Contribution à l'estimation des paramètres du système des carbonates en Mer Mediterranée

Elissar Gemayel

THÈSE

Pour obtenir le grade de

Docteur

Délivré par

UNIVERSITE DE PERPIGNAN VIA DOMITIA

Préparée au sein de l'école doctorale Énergie et Environnement 305, Et de l'unité de recherche IMAGES_ESPACE-DEV

Spécialité : **Océanologie**

Présentée par **Elissar GEMAYEL**

CONTRIBUTION A L'ESTIMATION DES PARAMETRES DU SYSTEME DES CARBONATES EN MER MEDITERRANEE

Soutenue le 21 Septembre 2015 devant le jury composé de

Mme Nadine LE BRIS Professeur, Laboratoire d'Écogéochimie des Environnements Benthiques, France	**Rapporteur**
Mme Evangelia KRASAKOPOULOU Professeur, University of the Aegean, Department of Marine Sciences, University Hill, Grece	**Rapporteur**
Mr Franck TOURATIER Maître de conférences, IMAGES_ESPACE-DEV, Université de Perpignan Via Domitia, France	**Examinateur**
Mme Catherine GOYET Professeur, IMAGES_ESPACE-DEV, Université de Perpignan Via Domitia, France	**Directrice**
Mme Marie ABBOUD - ABI SAAB Directeur de Recherche, CNRS, Centre National des Sciences Marines, Liban	**Co-directrice**

A ma petite famille, Antoine, Fadia et Joseph, qui m'ecouragent et me guident

A l'âme de mon grand père Farid, qui m'a appris à toujours sourire

A mon seul et unique Roy, qui fait ressortir le meilleur en moi-même

Remerciements

La thèse est l'aboutissement d'un parcours académique qui s'achève, et qui mène vers la vie professionnelle et le monde de la recherche. Ainsi j'ai eu l'occasion d'être entourée par plusieurs personnes qui sans eux mon chemin aurait été beaucoup plus difficile, même impossible. J'espère par les mots soulignés ci-dessous, leur rendre hommage et leur exprimer ma grande gratitude pour leurs accompagnements et leurs conseils.

Je tiens tout d'abord à remercier le CNRS Libanais représenté par le Directeur Général, Mr Mouïn Hamzé, qui m'a accordé le soutien financier de la thèse. Je remercie aussi le directeur du Centre National des Sciences Marines, Mr Gaby Khalaf, pour son aimable caractère et pour l'accueil chaleureux et l'ambiance favorable qu'il offre à tous les doctorants.

En vue de la coopération entre l'Université de Perpignan Via Domitia et le CNRS Libanais, j'ai eu l'opportunité d'être encadrée par deux professeurs très compétents. J'adresse ainsi mes remerciements à ma directrice Mme Catherine Goyet, qui a accepté de m'accueillir dans son unité de recherche. Je suis très reconnaissante pour la qualité de ces nombreux conseils, sa patience et son engagement continu. Mes remerciements vifs se dirigent ensuite à ma co-directrice Mme Marie Abboud-Abi Saab, qui m'a suivi depuis mon master et continue d'être un appui solide pour mon développement professionnel et personnel. Je tiens à lui exprimer ma grande gratitude pour son accompagnement journalier, son souci et sa confiance.

Mes remerciements s'adressent ensuite à Mme Nadine Le Bris et Mme Evangélina Krasakopoulou, pour l'effort et le temps qu'elles ont consacrées pour rédiger le rapport de la thèse ; ainsi que Mr Franck Touratier pour son évaluation pertinente de ce travail.

Je remercie très profondément tous les membres du Centre National des Sciences Marines, avec qui j'ai passé la plupart de mes années de thèse. J'apprécie de tout mon cœur l'ambiance familiale, l'amitié et les moments inoubliables qu'on a partagés. Je remercie ainsi tous les personnels: Mme Sana Chahine Tahan, Mme Roula El Rowayheb Mina, Mme Viviane Aouad El Osta, Mr Milad Fakhri, Mme Elise

Njeim Abi-Nader, Mr Elie Tarek, Mlle Carine Abi Ghanem, Mlle Nada Matar, Mlle Marie-Térèze Kassab ; ainsi que tous mes collègues: Mr Abed El Rahman Hassoun, Mr Anthony Ouba, Mr Sherif Jemaa, Mr Ali Badreddine, Mlle Aurore Assaker, Mlle Myriam Lteif, Mlle Laury Açaf et Mme Céline Mahfouz Karam.

J'adresse aussi mes remerciements à mes collègues et amis présents à l'unité IMAGES_ESPACE-DEV. Je remercie tout d'abord, Mr Cédric Falco pour son aide dans les mesures relatives à la mission MedSeA, sa gentillesse et son dévouement. Je remercie ensuite mes bons amis: Mme Hadjer Moussa Benallal et Mr Mohamed Anis Benallal, pour leur aide dans les aspects relatifs à la programmation ainsi que leur soutien moral et leur support continu. Merci aussi à Mme Françoise Petit pour son aide dans tous les papiers administratifs.

J'exprime aussi ma grande reconnaissance à toutes les personnes que j'ai rencontrées à l'Université de Perpignan Via Domitia, et qui ont rendu mes séjours très paisibles et agréables. Un grand merci à, Mr Hussein Kanso, Mr Ahmad Ramadan, Mr Issam Karrat, Mr Machti Kasem, Mr David Tsuyano, Mr David Roquis, Mr Amin Najahi, Mme Sara Fneich Choker, Mlle Rawa El Fallah, Mlle Nahil Lahoud, Mlle Mayla Salman, Mme Rafif Nheili, Mme Afraa Mansour et Mme Anais Bozo. Merci pour votre accueil généreux et pour tous les bons moments qu'on a passé ensemble.

Un grand merci aussi à ma famille, mon père Antoine, ma mère Fadia et mon frère Joseph. Sans vous je ne serais pas là aujourd'hui ! Bien plus que les mots ne peuvent l'exprimer, j'adresse un dernier grand merci à Roy Owayda, que j'aime énormément. Merci pour ton amour unique, et pour ton cœur à travers lequel tu as pu me voir telle que je suis.

Contribution à l'estimation des paramètres du système des carbonates en Mer Méditerranée

Résumé

L'objectif de la thèse s'inscrit dans le cadre de contribuer à l'estimation des paramètres du système des carbonates en Mer Méditerranée, en particulier la pression partielle du CO_2 dans l'eau (pCO_2^{sw}), l'alcalinité totale (A_T), le carbone inorganique total (C_T) et le pH.

En premier lieu, on a calculé à partir des données des campagnes Boum en 2008 et MedSeA en 2013 les coefficients de mélange des masses d'eau dans les bassins Ouest et Est. L'analyse de ces coefficients nous a permis d'étudier l'évolution des masses d'eau en Mer Méditerranée entre les années 2008 et 2013.

En deuxième lieu, on a présenté à partir des données de la mission MedSeA en mai 2013, les résultats des mesures récentes de pCO_2^{sw} sur une section longitudinale assez étendue allant du détroit de Gibraltar jusqu'au sous-bassin Levantin. Les résultats ont indiqué que les bassins Ouest et Est sont gouvernés par deux régimes différents de $pCO_2^{sw.}$ Ces deux régimes ont été influencés par les propriétés physico-chimiques assez distinctes des deux bassins. A partir des mesures directes de pCO_2^{sw} on a calculé les flux journaliers de CO_2 à travers l'interface air-mer en mai 2013 et cela pour le trajet couvert par la mission MedSeA. Pour aboutir à une analyse plus globale on s'est référé dans une étude ultérieure, aux données des campagnes Thresholds et MedSeA. On a établit ainsi deux équations pour estimer en mai 2007 et 2013, la pCO_2^{sw} à partir des données satellites de température de surface, Chlorophylle_a et l'index de la couleur de la matière organique dissoute. Puis, on a calculé et cartographié les flux air-mer de CO_2 en mai 2013 à l'échelle de toute la Mer Méditerranée et pour une résolution spatiale de 4 km.

Ensuite, on a établi à partir des données de la mission MedSeA, des régressions linéaires pour estimer l'A_T et le C_T à partir de la salinité, et cela pour chaque sous-bassin de la Mer Méditerranée et pour plusieurs intervalles de profondeur. Ultérieurement, on s'est concentré aux données physico-chimiques dans les eaux de surface, compilées de plusieurs campagnes océanographiques entre 1998 et 2013. Les équations établies pour estimer l'A_T et le C_T dans les eaux de surface, ont indiqué que le meilleur polynôme inclue la salinité et la température. Ces polynômes ont été appliqués sur les cartes climatologiques de température et de salinité du World Ocean Atlas, pour cartographier les variabilités spatiales et saisonnières de l'A_T et du C_T sur une moyenne de 7 ans. En outre, à partir des données de la mission MedSeA, on a estimé les concentrations en carbone anthropique (C_{ANT}) et la variation de l'acidification (ΔpH) en Mer Méditerranée. Les résultats ont indiqué que la Mer Méditerranée est fortement contaminée par le C_{ANT} avec des concentrations bien plus élevées que celles enregistrées dans l'océan Pacifique ou Indien. Le calcul du ΔpH a indiqué que la Mer Méditerranée est déjà acidifiée de la surface jusqu'en profondeur. Enfin, on a présenté un modèle pour prédire le ΔpH en fonction de concentrations théoriques de C_{ANT}. On a montré que le seuil en C_{ANT} pour lequel l'acidification va fortement s'intensifier en Mer Méditerranée est déjà atteint. Aussi, les eaux profondes des bassins Occidental et Oriental, deviendront très probablement sous saturées par rapport à la calcite et à l'aragonite d'ici la fin du siècle prochain.

Mots clés : Mer Méditerranée ; système des carbonates ; images satellites ; flux de CO_2 ; acidification

Contribution to the estimation of the carbonates system parameters in the Mediterranean Sea

Abstract

The objective of the thesis is to contribute to the estimation of the carbonate system parameters in the Mediterranean Sea, in particular the partial pressure of CO_2 in water (pCO_2^{sw}), total alkalinity (A_T), total inorganic carbon (C_T) and pH.

The study was initiated by an adequate calculation of the water masses mixing coefficients in the Western and Eastern basins, using data from the Boum and MedSeA cruises in 2008 and 2013, respectively. The analysis of the mixing coefficients, allowed us to study the evolution of water masses in the Mediterranean Sea between the years 2008 and 2013.

Subsequently, using data from the 2013 MedSeA cruise, we presented the results of recent measurements of pCO_2^{sw} on a wide longitudinal section from the Strait of Gibraltar to the Levantine sub-basin. The results indicated that the Western and Eastern basins were characterized by two different pCO_2^{sw} regimes. These regimes were mainly affected by the distinctive physico-chemical properties of each basin. From the direct measurements of pCO_2^{sw} we calculated along the track of the MedSeA cruise, the daily CO_2 fluxes across the air-sea interface in May 2013. To achieve a more comprehensive analysis, we referred in a consecutive study to the data of the Thresholds and MedSeA cruises. From these data, we provided two equations to estimate in May 2007 and 2013; pCO_2^{sw} from satellite data of sea surface temperature, Chlorophyll_a and the chromophoric dissolved organic matter index. Furthermore, we calculated and mapped the air-sea CO_2 fluxes in May 2013 across the whole Mediterranean Sea, with a spatial resolution of 4 km.

Successively, we established from the MedSeA cruise data, linear regressions to estimate A_T and C_T from salinity, in each sub-basin of the Mediterranean Sea and for several depths. Later on, we focused on the physico-chemical data in surface waters, compiled from several oceanographic cruises between 1998 and 2013. The equations developed to estimate the A_T and C_T in surface waters, indicated that it is best to include in these polynomials both salinity and temperature. These polynomials were applied to the climatological fields of salinity and temperature of the World Ocean Atlas, in order to map the spatial and seasonal variability of A_T and C_T on a 7 years average. Moreover, we estimated from the MedSeA cruise data, the concentrations of anthropogenic carbon (C_{ANT}) and the variation of acidification (ΔpH) in the Mediterranean Sea. The results indicated that the Mediterranean Sea is heavily contaminated by C_{ANT}, with higher concentrations than those recorded in the Pacific or Indian Ocean. Also, the calculated ΔpH indicated that the Mediterranean Sea is already acidified from the surface to the deep waters. Finally, we presented a model to predict the ΔpH according to theoretical concentrations of C_{ANT}. Consequently, we showed that we already reached the tipping point of C_{ANT}, for which the acidification will strongly intensify in the Mediterranean Sea. Moreover, the deep waters of the Western and Eastern basins are very likely to become under saturated in calcite and aragonite by the end of the next century.

Keywords: Mediterranean Sea; carbonates system; satellite images; CO_2 fluxes; acidification

Table des Matières

Introduction Générale

'Le réchauffement du système climatique est sans équivoque et, depuis les années 1950, beaucoup de changements observés sont sans précédent depuis des décennies voire des millénaires. L'atmosphère et l'océan se sont réchauffés, la couverture de neige et de glace a diminué, le niveau des mers s'est élevé et les concentrations des gaz à effet de serre ont augmenté (IPCC, 2013).'

C'est par cette assertion alarmante que le 'Groupe d'experts Intergouvernemental sur l'Evolution du Climat (GIEC)' s'adresse aux responsables politiques en affirmant le phénomène du réchauffement climatique et de ses différentes répercussions.

Le réchauffement climatique est fortement accéléré par l'influence de l'homme notamment par les rejets anthropiques de CO_2. En effet, suite aux rejets industriels et agricoles, les concentrations atmosphériques de CO_2 ont augmentées de 278 ppm depuis l'ère industrielle pour dépasser le seuil de 400 ppm en 2014 (Le Quéré *et al.*, 2015). Ces taux sont les plus élevés depuis 800 000 ans et les océans ont extrait 30 PgC de l'atmosphère, soit 30 % des émissions totales du CO_2 anthropique (IPCC, 2013; Wanninkhof *et al.*, 2013). L'océan contribue alors à minimiser certains impacts du réchauffement climatique en atténuant les taux de gaz à effet de serre émis dans l'atmosphère (Stocker *et al.*, 2013).

Face à cette perturbation des flux naturels, les propriétés physico-chimiques de l'océan ont été modifiées. Parmi les effets les plus importants on cite : le réchauffement des couches supérieures de l'océan (Marotzke and Forster, 2015), la modification de la salinité de surface (Kullenberg *et al.*, 2015), l'élévation du niveau moyen des mers (Hay *et al.*, 2015) et la diminution du pH à la surface d'environ 0.0018 ± 0.0004 an^{-1} entre 1991–2011, d'où une tendance nette à l'acidification des océans (Lauvset *et al.*, 2015).

A l'échelle globale, l'évaluation précise des flux de CO_2 à travers l'interface air-mer par les modèles couplant climat et cycle du carbone, présente une grande incertitude et cela dû au manque de connaissances relatives à la modification de la production et de la pompe biologique, à la répartition des pressions partielles du CO_2 (pCO_2) dans les océans, au rôle des mers marginales et des zones côtières, et au comportement du vivant face au changement abrupt du climat (IPCC, 2013). Ainsi, les données in-situ relatives aux paramètres hydrophysiques et du système des carbonates interviennent pour appuyer et valider les résultats des modèles climatiques et pour mieux contraindre la variabilité spatio-temporelle du puits du CO_2 océanique (Doney *et al.*, 2009; Le Quere *et al.*, 2009).

La mise au point d'un réseau de mesures directes nécessite de grands efforts et collaborations nationales et internationales. Ainsi, les mesures du système des carbonates en particulier le carbone inorganique et les données hydrographiques, ont été collectées au cours de

nombreuses campagnes océaniques comme : 'Geochemical Ocean Sections Study, GEOSECS' (Sabine *et al.*, 2010), 'World Ocean Circulation Experiment, WOCE', 'Joint Global Ocean Flux Study, JGOFS', avec des campagnes océaniques globales achevées à la fin des années 1990 (Tanhua *et al.*, 2013a). Depuis ces campagnes, les mesures du système des carbonates a continué à travers divers programmes comme : 'CLIVAR-CO_2, Climate Variability program', 'GO-SHIP : the Global Ocean Ship-based Hydrographic Investigations Program' (Tanhua *et al.*, 2013a) et le 'CO_2 Time-series and Moorings Project' (Sutton *et al.*, 2014).

En compilant ces données, Takahashi *et al.* (2009) ont établi à l'aide d'un modèle d'advection-diffusion, une carte climatologique des flux de CO_2 en référence à l'année 2000 et cela à partir de la synthèse de plus de 3 millions de mesures de pCO_2 dans les eaux de surface (pCO_2^{sw}) de l'océan mondial réalisées de 1970 à 2007 en dehors des conditions El Nino. Une observation assez remarquable dans cette carte est l'exclusion de la Mer Méditerranée dans la climatologie globale des flux de CO_2. Hors la Mer Méditerranée qui ne que représente que 0,8 % de la surface océanique globale, est considérée comme l'un des plus complexes environnements marins dû au divers processus physiques et biogéochimiques qui s'y manifeste (Lacombe and Tchernia, 1972; Béthoux *et al.*, 1999; Pinardi and Masetti, 2000; Tanhua *et al.*, 2013c).

La Mer Méditerranée est un bassin semi-fermé connecté seulement à l'océan Atlantique par le détroit de Gibraltar, où a lieu un échange important de masses d'eau de propriétés très distinctes qui affectent la circulation thermohaline globale (Baringer and Price, 1997; Serra and Ambar, 2002). Avec son échange limité avec l'océan et sa circulation spécifique, la Mer Méditerranée est considérée un "*océan miniature*" (Béthoux *et al.*, 1999; Bergamasco and Malanotte-Rizzoli, 2010), où l'on pourrait étudier les processus qui se produisent à l'échelle de l'océan mondial. La Mer Méditerranée est en mesure d'absorber plus de CO_2 anthropique et cela à cause des hautes concentrations d'alcalinité totale (Schneider *et al.*, 2007; Cossarini *et al.*, 2015) qui lui donne une plus grande capacité chimique pour absorber le CO_2 d'origine anthropique, et de la ventilation relativement rapide des eaux profondes ce qui permet une pénétration plus profonde de ce traceur anthropique (Touratier and Goyet, 2004). Ainsi elle a été identifiée comme un lieu de stockage important du carbone anthropique, où l'inventaire de la colonne d'eau est beaucoup plus élevé que dans l'Atlantique ou le Pacifique (Schneider *et al.*, 2010; Lee *et al.*, 2011), et alors sujette de faire face à une acidification relativement plus amplifiée comparée à la moyenne océanique globale (Touratier and Goyet, 2009, 2011; Palmiéri *et al.*, 2015).

Malgré l'importance de la Mer Méditerranée dans l'amélioration de notre compréhension des mécanismes et de l'évaluation du climat de la Terre; les mesures des paramètres du système des carbonates sont encore limitées du point de vue spatial et temporel (Álvarez, 2012). De ce fait, les estimations de pCO_2^{sw}, de l'Alcalinité Totale (A_T), du Carbone Inorganique Total (C_T) et du pH et ont été effectuées par des modèles empiriques qui couvrent des endroits spécifiques comme le détroit de Gibraltar (Santana-Casiano *et al.*, 2002), la mer d'Alboran (Copin-Montégut, 1993), le site DYFAMED (Copin-Montégut and Bégovic, 2002; Copin-

Montégut *et al.*, 2004), la mer Egée (Krasakopoulou *et al.*, 2009) et la Mer Adriatique (Luchetta *et al.*, 2010b). En outre, la pénétration du CO_2 anthropique (CANT) a été étudiée dans la région Catalo-Baléares (Delgado and Estrada, 1994), le détroit de Gibraltar (Sempéré *et al.*, 2003) dans le golfe de Cádiz (Aït-Ameur and Goyet, 2006) et le détroit d'Otrante (Krasakopoulou *et al.*, 2011). L'estimation de ces paramètres à l'échelle de la Méditerranée fut présentée par des travaux concentrés sur des campagnes mensuelles en mer (Schneider *et al.*, 2007; Touratier and Goyet, 2009; Rivaro *et al.*, 2010; Schneider *et al.*, 2010; Touratier and Goyet, 2011); ou basée sur des modèles couplés (D'Ortenzio *et al.*, 2008; Cossarini *et al.*, 2015; Palmiéri *et al.*, 2015). En vue de la limitation temporelle des données, les flux de CO_2 à l'interface air-mer sur l'ensemble du bassin ont été uniquement estimés par des simulations numériques du système des carbonates et cela entre les années 1960 et 2004 (D'Ortenzio *et al.*, 2008; Louanchi *et al.*, 2009; Taillandier *et al.*, 2012).

L'objectif de cette thèse se situe alors dans le cadre de mieux déterminé l'absorption du CO_2 dans la Mer Méditerranée, et cela à travers l'étude, l'estimation et la prédiction des différents mécanismes et paramètres qui affectent la variabilité du système du carbone océanique.

Dans le manuscrit de la thèse on présente deux chapitres introductifs, suivis d'une succession de sept d'articles scientifiques et on termine par la présentation des principales conclusions et perspectives

Le chapitre I est consacré à la présentation des équilibres chimiques, des définitions et usages des différents paramètres du système des carbonates dans l'eau de mer. On élabore aussi les méthodes de calcul du flux air-mer de CO_2, du coefficient d'échange du CO_2 et du carbone anthropique.

Le chapitre II a pour but d'introduire la zone d'étude, par la description de ses caractéristiques géographiques, météorologiques et hydrodynamiques. On présente aussi un état de lieux pour le système des carbonates en Mer Méditerranée avec une attention particulière sur les bases de données disponibles ainsi que l'estimation du système des carbonates dans les eaux de surface.

Dans le chapitre III, on présente une série d'articles divisés suivant quatre thématiques principales :

Thématique 1 : ' La circulation de la Mer Méditerranée : un débat continu'

Article I*: Hassoun, A.E.R., Guglielmi, V.,* ***Gemayel, E.****, Goyet, C., Abboud-Abi Saab, M., Giani, M., Ziveri, P., Ingrosso, G., Touratier, F., 2015c. Is the Mediterranean Sea Circulation in a Steady State. J. Water Resource Ocean Sci. 4 (1), 6-17. doi: 10.11648/j.wros.20150401.12*

Cet article teste l'hypothèse du 'régime permanent' ou 'quasi-stationnaire' de la circulation, en comparant l'évolution des coefficients de mélange des masses d'eaux mesurés lors de des campagnes Boum en 2008 et MedSeA en 2013.

Thématique 2 : 'Aperçu récent de la pCO_2 de surface et potentiels d'estimation des flux de CO_2 par les images satellites'

Article II: ***Gemayel, E.****, Hassoun, A.E.R., Benallal, M., Goyet, C., Krasakopoulou, E., Abboud-Abi Saab, M., Touratier, F. Distribution of surface water pCO_2 and air-sea fluxes in the Mediterranean Sea during May 2013. Submitted to Deep-Sea Research Part I.*

Dans ce papier on présente de nouvelles données de pCO_2^{sw} mesurées dans les eaux de surface au cours de la mission MedSeA en mai 2013. On décrit sur une section longitudinale assez étendue la distribution spatiale de la pCO_2^{sw} et des différents facteurs qui influencent sa variabilité dans les bassins Ouest et Est. Suite à ces mesures directes, on calcule le flux de CO_2 à travers l'interface air-mer durant le mois de mai 2013.

Article III: ***Gemayel, E.****, Benallal, M., Calleja, M., Hassoun, A.E.R, Goyet, C., Alvarez, M., Duarte, C., Abboud-Abi Saab, M. Estimates of pCO_2 and air-sea CO_2 fluxes in the Mediterranean Sea in May 2007 and 2013 from satellite data. Submitted to Remote sensing of Environment.*

Dans cette étude, nous introduisons une première comparaison entre différents algorithmes empiriques destinés à estimer la pCO_2^{sw} à partir de données de température, de Chlorophylle_a et de l'index de la couleur de la matière organique dissoute (CDOMi) acquis à partir des images satellites. Cette analyse est appliquée à deux campagnes dans la Mer Méditerranée menées en mai 2007 et 2013. On génère à partir de ces équations deux cartes de pCO_2^{sw} et des flux air-mer sur toute la Mer Méditerranée pour les mois de mai 2007 et 2013.

Thématique 3 : 'L'Alcalinité Totale et le Carbone Inorganique Total : estimations mensuelles et climatologiques'

Article IV: *Hassoun, A.E.R.,* ***Gemayel, E.****, Krasakopoulou, E., Goyet, C., Abboud-Abi Saab, M., Ziveri, P., Touratier, F., Guglielmi, V., Falco, C., 2015b. Modeling of the total alkalinity and the total inorganic carbon in the Mediterranean Sea. J. Water Resource Ocean Sci. 4 (1), 24-32. doi: 10.11648/j.wros.20150401.14*

Dans cette publication on établit à partir des données de la mission MedSeA 2013 des relations linéaires qui permettent d'estimer l'A_T et le C_T à partir de la salinité. Ces modèles sont établis pour différentes profondeur et cela pour chaque bassin et sous-bassin de la Mer Méditerranée.

Article V: ***Gemayel, E.****, Hassoun, A.E.R., Benallal, M., Goyet, C., Rivaro, P., Abboud-Abi Saab, M., Krasakopoulou, E., Touratier, F., Ziveri, P. Climatological variations of total alkalinity and total inorganic carbon in the Mediterranean Sea surface waters. Submitted to Journal of Oceanography.*

Cet article présente une compilation de mesures d'A_T et de C_T dans l'eau de surface (<10 m) à partir de différentes campagnes océaniques en Mer Méditerranée entre 1999 et 2013. On présente ainsi à partir de la température (T) et de la salinité (S): a) une équation améliorée pour l'estimation de l'A_T et b) la première estimation du C_T moyen annuel dans les eaux de surface. Ces équations sont utilisées pour cartographier à partir des climatologies de T et S du 'World Ocean Atlas 2013', la variabilité spatiale et saisonnière de l'A_T et du C_T en surface sur une moyenne de 7 ans.

Thématique 4 : 'La Mer Méditerranée face à l'acidification des eaux : état des lieux et prédictions'

Article VI: *Hassoun, A.E.R.,* ***Gemayel, E.****, Krasakopoulou, E., Goyet, C., Abboud-Abi Saab, M., Guglielmi, V., Touratier, F., Falco, C., 2015a. Acidification of the Mediterranean Sea from anthropogenic carbon penetration. Deep Sea Res. Part I Oceanogr. Res. Pap. 102 (0), 1-15.* http://dx.doi.org/10.1016/j.dsr.2015.04.005

Cette publication analyse à partir des données de la mission MedSeA, la distribution des concentrations du CO_2 anthropique (C_{ANT}) estimées par la méthode TrOCA. Ensuite, on caractérise les masses d'eau détectées en Mer Méditerranée en se basant sur les concentrations du C_{ANT}. Enfin on évalue les variations de l'acidification depuis l'ère préindustrielle jusqu'à l'année 2013.

Article VII: *Goyet, C., Hassoun, A.E.R.,* ***Gemayel, E.****, Touratier, F., Abboud-Abi Saab, M., Guglielmi, V. What are the tipping points for the Mediterranean Sea Acidification? Submitted to Climate Dynamics.*

Cette étude prédit les variations de l'acidification (ΔpH) en Mer Méditerranée pour les prochaines décennies et pour le siècle suivant. La prédiction du ΔpH est établie à partir d'un calcul purement théorique en se basant sur les conditions initiales des données de la mission MedSeA en 2013. Les estimations sont effectuées pour les deux bassins Ouest et Est et cela à partir de leur propriétés physico-chimiques respectives. Quatre seuils critiques sont ainsi déterminés, dont le seuil pour lequel les eaux de la Mer Méditerranée seront acides.

Suite à la succession de ces articles, on termine le manuscrit par le chapitre IV, où on illustre les conclusions principales de la thèse, ainsi que les perspectives issues de ce travail.

Contributions aux Articles

Cette thèse regroupe une série d'articles, auxquels plusieurs auteurs ont contribué. Je présente alors ci-dessous mes différentes contributions à chacun de ces articles.

Les articles I, IV et VI ont été initié par Hassoun, A.E.R., et sont le résultat de nombreuses discussions interdisciplinaires. J'ai effectué avec Hassoun A.E.R., toutes les mesures pour l'analyse des échantillons d'alcalinité totale et de carbone inorganique total collectés durant la mission MedSeA en mai 2013. Aussi, j'ai contribué aux corrections et révisions de ces articles.

D'autre part, j'ai initie, planifié et rédigé les articles II, III et V. Mes collègues m'ont épaulé pour l'évaluation et l'interprétation des données. J'ai été aussi responsable de la soumission de ces articles et pris en charge les corrections s'il y avait lieu. J'ai aussi effectué avec Falco, C., au bord du bateau Angeles alvarino ; le montage des appareils dediés pour mesurer en continu la pCO_2, la température, la salinité, le pH et la fluorescence. J'étais ainsi responsable avec l'aide de Hassoun A.E.R, de la surveillance du montage et la collecte des données durant la mission MedSeA en mai 2013.

L'article VII a été initié par Goyet, C. J'ai contribué à l'analyse des résultats et aux relectures de l'article.

Chapitre I : Le Puits Océanique

'Telle est la tâche d'une science naturelle : montrer que le merveilleux n'est pas incompréhensible, montrer comment il peut être compris – sans pour autant détruire l'émerveillement. Car lorsque nous avons expliqué le merveilleux, démasqué les structures cachées, un nouveau merveilleux surgit : la complexité était tissée de simplicité. L'esthétique d'une science naturelle ou des mathématiques est la même que celle de la musique ou de la peinture ; pour les unes comme pour les autres, elle est aspiration à la découverte d'une forme partiellement cachée…'

Simon, H. A. (2004). Les sciences de l'artificiel, trad. fr. Jean-Louis Le Moigne, Paris: Gallimard, coll. « Folio Essais »., p 27

I- Système des carbonates dans l'eau de mer

I.1- Equilibres chimiques

Le dioxyde de carbone (CO_2) est un gaz atmosphérique, soluble et présent dans toutes les eaux naturelles sous forme de molécules neutres. La réaction entre les formes gazeuses et dissoutes du CO_2 est régit par une série d'équilibres chimiques :

$$CO_2(g) \leftrightarrows CO_2(aq) \quad (1)$$

$$CO_2(aq) + H_2O \leftrightarrows H_2CO_3 \quad (2)$$

$$H_2CO_3 \leftrightarrows H^+ + HCO_3^- \quad (3)$$

$$HCO_3^- \leftrightarrows H^+ + CO_3^{2-} \quad (4)$$

A l'équilibre, la concentration de l'acide carbonique (H_2CO_3) est d'environ 1/1000 de la concentration de CO_2 dissous, et donc n'affecte pas les équilibres de base. Dans ce qui suit, la concentration totale des deux espèces non ionisées sera abrégée: $[CO_2^*] = [CO_2(aq)] + [H_2CO_3]$. Ainsi les réactions (1), (2) et (3) sont redéfinies suivant :

$$CO_2(g) \leftrightarrows CO_2^* \quad (5)$$

$$CO_2^* \leftrightarrows H^+ + HCO_3^- \quad (6)$$

Dans l'eau de mer, les constantes apparentes de dissociation (K_1 et K_2) s'expriment par les concentrations molaires des espèces ($mol.kg^{-1}$). Ces constantes dépendent de la pression, de la température et de la force ionique. Elles ont été déterminées dans l'eau de mer naturelle et artificielle en fonction de la salinité, de la température et sur différentes échelles de pH (Millero, 2007). Les différentes constantes sont déterminées par :

$$K_1 = [H^+][HCO_3^-]/[CO_2] \quad (7)$$

$$K_2 = [H^+][CO_3^{2-}]/[HCO_3^-] \quad (8)$$

A ces constantes apparentes de dissociation, s'ajoute la solubilité du carbonate de calcium ($CaCO_3$) selon la réaction (Mucci, 1983):

$$Ca^{2+} + CO_3^{2-} \leftrightarrows CaCO_3(s) \quad (9)$$

$$K_{sp} = [Ca^{2+}][CO_3^{2-}] \quad (10)$$

I.2- Propriétés mesurables

I.2.1- Carbone Inorganique Total

L'eau de mer constitue un milieu dans lequel [CO_2^*], [HCO_3^-] et [CO_3^{2-}] sont en équilibre permanent. On réfère la somme des concentrations de ces espèces dans l'eau de mer au carbone inorganique total (C_T).

$$C_T = [CO_2^*] + [HCO_3^-] + [CO_3^{2-}] \quad (11)$$

Les proportions relatives de ses espèces sont relativement bien connues, le C_T est constitué d'environ 90 % d'ions de HCO_3^-, 9 % de CO_3^{2-} et 1 % de CO_2^*.

I.2.2- Alcalinité Totale

L'alcalinité totale (A_T) est définie comme le nombre de moles d'ions hydrogène équivalent à l'excès d'accepteurs de protons (bases formées d'acides faibles avec une constante de dissociation $K \leq 10^{-4,5}$ à 25 °C et sans force ionique) relatif aux donneurs de protons (acides avec $K > 10^{-4,5}$) dans un échantillon d'eau d'un kilogramme (Dickson, 1981).

$$\begin{aligned} A_T = {} & [HCO_3^-] + 2[CO_3^{2-}] + [B(OH)_4^-] + [OH^-] + [HPO_4^{2-}] \\ & + 2[PO_4^{3-}] + [SiO(OH)_3^-] + [NH_3] + [HS^-] + \cdots \\ & - [H^+]_F - [HSO_4^-] - [HF] - [H_3PO_4] - \cdots \end{aligned} \quad (12)$$

Pour la majorité des eaux marines [HCO_3^-], [CO_3^{2-}] et [$B(OH)_4^-$] sont les bases les plus importantes. Dans les eaux anoxiques [NH_3] et [HS^-] peuvent contribuer à l'alcalinité totale (DOE, 1994).

L'alcalinité des carbonates est alors définie comme :

$$A_C = [HCO_3^-] + 2[CO_3^{2-}] = A_T - \Sigma\, Bases \quad (13)$$

L'acide borique se dissocie selon la réaction suivante :

$$B(OH)_3 + H_2O \leftrightarrows B(OH)_4^- + H^+ \quad (14)$$

$$K_B = [B(OH)_4^-] \times [H^+] / [B(OH)_3] \quad (15)$$

Le bore total, $B_T = [B(OH)_3] + [B(OH)_4^-]$ est conservatif avec un rapport presque constant avec la salinité : $B_T \cong 11{,}88 \times 10^{-6} \times S$ (Dickson, 1990b). Par conséquent, la relation précédente peut être reformulée suivant :

$$B_T \cong (K_B/([H^+] + K_B)) \times 11{,}88 \times 10^{-6} \times S \quad (16)$$

I.2.3- Pression partielle du CO_2

La dissolution du CO_2 dans l'eau de mer obéit à la loi de Henry (Eq 17).

$$\beta_0 = [CO_2]/pCO_2 \qquad (17)$$

Jusqu'à ce jour, β_0 est calculé en fonction de la température et de la salinité uniquement suivant l'algorithme proposé par (Weiss, 1974). En théorie et en toute rigueur scientifique, c'est la fugacité (fCO_2) - et non pas la pression partielle du CO_2 - qui doit être considérée pour prendre en compte le caractère non idéal de ce gaz (Weiss, 1974; DOE, 1994). En pratique la différence entre fCO_2 et pCO_2 est négligeable (0,5%), et les deux termes peuvent être utilisés indifféremment (Takahashi *et al.*, 1982; Peng *et al.*, 1987).

I.2.4- pH

La concentration en ions hydrogène dans l'eau de mer est généralement rapportée suivant:

$$pH = -\log[H^+] \qquad (18)$$

En pratique le pH peut être déterminé suivant plusieurs échelles :

- L'échelle NBS (National Bureau of Standards), basée sur des tampons de faible force ionique et de composition éloignée du milieu marin (Bates, 1973). Elle est utilisée pour la chimie des solutions aqueuses diluées dans l'eau douce, mais n'est pas recommandée pour les mesures dans l'eau de mer (Dickson, 1984; Millero, 1986). C'est l'échelle des protons libres (Khoo *et al.*, 1977; Ramette *et al.*, 1977) où le pH est déterminé par:

$$pH_F = -\log[H^+]_F \qquad (19)$$

- L'échelle des protons totaux (Total scale), tient compte des protons associés aux sulfates (Hansson, 1973c; Dickson, 1993).

$$pH_T = -\log[H^+]_T = -\log([H^+]_F(1 + [SO_4^{2-}]_T/K(HSO_4^-)) \approx -\log([H^+]_F + [HSO_4^-]) \qquad (20)$$

où $[SO_4^{2-}]_T = [SO_4^{2-}] + [HSO_4^-]$ est approximativement proportionnel à la salinité (Dickson and Millero, 1987) et $K(HSO_4^-)$ la constante de dissociation des ions bisulfates suivant Dickson (1990a).

- L'échelle de l'eau de mer (Sea Water Scale) prend en compte les sulfates et les fluorures présents dans l'eau de mer (Dickson and Riley, 1979; Dickson and Millero, 1987).

$$pH_{SWS} = -\log[H^+]_{SWS} = -\log([H^+]_F\,(1 + [SO_4^{2-}]_T/K(HSO_4^-) + [F^-]_T/K(HF)) \approx -\log([H^+]_F + [HSO_4^-] + [HF^-]) \qquad (21)$$

où $[F^-]_T = [F^-] + [HF]$ est proportionnel à la salinité (Dickson and Millero, 1987) et $K(HF)$ la constante de dissociation de l'acide fluorique par Dickson and Riley (1979).

II- Equations et calculs

II.1- Facteur de Revelle

Le CO_2 dans l'océan est un acide faible et donc le système des carbonates réagit à un ajout de CO_2 atmosphérique, en associant les ions CO_3^{2-} au CO_2 dissous en excès et neutralise son effet sur le pH. C'est l'effet tampon de l'océan. Le pouvoir tampon de l'eau de mer est caractérisé par le facteur de Revelle (R), qui exprime le rapport entre la variation relative de la pCO_2^{air} et la variation relative du C_T correspondant, à alcalinité constante (Revelle and Suess, 1957). Le facteur R est en moyenne de 10 et peut varier entre 7 et 19. Il est de l'ordre de 8 pour des températures autour de 30 ºC et de l'ordre de 14 pour des températures de 2 ºC.

$$R = [(\mathrm{dpCO_2}/\mathrm{pCO_2})/(\mathrm{dC_T}/\mathrm{C_T})]_{\mathrm{A_T=cst}} \qquad (22)$$

Un facteur de Revelle de 10 indique qu'une augmentation de pCO_2 de 10% correspond à une augmentation de C_T de 1%.

II.2- Equation locale du flux de CO_2

A l'échelle locale le flux air-mer d'un gaz (F) est calculé suivant l'équation 23:

$$F = k.s(C_{sw} - \mathrm{C_{air}}) \qquad (23)$$

où F est le flux entre l'océan et l'atmosphère, s est la solubilité du gaz, k est la vitesse de transfert du gaz, C_{sw} est la concentration aqueuse du gaz, et C_{air} est la concentration du gaz dans une eau de mer qui serait à l'équilibre avec l'atmosphère.

Les mesures du flux de CO_2 à l'interface air-mer ne sont pas possibles, et donc en pratique les mesures de pCO_2 sont effectuées à des profondeurs comprises entre 1 et 5 m. Par la suite, le flux local de CO_2 à l'interface air-mer d'après Smith (1985) peut s'écrire :

$$F = k\left(s \times pCO_2^{sw} - s_{skin} \times pCO_2^{air}\right) \qquad (24)$$

où pCO_2^{sw} est la pression partielle du CO_2 dans l'eau, pCO_2^{air} est la pression partielle du CO_2 dans l'air, s est la solubilité dans la couche de surface océanique et s_{skin} la solubilité à l'interface air-mer. La solubilité du CO_2 peut être calculée selon Weiss (1982) en fonction de la température et de la salinité.

La solubilité dans la couche de surface n'est pas la même que celle à l'interface air mer ($s_{skin} = s + \delta$). Le terme δ est dû à la différence de température entre l'interface air-mer et la couche de surface. En fait, l'évaporation à la surface de l'eau crée une pellicule de quelques centaines de micromètres d'épaisseur, plus froide de 0.1-0.5°C que les couches de surface

appelé l'effet de peau de l'eau (Goyet and Brewer, 1993). Il est a noté que l'équation 24 suit le principe de conservation de masse et donc ne tient pas en compte de l'effet biologique (Ward *et al*., 2004). Aussi cette équation ne tient pas en compte de l'effet de couche chaude dans l'océan créée par l'insolation dans les premiers mètres de la surface (Fairall *et al.*, 1996).

En pratique, étant donné les larges incertitudes sur k, s et ΔP, F peut-être alors approximé partir de la température et de la salinité mesurées simultanément aux mesures de pCO_2^{sw}:

$$F \approx k.s\left(pCO_2^{sw} - pCO_2^{air}\right) \approx k.s.\Delta P \qquad (25)$$

II.2.1- Vitesse de transfert et coefficient d'échange du CO_2

La vitesse de transfert d'un gaz (k) est proportionnelle à une puissance 'n' du nombre de Schmidt (Sc). Le nombre de Schmidt est défini comme le rapport de la viscosité cinématique de l'eau (v) et de la diffusion moléculaire du gaz dans l'eau (D) : $Sc = v/D$. Ce rapport dépend de la nature du gaz, de la salinité et de la température.

Dans l'eau de mer, la plupart des mesures de 'k' sont ramenées à un Sc constant de 660, correspondant au Sc du CO_2 dans l'eau de mer à 20 ºC et pour une salinité de 35 (Jähne *et al.*, 1987). Or, lors de l'étude des flux de CO_2 à travers l'interface air-mer, il est nécessaire de prendre en considération les variations de température, puisque pour le CO_2, k varie de plus d'un facteur 2 entre 0° et 30°C et cela due à la variation du nombre Schmidt avec la température. De ce fait il est convenable de considérer dans l'équation 25, le coefficient d'échange du CO_2, $\boldsymbol{K = k.s}$, puisque les variations de k et s dus à la température sont presque compensées (Etcheto and Merlivat, 1988). Ainsi en considérant que la variation du coefficient d'échange de CO_2 est proportionnelle à $(Sc/660)^{-0,5} \times s$, K varie de moins de 10% entre 0 et 30°C (Etcheto and Merlivat, 1988; Boutin *et al.*, 2009).

Plusieurs relations de k ont été proposées afin de calculer le coefficient d'échange du CO_2, et nous nous limiterons aux paramétérisations les plus utilisées en littérature (Tableau 1). Liss and Merlivat (1986) ont proposé une relation empirique entre la vitesse de transfert du CO_2 à l'interface air-mer (k), et le module de la vitesse du vent mesuré à dix mètres au-dessus de la surface de la mer (U_{10}). Cette relation est basée sur des mesures effectuées en soufflerie et sur des modèles théoriques pour la dépendance de k avec le vent à partir de mesures réalisées sur des lacs. Il s'agit d'une série d'équations linéaires dont les coefficients changent selon la gamme de vent. Wanninkhof (1992) a aussi proposé deux relations entre la vitesse de transfert k et U_{10}. Dans cette relation k est proportionnel au carré de la vitesse du vent. Les deux relations sont valables soit pour les champs de vents instantanés ou des champs de vents moyens. Plus tard, Wanninkhof and McGillis (1999) ont effectués des mesures de k au cours de la campagne Gas Ex-98 qui s'est déroulée dans l'Atlantique Nord en juin 1998. Leurs résultats indiquent qu'une relation de forme cubique en U_{10} s'accorde mieux à leurs mesures qu'une relation quadratique. Nightingale *et al.* (2000) ont fait la synthèse de mesures réalisées en mer à partir de traceurs chimiques en se servant du couple (SF_6, ^3He) et ils en ont

déduit une relation quadratique en U_{10}. Plus récemment, Ho *et al.* (2006) a reporté les résultats de SAGE (SOLAS Air-Sea Gas Exchange), qui a été menée dans le secteur Pacifique Occidental de l'océan Austral. Les vitesses de transfert de gaz ont été déterminées en utilisant le traceur double de gaz $^3He/SF_6$ et cela pour des vitesses de vents supérieures (16 $m.s^{-1}$) aux expérimentations précédentes. Les résultats montrent clairement une relation quadratique entre la vitesse du vent et de la vitesse de transfert de gaz plutôt qu'une relation cubique. La relation cubique reste cependant, très controversée et le débat n'est toujours pas clos (Ho *et al.*, 2011).

Tableau 1. Différentes équations pour la vitesse de transfert du CO_2

Référence	**Relation**
Liss and Merlivat (1986)	$k_{LM} = (2{,}85 \times U_{10} - 9{,}65) \times (Sc/660)^{-0{,}5}$
Wanninkhof (1992)	$k_{W92} = 0{,}31 \times U_{10}^2 \times (Sc/660)^{-0{,}5}$
Wanninkhof and McGillis (1999)	$k_{MG} = 0{,}0283 \times U_{10}^3 \times (Sc/660)^{-0{,}5}$
Nightingale *et al.* (2000)	$k_{NT} = (0{,}222 \times U_{10}^2 + 0{,}333 \times U_{10}) \times (Sc/660)^{-0{,}5}$
Ho *et al.* (2006)	$k_{H06} = (0{,}266 \pm 0{,}019) \times U_{10}^2 \times (Sc/660)^{-0{,}5}$
Sweeney *et al.* (2007)	$k_{So7} = 0{,}27 \times U_{10}^2 \times (Sc/660)^{-0{,}5}$
Wanninkhof *et al.* (2009)	$k_{W09} = 3 + 0{,}1(U_{10}) + 0{,}064(U_{10}^2) + 0{,}011(U_{10}^3) \times (Sc/660)^{-0{,}5}$
Ho *et al.* (2011)	$k_{H11a} = 0{,}286 \times U_{10}^2 \times (Sc/660)^{-0{,}5}$ $k_{H11b} = 0{,}0298 \times U_{10}^3 \times (Sc/660)^{-0{,}5}$

II.2.2- Données de la pression partielle du CO_2 dans l'air

Les échanges de CO_2 entre l'océan et l'atmosphère sont gouvernés en premier lieu par le gradient de la pression partielle du CO_2 à l'interface air-mer. Les variations spatio-temporelles de ce gradient dépendent surtout des variations de la pression partielle du CO_2 dans l'océan car les variations de la pression partielle du CO_2 dans l'atmosphère sont minimes par rapport à celles de l'océan.

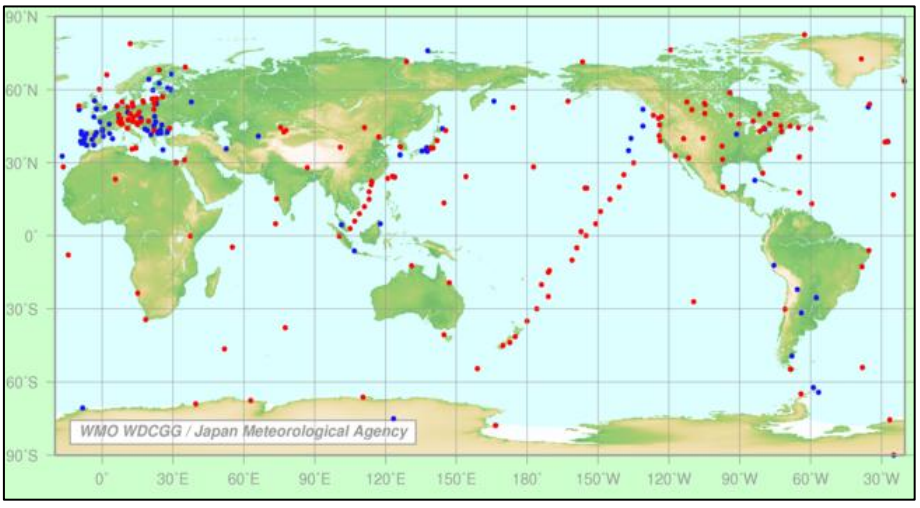

Figure 1. Localisations des stations atmosphériques pour le suivi de la concentration des gaz à effet de serre (en rouge les stations actualisées depuis moins d'un an). **Source :** **http://ds.data.jma.go.jp/gmd/wdcgg/**

La pCO_2^{air} varie par la photosynthèse et la respiration de la biosphère ainsi que par le rejet de CO_2 dans l'atmosphère dû aux activités humaines. Elle est relativement bien connue grâce au réseau mondial de stations de mesures atmosphériques (Figure 1). Les valeurs de la fraction molaire de CO_2 (en ppm) sont disponibles sur le site du World Meteorological Organization (WMO), World Data Centre for Greenhouse Gases (WDCGG) (http://ds.data.jma.go.jp/gmd/wdcgg/). A partir de la fraction molaire de CO_2 dans l'atmosphère, et de la connaissance de la pression atmosphérique, disponible sur le site de la NOAA (National Oceanic and Atmospheric Administration ; http://www.cdc.noaa.gov/cdc) grâce aux réanalyses du NCEP/NCAR (National Centers for Environmental Predictions/National Center for Atmospheric Research), la pCO_2^{air} peut être calculée suivant Weiss and Price (1980).

II.2.3- Données de la pression partielle du CO_2 dans les eaux de surface

L'importance mondiale d'échange du CO_2 se traduit par les ensembles de données de pCO_2^{sw} dans les océans du monde qui regroupent jusqu'à présent environ 6,4 et 10,1 millions de mesures, respectivement dans les bases de données du LDEO 2013 (Takahashi *et al.*, 2014b) et du 'Surface Ocean CO_2 Atlas' (SOCAT) version 2 (Bakker *et al.*, 2014).

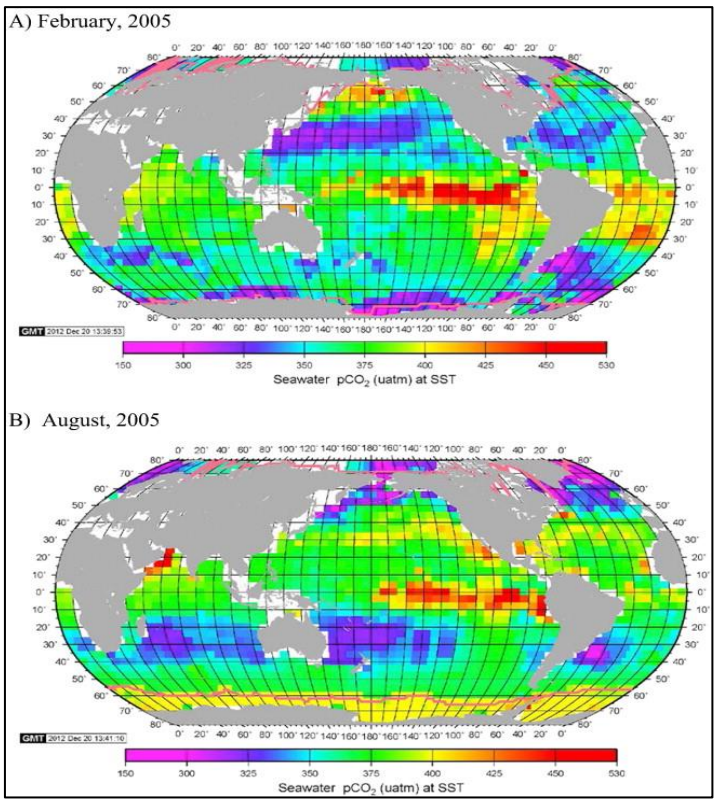

Figure 2. La distribution moyenne climatologique (1957-2012) de Takahashi *et al.* (2014a) pour la pCO_2^{sw} de l'océan global en référence à l'année 2005[1]

[1] Reprinted from Marine Chemistry, 164, Taro Takahashi, S.C. Sutherland, D.W. Chipman 1, J.G. Goddard, Cheng Ho, Timothy Newberger, Colm Sweeney, D.R. Munro, Climatological distributions of pH, pCO_2, total CO_2, alkalinity, and $CaCO_3$ saturation in the global surface ocean, and temporal changes at selected locations, Page 106, Copyright (2015), License number: 3640250753139, with permission from Elsevier (Annexes)

L'augmentation des mesures de pCO_2^{sw} dans l'océan permet de mieux comprendre leurs variabilités globales et locales et les processus qui affectent leurs distributions. Entre se référant à 5,6 million de mesures de pCO_2^{sw} entre 1957 et 2013 ; Takahashi *et al.* (2014a) ont présenté la distribution moyenne climatologique de la pCO_2^{sw} à partir d'un schéma d'advection-diffusion. Ils effectuent une correction des observations, à cause de l'augmentation de CO_2 au cours du temps, pour établir la climatologie en référence à l'année 2005. Cette climatologie mensuelle sert de référence pour valider les modèles globaux du cycle du carbone. Les couleurs jaune-orange indiquent les zones de source de CO_2 pour l'atmosphère, et les zones cyan et magenta-bleu sont des zones de puits de CO_2 atmosphérique (Figure 2).

II.2.4- Spéciation du système des carbonates

Dans l'eau de mer naturelle, les équilibres décrits précédemment se réalisent simultanément. Les 9 propriétés : pCO_2^{sw}, $[CO_{2aq}]$, $[H^+]\ ou\ pH$, $[OH^-]$, $[HCO_3^-]$, $[CO_3^{2-}]$, $[B(OH)_4^-]$, C_T $et\ A_T$ sont inter-reliés par plusieurs relations formant un système bivariant. Parmi les 9 propriétés, 4 seulement sont mesurables : pCO_2^{sw}, pH, C_T et A_T. La spéciation complète du système du carbone inorganique dans l'eau de mer peut être déterminée à partir de deux des quatre grandeurs mesurables (Millero *et al.*, 1979; Millero, 1995).

Afin de minimiser l'erreur entre les paramètres calculés et les mesures directes, il est nécessaire de connaître le plus exactement possible les constantes apparentes de dissociation. Les mesures directes de K_1 et K_2 ont été effectuées dans l'eau de mer artificielle (Goyet and Poisson, 1989; Roy et al., 1993) ; ou naturelle (Millero et al., 2006). D'autres groupes ont mesuré K_1 et le produit K_1K_2 dans l'eau de mer naturelle (Mehrbach *et al.*, 1973 ; Mojica-Prieto and Millero, 2002) ou artificielle (Hansson, 1973a, b). Cependant, ces constantes donnent des résultats très différents en raison de leur différente gamme de températures et de salinité (Millero, 2007). Les résultats de plusieurs analyses de cohérences pour le système de CO_2 dans l'eau de mer réalisées dans de nombreuses régions océaniques (Lee *et al.*, 1997; Wanninkhof *et al.*, 1999; Lee *et al.*, 2000; Millero *et al.*, 2002) et au laboratoire (Lee *et al.*, 1996; Lueker *et al.*, 2000) ; suggèrent que les mesures de [pK_2 - pK_1] de Mehrbach *et al.* (1973) réévaluées par Dickson and Millero (1987) sont applicables dans de nombreuses régions océaniques mais pas partout. Il est donc important de bien choisir ces constantes selon la région océanique considérée.

En tenant compte que les mesures sont effectuées avec une haute précision (A_T et C_T ± 1 µmol.kg^{-1} ; pH ± 0,0004 et pCO_2 ± 0,5 µatm**)**, les erreurs sur les différents paramètres dépendent des combinaisons choisies et du rapport X = A_T/C_T. Par exemple, le C_T et l'A_T ne devraient pas être calculés à partir du couple pH–pCO_2, et pour les eaux de surface la plus faible erreur sur le C_T calculé (± 3,2 µmol.kg^{-1}) est obtenue à partir du couple A_T–pCO_2 (Tableau 2). Lorsque le pH et l'A_T sont utilisés comme paramètres d'entrée pour calculer la pCO_2 et le C_T, l'effet des incertitudes du pK_1 sur la pCO_2 calculée dépend du rapport A_T/C_T mais a un effet moindre sur le C_T. L'effet des incertitudes du pK_2 sur le C_T calculé dépend du

rapport X : plus le rapport est élevé, plus la sensibilité pK_2 est élevée. En d'autres termes un rapport élevé implique une forte concentration de $[CO_3^{2-}]$ dont le calcul est sensible au pK_2. Toutefois indépendamment du rapport X, les incertitudes sur le pK_2 causent des différences minimes sur la pCO_2 calculée. Ces calculs indiquent que lorsque le pH et l'A_T sont utilisés comme paramètres d'entrées, seul un pK_1 fiable est nécessaire pour estimer la pCO_2, alors que seul un pK_2 fiable est nécessaire pour estimer le C_T. Lorsque la pCO_2 et l'A_T sont utilisés, les incertitudes du pK_1 et pK_2 sur le C_T calculé dépendent du rapport X, alors que seulement des erreurs sur le pK_1 affectent significativement le pH calculé et cela indépendamment du rapport X (Lee and Millero, 1995; Lee *et al.*, 1997; Lee *et al.*, 2000).

Tableau 2. Estimations des erreurs probables obtenues sur les paramètres calculés du système du carbone inorganique [d'après Millero (2007)].

Paramètres d'entrée	pH	A_T (µmol.kg^{-1})	C_T (µmol.kg^{-1})	pCO_2 (µatm)
pH-A_T	± 0,0004*	± 1	**± 3,8**	**± 2,1**
pH-C_T	± 0,0004	**± 2,7**	± 1	**± 1,8**
pH- pCO_2	± 0,0004	**± 21**	**± 18**	± 0,5
pCO_2 -C_T	**± 0,0025****	**± 3,4**	± 1	± 0,5
pCO_2 -A_T	**± 0,0026**	± 1	**± 3,2**	± 0,5
A_T-C_T	**± 0,0062**	± 1	± 1	**± 5,7**

* Précision des mesures

**** Erreurs probables calculées**

Néanmoins, les mesures des différents paramètres du système des carbonates peuvent ne pas être assez précises et cela à cause de la technique de mesure utilisée mais aussi à la manipulation de l'opérateur. Par exemple l'erreur sur les mesures de pH entre la spectrophotométrie et la potentiométrie est de ± 0,01 (Byrne *et al.*, 1988). Les erreurs sur les mesures de pCO_2 par les techniques infrarouges est de ± 2 µatm, et peut atteindre jusqu'à ± 10 µatm avec d'autres techniques comme la spectrophotométrie (DOE, 1994; Dickson *et al.*, 2007). Une étude récente d'inter-comparaison pour le système des carbonates entre plus de 60 laboratoires, a montré que les mesures actuelles d'A_T et de C_T ne sont probablement pas aussi précises qu'indiqué dans les publications. La majorité des laboratoires ont signalés des valeurs d'A_T et de C_T pour les mesures qui étaient dans une marge de ± 10 µmol.kg^{-1} de la valeur attribuée, mais peux d'entre eux ont pu obtenir des résultats inférieurs à ± 2 µmol.kg^{-1} en particulier pour le C_T. Certains laboratoires en utilisant un système de mesure donné, ont obtenu un excellent accord avec les valeurs attribuées, tandis que d'autres ont obtenus des résultats très différents même en utilisant un équipement apparemment identique. Ceci suggère qu'une contribution significative à l'incertitude globale de la mesure peut être attribuée à l'opérateur et à la procédure de laboratoire (Bockmon and Dickson, 2015).

Les incertitudes maximales sur les mesures de pH de ± 0,01 et de pCO_2, A_T et C_T de ± 10 µmol.kg^{-1}, impliquent que les erreurs probables sur les différents paramètres seront plus élevées que celle reportées dans le tableau 2. Pour mieux illustrer cet effet, on prend l'exemple de la mission MedSeA en mai 2013 pour laquelle on dispose des données d'A_T, de C_T et de pCO_2 dans les eaux de surface (Goyet *et al.*, 2015a, b). En tenant compte de ces incertitudes, on calcule ainsi à partir du logiciel CO_2SYS_2,1 (Pierrot *et al.*, 2006), les

nouvelles erreurs probables sur les différents paramètres en choisissant des différentes combinaisons de données d'entrées. Tous les calculs sont effectués en choisissant les constantes apparentes de dissociation (K_1 et K_2) de Goyet and Poisson (1989), les constantes des sulfates de Dickson (1990b), et les constantes des borates d'Uppström (1974). A noter que le choix de constantes à peu d'importance puisque nous cherchons à calculer les variations relatives. Le tableau 3 montre qu'en tenant compte des incertitudes maximales sur les mesures, les erreurs probables sur les différents paramètres par rapport au tableau 2, sont au moins dix fois plus élevées pour l'A_T, le C_T, le pH et la pCO_2^{sw}.

Tableau 3. Estimations des nouvelles erreurs probables obtenues sur les paramètres calculés du système du carbone inorganique en tenant compte des incertitudes maximales sur les mesures

Paramètres d'entrée	pH	A_T (µmol.kg^{-1})	C_T (µmol.kg^{-1})	pCO_2^{sw} (µatm)
pH-A_T	± 0,01*	± 10	**± 30**	**± 35**
pH-C_T	± 0,01	**± 18**	± 10	**± 29**
pH- pCO_2^{sw}	± 0,01	**± 47**	± **43**	± 10
pCO_2^{sw} -C_T	**± 0,09****	**± 20**	± 10	± 10
pCO_2^{sw} -A_T	**± 0,09**	± 10	**± 28**	± 10
A_T-C_T	**± 0,20**	± 10	± 10	**± 45**

* Incertitudes maximales sur les mesures

**** Nouvelles erreurs probables calculées**

II.2.5 – Versions disponibles

En ce qui concerne la spéciation du système des carbonates dans l'eau de mer, dix versions sont jusqu'à présent publiquement disponibles (Tableau 3). Tous nécessitent en entrée un minimum de deux variables du système afin de calculer les autres paramètres. Le logiciel CO_2calc permet aussi de calculer le flux de CO_2 à l'interface air-mer à partir de trois paraméterisations du coefficient d'échange notamment : Wanninkhof (1992), Nightingale *et al.* (2000) et Ho *et al.* (2006).

Tableau 3. Versions disponibles pour le calcul du système des carbonates [d'après Orr *et al.* (2015)]

Logiciel_Version	Language	Réference
CO_2SYS_1,05	DOS	Lewis and Wallace (1998)
CO_2SYS_1,4	Excel	Pelletier *et al.* (2007)
CO_2SYS_2,1	Excel	Pierrot *et al.* (2006)
CO_2SYS_1,1	Matlab	van Heuven *et al.* (2011)
CO_2calc_1,2,0	Visual Basic	Robbins *et al.* (2010)
csys_3	Matlab	Zeebe and Wolf-Gladrow (2001)
ODV_4,5,0	C++	Schlitzer (2002)
mocsy_1,2	Fortran 95	Orr and Epitalon (2015)
seacarb	R 2.4.8	Gattuso *et al.* (2015)
swco2_2	Excel; Visual basic	Hunter (2007); Mosley *et al.* (2010)

II.3- Approche TrOCA et calcul du CO_2 anthropique

L'estimation du dioxide de carbone anthropique (C_{ANT}) par le modèle TrOCA (Tracer combining Oxygen, inorganic Carbon, and total Alkalinity), a lieu à partir de quatre paramètres: la température potentielle (θ), l'oxygène dissous (O_2), le carbone inorganique total (C_T) et l'alcalinité totale (A_T). La description détaillée et la mise en œuvre de ce modèle a été établie par Touratier and Goyet (2004) et Touratier *et al.* (2011).

Le traceur semi-conservatif TrOCA peut être défini comme suit :

$$TrOCA = O_2 + a(C_T - 0{,}5A_T) \quad (26)$$

Le traceur TrOCA est utile pour caractériser les différentes masses d'eau, hors il diverge du comportement conservatif pour les eaux chargées de C_{ANT}. Ainsi le traceur conservatif TrOCA°, qui n'inclue pas de contribution anthropique, est définie comme suit :

$$TrOCA^0 = O_2^0 + a(C_T^0 - 0{,}5A_T^0) \quad (27)$$

où O_2^0, C_T^0 et A_T^0 sont les concentrations préindustrielles d'O_2, de C_T et d'A_T.

TrOCA° a été initialement calculé en fonction de θ uniquement (Touratier et Goyet, 2004), mais Touratier et al. (2007) ont proposé une équation améliorée déduite des traceurs ^{14}C et du CFC-11, en se basant sur θ et A_T (Eq 28).

$$TrOCA^0 = e^{(7{,}511-(1{,}087\times10^{-2})\theta-(7{,}81\times10^5)/(A_T)^2)} \quad (28)$$

La concentration de C_{ANT} est alors estimée suivant l'équation (30) en tenant en compte de deux considérations principales. En premier lieu l'A_T n'est pas influencée par l'augmentation du CO_2 anthropique (Chen and Millero, 1979; Goyet *et al.*, 1999), alors $A_T^0 = A_T$. En deuxième lieu, le réservoir atmosphérique en CO_2 est 500 fois plus sensible à la pression anthropique que le réservoir en O_2. Ceci en considérant que le rapport d'échange O_2/CO_2 de la combustion des combustibles fossiles est égal à -1,4 (Keeling and Shertz, 1992) et que les contributions relatives d'O_2 et du CO_2 dans l'atmosphère sont respectivement de ~ 21 et 0,04%. Il est donc supposé que la distribution d'oxygène n'est pas affectée significativement par les activités humaines, d'où $O_2^0 \approx O_2$.

$$C_{ANT} = C_T - C_T^0 = \frac{TrOCA - TrOCA^0}{a} \quad (29)$$

La valeur a = 1,279 a été déterminée avec un minimum d'erreur standard et par suite l'ensemble optimal des autres paramètres est la suivante (Touratier *et al.*, 2011):

$$C_{ANT} = \frac{O_2 + 1{,}279[C_T - 0{,}5A_T] - e^{(7{,}511-(1{,}087\times10^{-2})\theta-(7{,}81\times10^5)/(A_T)^2)}}{1{,}279} \quad (30)$$

Chapitre II : *Mare Nostrum*

'Lorsqu'on se sait pas vers quel port on navigue, aucun vent n'est le bon'

Sénèque

I- Caractéristiques géographiques et hydrodynamiques

La Mer Méditerranée appelé souvent en Latin « *Mare Nostrum* », est une mer semi-fermée entourée de grandes masses continentales : l'Europe au Nord, l'Asie à l'Est et l'Afrique au Sud. Elle s'étend sur environ 4000 km, de 6 °W à 36 °E en longitude et de 30 °N à 46 °N en latitude. Vu de sa position géographique, elle est considérée comme une mer semi-fermée se connectant uniquement à l'océan Atlantique par le détroit de Gibraltar. Elle est aussi reliée à la Mer Noire par les détroits de Bosphore et de Dardanelles, et à la Mer Rouge par le canal artificiel de Suez.

La Mer Méditerranée est composée de deux principaux bassins, le bassin Occidental et le bassin Oriental, connectés par le détroit de Sicile. Chaque bassin est subdivisé en plusieurs sous-bassins caractérisés par une topographie robuste, particulièrement dans la partie orientale où la profondeur atteint 4982 mètres. Le bassin Occidental est relativement plat, et le bassin Oriental est caractérisé par une alternance de dépressions profondes, vallées sous-marines, pentes raides, et plus de 700 îles et îlots répartis le long de l'archipel Égée à l'Est de la Grèce (Bergamasco and Malanotte-Rizzoli, 2010).

Le climat continental est particulièrement sec, même en hiver, et provoque une évaporation intense tout au long de l'année. Le bilan hydrique est donc fortement négatif et se traduit par une perte de 0,5 à 1 mètre d'eau par an sur l'ensemble du bassin méditerranéen (Béthoux, 1979). Les bilans en eau et en sel de la Méditerranée sont globalement équilibrés par les échanges avec l'océan Atlantique au détroit de Gibraltar où l'eau atlantique peu salée (S ~36) pénètre en surface en Méditerranée tandis qu'une eau Méditerranéenne plus salée (S > 38) s'écoule en profondeur vers l'Atlantique (Lacombe and Tchernia, 1972).

Un caractère météorologique distinctif en Mer Méditerranée, est la présence d'évènements de vents et de précipitations à petite échelle mais très violents. Les montagnes sont le principal contributeur au ruissellement d'eaux douces vers la Mer Méditerranée (Beniston, 2003; de Jong *et al.*, 2009). Des masses d'eau considérables, chargées en nutriments et riches en alcalinité totale, sont alors déversées à la mer par des fleuves côtiers, surtout dans la partie Nord-Ouest de la Méditerranée (Llasat *et al.*, 2013).

La Mer Méditerranée est donc un bassin de concentration qui transforme l'eau atlantique entrante en une eau méditerranéenne sortante. Ce fonctionnement est induit par la présence d'une circulation dans le plan vertical contrainte par les différences de salinité et de température. Cette circulation thermohaline anti-estuaire est favorisée par la présence d'un gradient horizontal de pression, au niveau du détroit de Gibraltar, dirigé vers la Mer Méditerranée dans la couche superficielle et vers l'océan Atlantique dans la couche profonde, ainsi que par la différence du niveau moyen des eaux entre les deux compartiments marins plus bas en Méditerranée qu'en Atlantique (Lacombe and Tchernia, 1972).

II- Régime du vent

La météorologie de la mer Méditerranée est largement décrite dans 'Her Majesty's Stationery Office' (HMSO, 1962). Cette zone presque entièrement entourée des chaînes montagneuses, est caractérisée par plusieurs sous-bassins où le flux d'air interagit souvent avec l'orographie environnante (Figure 3).

Dans la mer d'Alboran, le Sud-Ouest *Vendaval* se produit principalement d'octobre à novembre et de février à mars, alors que le *Levanter* provenant de l'Est souffle pendant toutes les saisons. Dans la Méditerranée centrale, le Nord-Ouest mistral froid et sec (Jansá, 1987; Jiang *et al.*, 2003; Guenard *et al.*, 2005) souffle dans le golfe du Lion, et peut atteindre parfois les côtes africaines. Quand il entre dans la mer Tyrrhénienne, le mistral prend le nom de *Maestrale*, prenant une direction plus marquée vers le Sud. La Méditerranée centrale est balayée, surtout en hiver, par le Sud-Ouest *Libeccio* et par le *Sirocco* humide et chaud, qui en l'automne souffle du Sud vers l'Est, induisant des tempêtes bien connues dans la Mer Adriatique, qui inondent la lagune de Venise. Le *Bora* est un vent Nord fort et froid affectant l'ensemble de la mer Adriatique (Jurčec, 1981; Smith, 1987; Pandžić and Likso, 2005). Les vents de type *Bora* existent dans d'autres régions, comme dans le Nord de la mer Egée. Dans le bassin Levantin les vents dominants sont le *Chlouk* provenant de l'Afrique au printemps (Abboud-ABi Saab, 1985), et les *Etesians* qui sont particulièrement forts en été (Ziv *et al.*, 2004).

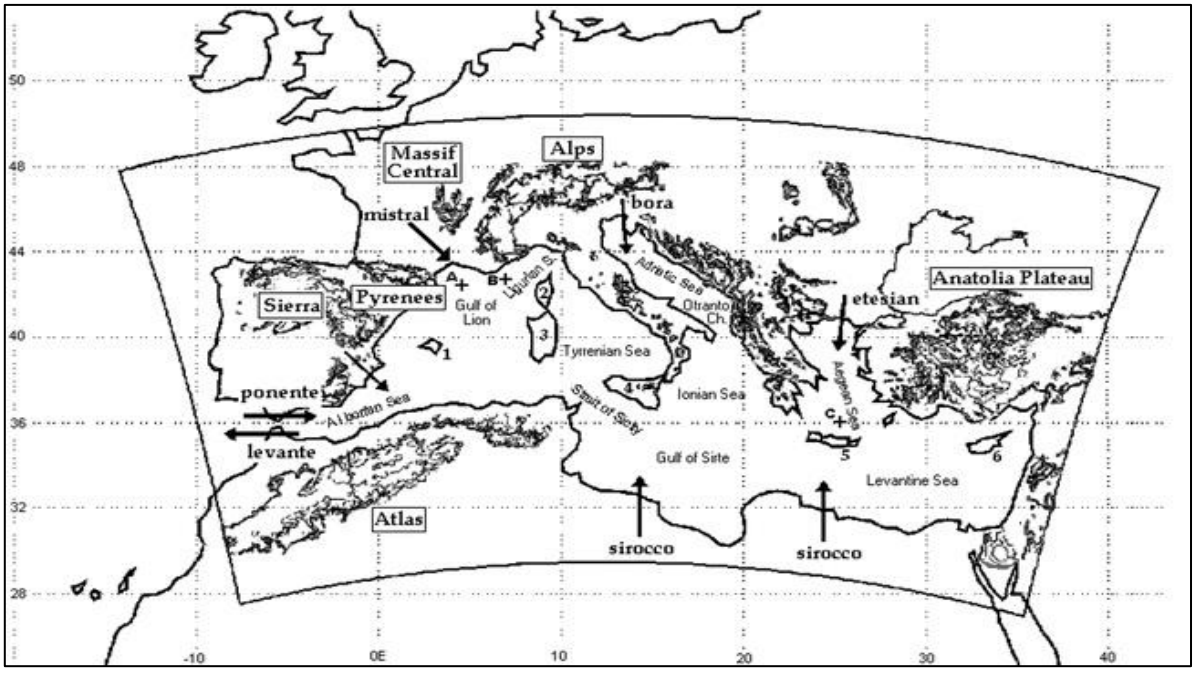

Figure 3. Carte de la région méditerranéenne montrant les vents dominants locaux qui sont indiqués par des flèches et les chaînes de montagnes importantes qui sont indiquées par des cases [d'après Accadia *et al.* (2007)][2]

[2] Accadia, C., Zecchetto, S., Lavagnini, A., Speranza, A., 2007. Comparison of 10-m Wind Forecasts from a Regional Area Model and QuikSCAT Scatterometer Wind Observations over the Mediterranean Sea. Mon. Weather Rev. 135 (5), 1945-1960. 10.1175/mwr3370.1. ©American Meteorological Society. Used with permission (Annexes).

III- Circulation globale

III.1- Circulation de l'eau Atlantique

La circulation générale de surface en Mer Méditerranée est fortement contrainte par le vent (Pinardi and Navarra, 1993) et la bathymétrie complexe (Testor *et al.*, 2005b). Par un circuit cyclonique de courants plus ou moins stables, l'eau Atlantique (AW) pénètre en mer d'Alboran par le détroit de Gibraltar en formant des méandres et de vastes tourbillons anticycloniques (Millot, 1999; Millot and Taupier-Letage, 2005).

Dans le sous-bassin d'Alboran, juste après son passage par le détroit de Gibraltar, l'AW forme un ou deux tourbillons anticycloniques suivant la saison: le Western Alboran Eddy (WAE) et le Eastern Alboran Eddy (EAE ; Vargas-Yáñez *et al.*, 2002). Puis, l'AW parcourt le Sud du bassin Occidental et le courant de bord Algérien (Algerian Current, AC) est déstabilisé par la pente très raide du talus continental. A cet endroit, la formation de tourbillons algériens s'accumulent dans deux gyres cycloniques profonds : le Western Algerian Gyre (WAG) et le Eastern Algerian Gyre (EAG ; Testor *et al.*, 2005b).

L'AW traverse le canal de Sardaigne et se sépare en deux branches au niveau du canal de Sicile. La première va dans le sous-bassin Tyrrhénien et poursuit son parcours le long de la côte italienne. Puis l'AW passe le détroit de Corse et entre dans le sous-bassin Liguro-Provençal pour former le Courant Nord (ou courant Liguro-Provençal) et longe les côtes Françaises et Espagnoles. Au niveau du canal de Sicile, la deuxième partie de l'AW entre dans le bassin Oriental, rejoint la côte Libyenne, en une ou plusieurs branches: l'Atlantic Tunisian Current (ATC), et l'Atlantic Ionian Stream (AIS ; Béranger *et al.*, 2004). Dans le sous-bassin Levantin, le courant de bord Libyo-Egyptian Current (LEC ; Hamad *et al.*, 2005; Hamad *et al.*, 2006; Gerin *et al.*, 2009), forme des tourbillons pouvant s'accumuler dans des zones préférentielles affectées par la topographie. Les eaux qui arrivent à l'extrémité du bassin oriental à la fin de l'été deviennent très chaudes et très salées (T = 26°C, S = 39,5) sous l'effet du climat estival.

Ensuite, l'AW longe les côtes du Proche-Orient puis les côtes Turques où elle forme le Courant d'Asie Mineure [Asia Minor Current (AMC)]. Une partie de l'AMC passe au Sud de la Crète et une autre partie entre dans le sous-bassin Egée et en fait le tour le long des côtes de manière cyclonique. Une branche de l'AW passe le détroit d'Otrante et circule cycloniquement le long des côtes du sous-bassin Adriatique, fortement marquée dans le Sud du sous-bassin par la présence du gyre Sud-Adriatique [South Adriatic Gyre (SAdG)]. L'AW retourne ensuite vers le canal de Sicile avec un trajet cyclonique le long des côtes Nord du sous-bassin Ionien (Figure 4).

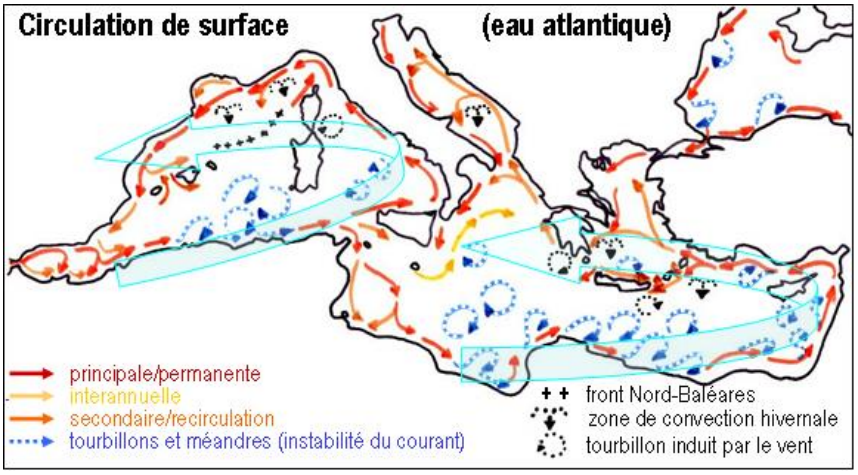

Figure 4. Circulation générale de la Mer Méditerranée [d'après Millot and Taupier-Letage (2005)][3]

III.2- Circulation intermédiaire et thermohaline

En hiver, les invasions irrégulières des masses d'air continentales et sèches au-dessus du bassin levantin sont fréquentes. Elles engendrent un refroidissement intense des eaux de surface et une augmentation de la salinité, qui est à l'origine de mélanges verticaux importants. Ainsi dans le Nord du sous-bassin Levantin, et plus précisément dans la zone du gyre de Rhodes, est formée l'eau Levantine intermédiaire [Levantine Intermediate Water (LIW)], à une profondeur moyenne de 200-300 m (Lascaratos *et al.*, 1993; Robinson *et al.*, 2001). La LIW est identifiable dans l'ensemble de la couche intermédiaire de la Méditerranée par un maximum de salinité entre 200 et 600 m.

Une partie de la LIW sort du sous-bassin Levantin et rejoint le canal de Sicile en traversant le sous-bassin Ionien de manière cyclonique le long du talus continental. Une fois passée dans le bassin occidental, la LIW circule majoritairement le long de la côte Est du sous-bassin Tyrrhénien. Une faible partie passe le détroit de Corse alors que la majorité revient vers le canal de Sardaigne. Une autre partie forme un gyre cyclonique entre les canaux de Sicile et de Sardaigne (Sorgente *et al.*, 2011) duquel s'échappent des tourbillons anticycloniques (Béranger *et al.*, 2004). Dans le sous-bassin Algéro-Provençal, une partie de la LIW est advectée vers le Nord le long des côtes de la Sardaigne et de la Corse. Une partie se sépare sous la forme de tourbillons (Sardinian Eddies, SE ; Testor *et al.*, 2005a), qui contribuent au transport de la LIW vers l'Ouest et Gibraltar par interaction avec les tourbillons algériens de surface (Millot and Taupier-Letage, 2005). Une autre partie de la LIW a un trajet moins direct et participe à la formation d'autres masses d'eau intermédiaires et profondes méditerranéennes. En passant les détroits de l'Arc Crétois, la LIW participe à la formation de l'eau crétoise intermédiaire [Cretan Intermediate Water (CIW)] ou profonde [Cretan Deep Water (CDW) ; Theocharis *et al.*, 1999]. Ces eaux crétoises ressortent parfois du sous-bassin

[3] Springer Berlin Heidelberg, 5K, 2005, 40, Circulation in the Mediterranean Sea, Claude, Millot, figure 2, Copyright (2015), License number 3640260257391 ; with kind permission from Springer Science and Business Media (Annexes)

Egée à travers les détroits de l'Arc Crétois et se retrouvent dans les sous-bassins Ionien et Levantin.

En passant le détroit d'Otrante vers le sous-bassin Adriatique, la LIW participe à la formation de l'eau profonde Sud-Adriatique [South Adriatic Deep Water (SAdDW)] dans le gyre Sud-Adriatique. L'eau profonde Nord-Adriatique [North Adriatic Deep Water (NAdDW)] est formée au Nord du sous-bassin Adriatique et cascade vers le Sud (Artegiani *et al.*, 1997). La NAdDW et la SAdDW se mélangent (Manca *et al.*, 2006), passent le détroit d'Otrante ou elles forment l'eau adriatique profonde [Adriatic Deep Water (ADW)], qui plonge vers le fond du sous-bassin Ionien. L'eau profonde Est-méditerranéenne [Eastern Mediterranean Deep Water (EMDW)] est alors principalement composée d'ADW, même si selon les periodes la CDW peut entrer dans sa composition. La partie de la LIW advectée vers le Nord du bassin Algéro-Provençal participe à la formation de l'eau profonde Ouest-méditerranéenne [Western Mediterranean Deep Water (WMDW)], dans le Golfe du Lion principalement. Cette région est dominée en hiver par les vents continentaux froids et secs (mistral et tramontane) qui entraînent le mélange de l'eau superficielle d'origine atlantique et l'eau levantine intermédiaire. La WMDW se propage au fond du sous-bassin Algéro-Provençal, vers l'Ouest et le détroit de Gibraltar ainsi que vers le sous-bassin Tyrrhénien par le fond du canal de Sardaigne.

Enfin, dans le sous-bassin Tyrrhénien est formée l'eau profonde tyrrhénienne [Tyrrhenian Deep Water (TDW)], soit localement à l'Est de Bonifacio (Fuda *et al.*, 2002), soit par interactions entre la LIW et la WMDW (Millot, 1999). La TDW sort du bassin Tyrrhénien par le canal de Sardaigne, au-dessus de la WMDW, et se propage également vers le détroit de Gibraltar (Millot *et al.*, 2006). En sortie à Gibraltar, l'eau méditerranéenne sortante [Mediterranean Outflow Water (MOW)] est principalement composée de LIW, de WMDW et de TDW (Millot *et al.*, 2006; Millot, 2009).

IV- Etat des lieux vis-à-vis du système des carbonates

IV.1- Bases de données

Les bases de données disponibles en Mer Méditerranée ont été présentées par Álvarez (2012) durant l'atelier du CIESM Nº 43 (CIESM, 2012). Dans ce qui suit, on va résumer les principales bases de données déjà citées, et y ajouter aussi les plus récentes.

IV.1.1- Observations jusqu'au IX^{ème} siècle

La base de donnée la plus connue qui rassemble les variables physiques et biogéochimiques de la Mer Méditerranée est le MEDAR-MEDATLAS II (Medar-Group, 2002) qui contient des données d'A_T, quelques données de pH, pratiquement pas de données de C_T et aucune pour la pCO_2^{sw} (Figure 5). D'autres bases de données accessibles au public comme CDIAC

(http://cdiac.ornl.gov/oceans/) contiennent des données de pCO_2^{sw} de surface de l'expédition INDOMED 3-4 (décembre 1977 par R.F.Weiss) et de la station 404 de l'expédition GEOSECS (1977-1978), échantillonnée dans le bassin Oriental de la Mer Méditerranée (Weiss *et al.*, 1983).

D'autres publications réfèrent aux données de CO_2 mais dont les résultats ne figurent pas dans aucune base de données (Álvarez, 2012):

- Copin-Montégut (1993): expédition Almofront (avril-mai 1991), le pH et l'A_T dans la mer d'Alboran.
- Millero *et al.* (1979) : expédition en septembre 1976 dans la mer d'Alboran et au Sud des Îles Baléares. Le pH et l'A_T ont été mesurés.
- Brunet *et al.* (1984): Mediprod IV, du 15 octobre au 17 novembre 1981. Mesures de pH A_T.
- Pérez *et al.* (1986) : campagne dans le mer Catalano-Baléare en juillet 1983. Mesures de pH et A_T.
- Delgado and Estrada (1994): plusieurs expéditions dans la mer Catalano-Baléare (1986, 1987, 1989). Mesures de pH et A_T.
- Luchetta *et al.* (2010b): données de pH_{NBS} et A_T mesurées au Nord de la mer Adriatique en 1983.

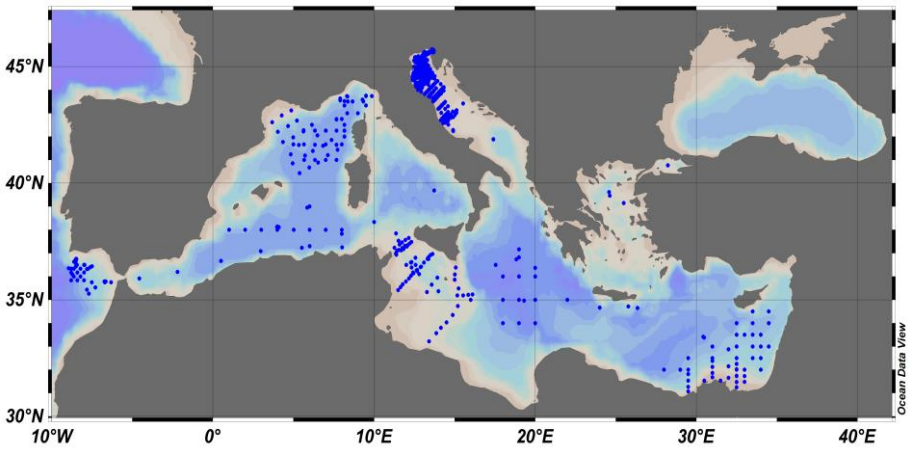

Figure 5. Mesures simultanées d'A_T et de pH dans les eaux de surface en Mer Méditerranée disponibles dans la base de donnée Medar-Medatalas II (Medar-Group, 2002)

IV.1.2- Observations récentes

- **Séries temporelles et bouées**

  - La mer Ligure: La série temporelle la plus connue au sein de la Mer Méditerranée est le site DYFAMED (Dynamics of Atmospheric Fluxes in the MEDiterranean sea) située dans la mer de Ligure, active depuis 1993. Les mesures de C_T et A_T ont été analysés seulement pour certaines périodes (entre 1998 et 2000; entre juillet 2003 et

décembre 2004; entre juin et décembre 2005). Ces résultats sont présentés dans plusieurs articles (Hood and Merlivat, 2001; Bégovic and Copin-Montégut, 2002; Copin-Montégut and Bégovic, 2002; Copin-Montégut *et al.*, 2004). En ce qui concerne la pCO_2^{sw}, plusieurs bouées CARIOCA ont été déployées entre 1995 et 1997 (Hood and Merlivat, 2001) et durant 1999 (Copin-Montégut *et al.*, 2004), pour étudier les variations saisonnières de pCO_2^{sw}. Actuellement deux bouées CARIOCA munies d'un capteur pour la mesure de la pCO_2^{sw} sont déployées dans le site BOUSSOLE (BOUée pour l'acquiSition d'une Série Optique à Long termE**)**.

- Îles Mèdes: à partir de 2008 un suivi continu pour de faibles profondeurs (80 m de profondeur) est en cours, où des échantillons d'A_T et de pH sont mesurés à quatre niveaux. A partir de 2009 une bouée avec un capteur SAMI-pH a été aussi déployée.
- Dans le golfe de Trieste la bouée Vida rapporté des données de pCO_2^{sw} à partir d'un capteur SAMI-CO_2 pendant plusieurs périodes en 2007 et 2008 (Turk *et al.*, 2010). Aussi à partir de 2011 des mesures saisonnières sont effectués pour le pH et l'A_T et d'autres variables biogéochimiques à plusieurs stations (Luchetta *et al.*, 2010a). En outre, depuis janvier 2008 le pH et l'A_T sont analysés dans toute la colonne d'eau du site côtier Paloma (Luchetta *et al.*, 2010b).
- Dans le Sud de l'Adriatique, cinq échantillonnages saisonnières (de septembre 2007 à octobre 2008) pour mesures l'A_T et le pH ont été effectués à la station AM1 (1250 m, 41º50'N et 17º45'E (Luchetta *et al.*, 2010b).
- Dans le projet Eurosites (www.eurosites.info) plusieurs sites d'observations mesurent à partir de bouées les paramètres de surface liée au CO_2: la bouée E2-M3A (Sud de la mer Adriatique) mesure la pCO_2^{sw} avec le capteur PRO-OCEANUS depuis octobre 2010.

Les différentes séries temporelles et bouées citées ci-dessus sont représentées dans la figure 6.

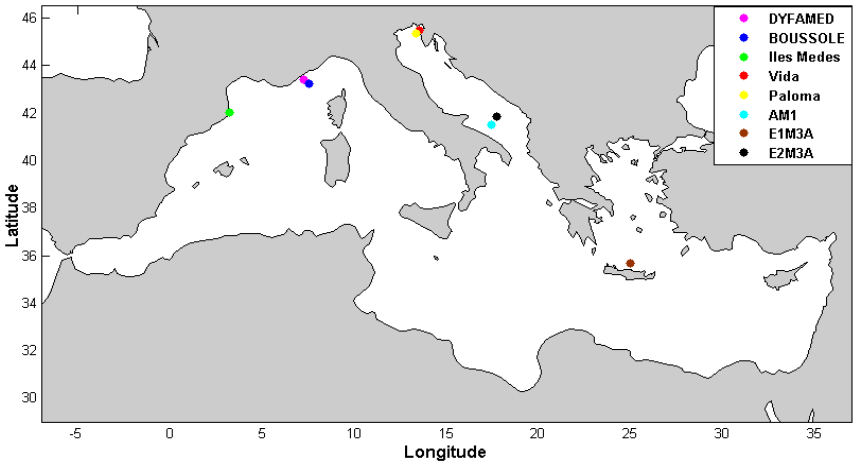

Figure 6. Séries temporelles et bouées dans la Mer Méditerranée

- **Campagnes en mer**

La pCO_2^{sw} a été mesurée en continu entre le bassin Ouest jusqu'au bassin Ionien seulement durant l'expédition PROSOPE en septembre-octobre 1999 (Claustre *et al.*, 2002). Aussi sur toute la profondeur de la colonne d'eau des mesures discrètes de pH et A_T ont été effectués. Les données de CO_2 peuvent être trouvées sur la base de données de Pangaea (Bégovic and Copin, 2013; Claustre and Bégovic, 2013).

Très récemment en mai 2013, la mission MedSeA a traversé toute la mer Méditerranée partant de l'Atlantique jusqu'au bassin Levantin. Des mesures discrètes de C_T et d'A_T ont été effectuées sur toute la colonne d'eau au niveau de 22 stations. Aussi la pCO_2^{sw} a été mesurée en continu avec le capteur SAMI-CO_2 sur une section d'environ 3820 km. Les résultats sont aussi disponibles sur la base de données de Pangaea (Goyet *et al.*, 2015a ; b).

Dans la base de données de CDIAC se trouvent les expéditions de la RV Meteor 51/2 (octobre-novembre 2001 ; Schneider and Roether, 2007) et RV Meteor 83/4 (avril 2011 ; Tanhua *et al.*, 2012) qui traversent la Mer Méditerranée d'Ouest en Est (Figure 7). Les paramètres mesurés sont l'A_T et le C_T pour la M51/2 et le pH, l'A_T et le C_T pour la M83/4. Les résultats de ces missions sont reportés dans les papiers de Schneider *et al.* (2007 ; 2010), Tanhua *et al.* (2013b) et Álvarez *et al.* (2014). Se trouvent aussi des données de pCO_2^{sw} dans la mer Égée en février 2006 (Krasakopoulou *et al.*, 2006), ainsi que des mesures d'A_T et de C_T au niveau du détroit d'Ortanto (Otranto-5, février 1995 ; Krasakopoulou and Souvermezoglou, 2012). Toujours sur CDIAC se trouvent des mesures d'A_T et de C_T pris au bord de la VOS Pacific Celebes entre 2007 et 2009 (Hydes *et al.*, 2012).

SESAME-Cast est aussi une base de données pertinente pour les variables liées au CO_2 dans la Méditerranée (http://isramar.ocean.org.il/SESAMEMETA/db_login.aspx). On note SESAME IT-7_BOT et SESAME IT-4_BOT pour des mesures d'A_T et C_T, respectivement entre le 8 et 14 septembre 2008 et le 15-26 février 2008 (Luchetta *et al.* 2010b), et S-IT4_BOT pour des mesures d'A_T, C_T et de pH de 18 mars au 5 avril 2008.

D'autres expéditions ont échantillonné le système des carbonates en Mer Méditerranée, mais dont les données ne sont pas disponibles publiquement :

- Borges *et al.* (2006) a rapporté des mesures pour la pCO_2^{sw}, C_T et A_T dans la Baie des Anges, près de Villefranche.
- La série temporelle RADMED (series tempoRAles de Datos oceanográficos del MEDiterráneo) de l'IEO (Instituto Español de Oceanografía) sonde trois fois par an, la côte méditerranéenne Espagnole pour mesurer l'A_T et le pH dans la colonne d'eau (López-Jurado *et al.*, 2015).
- Dans la baie de Palma, la pCO_2^{sw}, le pH et l'A_T ont été mesurés durant l'expédition EUBAL en mars et juin 2002 (Gazeau *et al.*, 2005).
- THRESHOLDS en mai 2007 sur un transect partant de la Sardaigne jusqu'à la mer Noire. Mesures en continu de la pCO_2^{sw} (Calleja *et al.*, 2013).

- TRANSMED entre mai et juin 2007, sur le transect Ouest-Est de la Mer Méditerranée. Dix stations ont été échantillonnées pour le pH et l'A_T (Rivaro *et al.*, 2010).
- Au Sud de la mer Tyrrhénienne, cinq expéditions allant de la côte vers la station de VTM, ont été effectués pour la mesure du pH et de l'A_T et cela pour les mois de novembre 2006, février, avril et juillet 2007 et février 2008 (Rivaro *et al.*, 2010).
- BOUM du 16 juin au 20 juillet 2008, sur un transect partant de Marseille jusqu'au bassin Levantin. Mesures extensives de C_T et d'A_T sur toute la colonne d'eau (Touratier *et al.*, 2012).

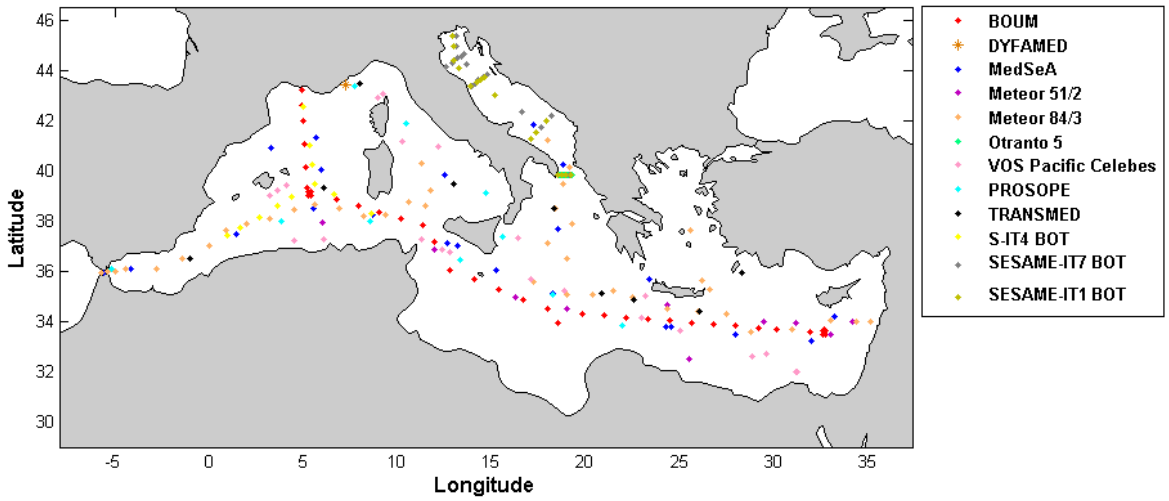

Figure 7. Stations des expéditions pour mesurer le système des carbonates en Mer Méditerranée

IV.2- Estimations du système des carbonates

En Mer Méditerranée, les mesures des paramètres du système de carbonate se concentrent généralement sur des échantillons discrets d'A_T et de C_T, ainsi que le pH (Schneider *et al.*, 2007; Krasakopoulou *et al.*, 2009; Rivaro *et al.*, 2010; Krasakopoulou *et al.*, 2011; Touratier *et al.*, 2012; De Carlo *et al.*, 2013; Álvarez *et al.*, 2014). En ce qui concernent les mesures directes de pCO_2, elles sont encore mal documentées, et sont essentiellement confinées dans le bassin Occidental (Bégovic and Copin-Montégut, 2002; Copin-Montégut and Bégovic, 2002; Copin-Montégut *et al.*, 2004). Jusqu'à présent, l'estimation du système des carbonates dans les eaux de surface sur l'échelle de toute la Mer Méditerranée est limitée à quelques études. Aussi le recours aux données des images satellites pour estimer les paramètres du système des carbonates est quasi-inexistant (D'Ortenzio *et al.*, 2008; Taillandier *et al.*, 2012).

Malgré l'importance de la Mer Méditerranée vis-à-vis du cycle du carbone océanique, celle-ci n'est pas toujours représentée dans la carte climatologique de pCO_2^{sw} pour l'océan global (Figure 2) établie par Takahashi *et al.* (2014a). Il est important aussi de noter que malgré son importance mondiale, la pCO_2^{sw} n'était pas mentionnée parmi les recommandations sur les

principaux paramètres des mesures du système des carbonates, qui seront implémentées au sein du programme Med-SHIP (CIESM, 2012).

De ce fait l'estimation de le pCO_2^{sw} sur l'échelle de toute la Mer Méditerranée a eu lieu uniquement à travers des modeles numeriques (D'Ortenzio *et al.*, 2008 ; Louanchi *et al.*, 2009 ; Taillandier *et al.*, 2012). Dans ces modèles, la pCO_2^{sw} a été estimée par des mesures discrètes d'A_T et pH ou A_T et C_T et cela en se basant sur la base de données du Medar/Medatlas II entre 1960 et 2004 (Medar-Group, 2002).

Ainsi, D'Ortenzio *et al.* (2008) ont proposé une simulation basée sur une matrice physico-bio-chimique unidimensionnelle (1D) couplée avec les images satellitaires. Ils simulent ainsi les dynamiques physiques et biogéochimiques dans les eaux de surface sur l'ensemble de la Mer Méditerranée au cours des années 1998-2004.

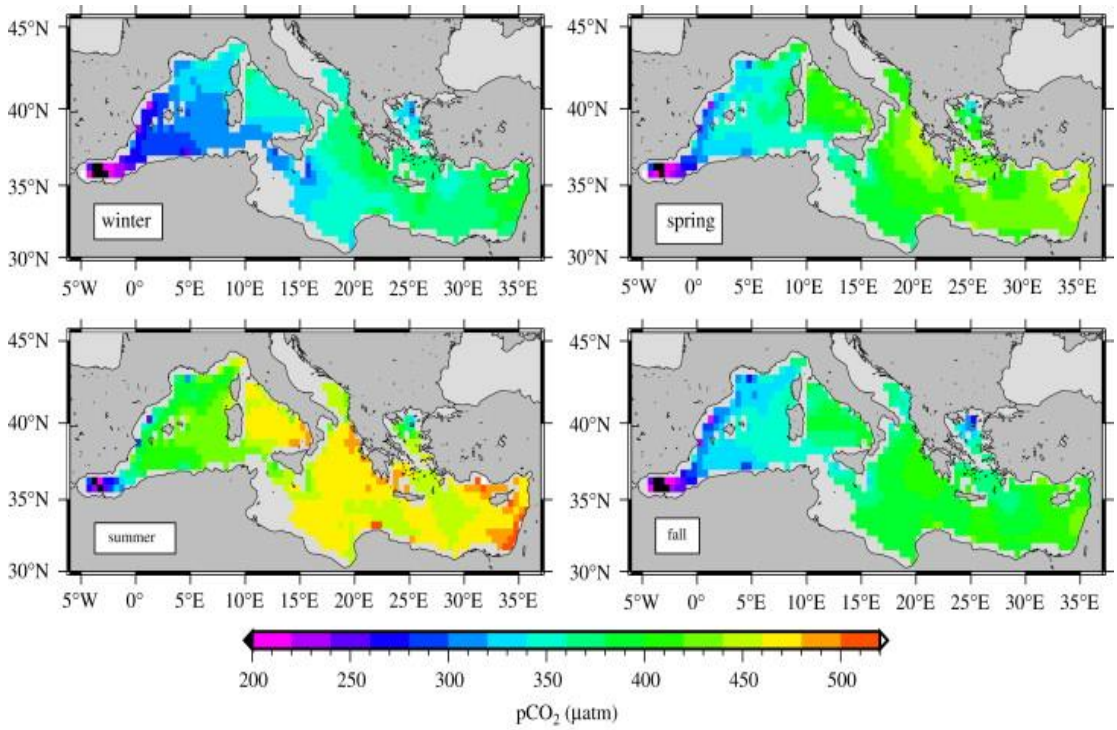

Figure 8. Variation saisonnière de la pCO_2 dans les eaux de surface simulée sur une moyenne de 7 ans [d'après D'Ortenzio et al. (2008)][4]

La pCO_2^{sw} simulée sur une moyenne saisonnière de 7 ans (1998-2004), montre un gradient permanent Ouest-Est. Les maximas de pCO_2^{sw} (près de 500 µatm) sont au niveau de la mer Ionienne et Levantine durant l'été, et les minimas sont dans la région de la mer d'Alboran (environ 250 µatm en hiver et 300 µatm en été). Les valeurs extrêmes et l'amplitude du cycle saisonnier diffèrent entre les deux sous-bassins. La pCO_2^{sw} varie entre environ 350 et 500 µatm dans la Méditerranée Orientale, qui est par conséquent au-dessus de l'équilibre par rapport à l'atmosphère. Alors que des valeurs beaucoup plus faibles se trouvent dans la

[4] Reprinted from Deep Sea Research Part I: Oceanographic Research Papers, 55, Fabrizio D'Ortenzio, David Antoine, Salvatore Marullo, Satellite driven modeling of the upper ocean mixed layer and air–sea CO_2 flux in the Mediterranean Sea, Page 421, Copyright (2015), License number 3640260502630, with permission from Elsevier (Annexes)

Méditerranée Occidentale (250 µatm), en particulier en hiver (Figure 8). Aussi Taillandier *et al.* (2012) ont présenté une comparaison de la variation saisonnière de la pCO_2^{sw} dans la couche de mélange entre les périodes du CZCS (Coastal Zone Color Scanner) en 1978 et SeaWifs (Sea-viewing Wide Field-of-view Sensor) en 2001.

En ce qui concerne le flux de CO_2 à l'interface air-mer, il n'a été alors calculé que par des modèles numériques sans avoir recours à des mesures directes de pCO_2^{sw}. En outre, aucune estimation récente des flux de CO_2 n'a eu lieu. D'Ortenzio *et al.* (2008) a montré que la Mer Méditerranée est proche de l'équilibre avec l'atmosphère et que les processus biologiques jouent un rôle important dans l'évolution saisonnière de la pCO_2^{sw} dans les bassins Ouest et Est. Louanchi *et al.* (2009) ont utilisé une approche basée sur un ensemble de données disponibles de température, salinité, oxygène, nutriments, Chlorophylle_a, couplée à un modèle en boite de la couche de mélange. Cette approche a permis de reconstituer dans la couche de mélange le C_T, l'A_T, et la fCO_2 entre les années 1960-1990. Ils ont conclu que la Mer Méditerranée a varié d'une source de 0,62 $TgC.an^{-1}$ à un puits net de -21,98 $TgC.an^{-1}$ pour le CO_2 atmosphérique, respectivement durant les années 1960 et 1990.

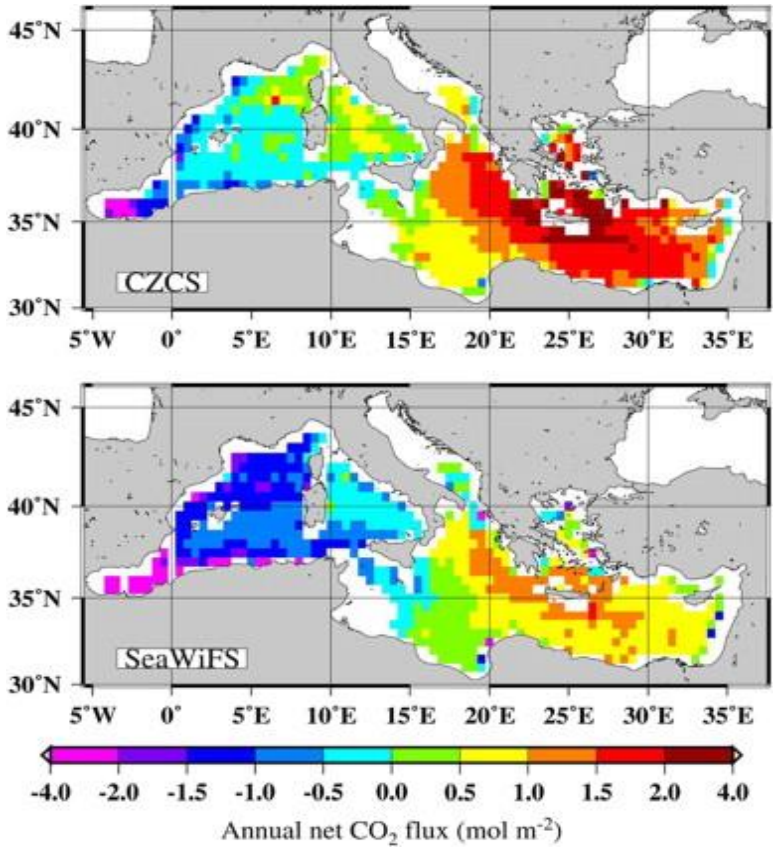

Figure 9. Comparaison du flux annuel net de CO_2 simulés entre les années 1980 (CZCS) et les années 2000 (SeaWiFS) [d'après Taillandier *et al.* (2012)][5]

[5] Reprinted from Deep Sea Research Part I: Oceanographic Research Papers, 55, Vincent Taillandier, Fabrizio D'Ortenzio, David Antoine, Carbon fluxes in the mixed layer of the Mediterranean Sea in the 1980s and the 2000s, Page 79, Copyright (2015), License number 3640260761132, with permission from Elsevier (Annexes)

Taillandier *et al.* (2012) ont présenté une analyse des flux de CO_2 dans la couche de mélange pour deux périodes séparées par un intervalle de 14 ans (1979 et 2001). L'analyse utilise une matrice physique-biologique-chimique à 1D couvrant tous les domaines où la profondeur est supérieure à 300 m. Les résultats indiquent que la Mer Méditerranée était biologiquement plus productive (d'environ 16 $gC.m^2.y^{-1}$) pendant les années 2000, avec une augmentation de l'exportation du carbone vers les couches profondes d'environ 7 $gC.m^2.y^{-1}$ par rapport aux années 1980 (Figure 9).

Pour l'A_T, les études ultérieures ont proposé d'estimer ce paramètre à partir de la salinité et/ou de la température par des régressions empiriques. Ces relations couvrent quelques campagnes en mer (Schneider *et al.*, 2007; Touratier and Goyet, 2009) ou des zones locales (Copin-Montégut, 1993; Santana-Casiano *et al.*, 2002). Récemment la reconstruction spatiale et temporelle de l'A_T a été réalisée grâce à un modèle 3D de transport biogéochimique (Cossarini *et al.*, 2015). Dans les eaux de surface, l'A_T montre un gradient prononcé de l'Ouest vers l'Est, avec des concentrations allant de 2400 $\mu mol.kg^{-1}$ près du détroit de Gibraltar à 2700 $\mu mol.kg^{-1}$ au niveau des mers marginales Orientales comme l'Adriatique et l'Egée. L'évaporation intense et les précipitations, contribuent à l'augmentation de l'alcalinité de surface, avec un taux moyen qui varie de 0,5 à 1 $\mu mol.m^{-2}.d^{-1}$ et de 1 à 2,5 $\mu mol.m^{-2}.d^{-1}$, respectivement dans les bassins Ouest et Est (Cossarini *et al.*, 2015).

A notre connaissance, l'estimation du C_T dans les eaux de surface n'a pas encore été effectuée dans la Mer Méditerranée. Les modèles empiriques existants ont été réalisés uniquement au niveau de la colonne d'eau et en dessous de la couche de mélange (Copin-Montégut and Bégovic, 2002; Touratier and Goyet, 2011; Lovato and Vichi, 2015). Ainsi, Lovato and Vichi (2015) ont récemment établis à partir des données de la campagne Meteor 84/3 un modèle de régression optimal pour estimer le C_T à partir de la température potentielle, la salinité, la pression et la concentration en nitrates. Ils trouvent que dans les couches proches de la surface, les concentrations de C_T variaient entre 2110 et 2240 $\mu mol.kg^{-1}$ selon un gradient Ouest-Est qui disparaît près de 250 m de profondeur. Les bassins Occidental et Oriental présentent des concentrations plus élevées à des profondeurs intermédiaires (500-1000m) avec des valeurs moyennes, respectivement de l'ordre de 2320 et 2315 $\mu mol.kg^{-1}$.

Les estimations du CO_2 anthropique (C_{ANT}) et de l'acidification des eaux en Mer Méditerranée, ont été menées principalement par Touratier and Goyet (2009), Touratier and Goyet (2011), Schneider *et al.* (2010) et Touratier *et al.* (2012). Les résultats montrent que le C_{ANT} varie entre 37 et 70 $\mu mol.kg^{-1}$, et que toutes les masses d'eaux méditerranéennes (même les plus profondes) semblent être fortement contaminées par le C_{ANT}. Ceci indique que le CO_2 atmosphérique, est efficacement transféré vers les couches les plus profondes des eaux méditerranéennes (Touratier *et al.*, 2012). Ainsi, l'acidification des eaux est plus prononcée dans la Mer Méditerranée que dans l'océan Atlantique et Pacifique (Lee *et al.*, 2011), avec une variation comprise entre 0,05 et 0,14 unité de pH depuis l'ère préindustrielle (Touratier and Goyet, 2011).

Références

Abboud-Abi Saab M., 1985. Contribution à l'étude des populations microplanctoniques des eaux côtières libanaises (Méditerranée Orientale), Doctorat d'Etat, Université d'Aix Marseille II.

Accadia, C., Zecchetto, S., Lavagnini, A., Speranza, A., 2007. Comparison of 10-m Wind Forecasts from a Regional Area Model and QuikSCAT Scatterometer Wind Observations over the Mediterranean Sea. Mon. Weather Rev. 135 (5), 1945-1960. 10.1175/mwr3370.1

Aït-Ameur, N., Goyet, C., 2006. Distribution and transport of natural and anthropogenic CO_2 in the Gulf of Cádiz. Deep Sea Res. Part II Top. Stud. Oceanogr. 53 (11–13), 1329-1343. http://dx.doi.org/10.1016/j.dsr2.2006.04.003

Álvarez, M., 2012. The CO_2 system observations in the Mediterranean Sea: past, present and future. In: Briand, F. (Ed.), Designing Med-SHIP: a Program for repeated oceanographic surveys. CIESM Monaco, p. 164.

Álvarez, M., Sanleón-Bartolomé, H., Tanhua, T., Mintrop, L., Luchetta, A., Cantoni, C., Schroeder, K., Civitarese, G., 2014. The CO_2 system in the Mediterranean Sea: a basin wide perspective. Ocean Sci. 10 (1), 69-92. 10.5194/os-10-69-2014

Artegiani, A., Bregant, D., Paschini, E., Pinardi, N., Raicich, F., Russo, A., 1997. The Adriatic Sea General Circulation. Part I: Air–Sea Interactions and Water Mass Structure. J. Phys. Oceanogr. 27, 1492-1514.

Bakker, D.C.E., Pfeil, B., Smith, K., Hankin, S., Olsen, A., Alin, S.R., Cosca, C., Harasawa, S., Kozyr, A., Nojiri, Y., O'Brien, K.M., Schuster, U., Telszewski, M., Tilbrook, B., Wada, C., Akl, J., Barbero, L., Bates, N.R., Boutin, J., Bozec, Y., Cai, W.J., Castle, R.D., Chavez, F.P., Chen, L., Chierici, M., Currie, K., de Baar, H.J.W., Evans, W., Feely, R.A., Fransson, A., Gao, Z., Hales, B., Hardman-Mountford, N.J., Hoppema, M., Huang, W.J., Hunt, C.W., Huss, B., Ichikawa, T., Johannessen, T., Jones, E.M., Jones, S.D., Jutterström, S., Kitidis, V., Körtzinger, A., Landschützer, P., Lauvset, S.K., Lefèvre, N., Manke, A.B., Mathis, J.T., Merlivat, L., Metzl, N., Murata, A., Newberger, T., Omar, A.M., Ono, T., Park, G.H., Paterson, K., Pierrot, D., Ríos, A.F., Sabine, C.L., Saito, S., Salisbury, J., Sarma, V.V.S.S., Schlitzer, R., Sieger, R., Skjelvan, I., Steinhoff, T., Sullivan, K.F., Sun, H., Sutton, A.J., Suzuki, T., Sweeney, C., Takahashi, T., Tjiputra, J., Tsurushima, N., van Heuven, S.M.A.C., Vandemark, D., Vlahos, P., Wallace, D.W.R., Wanninkhof, R., Watson, A.J., 2014. An update to the Surface Ocean CO_2 Atlas (SOCAT version 2). Earth Syst. Sci. Data 6 (1), 69-90. 10.5194/essd-6-69-2014

Baringer, M.O.N., Price, J.F., 1997. Mixing and Spreading of the Mediterranean Outflow. J. Phys. Oceanogr. 27 (8), 1654-1677. 10.1175/1520-0485(1997)027<1654:masotm>2.0.co;2

Bates, R.G., 1973. Determination of pH; theory and practice. Wiley, New York.

Bégovic, M., Copin-Montégut, C., 2002. Processes controlling annual variations in the partial pressure of CO_2 in surface waters of the central northwestern Mediterranean Sea (Dyfamed site). Deep Sea Res. Part II Top. Stud. Oceanogr. 49 (11), 2031-2047. http://dx.doi.org/10.1016/S0967-0645(02)00026-7

Bégovic, M., Copin, C., 2013. Alkalinity and pH measurements on water bottle samples during THALASSA cruise PROSOPE. doi:10.1594/PANGAEA.805265

Beniston, M., 2003. Climatic Change in Mountain Regions: A Review of Possible Impacts. Climatic Change 59 (1-2), 5-31. 10.1023/a:1024458411589

Béranger, K., Mortier, L., Gasparini, G.P., Gervasio, L., Astraldi, M., Crépon, M., 2004. The dynamics of the Sicily Strait: a comprehensive study from observations and models. Deep Sea Res. Part II Top. Stud. Oceanogr. 51 (4–5), 411-440. http://dx.doi.org/10.1016/j.dsr2.2003.08.004

Bergamasco, A., Malanotte-Rizzoli, P., 2010. The circulation of the Mediterranean Sea: a historical review of experimental investigations. Adv. Oceanogr. Limnol. 1 (1), 11-28. 10.1080/19475721.2010.491656

Béthoux, J.P., 1979. Budgets of the Mediterranean Sea. Their dependance on the local climate characteristics of the Atlantic waters. Oceanol. Acta 2 (2), 157-163.

Béthoux, J.P., Gentili, B., Morin, P., Nicolas, E., Pierre, C., Ruiz-Pino, D., 1999. The Mediterranean Sea: a miniature ocean for climatic and environmental studies and a key for the climatic functioning of the North Atlantic. Prog. Oceanogr. 44 (1–3), 131-146. http://dx.doi.org/10.1016/S0079-6611(99)00023-3

Bockmon, E.E., Dickson, A.G., 2015. An inter-laboratory comparison assessing the quality of seawater carbon dioxide measurements. Mar. Chem. 171 (0), 36-43. http://dx.doi.org/10.1016/j.marchem.2015.02.002

Borges, A.V., Schiettecatte, L.S., Abril, G., Delille, B., Gazeau, F., 2006. Carbon dioxide in European coastal waters. Estuar. Coast. Shelf Sci. 70 (3), 375-387. http://dx.doi.org/10.1016/j.ecss.2006.05.046

Boutin, J., Quilfen, Y., Merlivat, L., Piolle, J.F., 2009. Global average of air-sea CO_2 transfer velocity from QuikSCAT scatterometer wind speeds. J. Geophys. Res. 114 (C4). 10.1029/2007jc004168

Brunet, C., Poisson, A., Lebel, J., Porot, V., 1984. Alcalinité totale, carbone inorganique, calcium, densité. Propriétés hydrologiques et chimiques des eaux du bassin occidental de la Méditerranée: campagne MÉDIPROD IV, 15 octobre-17 novembre 1981. Centre National pour l'Exploitation des Océans, Brest, France, pp. 89-93.

Byrne, R.H., Robert-Baldo, G., Thompson, S.W., Chen, C.T.A., 1988. Seawater pH measurements: an at-sea comparison of spectrophotometric and potentiometric methods. Deep Sea Res. Part A Oceanogr. Res. Pap. 35 (8), 1405-1410. http://dx.doi.org/10.1016/0198-0149(88)90091-X

Calleja, M.L., Duarte, C.M., Álvarez, M., Vaquer-Sunyer, R., Agustí, S., Herndl, G.J., 2013. Prevalence of strong vertical CO_2 and O_2 variability in the top meters of the ocean. Global Biogeochem. Cycles 27 (3), 941-949. 10.1002/gbc.20081

Chen, G.-T., Millero, F.J., 1979. Gradual increase of oceanic CO_2. Nature 277 (5693), 205-206.

CIESM, 2012. Designing Med-SHIP: a Program for repeated oceanographic surveys. CIESM. N°43 CIESM Workshop Monographs, 164

Claustre, H., Bégovic, M., 2013. Underway measurements of pCO_2 in surface water during cruise PROSOPE. Pangaea. doi:10.1594/PANGAEA.805383

Claustre, H., Morel, A., Hooker, S.B., Babin, M., Antoine, D., Oubelkheir, K., Bricaud, A., Leblanc, K., Quéguiner, B., Maritorena, S., 2002. Is desert dust making oligotrophic waters greener? Geophys. Res. Lett. 29 (10), 107-101-107-104. 10.1029/2001gl014056

Copin-Montégut, C., 1993. Alkalinity and carbon budgets in the Mediterranean Sea. Global Biogeochem. Cycles 7 (4), 915-925. 10.1029/93gb01826

Copin-Montégut, C., Bégovic, M., 2002. Distributions of carbonate properties and oxygen along the water column (0–2000m) in the central part of the NW Mediterranean Sea (Dyfamed site): influence of winter vertical mixing on air–sea CO_2 and O_2 exchanges. Deep Sea Res. Part II Top. Stud. Oceanogr. 49 (11), 2049-2066. http://dx.doi.org/10.1016/S0967-0645(02)00027-9

Copin-Montégut, C., Bégovic, M., Merlivat, L., 2004. Variability of the partial pressure of CO_2 on diel to annual time scales in the Northwestern Mediterranean Sea. Mar. Chem. 85 (3–4), 169-189. http://dx.doi.org/10.1016/j.marchem.2003.10.005

Cossarini, G., Lazzari, P., Solidoro, C., 2015. Spatiotemporal variability of alkalinity in the Mediterranean Sea. Biogeosciences 12 (6), 1647-1658. 10.5194/bg-12-1647-2015

D'Ortenzio, F., Antoine, D., Marullo, S., 2008. Satellite-driven modeling of the upper ocean mixed layer and air–sea CO_2 flux in the Mediterranean Sea. Deep Sea Res. Part I Oceanogr. Res. Pap. 55 (4), 405-434. http://dx.doi.org/10.1016/j.dsr.2007.12.008

De Carlo, E., Mousseau, L., Passafiume, O., Drupp, P., Gattuso, J.-P., 2013. Carbonate chemistry and air–sea CO_2 flux in a NW Mediterranean Bay over a four-year period: 2007–2011. Aquat. Geochem. 19 (5-6), 399-442. 10.1007/s10498-013-9217-4

de Jong, C., Lawler, D., Essery, R., 2009. Mountain Hydroclimatology and Snow Seasonality—Perspectives on climate impacts, snow seasonality and hydrological change in mountain environments. Hydrol. Process. 23 (7), 955-961. 10.1002/hyp.7193

Delgado, O., Estrada, M., 1994. CO_2 system in a Mediterranean frontal zone. Sci. Mar. 58, 237-250.

Dickson, A.G., 1981. An exact definition of total alkalinity and a procedure for the estimation of alkalinity and total inorganic carbon from titration data. Deep Sea Res. Part A Oceanogr. Res. Pap. 28 (6), 609-623. http://dx.doi.org/10.1016/0198-0149(81)90121-7

Dickson, A.G., 1984. pH scales and proton-transfer reactions in saline media such as sea water. Geochim. Cosmochim. Acta 48 (11), 2299-2308. http://dx.doi.org/10.1016/0016-7037(84)90225-4

Dickson, A.G., 1990a. Standard potential of the reaction: $AgCl(s) + 12H_2(g) = Ag(s) + HCl(aq)$, and and the standard acidity constant of the ion HSO_4^- in synthetic sea water from 273.15 to 318.15 K. J. Chem. Thermodyn. 22 (2), 113-127. http://dx.doi.org/10.1016/0021-9614(90)90074-Z

Dickson, A.G., 1990b. Thermodynamics of the dissociation of boric acid in synthetic seawater from 273.15 to 318.15 K. Deep Sea Res. Part A Oceanogr. Res. Pap. 37 (5), 755-766. http://dx.doi.org/10.1016/0198-0149(90)90004-F

Dickson, A.G., 1993. pH buffers for sea water media based on the total hydrogen ion concentration scale. Deep Sea Res. Part I Oceanogr. Res. Pap. 40 (1), 107-118. http://dx.doi.org/10.1016/0967-0637(93)90055-8

Dickson, A.G., Millero, F.J., 1987. A comparison of the equilibrium constants for the dissociation of carbonic acid in seawater media. Deep Sea Res. Part A Oceanogr. Res. Pap. 34 (10), 1733-1743. http://dx.doi.org/10.1016/0198-0149(87)90021-5

Dickson, A.G., Riley, J.P., 1979. The estimation of acid dissociation constants in seawater media from potentionmetric titrations with strong base. I. The ionic product of water — Kw. Mar. Chem. 7 (2), 89-99. http://dx.doi.org/10.1016/0304-4203(79)90001-X

Dickson, A.G., Sabine, C.L., Christian, J.R., 2007. Guide to best practices for ocean CO_2 measurements. PICES Special Publication 3, 191.

DOE, 1994. Handbook of methods for the analysis of the various parameters of the carbon dioxide system in sea water; version 2. A. G. Dickson & C. Goyet, eds., ORNL/CDIAC-74.

Doney, S.C., Tilbrook, B., Roy, S., Metzl, N., Le Quéré, C., Hood, M., Feely, R.A., Bakker, D., 2009. Surface-ocean CO_2 variability and vulnerability. Deep Sea Res. Part II Top. Stud. Oceanogr. 56 (8–10), 504-511. http://dx.doi.org/10.1016/j.dsr2.2008.12.016

Etcheto, J., Merlivat, L., 1988. Satellite determination of the carbon dioxide exchange coefficient at the ocean-atmosphere interface: A first step. J. Geophys. Res. 93 (C12), 15669-15678. 10.1029/JC093iC12p15669

Fairall, C.W., Bradley, E.F., Godfrey, J.S., Wick, G.A., Edson, J.B., Young, G.S., 1996. Cool-skin and warm-layer effects on sea surface temperature. J. Geophys. Res. 101 (C1), 1295-1308. 10.1029/95jc03190

Fuda, J.L., Etipe, G., Millot, C., Favali, P., Calcara, M., Smriglio, G., Boshi, E., 2002. Warming, salting and origin of the Tyrrhenian Deep Water. Geophys. Res. Lett. 29 (19), 1898. doi :10,1029/2001GL014072.

Gattuso, J.P., Epitalon, J.M., Lavigne, H., 2015. seacarb: seawater carbonate chemistry with R. The Comprehensive R Archive Network, http://CRAN.R-project.org/package=seacarb.

Gazeau, F., Duarte, C.M., Gattuso, J.P., Barrón, C., Navarro, N., Ruiz, S., Prairie, Y.T., Calleja, M., Delille, B., Frankignoulle, M., Borges, A.V., 2005. Whole-system metabolism and CO_2 fluxes in a Mediterranean Bay dominated by seagrass beds (Palma Bay, NW Mediterranean). Biogeosciences 2 (1), 43-60. 10.5194/bg-2-43-2005

Gerin, R., Poulain, P.M., Taupier-Letage, I., Millot, C., Ben Ismail, S., Sammari, C., 2009. Surface circulation in the Eastern Mediterranean using drifters (2005–2007). Ocean Sci. 5 (4), 559-574. 10.5194/os-5-559-2009

Goyet, C., Brewer, P., 1993. Biochemical Properties of the Oceanic Carbon Cycle. In: Willebrand, J., Anderson, D.T. (Eds.), Modelling Oceanic Climate Interactions. Springer Berlin Heidelberg, pp. 271-297. 10.1007/978-3-642-84975-6_8

Goyet, C., Coatanoan, C., Eischeid, G., Amaoka, T., Okuda, K., Healy, R., Tsunogai, S., 1999. Spatial variation of total CO_2 and total alkalinity in the northern Indian Ocean: A novel approach for the quantification of anthropogenic CO_2 in seawater. J. Mar. Res. 57 (1), 135-163. 10.1357/002224099765038599

Goyet, C., Gemayel, E., Hassoun, A.E.R., 2015a. Underway pCO_2 in surface water during the 2013 MedSeA cruise. Pangaea. Dataset #841928 (DOI registration in progress)

Goyet, C., Hassoun, A.E.R., Gemayel, E., 2015b. Carbonate system during the May 2013 MedSeA cruise. Pangaea. Dataset #841933 (DOI registration in progress)

Goyet, C., Poisson, A., 1989. New determination of carbonic acid dissociation constants in seawater as a function of temperature and salinity. Deep Sea Res. Part A Oceanogr. Res. Pap. 36 (11), 1635-1654. http://dx.doi.org/10.1016/0198-0149(89)90064-2

Guenard, V., Drobinski, P., Caccia, J.-L., Campistron, B., Bench, B., 2005. An Observational Study of the Mesoscale Mistral Dynamics. Boundary-Layer Meteorology 115 (2), 263-288. 10.1007/s10546-004-3406-z

Hamad, N., Millot, C., Taupier-Letage, I., 2005. A new hypothesis about the surface circulation in the eastern basin of the mediterranean sea. Prog. Oceanogr. 66 (2–4), 287-298. http://dx.doi.org/10.1016/j.pocean.2005.04.002

Hamad, N., Millot, C., Taupier-Letage, I., 2006. The surface circulation in the eastern basin of the Mediterranean Sea. Sci. Mar. 70 (3), 457-503.

Hansson, I., 1973a. The determination of dissociation constants of carbonic acid in synthetic sea water in the salinity range of 20-40 ‰ and temperature range of 5-30 ºC. Acta Chem. Scand. 27, 931-944.

Hansson, I., 1973b. A new set of acidity constants for carbonic acid and boric acid in sea water. Deep Sea Res.: Oceanogr. Abstr. 20 (5), 461-478. http://dx.doi.org/10.1016/0011-7471(73)90100-9

Hansson, I., 1973c. A new set of pH-scales and standard buffers for sea water. Deep Sea Res.: Oceanogr. Abstr. 20 (5), 479-491. http://dx.doi.org/10.1016/0011-7471(73)90101-0

Hay, C.C., Morrow, E., Kopp, R.E., Mitrovica, J.X., 2015. Probabilistic reanalysis of twentieth-century sea-level rise. Nature 517 (7535), 481-484. 10.1038/nature14093

HMSO, 1962. Weather in the Mediterranean I: General Meteorology. 2d ed. Her Majesty's Stationery Office, 362.

Ho, D.T., Law, C.S., Smith, M.J., Schlosser, P., Harvey, M., Hill, P., 2006. Measurements of air-sea gas exchange at high wind speeds in the Southern Ocean: Implications for global parameterizations. Geophys. Res. Lett. 33 (16), L16611. 10.1029/2006gl026817

Ho, D.T., Wanninkhof, R., Schlosser, P., Ullman, D.S., Hebert, D., Sullivan, K.F., 2011. Toward a universal relationship between wind speed and gas exchange: Gas transfer velocities measured with $^3He/SF_6$ during the Southern Ocean Gas Exchange Experiment. J. Geophys. Res. 116 (C4), C00F04. 10.1029/2010jc006854

Hood, E.M., Merlivat, L., 2001. Annual to interannual variations of fCO_2 in the northwestern Mediterranean Sea: Results from hourly measurements made by CARIOCA buoys, 1995-1997. J. Mar. Res. 59 (1), 113-131. http://dx.doi.org/10.1357/002224001321237399

Hunter, K.A., 2007. XLCO2 – Seawater CO_2 Equilibrium Calculations Using Excel Version 2. University of Otago, New Zealand.

Hydes, D., Jiang, Z., Hartman, M.C., Campbell, J.M., Hartman, S.E., Pagnani, M.R., B.A., K.-G., 2012. Surface DIC and TALK measurements along the M/V Pacific Celebes VOS Line during the 2007-2012 cruises. http://cdiac.ornl.gov/ftp/oceans/VOS_Pacific_Celebes_line/. Carbon Dioxide Information Analysis Center, Oak Ridge National Laboratory, US Department of Energy, Oak Ridge, Tennessee. doi: 10.3334/CDIAC/OTG.VOS_PC_2007-2012.

IPCC, 2013. Climate Change 2013: The Physical Science Basis. Contribution of Working Group I to the Fifth Assessment Report of the Intergovernmental Panel on Climate Change. Cambridge University Press, Cambridge, United Kingdom and New York, NY, USA. 10.1017/CBO9781107415324

Jähne, B., Heinz, G., Dietrich, W., 1987. Measurement of the diffusion coefficients of sparingly soluble gases in water. J. Geophys. Res. 92 (C10), 10767-10776. 10.1029/JC092iC10p10767

Jansá, A., 1987. Distribution of the Mistral: A satellite observation. Meteorology and Atmospheric Physics 36 (1-4), 201-214. 10.1007/bf01045149

Jiang, Q., Smith, R.B., Doyle, J., 2003. The nature of the mistral: Observations and modelling of two MAP events. Q. J. Roy. Meteor. Soc. 129 (588), 857-875. 10.1256/qj.02.21

Jurčec, V., 1981. On Mesoscale Characteristics of Bora Conditions in Yugoslavia. In: Liljequist, G. (Ed.), Weather and Weather Maps. Birkhäuser Basel, pp. 640-657. 10.1007/978-3-0348-5148-0_15

Keeling, R.F., Shertz, S.R., 1992. Seasonal and interannual variations in atmospheric oxygen and implications for the global carbon cycle. Nature 358 (6389), 723-727.

Khoo, K.H., Ramette, R.W., Culberson, C.H., Bates, R.G., 1977. Determination of hydrogen ion concentrations in seawater from 5 to 40 ºC: standard potentials at salinities from 20 to 45%. Anal. Chem. 49 (1), 29-34. 10.1021/ac50009a016

Krasakopoulou, E., Rapsomanikis, S., Papadopoulos, A., Papathanassiou, E., 2006. Partial pressure and air sea CO_2 flux in the Aegean Sea during February 2006. http://cdiac.ornl.gov/ftp/oceans/HCMR_Aegean_Sea/. Carbon Dioxide Information Analysis Center, Oak Ridge National Laboratory, US Department of Energy, Oak Ridge, Tennessee. doi: 10.3334/CDIAC/otg.GCP_HCMR_2006

Krasakopoulou, E., Rapsomanikis, S., Papadopoulos, A., Papathanassiou, E., 2009. Partial pressure and air–sea CO_2 flux in the Aegean Sea during February 2006. Cont. Shelf. Res. 29 (11–12), 1477-1488. http://dx.doi.org/10.1016/j.csr.2009.03.015

Krasakopoulou, E., Souvermezoglou, E., 2012. Discrete measurements of carbon dioxide in the Aegean Sea during the HCMR OTRANTO-5 cruise, February 1995.

http://cdiac.ornl.gov/ftp/oceans/HCMR_OTR5/. Carbon Dioxide Information Analysis Center, Oak Ridge National Laboratory, US Department of Energy, Oak Ridge, Tennessee. doi: 10.3334/CDIAC/OTG.HCMR_OTR5_1995.

Krasakopoulou, E., Souvermezoglou, E., Goyet, C., 2011. Anthropogenic CO_2 fluxes in the Otranto Strait (E. Mediterranean) in February 1995. Deep Sea Res. Part I Oceanogr. Res. Pap. 58 (11), 1103-1114. http://dx.doi.org/10.1016/j.dsr.2011.08.008

Kullenberg, G., Carmack, E., Denman, K., 2015. Physical and chemical changes in the ocean over basin-wide zones and decadal or longer time-scales: perspectives on current and future conditions. In: Arico, S. (Ed.), Ocean sustainability in the 21st century. Cambridge University Press and UNESCO, p. 320.

Lacombe, H., Tchernia, P., 1972. Caractères hydrologiques et circulation des eaux en Méditerranée. In: Stanley, D.J. (Ed.), The Mediterranean Sea. Dowden, Hutchinson and Ross, Stroudsberg, pp. 26-36.

Lascaratos, A., Williams, R.G., Tragou, E., 1993. A mixed-layer study of the formation of Levantine intermediate water. J. Geophys. Res. 98 (C8), 14739-14749. 10.1029/93jc00912

Lauvset, S.K., Gruber, N., Landschützer, P., Olsen, A., Tjiputra, J., 2015. Trends and drivers in global surface ocean pH over the past 3 decades. Biogeosciences 12 (5), 1285-1298. 10.5194/bg-12-1285-2015

Le Quéré, C., Moriarty, R., Andrew, R.M., Peters, G.P., Ciais, P., Friedlingstein, P., Jones, S.D., Sitch, S., Tans, P., Arneth, A., Boden, T.A., Bopp, L., Bozec, Y., Canadell, J.G., Chini, L.P., Chevallier, F., Cosca, C.E., Harris, I., Hoppema, M., Houghton, R.A., House, J.I., Jain, A.K., Johannessen, T., Kato, E., Keeling, R.F., Kitidis, V., Klein Goldewijk, K., Koven, C., Landa, C.S., Landschützer, P., Lenton, A., Lima, I.D., Marland, G., Mathis, J.T., Metzl, N., Nojiri, Y., Olsen, A., Ono, T., Peng, S., Peters, W., Pfeil, B., Poulter, B., Raupach, M.R., Regnier, P., Rödenbeck, C., Saito, S., Salisbury, J.E., Schuster, U., Schwinger, J., Séférian, R., Segschneider, J., Steinhoff, T., Stocker, B.D., Sutton, A.J., Takahashi, T., Tilbrook, B., van der Werf, G.R., Viovy, N., Wang, Y.P., Wanninkhof, R., Wiltshire, A., Zeng, N., 2015. Global carbon budget 2014. Earth Syst. Sci. Data 7 (1), 47-85. 10.5194/essd-7-47-2015

Le Quere, C., Raupach, M.R., Canadell, J.G., Marland, G., et al., 2009. Trends in the sources and sinks of carbon dioxide. Nature Geosci, 2 (12), 831-836. http://www.nature.com/ngeo/journal/v2/n12/suppinfo/ngeo689_S1.html

Lee, K., Millero, F.J., 1995. Thermodynamic studies of the carbonate system in seawater. Deep Sea Res. Part I Oceanogr. Res. Pap. 42 (11–12), 2035-2061. http://dx.doi.org/10.1016/0967-0637(95)00077-1

Lee, K., Millero, F.J., Byrne, R.H., Feely, R.A., Wanninkhof, R., 2000. The recommended dissociation constants for carbonic acid in seawater. Geophys. Res. Lett. 27 (2), 229-232. 10.1029/1999gl002345

Lee, K., Millero, F.J., Campbell, D.M., 1996. The reliability of the thermodynamic constants for the dissociation of carbonic acid in seawater. Mar. Chem. 55 (3–4), 233-245. http://dx.doi.org/10.1016/S0304-4203(96)00064-3

Lee, K., Millero, F.J., Wanninkhof, R., 1997. The carbon dioxide system in the Atlantic Ocean. J. Geophys. Res. 102 (C7), 15693-15707. 10.1029/97jc00067

Lee, K., Sabine, C.L., Tanhua, T., Kim, T.-W., Feely, R.A., Kim, H.-C., 2011. Roles of marginal seas in absorbing and storing fossil fuel CO_2. Energy Environ. Sci. 4 (4), 1133-1146. 10.1039/c0ee00663g

Lewis, E., Wallace, D.W.R., 1998. Program Developed for CO_2 System Calculations. In: ORNL/CDIAC-105 (Ed.). Carbon Dioxide Information Analysis Center, Oak Ridge National Laboratory, U.S. Department of Energy, Oak Ridge,Tennessee.

Liss, P., Merlivat, L., 1986. Air-sea gas exchange rates: Introduction and synthesis. In: Buat-Ménard, P. (Ed.), The role of air-sea exchange in geochemical cycling. Springer Netherlands, pp. 113-127. 10.1007/978-94-009-4738-2_5

Llasat, M.C., Llasat-Botija, M., Petrucci, O., Pasqua, A.A., Rosselló, J., Vinet, F., Boissier, L., 2013. Towards a database on societal impact of Mediterranean floods within the framework of the HYMEX project. Nat. Hazards Earth Syst. Sci. 13 (5), 1337-1350. 10.5194/nhess-13-1337-2013

López-Jurado, J.L., Balbín, R., Amengual, B., Aparicio-González, A., Fernández de Puelles, M.L., García-Martínez, M.C., Gazá, M., Jansá, J., Morillas-Kieffer, A., Moyá, F., Santiago, R., Serra, M., Vargas-Yáñez, M., Vicente, L., 2015. The RADMED monitoring program: towards an ecosystem approach. Ocean Sci. Discuss. 12 (3), 645-671. 10.5194/osd-12-645-2015

Louanchi, F., Boudjakdji, M., Nacef, L., 2009. Decadal changes in surface carbon dioxide and related variables in the Mediterranean Sea as inferred from a coupled data-diagnostic model approach. ICES J. Mar. Sci. 66 (7), 1538-1546. 10.1093/icesjms/fsp049

Lovato, T., Vichi, M., 2015. An objective reconstruction of the Mediterranean sea carbonate system. Deep Sea Res. Part I Oceanogr. Res. Pap. 98 (0), 21-30. http://dx.doi.org/10.1016/j.dsr.2014.11.018

Luchetta, A., Cantoni, C., Catalano, G., 2010a. New observations of CO_2 induced acidification in the northern Adriatic Sea over the last quarter century. Chem. Ecol. 26 (sup1), 1-17. 10.1080/02757541003627688

Luchetta, A., Cantoni, C., Catalano, G., Civitarese, G., Celio, M., 2010b. Monitoring pH of seawater in the Adriatic Sea. Results from a regional observing effort. In: Hall, J., Harrison, D.E., Stammer, D. (Eds.), Proceedings of OceanObs'09: Sustained Ocean Observations and Information for Society (Annex). ESA Publication WPP-306, Venice, Italy, 21-25 September 2009. doi:10.5270/OceanObs09

Lueker, T.J., Dickson, A.G., Keeling, C.D., 2000. Ocean pCO_2 calculated from dissolved inorganic carbon, alkalinity, and equations for K_1 and K_2 : validation based on laboratory measurements of CO_2 in gas and seawater at equilibrium. Mar. Chem. 70, 105-119.

Manca, B.B., Ibello, V., Pacciaroni, M., Scarazzato, P., Giorgetti, A., 2006. Ventilation of deep waters in the Adriatic and Ionian Seas following changes in thermohaline circulation of the Eastern Mediterranean. Clim. Res. 31, 239-256.

Marotzke, J., Forster, P.M., 2015. Forcing, feedback and internal variability in global temperature trends. Nature 517 (7536), 565-570. 10.1038/nature14117

Medar-Group, 2002. MEDATLAS 2002. Mediterranean and Black Sea database of temperature, salinity and biochemical parameters. Climatological Atlas.

Mehrbach, C., Culberson, C.H., Hawley, J.E., Pytkowicz, R.M., 1973. Measurements of the apparent dissociation constants of carbonic acid in seawater at atmospheric pressure. A.S.L.O. 18 (6), 879-907.

Millero, F.J., 1986. The pH of estuarine waters. A.S.L.O. 31 (4), 839-847.

Millero, F.J., 1995. Thermodynamics of the carbon dioxide system in the oceans. Geochim. Cosmochim. Acta 59 (4), 661-677. http://dx.doi.org/10.1016/0016-7037(94)00354-O

Millero, F.J., 2007. The Marine inorganic carbon cycle. Chem. Rev. 107 (2), 308-341. 10.1021/cr0503557

Millero, F.J., Graham, T.B., Huang, F., Bustos-Serrano, H., Pierrot, D., 2006. Dissociation constants of carbonic acid in seawater as a function of salinity and temperature. Mar. Chem. 100 (1–2), 80-94. http://dx.doi.org/10.1016/j.marchem.2005.12.001

Millero, F.J., Morse, J., Chen, C.-T., 1979. The carbonate system in the western Mediterranean sea. Deep Sea Res. Part A Oceanogr. Res. Pap. 26 (12), 1395-1404. http://dx.doi.org/10.1016/0198-0149(79)90007-4

Millero, F.J., Pierrot, D., Lee, K., Wanninkhof, R., Feely, R., Sabine, C.L., Key, R.M., Takahashi, T., 2002. Dissociation constants for carbonic acid determined from field measurements. Deep Sea Res. Part I Oceanogr. Res. Pap. 49 (10), 1705-1723. http://dx.doi.org/10.1016/S0967-0637(02)00093-6

Millot, C., 1999. Circulation in the Western Mediterranean Sea. J. Mar. Syst. 20 (1–4), 423-442. http://dx.doi.org/10.1016/S0924-7963(98)00078-5

Millot, C., 2009. Another description of the Mediterranean Sea outflow. Prog. Oceanogr. 82 (2), 101-124. http://dx.doi.org/10.1016/j.pocean.2009.04.016

Millot, C., Candela, J., Fuda, J.-L., Tber, Y., 2006. Large warming and salinification of the Mediterranean outflow due to changes in its composition. Deep Sea Res. Part I Oceanogr. Res. Pap. 53 (4), 656-666. http://dx.doi.org/10.1016/j.dsr.2005.12.017

Millot, C., Taupier-Letage, I., 2005. Circulation in the Mediterranean Sea In: Saliot, A. (Ed.), The Mediterranean Sea Handbook of Envrionmental Chemistry. Springer Berlin Heidelberg, pp. 29-66. 10.1007/b107143

Mojica-Prieto, F.J., Millero, F.J., 2002. The values of pK_1 + pK_2 for the dissociation of carbonic acid in seawater. Geochim. Cosmochim. Acta 66 (14), 2529-2540.

Mosley, L.M., Peake, B.M., Hunter, K.A., 2010. Modelling of pH and inorganic carbon speciation in estuaries using the composition of the river and seawater end members. Environ. Model Softw. 25 (12), 1658-1663. http://dx.doi.org/10.1016/j.envsoft.2010.06.014

Mucci, A., 1983. The solubility of calcite and aragonite in seawater at various salinities, temperatures, and one atmosphere total pressure. American Journal of Science 283 (7), 780-799. 10.2475/ajs.283.7.780

Nightingale, P.D., Malin, G., Law, C.S., Watson, A.J., Liss, P.S., Liddicoat, M.I., Boutin, J., Upstill-Goddard, R.C., 2000. In situ evaluation of air-sea gas exchange parameterizations using novel conservative and volatile tracers. Global Biogeochem. Cycles 14 (1), 373-387. 10.1029/1999gb900091

Orr, J.C., Epitalon, J.M., 2015. Improved routines to model the ocean carbonate system: mocsy 2.0. Geosci. Model. Dev. 8 (3), 485-499. 10.5194/gmd-8-485-2015

Orr, J.C., Epitalon, J.M., Gattuso, J.P., 2015. Comparison of ten packages that compute ocean carbonate chemistry. Biogeosciences 12 (5), 1483-1510. 10.5194/bg-12-1483-2015

Palmiéri, J., Orr, J.C., Dutay, J.C., Béranger, K., Schneider, A., Beuvier, J., Somot, S., 2015. Simulated anthropogenic CO_2 storage and acidification of the Mediterranean Sea. Biogeosciences 12 (3), 781-802. 10.5194/bg-12-781-2015

Pandžić, K., Likso, T., 2005. Eastern Adriatic typical wind field patterns and large-scale atmospheric conditions. Int. J. Climatol. 25 (1), 81-98. 10.1002/joc.1085

Pelletier, G., Lewis, E., Wallace, D., 2007. CO2SYS.XLS: A calculator for the CO_2 system in seawater for Microsoft Excel/VBA. Wash. State Dept. of Ecology/Brookhaven Nat. Lab., Olympia, WA/Upton, NY, USA.

Peng, T.-H., Takahashi, T., Broecker, W.S., Olafsson, J.O.N., 1987. Seasonal variability of carbon dioxide, nutrients and oxygen in the northern North Atlantic surface water: observations and a model. Tellus B 39B (5), 439-458. 10.1111/j.1600-0889.1987.tb00205.x

Pérez, F.F., Estrada, M., Salat, J., 1986. Sistema del carbónico, oxígeno y nutrientes en el Mediterráneo occidental. Inv. Pesq. 50 (3), 333-351

Pierrot, D., Lewis, E., Wallace, D.W.R., 2006. MS Excel program developed for CO_2 system calculations. ORNL/CDIAC-105a, Carbon Dioxide Information Analysis Center, Oak

Ridge National Laboratory, U.S. Department of Energy, Oak Ridge, Tennessee. 10.3334/CDIAC/otg.CO2SYS_XLS_CDIAC105a

Pinardi, N., Masetti, E., 2000. Variability of the large scale general circulation of the Mediterranean Sea from observations and modelling: a review. Palaeogeogr. Palaeoclimatol. Palaeoecol. 158 (3–4), 153-173. http://dx.doi.org/10.1016/S0031-0182(00)00048-1

Pinardi, N., Navarra, A., 1993. Baroclinic wind adjustment processes in the Mediterranean Sea. Deep Sea Res. Part II Top. Stud. Oceanogr. 40 (6), 1299-1326. http://dx.doi.org/10.1016/0967-0645(93)90071-T

Ramette, R.W., Culberson, C.H., Bates, R.G., 1977. Acid-base properties of tris(hydroxymethyl)aminomethane (Tris) buffers in sea water from 5 to 40 ºC. Anal. Chem. 49 (6), 867-870. 10.1021/ac50014a049

Revelle, R., Suess, H.E., 1957. Carbon Dioxide Exchange Between Atmosphere and Ocean and the Question of an Increase of Atmospheric CO_2 during the Past Decades. Tellus 9 (1), 18-27. 10.1111/j.2153-3490.1957.tb01849.x

Rivaro, P., Messa, R., Massolo, S., Frache, R., 2010. Distributions of carbonate properties along the water column in the Mediterranean Sea: Spatial and temporal variations. Mar. Chem. 121 (1–4), 236-245. http://dx.doi.org/10.1016/j.marchem.2010.05.003

Robbins, L.L., Hansen, M.E., Kleypas, J.A., Meylan, S.C., 2010. CO_2calc—A user-friendly seawater carbon calculator for Windows, Max OS X, and iOS (iPhone). U.S. Geological Survey Open-File Report 2010-1280, 17

Robinson, A.R., Leslie, W.G., Theocharis, A., Lascaratos, A., 2001. Mediterranean Sea Circulation. In: Steele, J.H. (Ed.), Encyclopedia of Ocean Sciences (Second Edition). Academic Press, Oxford, pp. 710-725. http://dx.doi.org/10.1016/B978-012374473-9.00376-3

Roy, R.N., Roy, L.N., Vogel, K.M., Porter-Moore, C., Pearson, T., Good, C.E., Millero, F.J., Campbell, D.M., 1993. The dissociation constants of carbonic acid in seawater at salinities 5 to 45 and temperatures 0 to 45°C. Mar. Chem. 44 (2–4), 249-267. http://dx.doi.org/10.1016/0304-4203(93)90207-5

Sabine, C., Ducklow, H., Hood, M., 2010. International carbon coordination: Roger Revelle's legacy in the Intergovernmental Oceanographic Commission. Oceanogr. 23 (3), 48-61. http://dx.doi.org/10.5670/oceanog.2010.23

Santana-Casiano, J.M., Gonzalez-Davila, M., Laglera, L.M., 2002. The carbon dioxide system in the Strait of Gibraltar. Deep Sea Res. Part II Top. Stud. Oceanogr. 49 (19), 4145-4161. http://dx.doi.org/10.1016/S0967-0645(02)00147-9

Schlitzer, R., 2002. Interactive analysis and visualization of geoscience data with Ocean Data View. Comput. Geosci. 28 (10), 1211-1218. http://dx.doi.org/10.1016/S0098-3004(02)00040-7

Schneider, A., Tanhua, T., Körtzinger, A., Wallace, D.W.R., 2010. High anthropogenic carbon content in the Eastern Mediterranean. J. Geophys. Res. 115 (C12), C12050. 10.1029/2010jc006171

Schneider, A., Wallace, D.W.R., Körtzinger, A., 2007. Alkalinity of the Mediterranean Sea. Geophys. Res. Lett. 34 (15), L15608. 10.1029/2006gl028842

Schneider, B., Roether, W., 2007. Meteor 06MT20011018 cruise data from the 2001 cruises, CARINA Data Set. http://cdiac.ornl.gov/ftp/oceans/CARINA/Meteor/06MT512/. Carbon Dioxide Information Analysis Center, Oak Ridge National Laboratory, US Department of Energy, Oak Ridge, Tennessee. doi: 10.3334/CDIAC/otg.CARINA 06MT20011018.

Sempéré, R., Dafner, E., Van Wambeke, F., Lefèvre, D., Magen, C., Allègre, S., Bruyant, F., Bianchi, M., Prieur, L., 2003. Distribution and cycling of total organic carbon across the

Almeria-Oran Front in the Mediterranean Sea: Implications for carbon cycling in the western basin. J. Geophys. Res. 108 (C11). 10.1029/2002jc001475

Serra, N., Ambar, I., 2002. Eddy generation in the Mediterranean undercurrent. Deep Sea Res. Part II Top. Stud. Oceanogr. 49 (19), 4225-4243. http://dx.doi.org/10.1016/S0967-0645(02)00152-2

Smith, R.B., 1987. Aerial Observations of the Yugoslavian Bora. J. Atmos. Sci. 44 (2), 269-297. 10.1175/1520-0469(1987)044<0269:aootyb>2.0.co;2

Smith, S.V., 1985. Physical, chemical and biological characteristics* of CO_2 gas flux across the air-water interface. Plant, Cell & Environment 8 (6), 387-398. 10.1111/j.1365-3040.1985.tb01674.x

Sorgente, R., Olita, A., Oddo, P., Fazioli, L., Ribotti, A., 2011. Numerical simulation and decomposition of kinetic energy in the Central Mediterranean: insight on mesoscale circulation and energy conversion. Ocean Sci. 7 (4), 503-519. 10.5194/os-7-503-2011

Stocker, T.F., Qin, D., Plattner, G.-K., Alexander, L.V., Allen, S.K., Bindoff, N.L., Bréon, F.-M., Church, J.A., Cubasch, U., Emori, S., Forster, P., Friedlingstein, P., Gillett, N., Gregory, J.M., Hartmann, D.L., Jansen, E., Kirtman, B., Knutti, R., Krishna Kumar, K., Lemke, P., Marotzke, J., Masson-Delmotte, V., Meehl, G.A., Mokhov, I.I., Piao, S., Ramaswamy, V., Randall, D., Rhein, M., Rojas, M., Sabine, C., Shindell, D., Talley, L.D., Vaughan, D.G., Xie, S.-P., 2013. Technical Summary. In: Stocker, T.F., Qin, D., Plattner, G.-K., Tignor, M., Allen, S.K., Boschung, J., Nauels, A., Xia, Y., Bex, V., Midgley, P.M. (Eds.), Climate Change 2013: The Physical Science Basis. Contribution of Working Group I to the Fifth Assessment Report of the Intergovernmental Panel on Climate Change. Cambridge University Press, Cambridge, United Kingdom and New York, NY, USA, pp. 33–115. 10.1017/CBO9781107415324.005

Sutton, A.J., Sabine, C.L., Maenner-Jones, S., Lawrence-Slavas, N., Meinig, C., Feely, R.A., Mathis, J.T., Musielewicz, S., Bott, R., McLain, P.D., Fought, H.J., Kozyr, A., 2014. A high-frequency atmospheric and seawater pCO_2 data set from 14 open-ocean sites using a moored autonomous system. Earth Syst. Sci. Data 6 (2), 353-366. 10.5194/essd-6-353-2014

Sweeney, C., Gloor, E., Jacobson, A.R., Key, R.M., McKinley, G., Sarmiento, J.L., Wanninkhof, R., 2007. Constraining global air-sea gas exchange for CO2 with recent bomb 14C measurements. Global Biogeochem. Cycles 21 (2). 10.1029/2006gb002784

Taillandier, V., D'Ortenzio, F., Antoine, D., 2012. Carbon fluxes in the mixed layer of the Mediterranean Sea in the 1980s and the 2000s. Deep Sea Res. Part I Oceanogr. Res. Pap. 65 (0), 73-84. http://dx.doi.org/10.1016/j.dsr.2012.03.004

Takahashi, T., Sutherland, S.C., Chipman, D.W., Goddard, J.G., Ho, C., Newberger, T., Sweeney, C., Munro, D.R., 2014a. Climatological distributions of pH, pCO_2, total CO_2, alkalinity, and $CaCO_3$ saturation in the global surface ocean, and temporal changes at selected locations. Mar. Chem. 164 (0), 95-125. http://dx.doi.org/10.1016/j.marchem.2014.06.004

Takahashi, T., Sutherland, S.C., Kozyr, A., 2014b. Global ocean surface water partial pressure of CO_2 database: Measurements performed during 1957-2013 (Version 2013). Carbon Dioxide Information Analysis Center, Oak Ridge National Laboratory, U.S. Department of Energy, Oak Ridge, Tennessee. 10.3334/CDIAC/OTG.NDP088(V2013)

Takahashi, T., Sutherland, S.C., Wanninkhof, R., Sweeney, C., Feely, R.A., Chipman, D.W., Hales, B., Friederich, G., Chavez, F., Sabine, C., Watson, A., Bakker, D.C.E., Schuster, U., Metzl, N., Yoshikawa-Inoue, H., Ishii, M., Midorikawa, T., Nojiri, Y., Körtzinger, A., Steinhoff, T., Hoppema, M., Olafsson, J., Arnarson, T.S., Tilbrook, B., Johannessen, T., Olsen, A., Bellerby, R., Wong, C.S., Delille, B., Bates, N.R., de Baar, H.J.W., 2009. Climatological mean and decadal change in surface ocean pCO_2, and net sea–air CO_2

flux over the global oceans. Deep Sea Res. Part II Top. Stud. Oceanogr. 56 (8–10), 554-577. http://dx.doi.org/10.1016/j.dsr2.2008.12.009

Takahashi, T., Williams, R.T., Bos, D.L., 1982. Carbonate chemistry. National Science Foundation. GEOSECS Pacific Expedition, Volume 3, Hydrographic Data 1973-1974 3, 77-83

Tanhua, T., Alvarez, M., Mintrop, L., 2012. Carbon dioxide, hydrographic, and chemical data obtained during the R/V Meteor MT84_3 Mediterranean Sea cruise (April 5. - April 28, 2011). http://cdiac.ornl.gov/ftp/oceans/CLIVAR/Met_84_3_Med_Sea/. Carbon Dioxide Information Analysis Center, Oak Ridge National Laboratory, US Department of Energy, Oak Ridge, Tennessee. doi: 10.3334/CDIAC/OTG.CLIVAR_06MT20110405.

Tanhua, T., Bates, N.R., Kortzinger, A., 2013a. The Marine Carbon Cycle and Ocean Anthropogenic CO_2 Inventories. In: Siedler, G., Griffies, S., Gould, J., Church, J. (Eds.), Ocean Circulation and Climate: A 21st Century Perspective. 2nd Ed. Academic Press, pp. 787-816.

Tanhua, T., Hainbucher, D., Cardin, V., Álvarez, M., Civitarese, G., McNichol, A.P., Key, R.M., 2013b. Repeat hydrography in the Mediterranean Sea, data from the Meteor cruise 84/3 in 2011. Earth Syst. Sci. Data 5 (2), 289-294. 10.5194/essd-5-289-2013

Tanhua, T., Hainbucher, D., Schroeder, K., Cardin, V., Álvarez, M., Civitarese, G., 2013c. The Mediterranean Sea system: a review and an introduction to the special issue. Ocean Sci. 9 (5), 789-803. 10.5194/os-9-789-2013

Testor, P., Béranger, K., Mortier, L., 2005a. Modeling the deep eddy field in the southwestern Mediterranean: The life cycle of Sardinian eddies. Geophys. Res. Lett. 32 (13). 10.1029/2004gl022283

Testor, P., Send, U., Gascard, J.C., Millot, C., Taupier-Letage, I., Béranger, K., 2005b. The mean circulation of the southwestern Mediterranean Sea: Algerian Gyres. J. Geophys. Res. 110 (C11), C11017. 10.1029/2004jc002861

Theocharis, A., Balopoulos, E., Kioroglou, S., Kontoyiannis, H., Iona, A., 1999. A synthesis of the circulation and hydrography of the South Aegean Sea and the Straits of the Cretan Arc (March 1994–January 1995). Prog. Oceanogr. 44 (4), 469-509. http://dx.doi.org/10.1016/S0079-6611(99)00041-5

Touratier, F., Azouzi, L., Goyet, C., 2011. CFC-11, Δ ^{14}C and ^{3}H tracers as a means to assess anthropogenic CO_2 concentrations in the ocean. Tellus B 59 (2). 10.3402/tellusb.v59i2.16991

Touratier, F., Goyet, C., 2004. Applying the new TrOCA approach to assess the distribution of anthropogenic CO_2 in the Atlantic Ocean. J. Mar. Syst. 46 (1–4), 181-197. http://dx.doi.org/10.1016/j.jmarsys.2003.11.020

Touratier, F., Goyet, C., 2009. Decadal evolution of anthropogenic CO_2 in the northwestern Mediterranean Sea from the mid-1990s to the mid-2000s. Deep Sea Res. Part I Oceanogr. Res. Pap. 56 (10), 1708-1716. http://dx.doi.org/10.1016/j.dsr.2009.05.015

Touratier, F., Goyet, C., 2011. Impact of the Eastern Mediterranean Transient on the distribution of anthropogenic CO_2 and first estimate of acidification for the Mediterranean Sea. Deep Sea Res. Part I Oceanogr. Res. Pap. 58 (1), 1-15. http://dx.doi.org/10.1016/j.dsr.2010.10.002

Touratier, F., Guglielmi, V., Goyet, C., Prieur, L., Pujo-Pay, M., Conan, P., Falco, C., 2012. Distributions of the carbonate system properties, anthropogenic CO_2, and acidification during the 2008 BOUM cruise (Mediterranean Sea). Biogeosci. Discuss. 9 (3), 2709-2753. 10.5194/bgd-9-2709-2012

Turk, D., Malačič, V., DeGrandpre, M.D., McGillis, W.R., 2010. Carbon dioxide variability and air-sea fluxes in the northern Adriatic Sea. J. Geophys. Res. 115 (C10), C10043. 10.1029/2009jc006034

Uppström, L.R., 1974. The boron/chlorinity ratio of deep-sea water from the Pacific Ocean. Deep Sea Res.: Oceanogr. Abstr. 21 (2), 161-162. http://dx.doi.org/10.1016/0011-7471(74)90074-6

van Heuven, S., Pierrot, D., Rae, J.W.B., Lewis, E., Wallace, D.W.R., 2011. MATLAB program developed for CO_2 system calculations. In: ORNL/CDIAC-105 (Ed.). Carbon Dioxide Information Analysis Center, Oak Ridge National Laboratory, U.S. Department of Energy, Oak Ridge,Tennessee.

Vargas-Yáñez, M., Plaza, F., García-Lafuente, J., Sarhan, T., Vargas, J.M., Vélez-Belchi, P., 2002. About the seasonal variability of the Alboran Sea circulation. J. Mar. Syst. 35 (3–4), 229-248. http://dx.doi.org/10.1016/S0924-7963(02)00128-8

Wanninkhof, R., 1992. Relationship between wind speed and gas exchange over the ocean. J. Geophys. Res. 97 (C5), 7373-7382. 10.1029/92jc00188

Wanninkhof, R., Asher, W.E., Ho, D.T., Sweeney, C., McGillis, W.R., 2009. Advances in quantifying air-sea gas exchange and environmental forcing. Ann. Rev. Mar. Sci. 1 (1), 213-244. doi:10.1146/annurev.marine.010908.163742

Wanninkhof, R., Lewis, E., Feely, R.A., Millero, F.J., 1999. The optimal carbonate dissociation constants for determining surface water pCO_2 from alkalinity and total inorganic carbon. Mar. Chem. 65 (3–4), 291-301. http://dx.doi.org/10.1016/S0304-4203(99)00021-3

Wanninkhof, R., McGillis, W.R., 1999. A cubic relationship between air-sea CO_2 exchange and wind speed. Geophys. Res. Lett. 26 (13), 1889-1892. 10.1029/1999gl900363

Wanninkhof, R., Park, G.H., Takahashi, T., Sweeney, C., Feely, R., Nojiri, Y., Gruber, N., Doney, S.C., McKinley, G.A., Lenton, A., Le Quéré, C., Heinze, C., Schwinger, J., Graven, H., Khatiwala, S., 2013. Global ocean carbon uptake: magnitude, variability and trends. Biogeosciences 10 (3), 1983-2000. 10.5194/bg-10-1983-2013

Ward, B., Wanninkhof, R., McGillis, W.R., Jessup, A.T., DeGrandpre, M.D., Hare, J.E., Edson, J.B., 2004. Biases in the air-sea flux of CO2 resulting from ocean surface temperature gradients. J. Geophys. Res. 109 (C8). 10.1029/2003jc001800

Weiss, R.F., 1974. Carbon dioxide in water and seawater: the solubility of a non-ideal gas. Mar. Chem. 2 (3), 203-215. http://dx.doi.org/10.1016/0304-4203(74)90015-2

Weiss, R.F., , et al., 1983. GEOSECS Indian Ocean Expedition: Hydrographic data 1977-1978. National Science Foundation, Washington.

Weiss, R.F., Price, B.A., 1980. Nitrous oxide solubility in water and seawater. Mar. Chem. 8 (4), 347-359. http://dx.doi.org/10.1016/0304-4203(80)90024-9

Zeebe, R.E., Wolf-Gladrow, D.A., 2001. CO_2 in Seawater: Equilibrium, Kinetics, Isotopes. Elsevier, Amsterdam.

Ziv, B., Saaroni, H., Alpert, P., 2004. The factors governing the summer regime of the eastern Mediterranean. Int. J. Climatol. 24 (14), 1859-1871. 10.1002/joc.1113

Chapitre III: Articles Scientifiques

'Si tu veux construire un bateau, ne rassemble pas tes hommes et femmes pour leur donner des ordres, pour expliquer chaque détail, pour leur dire où trouver chaque chose... Si tu veux construire un bateau, fais naître dans le cœur de tes hommes et femmes le désir de la mer'

Antoine de Saint Exupéry

Article I: Is the Mediterranean Sea circulation in a steady state

Hassoun, A.E.R., Guglielmi, V., **Gemayel, E.,** et al. (2015)

Journal of Water Resources and Ocean Science, 4 (1), 6-17. doi: 10.11648/j.wros.20150401.12

Is the Mediterranean Sea circulation in a steady state

Abed El Rahman HASSOUN[1], Véronique GUGLIELMI[2,3], Elissar GEMAYEL[1,2,3], Catherine GOYET[2,3], Marie ABBOUD-ABI SAAB[1], Michele GIANI[4], Patrizia ZIVERI[5], Gianmarco INGROSSO[4], Franck TOURATIER[2,3]

[1]National Council for Scientific Research, National Center for Marine Sciences, Batroun, Lebanon
[2]IMAGES_ESPACE-DEV, Université de Perpignan Via Domitia, Perpignan Cedex, France
[3]ESPACE-DEV, UG UA UR UM IRD, Maison de la télédétection, Montpellier Cedex, France
[4]OGS (Istituto Nazionale di Oceanografia e di Geofisica Sperimentale), Oceanography Section, Via A. Piccard, Trieste, Italy
[5]ICREA - Institute of Environmental Science and Technology (ICTA), Universitat Autònoma de Barcelona, Ed. Z, ICTA-ICP, Carrer de les columnes, E- 08193 Bellaterra, Barcelona, Spain

Abstract: Most global ocean models are based on the assumption of a "steady state" ocean. Here, we investigate the validation of this hypothesis for the anthropized Mediterranean Sea. In order to do so, we calculated the mixing coefficients of the water masses detected in this sea via an optimum multiparameter analysis referred to as the MIX approach, using data from the BOUM (2008) and MedSeA (2013) cruises. The comparison of the mixing coefficients of each water mass, between 2008 and 2013, indicates that some of their proportions have significantly changed. Surface water mass proportions did not change significantly (Δ 0.05-0.1), while intermediate and deep water mass mixing coefficients of both Eastern and Western basins were significantly modified (~Δ 0.35). This study clearly shows that the Mediterranean seawater is not in a "steady state".

Keywords: Mixing Coefficient; MIX Approach; Water Masses; Seawater Circulation; Mediterranean Sea; Climate Change

1. Introduction

The Mediterranean Sea is a mid-latitude semi-enclosed sea. It witnesses two well-defined seasons, wet-cold winter and dry-warm summer, with short period of transition between them [1] [2]. An excess of evaporation over precipitation can be quantified by calculating the annual mean budget "evaporation minus precipitation" (E-P) over the whole Mediterranean Sea (350-750 mm yr^{-1}) [1]. Thus, Atlantic Water (AW) inflows at the surface and Mediterranean Water outflows along the bottom. The Atlantic water entering into Gibraltar in the surface layer, after travelling to the easternmost Levantine Sub-basin, is transformed into one of the saltiest seawater masses through air-sea heat and moisture fluxes. This relatively cold and salty water, which crosses the entire Mediterranean Sea in the opposite direction of the surface Atlantic Water, finally exits from the Strait of Gibraltar at the mid-depths. In wintertime, a significant negative heat budget [1] [3] causes a buoyancy loss, initiating deep and/or intermediate dense water formation. These events are frequent over the shelf areas and

in the offshore regions, both in the Western and the Eastern basins [4] [5]. The Mediterranean Sea also exchanges water with the Black Sea through the Turkish Strait System (the Dardanelles, the Marmara Sea and the Bosphorus Strait) and receives significant amounts of freshwater from river discharge. In addition, this sea is always provided by groundwater discharges and sewage, which are likely, an important source of freshwater, nutrients, trace metals, alkalinity and other elements to the Mediterranean System [6] [7]. The Mediterranean Sea is composed mainly of two nearly equal size basins, the Western and the Eastern ones, connected by the relatively shallow Strait of Sicily (sill depth ~ 500 m). In each basin a number of sub-basins are characterized by different water masses circulations, chemical and biological features and rough bottom topography. Note that we reserve the term ‘‘sea’’ for the Mediterranean Sea and ‘‘basin’’ for the Eastern and Western parts of it; any smaller entity is a sub-basin.

The Mediterranean Sea is a particular system, characterized by a complex thermohaline, wind, and water flux-driven multi-scale circulation with interactive variability [8]. This land-locked sea is exporting warm and salty intermediate waters to the North Atlantic Ocean by the narrow and shallow Strait of Gibraltar [width ~ 13 km ; sill depth ~ 300 m] affecting the global thermohaline conveyor belt [9] [10]. Through pathways to the Atlantic Polar regions or through indirect mixing processes, the salty Mediterranean water preconditions the deep convection cells of the Polar Atlantic. There the North Atlantic Deep Water is formed and successively spreads throughout the world ocean constituting the core of the global thermohaline circulation [11] [12]. Thus, the salty water of Mediterranean origin may affect water formation processes and variability and even the stability of the global thermohaline equilibrium state. Hence, the study of the Mediterranean water masses (their formation, spreading, mixing, and impact on general circulation) is essential for a better understanding of the ocean circulation and variability. Moreover, the existence of a thermohaline cell (the Eastern Mediterranean “Conveyor Belt”), multiple scales of motion defining the general circulation (basin/sub-basin/mesoscale), and deep water mass formation processes, make this sea a “test basin” for general circulation studies.

Aiming to study the hydrographic situation in the Mediterranean Sea, many researchers have used an optimum multiparameter analysis ([13] in the Adriatic Sub-basin, and [14] in the Eastern Mediterranean Sub-basin; [15] in the Western Mediterranean Sub-basin; [16] in the entire Mediterranean Sea). However, a study of the evolution of water mass mixing coefficients in this semi-enclosed sea is needed to better understand the hydrographic system in this sea. Reference [17] introduced the MIX approach based upon an optimum multiparameter mixing analysis. The use of this approach is particularly recommended for regional studies where the distribution of water masses can be clearly defined (this is the case of the Mediterranean Sea). In the present paper, our main objective is to evaluate the variation (if any) of the water mass circulation in the Mediterranean Sea based on their mixing coefficients calculated via the MIX approach using data collected in 2008 and 2013.

2. Methodology

2.1. Study Area

The BOUM cruise (Biogeochemistry from the Oligotrophic to the Ultra oligotrophic Mediterranean Sea [18]) was conducted during summer 2008, from 20 June to 22 July, on board the R/V L'Atalante [19]. It consists of a longitudinal transect (more than 3000 km long from the Levantine Sub-basin to the Northwestern Mediterranean Sea) of 27 short-term stations and 3 long-term stations referred as A, B, and C (Fig.1).

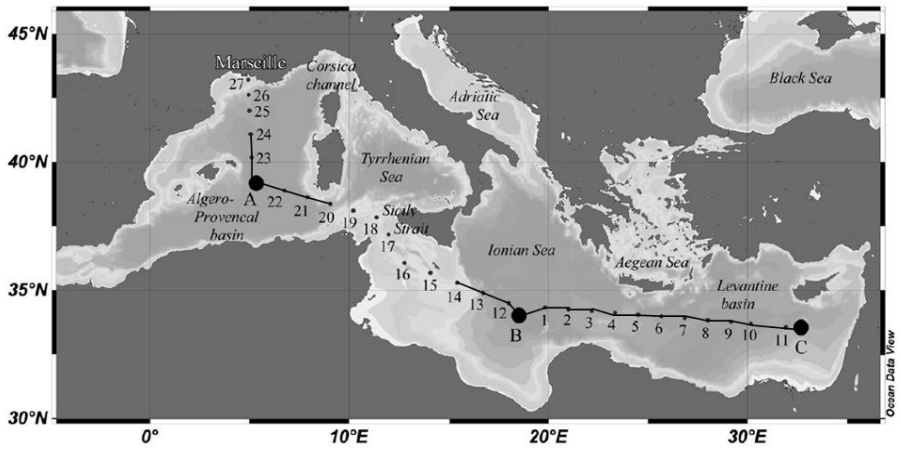

Figure 1. Map of the 2008 BOUM cruise in the Mediterranean Sea. Short-term stations are indicated by numbers (from 1 to 27); the three long-term stations are referred as A, B, and C (Touratier et al., 2012). The thick black lines referred to the sections used in this study.

The MedSeA (Mediterranean Sea Acidification in a Changing Climate; [20] [21]) cruise occurred during spring 2013, on board of the Spanish R/V Angeles Alvariño, from 2 May to 2 June.

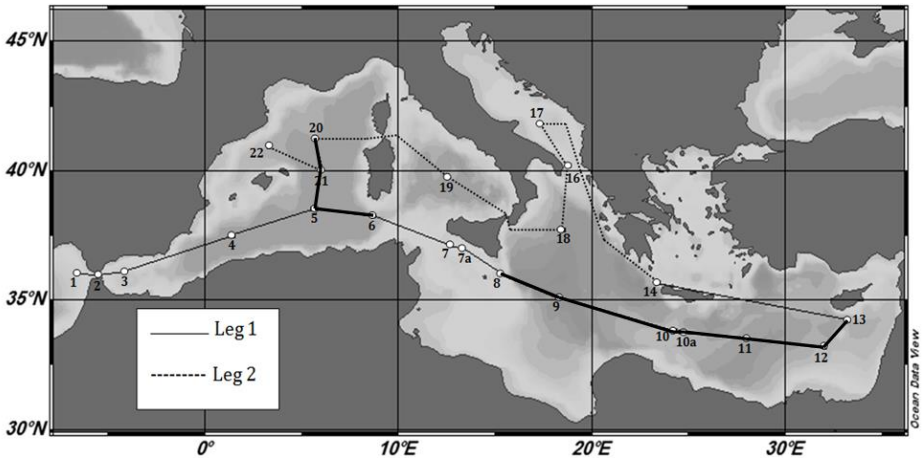

Figure 2. Map of the 2013 MedSeA cruise in the Mediterranean Sea. The numbers from 1 to 22 correspond to the sampled stations. The thick black lines referred to the sections used in this study.

The full cruise track (more than 8000 km long) consisted of two longitudinal legs where 23 stations along the Mediterranean Sea were sampled throughout the water column. During the first leg, samples were collected from Atlantic waters off Cadiz, Spain to the Levantine Sub-basin in the Eastern Mediterranean basin (3879 km long, 15 stations, 279 sampled points, maximum sampled depth = 3720 m). The second leg was conducted in the Northern part of the Mediterranean from Heraklion, Crete, Greece in the Eastern Mediterranean basin to Barcelona, Spain in the North Western Mediterranean basin (3232.5 km long, 8 stations, 183 sampled points, maximum sampled depth = 3000 m ; Fig.2).

2.2. Sampling and Measurements

In the present study, we use the following properties: potential temperature (θ ; °C), salinity (S), dissolved oxygen (O_2 ; μmol kg^{-1}), nitrates (NO_3 ; μmol kg^{-1}), and phosphates (PO_4 ; μmol kg^{-1}). For the 2008 BOUM cruise, the profiles for θ, S, and O_2 were obtained using a Sea-Bird Electronics 911 PLUS CTD system. Each CTD cast was associated with a carousel of 24 Niskin bottles to collect seawater samples used to perform the analysis of the other chemical and biological properties. Concerning the nutrients (NO_3 and PO_4), the description of the methods used for the analysis are explained by [22] and [23].

For the 2013 MedSeA cruise, hydrologic properties [S and T (ºC)] were measured *in situ* using a Sea-Bird Electronics CTD system (SBE 911plus) associated with a General Oceanic rosette sampler, equipped with twenty four 12 L Niskin bottles. The precision of measurements is ± 0.001 ºC for T and ± 0.0003 for S. Water samples for dissolved oxygen determination were collected in calibrated BOD 60 ml bottles. Oxygen concentrations were measured using a Winkler iodometric titration [24] with a Mettler-Toledo. DL-21 potentiometric titrator with a Pt ring redox electrode for the determination of the equivalence point [25]. The analytical precision and accuracy are ± 1.5 μmol kg^{-1}. For the nitrates (NO_3) and phosphates (PO_4), water samples were pre-filtered over glass fiber filters (Whatman GF/F) with a pore size of 0.7 microns, immediately after sampling. Then, they were stored at -20°C in polyethylene bottles until their analysis. The samples were thawed and analyzed colorimetrically with a Bran + Luebbe 3 autoanalyzer according to [26], at OGS laboratory in Trieste, Italy.

2.3. Modeling: The MIX Approach

Aiming to quantify the contribution of the different water sources to the collected data, we used the MIX approach developed by [17]. This approach uses a multi-parameter analysis. Optimum multiparameter methods [27] [28] are based on the assumption that observed water properties at a hydrographic station are the result of mixing among two or more ‘‘source waters’’. They have been used to evaluate water mass properties in both the Southern Ocean [29] [30] and other regions [28] [31].

In the present study, four conservative tracers (S, θ, NO, and PO) are used in the MIX approach. Reference [32] defined the conservative tracers NO and PO as follows:

$$NO = O_2 + R_{ON}NO_3 \qquad (1)$$

$$PO = O_2 + R_{OP}PO_4 \qquad (2)$$

where NO and PO are composite tracers of the non conservative tracers O_2 (dissolved oxygen concentration in µmol kg^{-1}) and NO_3 (nitrate concentration in µmol kg^{-1}), and PO_4 (phosphate concentration in µmol kg^{-1}), respectively. According to the equation of [33] which describes the average photosynthesis and aerobic respiration in the interior of the ocean, the composite tracers NO and PO were built using the fact that the consumption of oxygen is balanced by the production of nutrients during the processes of respiration and decomposition. The two constants R_{ON} and R_{OP} are the ratios of the stoechiometric coefficients (ψ) involved in the Redfield equation ($R_{ON} = \psi O_2/\psi NO_3$; $R_{OP} = \psi O_2/\psi PO_4$).

The general conservation equation for a conservative tracer (Ω) is given by:

$$\Omega = \sum_{j=1}^{n} Kj\ \Omega j \qquad (3)$$

where K_j represents the contribution (also called "mixing coefficient") of a water source j, n is the number of water sources in the system, and Ω_j is the value of the conservative tracer for the water source j.

For each seawater sample, where the conservative tracers Ω are either measured (S and θ) or calculated (NO and PO ; see equations 1 and 2), the contributions K_j are estimated after resolving the system of equations with the following constraints :

$$\sum_{j=1}^{n} Kj = 1 \text{ (mass conservation)} \qquad (4)$$

$$\forall_j,\ 0 \le K_j \le 1 \qquad (5)$$

It is a constrained linear least-squares problem, with one equality constraint and n inequality constraints. To solve it, we use a medium-scale optimization algorithm (with MATLAB) similar to that described by [34]. The difference in range between tracers leads to an ill-conditioned problem: the linear equation solution involves the inversion of the matrix containing the water sources characteristics, but this matrix is really badly scaled. So, prior to the inversion, rows and columns of the matrix are normalized. The stability of the results (linked to the correct placement of sources) is then tested by adding thirty perturbations to the values of Ω and the Ω_j which provide at each point a mean solution for each K_j [17]. These perturbations are independent Gaussian random variables with zero mean and given standard deviation. We entered the standard deviations for each tracer with a given value for the measurement points and another (larger) value for sources. These thirty Gaussian perturbations allowed us not only to test the stability of the results but also to take into account the differences between the errors of measurement based on the tracers.

2.4. Determination of the Water Sources

The Appropriate definition of water source properties is crucial to achieving physically meaningful results from the MIX approach. The different water sources j were typically identified using the conservative tracers S and θ, their corresponding θ/S diagrams (Fig. 3 and 6) and referring to the literature. In order to lower the number of water sources, the Mediterranean Sea was tested as two independent systems : the Western basin (5° E ≤ longitude ≤ 9.5°E) and the Eastern basin (longitude ≥ 15°E). Consequently, the relatively shallow stations located in the Sicily Strait between 9.5°E and 15°E were ignored when the MIX approach was applied.

Table 1. Physical and chemical properties of water sources used by the MIX approach in the Western Mediterranean basin for BOUM 2008 and MedSeA 2013.

Water Sources	Depth	T (°C)	S	θ (°C)	NO_3 (µmol kg^{-1})	PO_4 (µmol kg^{-1})	O_2 (µmol kg^{-1})
BOUM 2008							
AW	50	17.21	37.269	17.20	0.00	0.002	240.8
EOW	50	15.12	38.163	15.12	0.05	0.032	259.0
LIW	496	14.15	38.853	14.07	5.69	0.192	181.8
TDW	2839	13.31	38.472	12.86	8.61	0.391	196.2
WMDW	1483	13.08	38.459	12.86	8.78	0.383	190.0
MedSeA 2013							
AW	50	16.17	36.607	16.16	0.63	0.058	234.8
EOW	50	15.12	38.163	15.12	0.05	0.032	259.0
LIW	496	14.15	38.853	14.07	5.69	0.192	181.8
TDW	2839	13.31	38.472	12.86	8.61	0.391	196.2
WMDW	1483	13.08	38.459	12.86	8.78	0.383	190.0

AW, Atlantic Water;
EOW, Effluent Outflow Water;
LIW, Levantine Intermediate Water;
TDW, Tyrrhenian Deep Water;
WMDW, Western Mediterranean Deep Water.

For the Western basin, we used five water sources (n = 5). Whereas, six ones were used for the Eastern basin (n = 6). The physical and chemical properties of these water sources, for both BOUM 2008 and MedSeA 2013 cruises, are shown in Tables 1 and 2 for the Western and the Eastern Mediterranean basins respectively. These water sources were identified based on the data of the two cruises and on the availability of the input parameters (S, θ, O_2, NO_3, PO_4) manipulated by MIX approach to calculate the mixing coefficients. The main water sources are indicated on the corresponding θ/S diagrams of the Western and Eastern basins (Fig. 3 and 4). When the water sources of the MedSeA cruise have similar θ/S characteristics compared to the BOUM ones, we decided to take into consideration the characteristics of the BOUM water masses in our mixing coefficients calculation to maintain the same ratios previously calculated for the Mediterranean Sea based on the 2008 BOUM cruise.

Table 2. Physical and chemical properties of water sources used by the MIX approach in the Eastern Mediterranean basin for BOUM 2008 and MedSeA 2013.

Water Sources	Depth	T (°C)	S	θ (°C)	NO_3 (µmol kg^{-1})	PO_4 (µmol kg^{-1})	O_2 (µmol kg^{-1})
BOUM 2008							
MAW	73	15.73	37.618	15.72	0.00	0.001	239.7
EOW	174	15.59	38.436	15.56	2.37	0.102	205.9
LIW	248	16.25	39.163	16.21	0.96	0.013	220.6
CIW	173	15.17	39.045	15.14	3.34	0.090	204.9
EMDW-Adr	2965	13.86	38.710	13.38	4.91	0.142	195.4
EMDW-Ag	2222	14.00	38.789	13.64	4.84	0.167	189.3
MedSeA 2013							
MAW	50	17.72	38.873	17.72	0.01	0.029	241.3
EOW	174	15.59	38.436	15.56	2.37	0.102	205.9
LIW	248	16.25	39.163	16.21	0.96	0.013	220.6
CIW	173	15.17	39.045	15.14	3.34	0.090	204.9
$EMDW_{Adr}$	950	13.18	38.702	13.04	1.65	0.087	219.7
$EMDW_{Ag}$	2222	14.00	38.789	13.64	4.83	0.167	189.3

MAW, Modified Atlantic Water;
EOW, Effluent Outflow Water ;
LIW, Levantine Intermediate Water ;
CIW, Cretan Intermediate Water ;
$EMDW_{Adr}$, Eastern Mediterranean Water-Adriatic origin; $EMDW_{Ag}$, Eastern Mediterranean Deep Water-Aegean origin.

2.5. Determination of the Redfield Ratios R_{ON} and R_{OP}

Typical values given by [33] are R_{ON} = 8.6 and R_{OP} = 138 (molar ratios). However, these ratios cannot be representative for the Mediterranean waters since [33] never used observations from this region. In this paper, we use the R_{ON} and R_{OP} ratios previously estimated, specifically for the Mediterranean Sea by [35] using the 2008 BOUM database. The best results for the regressions between the nutrients and O_2 were obtained after considering two different layers for both the Western and the Eastern basins : the surface/intermediate layer (from 50 up to 750 m), and the deep layer (from 750 m to the bottom). We hypothesize that these layers are related to the traditional Mediterranean circulation scheme which is described by two cells [36] : the well ventilated surface cell which contains water masses like MAW, WIW, and LIW ; and the deep cells which contains the WMDW and TDW in the Western basin, and the $EMDW_{Adr}$ and $EMDW_{Ag}$ in the Eastern basin.

3. Results and Discussion

In order to assess the goodness of the solutions and to check possible errors due to the water-source description and to uncertainties associated with the measurements, the residual vector was calculated for each of the four conservative tracers. This vector corresponds to the difference between the predicted and the measured data. For BOUM 2008 and MedSeA 2013, the MIX method performs well, producing unbiased small residuals (always less than 10%) for all measures. Hereafter, we discuss the evolution of the main water sources mixing coefficients for the Western and Eastern Mediterranean basins.

3.1. Western Basin

3.1.1. Atlantic Water, AW

The mixing coefficients of the surface water masses did not change significantly since 2008 till 2013 (Fig.5). The Mediterranean Sea has an active water exchange with the Northern Atlantic through the Strait of Gibraltar. The surface Atlantic flow entering the Mediterranean Sea does not only fill the water deficit of 1 m per year, but it also replaces the Mediterranean deep outflow, which represents a loss of 20 m of water per year for the whole Mediterranean Sea [37]. As a consequence of the excess of evaporation over precipitation (~ 0.62 – 1.16 m year^{-1}) [38], heating and various physical phenomena (gyres, eddies), the proportion of the AW decreases progressively because its characteristics change while propagating Eastward to be referred as Modified Atlantic Water (MAW). This trend was comparable during the two oceanographic surveys (BOUM 2008 and MedSeA 2013).

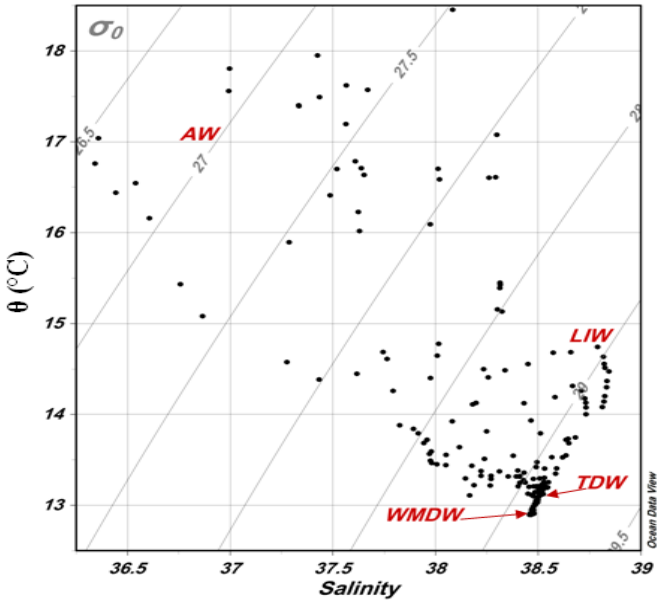

Figure 3. θ/S diagram illustrating the main water masses detected in the Western basin during the MedSeA cruise in May 2013 (AW: Atlantic Water, LIW: Levantine Intermediate Water, TDW: Tyrrhenian Deep Water, WMDW: Western Mediterranean Deep Water).

3.1.2. Levantine Intermediate Water, LIW

The amount of this water mass has increased during the study period (2008-2013). For example, its proportion increased from 0.55 in 2008 to 0.9 in 2013 within the intermediate layers (~ 300 m) of the Sardinia Strait (Fig.5). The LIW contributes predominately to the non-returning efflux, mixed with both EMDW and WMDW in the Strait of Gibraltar, and to the outflow into the Atlantic Ocean [2] [8] [39]. Our results show recent changes in the Mediterranean outflow. These increasing proportions could be caused by the excessive evaporation and the decrease in precipitation and freshwater supplies to the Eastern Mediterranean Sea [40] which can be direct consequences of the unequivocal global warming [41]. Decreasing trends of river discharges in the Eastern Mediterranean Sea [42] has been observed, as in the Adriatic Sub-basin [43].

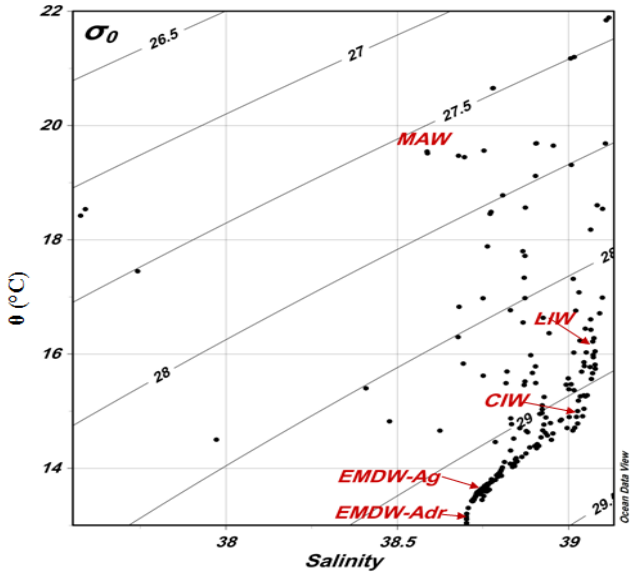

Figure. 4. θ/S diagram illustrating the main water masses detected in the Eastern basin during the MedSeA cruise in May 2013 (MAW: Modified Atlantic Water, LIW: Levantine Intermediate Water, CIW: Cretan Intermediate Water, EMDW-Ag: Eastern Mediterranean Deep Water originated from the Aegean Sub-basin, EMDW-Adr: Eastern Mediterranean Deep Water originated from the Adriatic Sub-basin).

3.1.3. Tyrrhenian Deep Water, TDW

The proportion of this water mass has clearly decreased below 1000 m in the Western basin. Its amount during 2013 become less abundant in the Southern sub-basins compared to the one recorded for 2008 (Fig.5). This water, which is a product of the mixing between Eastern (LIW and EMDW) and western waters (WMDW), fills the Tyrrhenian Sub-basin down to the bottom [44]. Thus, this decrease could be attributed to the modification in the EMDW formation, since the Adriatic Sub-basin seems to retrieve its role as a main contributor in the deep water mass formation in the Eastern basin instead of the Aegean during the EMT (Eastern Mediterranean Transient ; data of the MedSeA cruise 2013). However, [45] argue that the TDW might result from a dense water formation process occurring within the Tyrrhenian itself, in the East of the Bonifacio Strait. This means that the decrease in the mixing proportion could also be attributed to climatic changes affecting temperature and salinity, thus the deep water formation. Nevertheless, the mixing coefficients proportions of the TDW have slightly increased from 0.05 in 2008 to 0.2 in 2013, exclusively in the North of the Western basin between 0 and 500 m. This fact could be firstly related to the harsh winter convective mixing in this wind-driven area [46]. Secondly, this smooth proportions increase could be also connected to the mixing caused by heavy freshwater inputs from the Northern rivers during May (time of the snow melting) [47].

3.1.4. Western Mediterranean Deep Water, WMDW

The mixing coefficients schemes of this water mass (Fig.5) show that its amount decreased slightly below 1000 m, between 2008 and 2013, particularly in the South of the Western basin. The WMDW remains well distributed in the Western basin with higher proportions in the North of this basin, where it is originated (Fig.5).

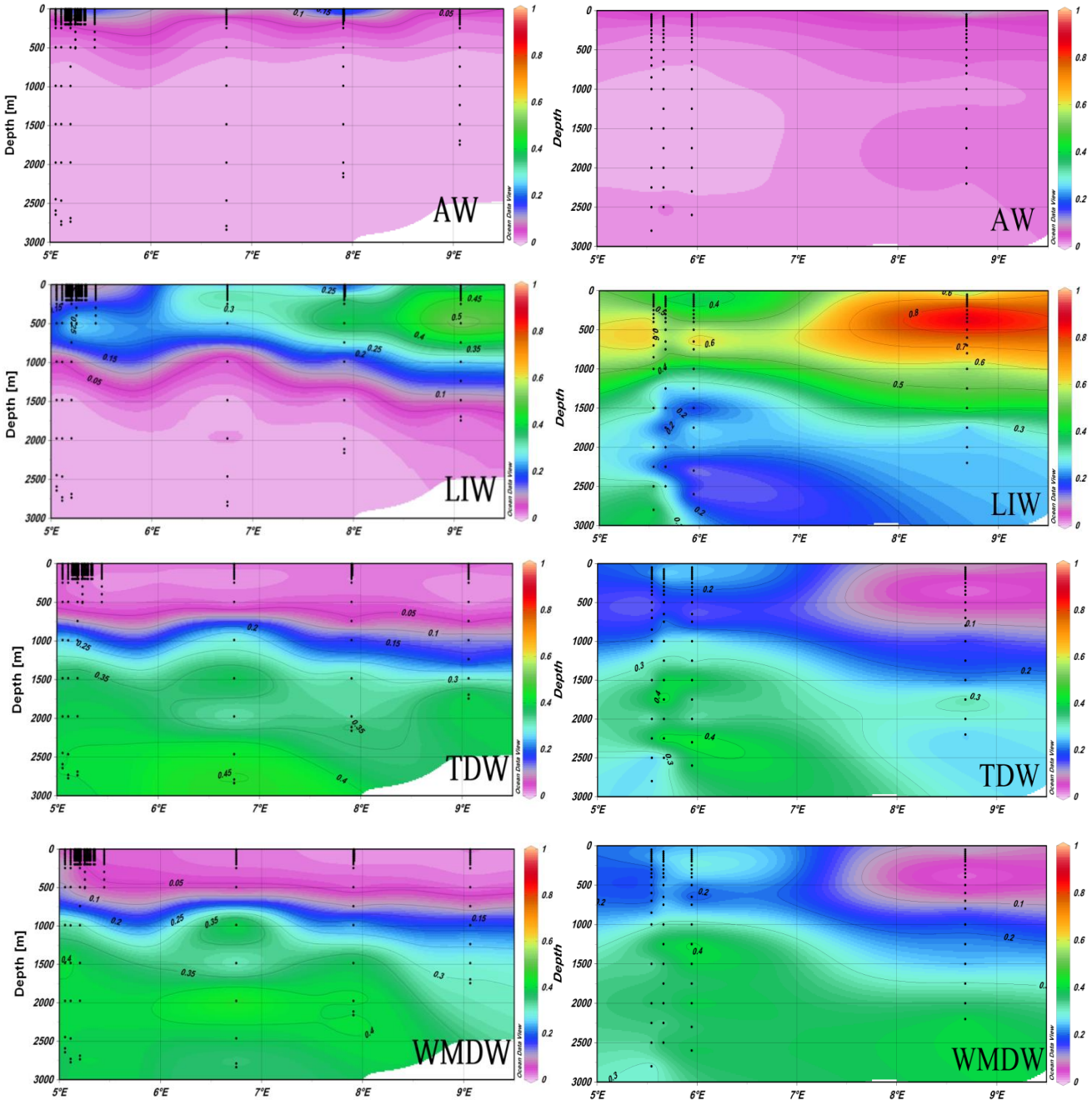

Figure 5. Profiles of the mixing coefficients of water masses in the Western Mediterranean basin during the 2013 MedSeA cruise (right column) and the 2008 BOUM cruise (left column)

The observed decrease could be due to the significant warming and salinification, widely mentioned in the literature [48] [49] [50] [51] [52]. However, at a station in the south of the Tyrrhenian Sub-basin sampled in September 1999 during the PROSOPE cruise [53], the total alkalinity in deep water was higher than in deep water at the Dyfamed site [54]. If it is confirmed that the Tyrrhenian deep water contributes to the deep water in the Liguro-Provençal Sub-basin, this observation could explain the modifications in the WMDW proportions which could also be attributed to the changes in the TDW linked to the Eastern

deep water formation. Based on 23 years eddy-permitting reanalysis, [55] argued that the largest water mass formation event of the past 23 years occurred in the Western Mediterranean basin in 2005-2006. This event was presumably preconditioned by the EMT which modified the characteristics of the LIW crossing the Sicily Strait.

3.2. Eastern Basin

However, similarly to the TDW, a slight rise of the mixing coefficients has been registered within the layer above 1000 m in the Northern part of the Western basin. This boost could also be attached to the vertical mixing related to the tough meteorological winter conditions in the Gulf of Lions, as well as in Balearic and Liguro-Provençal Sub-basins [46] [56].

3.2.1. Modified Atlantic Water, MAW

The proportion of the MAW increased from 2008 to 2013. During 2013, it is clear that its amount increases while propagating Eastward from the Sicily Strait (Fig.6). This water mass is initially made as a result of the mixing of comparatively fresh Atlantic water ($S < 36.5$) flowing via the Strait of Gibraltar into the Mediterranean Sea with the surface waters of the Alboran Sub-basin [57]. The incoming MAW is continuously modified by interactions with the atmosphere and mixing with older surface waters and with the waters underneath. All along its course, it is seasonally warmed or cooled, but overall its salt content increases and it becomes denser [58]. Thus, its increasing proportion could be attributed to the excessive evaporation trend in the context of global warming occurring in the Mediterranean Sea [59] [60]. Satellite observations from 1985–2006 indicate that in the last two decades the temperature in the upper layer of the Mediterranean Sea has been increasing at an average (± SD) rate of 0.03 ± 0.008°C yr^{-1} for the Western basin and 0.05 ± 0.009°C yr^{-1} for the Eastern basin [60]. Nevertheless, these changes could also be due to the modifications in circulation patterns leading to blocking situations during the EMT (i.e. gyres, eddies, …), to the Adriatic-Ionian Bimodal Oscillating System (BiOS) [61] and/or to variations in the fresher water of Black Sea origin input through the Strait of Dardanelles [8].

3.2.2. Levantine Intermediate Water, LIW

The amount of this water mass has increased during the study period (2008-2013; Fig.6). Its proportion increased from 0.27 in 2008 to 0.37 in 2013 within the intermediate layers (~ 175 m) in the South of Cyprus. The increasing proportion could be related to the occurrence of high amount of MAW in this area which becomes denser. Thus, this latter sinks more quickly to participate in the formation of the LIW. This fact could be caused by the excessive evaporation and the decrease in precipitation and freshwater supplies to the Mediterranean Sea. This can be direct consequences of the global warming, well described in literature [62] [63] [64].

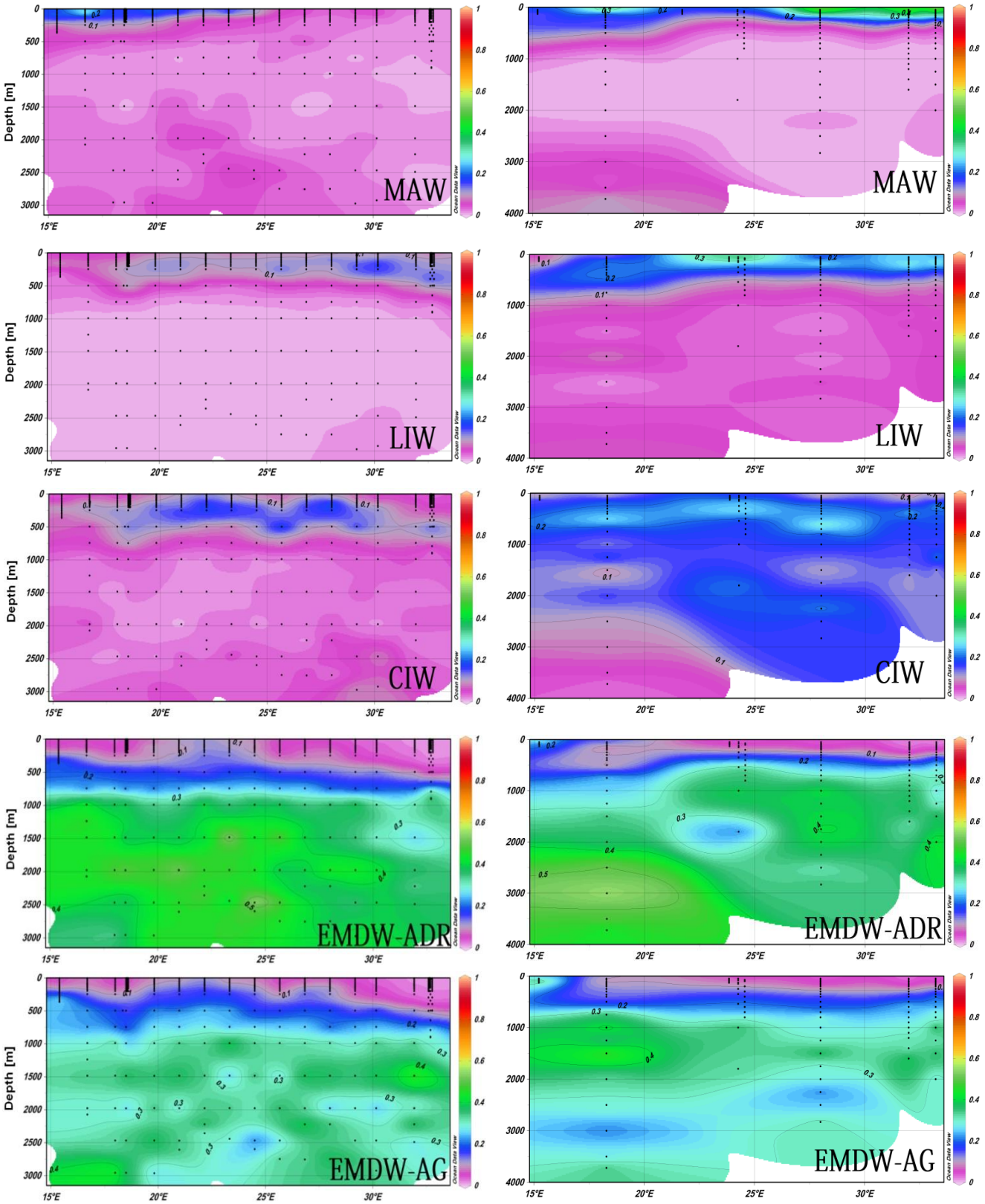

Figure 6. Profiles of the mixing coefficients of water masses in the Eastern Mediterranean basin during the 2013 MedSeA cruise (right column) and the 2008 BOUM cruise (left column).

3.2.3. Cretan Intermediate Water, CIW

The proportion of this intermediate water mass has increased in the entire Eastern basin, particularly in the South of Crete where it has the highest proportions (~ 0.35 at ~ 170 m; Fig. 6). This fact is due to changes in circulation patterns leading to blocking situations concerning the MAW and the LIW, and to variations in the fresher water of Black Sea origin input through the Strait of Dardanelles [8] [42]. These results could also be attributed to specific atmospheric conditions which created large buoyancy fluxes from the Aegean Sub-basin, similarly to the ones mentioned by [65] during winters 1991/1992 and 1992/1993 (the "enhanced EMT winters"), intensifying intermediate and deep water production, although with modified characteristics [66].

3.2.4. Eastern Mediterranean Deep Water Originated in the Adriatic Sub-Basin, $EMDW_{Adr}$

During the study period, it is clear that the mixing coefficients of the $EMDW_{Adr}$ decreased in the Levantine Sub-basin from a range of 0.33-0.4 to 0.2-0.39 in deep layers (below 1000 m ; Fig. 6). However, its mixing proportion remains high in the South of the Ionian Sub-basin (~ 0.54). These results indicate that the $EMDW_{Adr}$ stays a minor deep water mass in the Levantine Sub-basin. Moreover, it shows that the EMDW originated from the Adriatic Sub-basin is reaching the South of the Ionian Sub-basin but maybe physical phenomena (like the more defined open ocean, free jet intensified structures mentioned by [55] : the Atlantic-Ionian Stream and the Mid-Mediterranean Jet in the Eastern basin) are disabling its dissemination all over the Eastern basin.

3.2.5. Eastern Mediterranean Deep Water Originated in the Aegean Sub-Basin, $EMDW_{Ag}$

The mixing coefficients of this water mass show a remarkable increase, particularly in the Levantine Sub-basin (from 0.29 to 0.54 at 1500 m ; Fig.6). The steady occurrence of this dominant deep water mass in the Levantine Sub-basin, instead of $EMDW_{Adr}$, could be due to many factors : 1- the waters formed in the Aegean Sub-basin still sufficiently denser than those originated in the Adriatic one, hence, it is able to enter the deep layers of the Eastern basin and not address the intermediate water range depth [67], 2- the deep water formation in the Adriatic Sub-basin seems to be significantly impacted by the EMT [68], thus it is not able to match its previous distribution in the Eastern basin, 3- the atmospheric and physical conditions favorable for the formation of this dense water still dominant in this area, 4- our results could also be attributed to the long residence time of deep water masses in the Levantine Sub-basin due the robust topography which could trap the deep waters for a long period (~ 100 years) [69] [70].

4. Conclusion

Overall, based upon data from the 2008 BOUM and 2013 MedSeA cruises, the present study shows a significant evolution of some water masses mixing coefficients, calculated via the MIX approach. Surface water mass proportions did not change significantly. However, intermediate and deep water mass mixing coefficients of both Eastern and Western basins were noticeably modified. Moreover, these results indicate that the mixing coefficient of the $EMDW_{Adr}$ is always high in the Ionian Sub-basin, while it remains low in the Levantine Sub-basin compared to the $EMDW_{Ag}$. Furthermore, the observed decrease of the mixing coefficient in the deep Western water masses (TDW, WMDW) is mainly attributed to changes in the deep Eastern water masses circulation. This study proves that the hypothesis of "steady state" situation for the Mediterranean Sea is far from being validated. This sea witnesses continuous and significant water masses changes [ex. The Eastern Mediterranean Transient, EMT [66] [71] [72] [73] [74], changes in circulation pattern in the Ionian Sub-basin which affect the contiguous sub-basins [61] [75]. Therefore, this work could be an incentive for further studies to innovate new oceanic models that take into considerations the unsteady state situation of the water masses circulation in the Mediterranean Sea (and probably in other oceanic areas). In the context of the global warming, further measurements of these water masses properties are necessary, to assess their evolutions and to evaluate the consequences of any modification on the global circulation.

Acknowledgements

This work was funded by the EC FP7 "Mediterranean Sea Acidification in a changing climate – MEDSEA" project (MedSeA ; grant agreement 265103 ; medsea-project.eu). The authors are pleased to thank the captains and the crew of the Spanish research vessel R/V Ángeles Alvariño. They would like furthermore to thank Mr. Michael GRELAUD for uploading the data of this cruise on Pangaea data repository [76, 77, 78, 79, 80]. Authors are grateful to the National Council for Scientific Research (CNRS) in Lebanon for the Ph.D. thesis scholarship granted to Mr. Abed El Rahman HASSOUN.

References

[1] Mariotti A., Struglia M.V., Zeng N., Lau K.-M., 2002. The Hydrological Cycle in the Mediterranean Region and Implications for the Water Budget of the Mediterranean Sea. Journal of Climate, 15, 1674–1690.

[2] Manca B., Burca M., Giorgetti A., Coatanoan C., Garcia M.-J., Iona A., 2004. Physical and biochemical averaged vertical profiles in the Mediterranean regions: an important tool to trace the climatology of water masses and to validate incoming data from operational oceanography. Journal of Marine Systems, 48, 83–116.

[3] Castellari S., Pinardi N., Leaman K., 2000. Simulation of water mass formation processes in the Mediterranean Sea : influence of the time frequency of the atmospheric forcing. Journal of Geophysical research, 105 (C10), 24157-24181.

[4] Malanotte-Rizzoli P., 1991. The Northern Adriatic Sea as a prototype of convection and

water mass formation on the continental shelf. In: Chu, P.C., Gascard, J.C. (Eds.), Deep Convection and Deep Water Formation in the Oceans. Elsevier Oceanography Series. 57. Elsevier, Amsterdam, pp. 229– 239.

[5] POEM Group, 1992. General circulation of the Eastern Mediterranean Sea. Earth-Science Reviews, 32, 285–308.

[6] Moore W.S., 2006 a. The role of submarine groundwater discharge in coastal biogeochemistry. Journal of Geochemical Exploration, 88, 389–393, doi:10.1016/j.gexplo.2005.08.082.

[7] Moore W. S., 2006 b. Radium isotopes as tracers of submarine groundwater discharge in Sicily. Continental Shelf Research, 26, 852–861, doi:10.1016/j.csr.2005.12.004.

[8] Robinson A.R., Leslie W., Theocharis A., Lascaratos A., 2001. Mediterranean Sea circulation. Encyclopedia of Ocean Science, Vol. 3. Academic Press, San Diego, CA, pp. 1689–1705.

[9] Lacombe H. and Richez C., 1982. The Regime of the Strait of Gibraltar. Hydrodynamics of Semi-Enclosed Seas. Proceedings of the 13th International Liege Colloquium on Ocean Hydrodynamics. Elsevier Oceanography Series, 34, 13–73.

[10] Bergamasco A. and Malanotte-Rizzoli P., 2010. The circulation of the Mediterranean Sea: a historical review of experimental investigations. Advances in Oceanography and Limnology, 1 (1), 11–28.

[11] Candela J., 2001. Mediterranean water and the global circulation. In: Siedler, G., Chuch, J., Gould, J., (Eds.), Ocean circulation and Climate. Observing and modeling the global ocean. Academic Press, New York, pp. 419–429.

[12] Malanotte-Rizzoli P. and the Pan-Med Group, 2012. Physical forcing and physical/biochemical variability of the Mediterranean Sea: A review of unresolved issues and directions of future research. Report of the Workshop "Variability of the Eastern and Western Mediterranean circulation and thermohaline properties: similarities and differences", Rome, 7-9 November, 2011, pp. 48.

[13] Cardin V., Bensi M., and Pacciaroni M., 2011. Variability of water mass properties in the last two decades in the South Adriatic Sea with emphasis on the period 2006–2009. Continental Shelf Research, 5 (31), 951–965.

[14] Kovačević V., Manca B.B., Ursella L., Schroeder K., Cozzi S., Burca M., Mauri E., Gerin R., Notarstefano G., and Deponte D., 2012. Water mass properties and dynamic conditions of the Eastern Mediterranean in June 2007. Progress in Oceanography, 104, 59–79.

[15] Schroeder K., Borghini M., Cerrati G., Difesca V., Delfanti R., Santinelli C., et Gasparini G.P., 2008. Multiparametric mixing analysis of the deep waters in the western Mediterranean Sea. Chemistry and Ecology, 24 (1), 47–56.

[16] Hainbucher D., Rubino A., Cardin V., Tanhua T., Schroeder K., and Bensi M., 2013. Hydrographic situation during cruise M84/3 and P414 (spring 2011) in the Mediterranean Sea. Ocean Science Discussion, 10, 2399–2432, doi:10.5194/osd-10-2399-2013

[17] Goyet C., Coatanoan C., Eischeid G., Amaoka T., Okuda K., Healy R., and Tsunogai S., 1999. Spatial variation of total CO_2 and total alkalinity in the northern Indian Ocean: A novel approach for the quantification of anthropogenic CO_2 in seawater. Journal Of Marine Research, 57, 135–163, doi: 10.1357/002224099765038599.

[18] BOUM (Biogeochemistry from the Oligotrophic to the Ultra-oligotrophic Mediterranean): http://www.com.univ-mrs.fr/BOUM/. Moutin T. and Torre M.P., Centre d'oceanologie de Marseille - Campus de Luminy.

[19] Moutin T., Van Wambeke F., and Prieur L., 2012. Introduction to the Biogeochemistry from the Oligotrophic to the Ultraoligotrophic Mediterranean (BOUM) experiment.

Biogeosciences, 9, 3817–3825, doi:10.5194/bg-9-3817-2012
[20] MedSeA (Mediterranean Sea Acidification in a changing climate) project, 2015 : http://medsea-project.eu/
[21] 2013 MedSeA research cruise on ocean acidification and warming : http://medseaoceancruise.wordpress.com/
[22] Pujo-Pay M., Conan P., Oriol L., Cornet-Barthaux V., Falco C., Ghiglione J.-F., Goyet C., Moutin T., and Prieur L., 2011. Integrated survey of elemental stoichiometry (C, N, P) from the western to eastern Mediterranean Sea. Biogeosciences, 8, 883–899, doi: 10.5194/bg-8-883-2011.
[23] Crombet Y., Leblanc K., Quéguiner B., Moutin T., Rimmelin P., Ras J., Claustre H., Leblond N., Oriol L., and Pujo-Pay M., 2011. Deep silicon maxima in the stratified oligotrophic Mediterranean Sea. Biogeosciences, 8, 459–475, doi: 10.5194/bg-8-459-2011.
[24] Hansen H.P., 1999. Determination of oxygen. In: Grasshoff, K., Kremling, K., Ehrhardt, M., Methods of Seawater Analysis, 3rd Edition, Wiley-VCH, Weinheim, pp. 600.
[25] Outdot C., Gerard R., Morin P., 1988. Precise shipboard determination of dissolved oxygen (Winkler procedure) for productivity studies with commercial system. Limnology and Oceanography, 33, 146-150. Edition, Wiley-VCH, Weinheim, pp. 600.
[26] Grasshoff K., Kremling K., Ehrhardt M., 1999. Methods of Seawater Analysis, 3rd ed. Wiley-VCH, Weinheim, Germany.
[27] Tomczak M., 1981. A multiparameter extension of temperature/salinity diagram techniques for the analysis of non-isopycnal mixing. Progress in Oceanography, 10, 147–171.
[28] Tomczak M. and Large D.G.B., 1989. Optimum multiparameter analysis of mixing in the thermocline of the Eastern Indian Ocean. Journal of Geophysical Research, 94 (C11), 16141–16149.
[29] Budillon G., Pacciaroni M., Cozzi S., Rivaro P., Catalano G., Ianni C. and Cantoni C., 2003. An optimum multiparameter mixing analysis of the shelf waters in the Ross Sea. Antarctic Science, 15,105–118.
[30] Tomczak M. and Liefrink S., 2005. Interannual variations of water mass volumes in the Southern Ocean. Journal of Atmospheric and Ocean Science, 10, 31–42.
[31] Tomczak M. and Poole R., 1999. Optimum multiparameter analysis of the water mass structure in the Atlantic Ocean thermocline. Deep Sea Research Part I: Oceanographic Research Papers, 46, 1895–1921.
[32] Broecker W. S., 1974. “NO”, a conservative water-mass tracer, Earth and Planetary Science Letters, 23, 100–107, doi: 10.1016/0012-821X(74)90036-3.
[33] Redfield A.C., Ketchum B.H., and Richards F.A., 1963. The influence of organisms on the composition of seawater, in: The Sea, Hill M. N., pp. 26–77.
[34] Gill P.E., Murray W., Wright M.H., 1991. Numerical Linear Algebra and Optimization, Addison Wesley.
[35] Touratier F., Guglielmi V., Goyet C., Prieur L., Pujo-Pay M., Conan P., Falco C., 2012. Distributions of the carbonate system properties, anthropogenic CO_2, and acidification during the 2008 BOUM cruise (Mediterranean Sea). Biogeosciences Discussions, 9, 2709-2753, doi:10.5194/bgd-9-2709-2012.
[36] Malanotte-Rizzoli P., Manca B.B., D’ Alcala M.R., Theocharis A., Brenner S., Budillon G., and Ozsoy E., 1999. The Eastern Mediterranean in the 80s and in the 90s: the big transition in the intermediate and deep circulations. Dynamics of Atmospheres and Oceans, 29, 365–395, doi: 10.1016/S0377-0265(99)00011-1.
[37] Béthoux J.-P., 1980. Mean water fluxes across sections in the Mediterranean Sea, evaluated on the basis of water and salt budget and of observed salinities. Oceanologica

Acta, 3, 79–88.
[38] Hopkins T.S., 1978. Physical Processes in the Mediterranean basins. In: Kjerfve, B. (Eds.), Estuarine Transport Processes. Univ. of South Carolina Press, Columbia, SC. pp. 269–310.
[39] Özsoy E., Hecht A., Unluata U., Brenner S., Sur H.I., Bishop J., Latif M.A., Rozentraub Z., Oguz T., 1993. A synthesis of the Levantine Basin circulation and hydrography, 1985– 1990. Deep-Sea Research Part II: Topical Studies in Oceanography, 40, 1075–1119.
[40] Marcos M. and Tsimplis M.N., 2008. Comparison of results of AOGCMs in the Mediterranean Sea during the 21st century. Journal of Geophysical Research: Oceans, 113 (C12), doi: 10.1029/2008JC004820.
[41] IPCC, 2014. Climate Change 2014: Impacts, Adaptation, and Vulnerability. The Fifth Assessment Report of the Intergovernmental Panel on Climate Change.
[42] Ludwig W., Dumont E., Meybeck M., Heussner S., 2009. River discharges of water and nutrients to the Mediterranean and Black Sea : Major drivers for ecosystem changes during past and future decades? Progress in Oceanography, 80, 199–217.
[43] Cozzi S. and Giani M., 2011. River water and nutrient discharges in the northern Adriatic Sea : current importance and long term changes. Continental Shelf Research, 31, 1881–1893.
[44] Sparnocchia S., Gasparini G.P., Astraldi M., Borghini M., Pistek P., 1999. Dynamics and mixing of the Eastern Mediterranean outflow in the Tyrrhenian Sea. Journal of Marine Systems, 20, 301–317.
[45] Fuda J.-L., Etiope G., Millot C., Favali P., Calcara M., Smriglio G. and Boschi E., 2002. Warming, salting and origin of the Tyrrhenian Deep Water. Geophysical Research Letters, 29 (19), 41–44, doi: 10.1029/2001GL014072.
[46] Bakun A. and Agostini V.N., 2001. Seasonal patterns of wind-induced upwelling/downwelling in the Mediterranean Sea. Scientia Marina, 65, 243–257.
[47] Estrada M., 1996. Primary production in the northwestern Mediterranean. Scientia Marina, 60 (2), 55–64.
[48] Lacombe H., Tchernia P., Gamberoni L., 1985. Variable bottom water in the Western Mediterranean basin. Progress in Oceanography, 14, 319–338.
[49] Béthoux J.P., Gentili B., Raunet J., and Tailliez D., 1990. Warming trend in the western Mediterranean deep water. Nature, 347, 660–662, doi: 10.1038/347660a0.
[50] Rohling E.J. and Bryden H.L., 1992. Man-induced salinity and temperature increases in Western Mediterranean deep water. Journal of Geophysical Research, 97, 11191-11198.
[51] Vargas-Yáñez M., Moya F., García-Martínez M.C., Tel E., Zunino P., Plaza F., Salat J., Pascual J., López-Jurado J. L., and Serra M., 2010. Climate change in the Western Mediterranean Sea 1900–2008. Journal of Marine Systems, 82, 171–176.
[52] Malanotte-Rizzoli P., Artale V., Borzelli-Eusebi G.L., Brenner S., Crise A., Gacic M., Kress N., Marullo S., Ribera d'Alcalà M., Sofianos S., Tanhua T., Theocharis A., Alvarez M., Ashkenazy Y., Bergamasco A., Cardin V., Carniel S., Civitarese G., D'Ortenzio F., Font J., Garcia-Ladona E., Garcia-Lafuente J.M., Gogou A., Gregoire M., Hainbucher D., Kontoyannis H., Kovacevic V., Kraskapoulou E., Kroskos G., Incarbona A., Mazzocchi M.G., Orlic M., Ozsoy E., Pascual A., Poulain P.-M., Roether W., Rubino A., Schroeder K., Siokou-Frangou J., Souvermezoglou E., Sprovieri M., Tintoré J., and Triantafyllou G., 2014. Physical forcing and physical/biochemical variability of the Mediterranean Sea: a review of unresolved issues and directions for future research. Ocean Science, 10, 281–322, doi: 10.5194/os-10-281-2014.
[53] PROOF program, 2015, http://www.obsvlfr.fr/jgofs/html/prosope/home.htm.
[54] Copin-Montégut C. and Bégovic M., 2002. Distributions of carbonate properties and

oxygen along the water column (0-2000 m) in the central part of the NW Mediterranean Sea (Dyfamed site): influence of winter vertical mixing on air-sea CO2 and O2 exchanges. Deep-Sea Research Part II: Topical Studies in Oceanography, 49 (11), 2049–2066.

[55] Pinardi N., Zavatarelli M., Adani M., Coppini G., Fratianni C., Oddo P., Simoncelli S., Tonani M., Lyubartsev V., Dobricic S. and Bonaduce A., 2013. Mediterranean Sea large-scale low-frequency ocean variability and water mass formation rates from 1987 to 2007: A retrospective analysis. Progress in Oceanography, doi:10.1016/j.pocean.2013.11.003 (In Press).

[56] Millot C., 1979. Wind induced upwellings in the Gulf of Lions. Oceanologica Acta, 2, 261–274.

[57] Gascard J.C. and Richez C., 1985. Water masses and circulation in the western Alboran Sea and in the Strait of Gibraltar. Progress in Oceanography, 15, 157–216.

[58] Zavatarelli M., and Mellor G.L., 1995. A Numerical Study of the Mediterranean Sea Circulation. American Meteorological Society, 2013 GRID-Arendal.

[59] Millot C., Candela J., Jean-Luc F. and Youssef T., 2006. Large warming and salinification of the Mediterranean outflow due to changes in its composition. Deep Sea Research Part I: Oceanographic Research Papers, 53, 656–666.

[60] Nykjaer L., 2009. Mediterranean Sea surface warming 1985–2006. Climate Research, 39, 11–17, doi: 10.3354/cr00794

[61] Civitarese G., Gačić M., Lipizer M., and Eusebi Borzelli G. L., 2010. On the impact of the Bimodal Oscillating System (BiOS) on the biogeochemistry and biology of the Adriatic and Ionian Seas (Eastern Mediterranean). Biogeosciences, 7, 3987–3997, doi:10.5194/bg-7-3987-2010.

[62] Abboud-Abi Saab M., Romano J.-C., Bensoussan N., Fakhri M., 2004. Suivis temporels comparés de la structure thermique d'eaux côtières libanaises (Batroun) et françaises (Marseille) entre juin 1999 et octobre 2002. Comptes Rendus Geoscience, 336 (15), 1379–1390.

[63] IUCN and MedPanA, 2012. Changing mediterranean coastal marine environment under predicted climate-change scenarios. www.medpan.org and www.iucn.org/mediterranean

[64] Lelieveld J., Hadjinicolaou P., Kostopoulou E., El Maayar M., Hannides C., Lange M.A., Tanarhte M., Tyrlis E., Xoplaki E., 2012. Climate change and impacts in the Eastern Mediterranean and the Middle East. Climatic Change, 114 (3), 667–687, http://dx.doi.org/10.1007/s10584-012-0418-4.

[65] Romanski J., Romanou A., Bauer M., and Tselioudis G., 2012. Atmospheric forcing of the Eastern Mediterranean Transient by midlatitude cyclones. Geophysical Research Letters, 39 (L03703), doi: 10.1029/2011GL050298.

[66] Theocharis A., Klein B., Nittis K., Roether W., 2002. Evolution and status of the Eastern Mediterranean Transient (1997–1999). Journal of Marine Systems, 33–34, 91–116.

[67] Borzelli G. E., Gacic M., Lionello P., Malanotte-Rizzoli P., 2014. The Mediterranean Sea: Temporal Variability and Spatial Patterns. Geophysical Monograph Series. Editors: John Wiley & Sons, 2014, pp. 75-82.

[68] Vilibić I., Matijević S., Šepić J., and Kušpilić G., 2012. Changes in the Adriatic oceanographic properties induced by the Eastern Mediterranean Transient. Biogeosciences, 9, 2085–2097, doi: 10.5194/bg-9-2085-2012.

[69] Roether W., Manca B.B., Klein B., Bregant D., Georgopoulos D., Beitzel V., Kovačević V., and Luchetta A., 1996. Recent Changes in Eastern Mediterranean Deep Waters. Science, 271, 333–335, doi: 10.1126/science.271.5247.333.

[70] Stratford K., Williams R.G., and Drakopoulos P.G., 1998. Estimating climatological age from a model-derived oxygen-age relationship in the Mediterranean. Journal of Marine

Systems, 18, 215–226.
[71] Gasparini G.P., Ortonab A., Budillon G., Astraldi M. and Sansone E., 2005. The effect of the Eastern Mediterranean Transient on the hydrographic characteristics in the Strait of Sicily and in the Tyrrhenian Sea. Deep Sea Research Part I: Oceanographic Research Papers, 52 (6), 915–935.
[72] Schröder K., Gasparini G.P., Tangherlini M., and Astraldi M., 2006. Deep and intermediate water in the western Mediterranean under the influence of the Eastern Mediterranean Transient. Geophysical Research Letters, 33 (L21607, doi: 10.1029/2006GL027121.
[73] Touratier, F. and Goyet, C., 2011. Impact of the Eastern Mediterranean Transient on the distribution of anthropogenic CO2 and first estimate of acidification for the Mediterranean Sea. Deep Sea Research Part I: Oceanographic Research Papers, 58, 1–15.
[74] Tanhua T., Hainbucher D., Schroeder K., Cardin V., Alvarez M., and Civitarese G., 2013. The Mediterranean Sea system: a review and an introduction to the special issue. Ocean Sciences, 9, 789–803, doi:10.5194/os-9-789-2013.
[75] Gačić M., Civitarese G., Eusebi Borzelli G.L., Kovačević V.,Poulain P.-M.,Theocharis A., Menna M., Catucci A., Zarokanellos N., 2011.On the relationship between the decadal oscillations of the northern Ionian Sea and the salinity distributions in the eastern Mediterranean. Journal of Geophysical Research: Oceans, 116 (C12002), doi: 10.1029/2011JC007280.
[76] Goyet C., Hassoun A.E.R., Gemayel E., 2015. Carbonate system during the May 2013 MedSeA cruise. Dataset #841933 (DOI registration in progress).
[77] Goyet C., Gemayel E., Hassoun A.E.R., 2015. Underway pCO2 in surface water during the 2013 MedSEA cruise. Dataset #841928 (DOI registration in progress).
[78] Ziveri P., and Grelaud M., 2013. Continuous thermosalinograph oceanography along Ángeles Alvariño cruise track MedSeA2013. Universitat Autònoma de Barcelona, doi:10.1594/PANGAEA.822153.
[79] Ziveri P., and Grelaud M., 2013. Physical oceanography during Ángeles Alvariño cruise MedSeA2013. Universitat Autònoma de Barcelona, doi:10.1594/PANGAEA.822162.
[80] Ziveri P., and Grelaud M., 2013. Physical oceanography measured on water bottle samples during Ángeles Alvariño cruise MedSeA2013. Universitat Autònoma de Barcelona, doi:10.1594/PANGAEA.822163.

Article II: Distribution of surface water pCO_2 and air-sea fluxes in the Mediterranean Sea during May 2013

Gemayel, E., et al. (2015)

Submitted to Deep Sea Research Part I

Distribution of surface water pCO_2 and air-sea fluxes in the Mediterranean Sea during May 2013

Elissar GEMAYEL[1,2,3], Abed El Rahman HASSOUN[3], Mohamed Anis BENALLAL[1,2], Catherine GOYET[1,2], Evangelina KRASAKOPOULOU[4], Marie ABBOUD-ABI SAAB[3], and Franck TOURATIER[1,2]

[1] Université de Perpignan Via Domitia, IMAGES_ESPACE-DEV, 52 avenue Paul Alduy, 66860 Perpignan Cedex 9, France
[2] ESPACE-DEV, UG UA UR UM IRD, Maison de la télédétection, 500 rue Jean-François Breton, 34093 Montpellier Cedex 5, France
[3] National Council for Scientific Research, National Center for Marines Sciences, P.O Box 534, Batroun, Lebanon
[4] University of the Aegean, Department of Marine Sciences, University Hill, Mytilene 81100, Greece

Abstract

Recent measurements of surface water pCO_2 (pCO_2^{sw}) were carried out continuously during the MedSeA cruise in May 2013. A clear increasing Eastward pCO_2^{sw} trend was observed with values ranging from 340 µatm in the Strait of Gibraltar up to 434 µatm in the Levantine sub-basin. On a short time scale the pCO_2^{sw} range was comparable to the seasonal amplitude and the Western and Eastern basin were characterized by two different pCO_2^{sw} regimes. The factors influencing the pCO_2^{sw} spatial variability were also basin dependent. In the Western basin, the effects of mixing with surface Atlantic Waters along with the increase in salinity of 1.72 units were the main drivers of the pCO_2^{sw} variations. The highest surface Chlorophyll_a concentrations of 0.23 µg/L were detected in the Strait of Gibraltar and the Alboran sub-basin, which marked these areas with the lowest pCO_2^{sw}. In the Eastern basin, the sea surface temperature explained 61% of the pCO_2^{sw} variations. The low Chlorophyll_a concentrations decreasing sharply to reach as low 0.014 µg/L did not counteract the pCO_2^{sw}-temperature related increase. The air-sea disequilibrium (ΔpCO_2) followed a similar longitudinal distribution as the pCO_2^{sw} varying from - 31 µatm in the Strait of Gibraltar to + 57 µatm in the Levantine sub-basin. The computed daily CO_2 fluxes were affected by the local winds and yielded higher CO_2 exchange rates than the climatological CO_2 fluxes. The latter showed that during May 2013 the Mediterranean Sea released CO_2 into the atmosphere at rate of 0.97 to 1.18 $mmol.m^{-2}.day^{-1}$. Overall the Western and Eastern basin were found to act respectively as a sink and source for CO_2 to the atmosphere during May 2013.

Keywords: Mediterranean Sea; surface water; pCO_2; spatial variations; air-sea CO_2 fluxes

1. Introduction

Any estimate of a CO_2 flux across the ocean-atmosphere interface requires the knowledge of the partial pressure of CO_2 (pCO_2) distribution in the surface oceans. The global importance of CO_2 exchange is reflected by the pCO_2 datasets in the world oceans that assemble so far about 6.4 and 10.1 million measurements in the LDEO database (Takahashi et al., 2014) and the Surface Ocean CO_2 Atlas (SOCAT) version 2 database (Bakker et al., 2014), respectively.

In the Mediterranean Sea, surface water pCO_2 measurements are still poorly documented and when available they are mainly confined within the Western basin. The measurements of the carbonate system are more focused on discrete samples of Total Alkalinity (A_T) and Total Inorganic Carbon (C_T), along with pH (Álvarez et al., 2014; De Carlo et al., 2013; Krasakopoulou et al., 2009; Krasakopoulou et al., 2011; Rivaro et al., 2010; Schneider et al., 2007; Touratier et al., 2012). Also, the recommendations of the Med-SHIP program regarding water column sampling for the CO_2 parameters include A_T, C_T, or alternatively pH with no mention for pCO_2 (CIESM, 2012). Consequently the CO_2 air-sea exchange on the scale of the entire basin has only been estimated through modeling approaches. D'Ortenzio et al. (2008), based on satellite-driven modeling of the upper mixed layer, estimated that the Mediterranean Sea is close to equilibrium with the atmosphere. Louanchi et al. (2009) based on a layer surface box model concluded that the Mediterranean Sea varied from a source of 0.62 $Tg.C.yr^{-1}$ in the 1960's to a net sink of - 21.98 $Tg.C.yr^{-1}$ in the 1990's for atmospheric CO_2.

The first study that dealt with the seasonal variability of pCO_2 was conducted between 1995 and 1997 by Hood and Merlivat (2001) in the DYFAMED (Dynamics of atmospheric fluxes in the Mediterranean Sea) time-series site in the Ligurian Sea. Their results show a strong seasonal variation of pCO_2 from 300 to 500 µatm that is mainly due to the temperature variations (13 to 28 °C). This site is so far the most documented as to direct measurements of pCO_2 by moored Carioca buoys or cruises (Bégovic and Copin-Montégut, 2002; Copin-Montégut and Bégovic, 2002; Copin-Montégut et al., 2004). Over a large scale, the pCO_2 in surface waters was continuously measured along two cruises: the 1999 PROSOPE cruise (Bégovic, 2001) and the 2006 THRESHOLD cruise (Calleja et al., 2013). Other local studies cover the Strait of Gibraltar (de la Paz et al., 2009; de la Paz et al., 2011; Santana-Casiano et al., 2002), the Aegean Sea (Krasakopoulou et al., 2009), the Adriatic Sea (Luchetta et al., 2010), and coastal areas such as the Bay of Palma in the Iberian Sea (Gazeau et al., 2005), the Gulf of Trieste in the Adriatic Sea (Cantoni et al., 2012; Turk et al., 2010), and the Point-B time-series station in the Rade de Villefranche (De Carlo et al., 2013). To our knowledge and as mentioned by Álvarez (2012) no continuous pCO_2 measurements are currently performed.

In this study, we present recent continuous pCO_2 surface data measured over the entire Western-Eastern transect of the MedSeA cruise conducted in May 2013. Then we discuss the spatial variations of pCO_2 in the Western and Eastern basin and the different factors affecting their distributions. Finally we calculate the daily and climatological air-sea CO_2 fluxes using three different parameterizations for the gas transfer velocity.

2. Methods

2.1. Study area

The MedSeA 2013 oceanographic cruise was conducted from the 2nd of May to the 2nd of June 2013, as part of the "European Mediterranean Sea Acidification in a changing climate" (MedSeA) project.

The cruise (with two legs), covered all the major sub-basins of the Mediterranean Sea. The first leg covered the two main basins of the Mediterranean Sea, with a section from the Atlantic Ocean to the Levantine sub-basin in the Eastern Mediterranean. Measurements were collected both by continuous underway surface water sampling and by discrete sampling throughout the water column on a total of 14 stations (Figure 1).

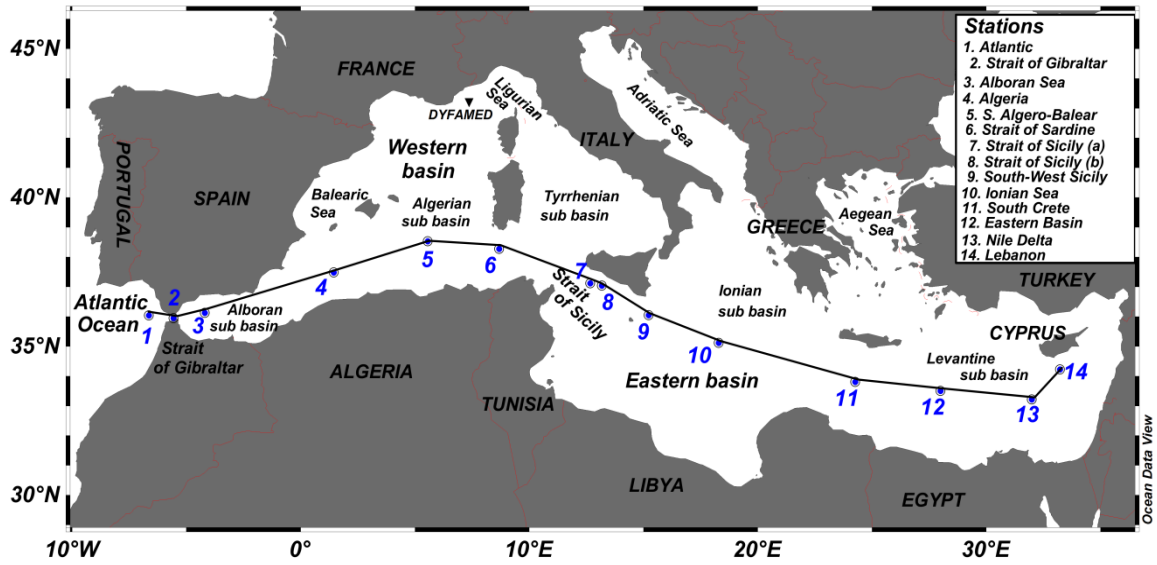

Figure 1. First leg sampling scheme of the 2013 MedSeA oceanographic cruise

2.2. Surface water sampling

The seawater was pumped from an intake at the bow located at ~5 m below the surface. At the ship's inlet, temperature and salinity were measured continuously using a SeaBird SBE 21 thermosalinometer and fluorescence signal with a TURNER $_{10}$AU fluorometer. Surface Chlorophyll_a (Chl*a*) samples were collected from all stations, except the Strait of Sicily (b) station. In the dry lab, the partial pressure of CO_2 in surface seawater (pCO_2^{SW}) was measured using an AFT-CO_2 (Autonomous Flow Thru) sensor connected to the seawater network. The AFT-CO_2 has the same technology as the Submersible Autonomous Moored Instrument (SAMI-CO_2); however it is not submersible and can only be installed on dry areas such as the bench top of a table. The measurements of pCO_2^{SW} are made by spectrophotometry based on the optical absorbance of the pH indicator solution bromothymol blue diluted in seawater (DeGrandpre et al., 1999). The AFT-CO_2 can measure pCO_2^{SW} in seawater in the range of 150 to 700 µatm and it is accurate to within ± 3 µatm.

To account for the temperature difference due to the tubes heating, temperature and salinity were also measured at the sensor's inlet with a microTSG SBE thermosalinometer. A debubbler was inserted in the flow to avoid gas exchange with the atmosphere. Also to ensure the proper functioning of the system, constant flow rate and pressure were maintained by regulating the valves of the hoses at the sensor's inlet. The AFT-CO_2 and the microTSG were connected to a datalogger, and records were retrieved at a 20 minutes interval, with the "LoggerNet 4.1" by "Campbell Scientific". The retrieved pCO_2^{sw} measurements were corrected for temperature difference between the seawater and the AFT-CO_2 sensor, using the algorithm proposed by Takahashi et al. (1993). Moreover, when the ship was stationary, all the measurements were discarded to minimize the error derived from the water turbulence induced by the propellers.

Between the 2nd and the 17th of May 2013, navigating from the Atlantic Ocean (6.437°W/36.382°N), to the Levantine sub-basin (33.225°W/34.224°N), a total of 654 pCO_2^{sw} measurements were performed. The total section distance was 3820 km, and the mean vessel speed was 5 $m.s^{-1}$; yielding an average distance of 5.6 km between every two data points.

2.3. Air-sea CO_2 fluxes

The daily air-sea CO_2 fluxes ($mmol.m^{-2}.d^{-1}$) were computed according to Eq (1) using the "CO_2calc 1.2.0" software (Robbins et al., 2010).

$$FCO_2 = \beta o \times k \times \Delta pCO_2 \qquad \text{(Eq 1)}$$

The different terms in Eq (1) are:

a) The solubility coefficient β_0 of CO_2 in seawater ($mol.L^{-1}.atm^{-1}$), determined according to Weiss (1974), as a function of temperature and salinity.

b) The gas transfer velocity k ($cm.h^{-1}$), is calculated as a function of the wind speed (u) and the Schmidt number (Sc) of CO_2 in seawater. There are several algorithms such as those of Liss and Merlivat (1986), Wanninkhof (1992), Nightingale et al. (2000) and more recently those of Ho et al. (2006) and Wanninkhof et al. (2009). However they all yield large differences in estimating the oceanic CO_2 uptake in different wind speed conditions. In order to calculate k ($cm\ h^{-1}$), the wind speed was recorded every minute by an automated Aanderaa weather station located close to the bridge of the ship, at about 10m above sea level. Wind speed records were corrected using the ship's heading and velocity and averaged over a 20 min period in accordance with the pCO_2^{sw} recording cycles. We also downloaded monthly averaged wind fields in 0.25° geographical grid from the Advanced SCATterometer (ASCAT) carried onboard of the Meteorological Operational Polar (Metop-A) satellites (http://cersat.ifremer.fr/). The daily and climatological CO_2 fluxes were computed using respectively, the onboard wind speeds (Aanderaa) and the monthly averaged wind fields (ASCAT), and by applying the three different wind parameterizations of the gas transfer

velocity that are integrated in the CO_2calc software: Wanninkhof (1992), Nightingale et al. (2000) and Ho et al. (2006).

c) The air-sea gradient of pCO_2 ($\Delta pCO_2 = pCO_2^{sw} - pCO_2^{air}$) determines the direction of the exchange. Positive air-sea CO_2 fluxes indicate oceanic source of CO_2 to the atmosphere and negative values indicate an oceanic CO_2 sink.

The calculation of the partial pressure of CO_2 in the atmosphere (pCO_2^{air}) follows Eq (2):

$$pCO_2^{air} = xCO_2(p_{atm} - pH_2O) \quad \text{(Eq 2)}$$

where xCO_2 is the atmospheric monthly mean of the mole fraction of CO_2, p_{atm} is the atmospheric pressure and pH_2O is the water vapor pressure.

The xCO_2 was computed from the average of 5 different stations spread across the Mediterranean Sea (Table 1), downloaded from the World Data Center for Greenhouse Gases (http://ds.data.jma.go.jp/gmd/wdcgg/). The atmospheric pressure (p_{atm}) was retrieved from the NCEP/DOE AMIP-II Reanalysis (Reanalysis 2) daily averages gridded at a 2.5º resolution (http://www.esrl.noaa.gov/psd/). The mean atmospheric concentration (xCO_2) of 398 ppm was corrected to saturated humidity by computing the water vapor pressure (pH_2O) according to Weiss and Price (1980).

Table 1. Records of monthly average atmospheric CO_2 concentration during May 2013 from 5 different ground stations

Station-GAW ID-Country	Geographic Coordinates	May 2013 monthly mean xCO_2 (ppm)
Monte Cimone-CMN-Italy	44.18ºN, 10.70ºE, 2165m	398.84
Giordan Lighthouse-GLH-Malta	36.07 ºN, 14.22ºE, 160m	389.37
Sede Boker-WIS-Israel	31.12ºN, 34.87ºE, 400m	399.13
Plateau Rosa-PRS-Italy	45.93ºN, 7.70ºE, 3480m	399.10
Lampedusa-LMP-Italy	35.52ºN, 12.63ºE, 45m	399.28

3. Spatial variations on the Western/Eastern transect

3.1. Hydrological characteristics in May 2013

The daily on board wind speed recorded during the cruise was on average 5.19 ± 2.94 $m.s^{-1}$; however it varied greatly between the Western and the Eastern basin, with mean wind speeds of 3.31 and 7.04 $m.s^{-1}$, respectively (Figure 2a). In the Eastern basin velocities reached as high as 17 $m.s^{-1}$, associated with a bad weather event encountered near the South of Crete station. However the monthly mean satellite-derived wind speed was 6.07 ± 0.32 $m.s^{-1}$ with no apparent differences between the Western and the Eastern basin (Figure 2b).

The θ/S diagram plotted using Ocean Data View (ODV); (Schlitzer, 2014) showed that temperature and salinity increased in an Eastward direction from the Strait of Gibraltar to the

Levantine sub-basin. The Western basin was characterized by the lowest temperature and salinity values (16.37°C and 34.175 respectively). The presence of this water mass with low salinity, low temperature is due to the inflow of surface Atlantic Waters (AW) through the Strait of Gibraltar, and is traceable through the Strait of Sicily with an increased salinity to 37.36. In the Eastern basin, temperature and salinity continue to rise in the same Eastward direction reaching a maximum of 21.91°C and 39.112 respectively, in accordance with the presence of Levantine Surface Waters (LSW). In addition, we can clearly see that the water masses are exchanged through the Strait of Gibraltar and the Strait of Sicily by an Eastward surface flow (Figure 3).

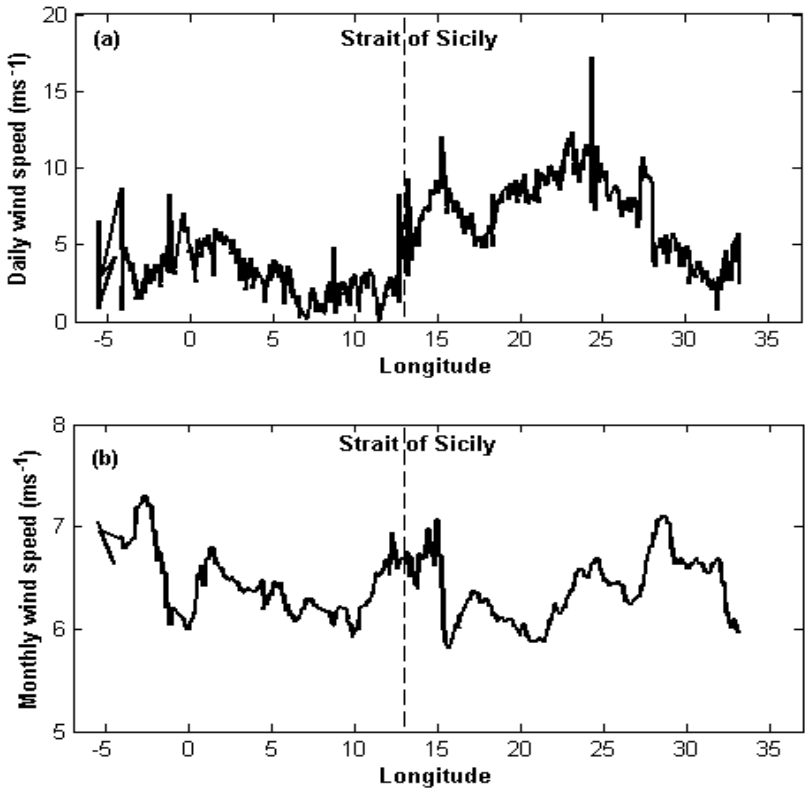

Figure 2. Longitudinal variation of the wind speed from (a) the daily on-board measurements and from (b) the satellite monthly averages of the ASCAT

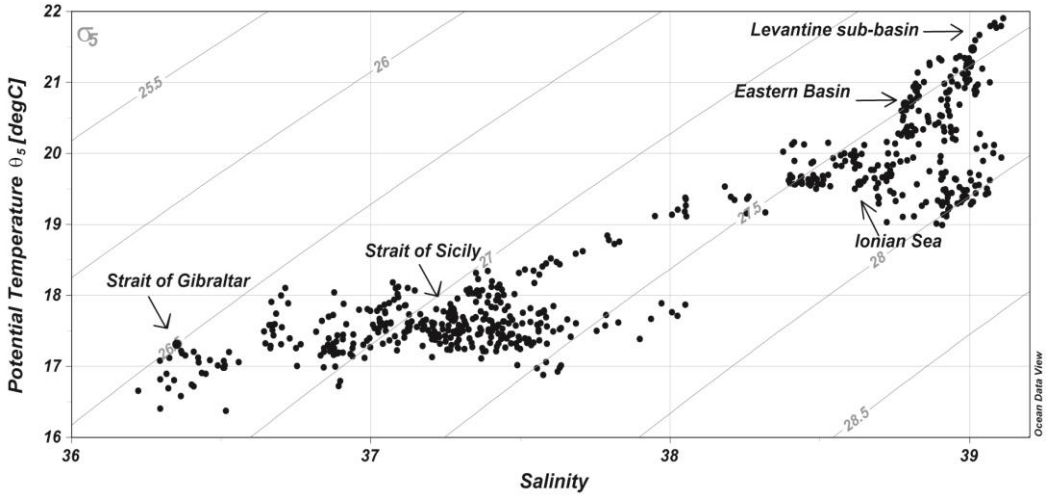

Figure 3. The θ/S diagram during the MedSeA cruise 2013

3.2.Variability of surface water pCO_2

Between the Strait of Gibraltar and the Levantine sub-basin, the pCO_2^{sw} varied from 340 to 434.75 µatm with an average of 395.21 ± 22.58 µatm. An Eastward increase was clearly observed with minima pCO_2^{sw} encountered near the Strait of Gibraltar and the Alboran sub-basin and maxima pCO_2^{sw} in the Ionian and the Levantine sub-basins (Figure 4a).

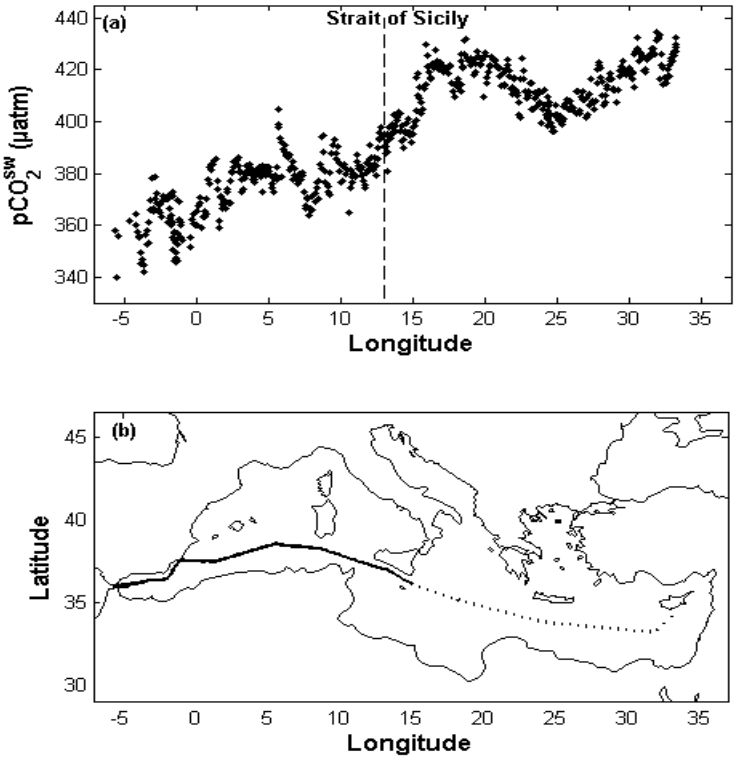

Figure 10. Diagrams showing a) the pCO_2^{sw} spatial variation during the 2013 MedSeA cruise and b) the two pCO_2^{sw} regimes in the Mediterranean Sea following the K-means two groups clustering

The pCO_2^{sw} was higher in the Easternmost part of the Mediterranean Sea where salinity and temperature were above 38 and 19°C respectively. The spatial variation of pCO_2^{sw} correlated strongly with sea surface temperature (r = 0.80). Hence, the pCO_2^{sw} gradual Eastward increase is mainly related to the Eastward driven warming of surface waters that is associated with the elevated salinity. The observed spatial variation is in agreement with the simulated seasonal averages of pCO_2^{sw} that show a permanent and slightly more pronounced Eastward gradient of pCO_2^{sw} in the spring and summer periods (D'Ortenzio et al., 2008; Taillandier et al., 2012). During the short time of the cruise the pCO_2^{sw} range of ~100 µatm was close to the seasonal amplitude (120–140 µatm), that was earlier estimated in the 1980's and the 2000's (Taillandier et al., 2012). Therefore, a two groups K-means clustering analysis was conducted based on the wide range of the pCO_2^{sw} measurements. The analysis revealed that two pCO_2^{sw} regimes prevail in the Mediterranean Sea: a) between 6º50'W and 13ºE, namely the Western Mediterranean basin (full line), and b) between 13º and 33º20'E corresponding to the Eastern Mediterranean basin (dotted line). The tipping point of the two regimes is in the Strait of

Sicily, which naturally divides the Mediterranean Sea into a Western and Eastern basin (Figure 4b).

Due to the scarcity of the pCO_2^{sw} data in the Mediterranean Sea, the interannual variability can be neglected compared to seasonal variability (Lefèvre and Taylor, 2002). The seasonal cycle of pCO_2^{sw} can then be characterized by comparing similar large scale cruises that were conducted in this area (Table 2). The average pCO_2^{sw} of 395 µatm in late spring (MedSeA 2013) was followed by an increase of about 18 µatm in the summer during the TRANSMED cruise (Rivaro et al., 2010) and the THRESHOLDS cruise (Calleja et al., 2013). Compared to the late spring (MedSeA 2013), the pCO_2^{sw} increased by 35 µatm in autumn during the PROSOPE cruise (Bégovic, 2001). During the spring bloom, the increased photosynthetic activity lowers the pCO_2^{sw}, whereas the warming of surface waters in the late spring and summer induces an increase in pCO_2^{sw}. The higher pCO_2^{sw} in autumn could be related to the vertical mixing that bring up the deep waters rich in CO_2 (Hood and Merlivat, 2001).

Table 2. Data of pCO_2^{sw} from different cruises in the Mediterranean Sea

pCO_2^{sw} (µatm)	PROSOPE (Sep-Oct 1999)	TRANSMED (June 2007)	THRESHOLDS (June-July 2006)	MedSeA (May 2013)
Mean	430	416	410	395
Min	310	375	309	340
Max	470	460	495	435

3.3. Factors affecting the pCO_2^{sw} surface variability

In surface waters, the pCO_2^{sw} is mainly a function of the temperature, total CO_2 concentrations (C_T), alkalinity (A_T) and salinity (Takahashi et al., 1993). But the biological processes and upwelling of subsurface waters can also control the A_T and C_T concentrations, which in their turn affect the pCO_2^{sw} distributions (Takahashi et al., 2002).

Table 3. Equations and RMSE and coefficient of determination for the pCO_2 as function of Temperature (T), Salinity (S) and Fluorescence (F)

pCO_2^{sw} = f(Temperature)		RMSE (µatm)	r^2
Mediterranean Sea	$pCO_2^{sw} = 14.85T + 117.30$	± 10	0.79
Western basin	$pCO_2^{sw} = 17.49T + 67.89$	± 9	0.20
Eastern basin	$pCO_2^{sw} = 8.34T + 248.70$	± 6	0.61

pCO_2^{sw} = f(Salinity)		RMSE (µatm)	r^2
Mediterranean Sea	$pCO_2^{sw} = 24.33S - 527.6$	± 10	0.78
Western basin	$pCO_2^{sw} = 25.2S - 563$	± 8	0.51
Eastern basin	$pCO_2^{sw} = 9.74S + 38.09$	± 8	0.23

pCO_2^{sw} = f(Fluorescence)		RMSE (µatm)	r^2
Mediterranean Sea	$pCO_2^{sw} = -70.76F + 502.90$	± 13	0.66
Western basin	$pCO_2^{sw} = 81.9F + 232.60$	± 8	0.34
Eastern basin	$pCO_2^{sw} = -39.72F + 466.40$	± 6	0.56

Based on the K-mean clustering analysis (section 3.2), the Western and Eastern basin are characterized by two different pCO_2^{sw} regimes. In fact, we found that considering each basin separately reduces the Root Mean Square Error (RMSE) produced by the pCO_2^{sw} fitted to temperature (T) salinity (S) or fluorescence (F). Moreover the fits in the Eastern basin yield smaller RMSE than the fits for the Western basin (Table 3).

The shift in sea surface temperature between the two basins is one of the main drivers of the pCO_2^{sw} variability (Figure 5a). In the Western basin, a weak correlation between temperature and pCO_2^{sw} ($r = 0.40$) is detected (Figure 5b) and the accuracy of the fit is very low with $r^2 = 0.20$. In fact, the sea surface temperature changes were very small with a range of only 1.8 ºC along the entire Western basin. This suggests that in this basin other processes such as mixing and biological uptake are driving the pCO_2^{sw} variability. In the Eastern basin (Figure 5c), the increase in temperature exhibits a pronounced positive effect on the pCO_2^{sw} ($r = 0.78$) and the temperature contributes to 61% of the pCO_2^{sw} variability (Table 3).

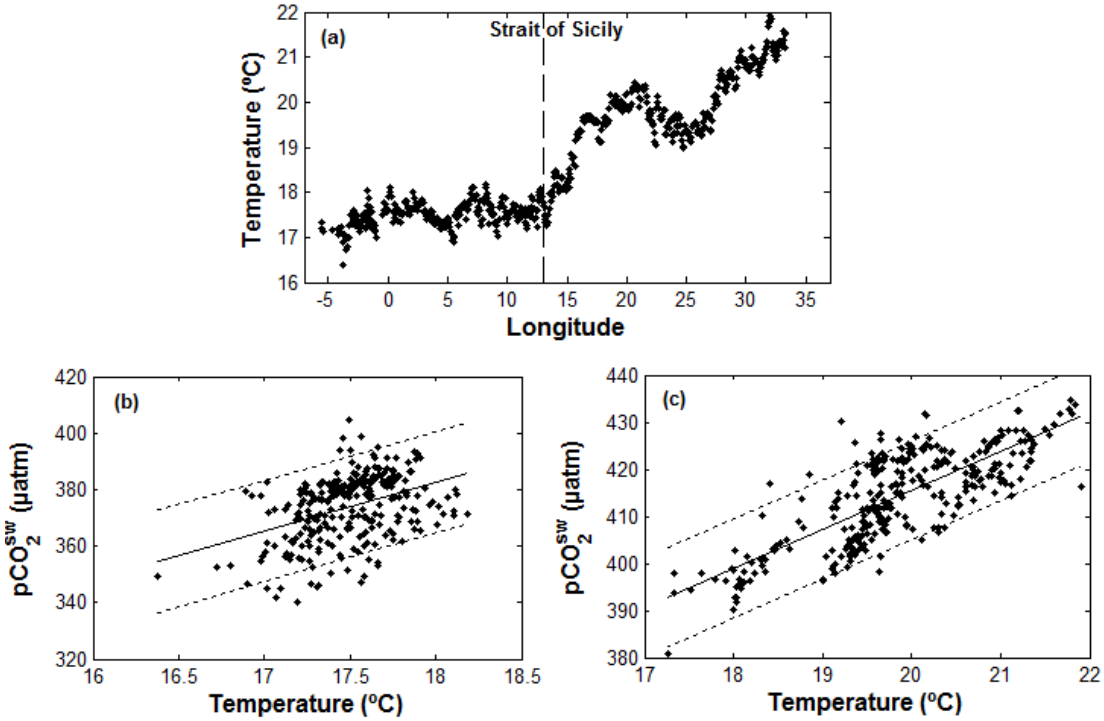

Figure 5. Diagrams showing (a) the sea surface temperature longitudinal variation during the 2013 MedSeA cruise and the pCO_2-temperature dependence in (b) the Western basin and (c) the Eastern basin

The rise in pCO_2^{sw} is explained by the effect of temperature on the carbonate equilibrium constants and the solubility coefficient of CO_2 (Takahashi et al., 1993). Several researchers proposed relationships to quantify the effect of temperature on pCO_2^{sw}. Copin-Montégut (1988) proposed a quadratic function of pCO_2 fitted to the values of $\Delta pCO_2/\Delta t$. Goyet et al. (1993) presented a forth degree polynomial function to estimate the effect of temperature on fCO_2 at different salinity and C_T/A_T ratios. They computed this effect thermodynamically using the carbonic acid dissociation constants of Goyet and Poisson (1989). Takahashi et al.

(1993) computed experimentally the effect of temperature on pCO_2 from a set of measurements made on a single surface water sample with a specific salinity in the North Atlantic. The differences between the Goyet et al. (1993) and the Takahashi et al. (1993) parameterizations are within the uncertainty of the measurements (± 3 µatm); which shows that the changes of fCO_2 as function of the ratios C_T/A_T as established by Goyet et al. (1993) could also be applicable in specific regions such as the Mediterranean Sea.

The effect on pCO_2 of changes in temperature often counteracts that of C_T, and their net effect largely determines whether an oceanic area becomes a sink or source for atmospheric CO_2. The effect of A_T on pCO_2 has a similar magnitude as the C_T, however it is smaller than that of the CO_2 removal by photosynthesis (Takahashi et al., 1993). During the MedSeA cruise, the A_T and C_T concentrations in the water column varied in each basin and sub-basin. An increasing Eastward trend for the A_T was noticed with the highest concentrations measured in the Eastern basin, however the C_T concentrations were more pronounced in the intermediate and deep layers of the Western basin (Hassoun et al., 2015).

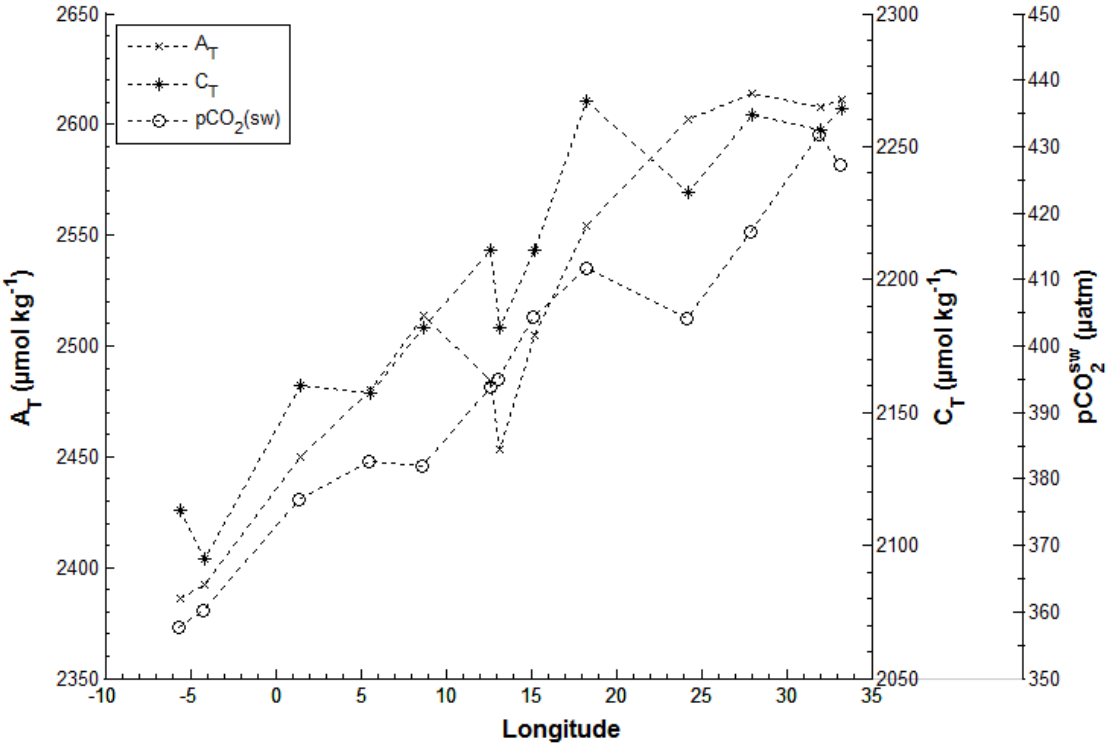

Figure 6. Diagram showing the A_T and C_T surface concentrations measured at all the stations as well as the correspondent pCO_2^{sw}

Referring to the A_T and C_T measured at 5m depth, they have a general Eastward increase as the pCO_2^{sw}. A clear shift is observed after the Strait of Sicily with concentrations in the Lebanon station (35 ºE longitude) reaching as high as 2614 and 2267 µmol.kg^{-1} for A_T and C_T respectively (Figure 6). Also both A_T and C_T concentrations increased by ~ 70 µmol.kg^{-1} between the Strait of Sicily and the Ionian sub-basin. In the Eastern basin temperatures as low as 17 ºC were recorded. According to figure 5a these low temperatures were also observed in

the Western basin, hence the Eastern basin seems to include waters from the Western basin. During the late spring, strong currents flowing in the Strait of Sicily (Bonanno et al., 2014) could enrich the Eastern basin with high A_T and C_T concentrations. In the Western basin, the increase of pCO_2^{sw} was parallel to that of A_T and C_T, whereas in the Strait of Sicily the decrease of A_T and C_T was accompanied with an increase of pCO_2^{sw}. In the Eastern basin, the pCO_2^{sw} appears to be more regulated by the C_T than the A_T concentrations. The peak and drop in C_T at 18 and 25 ºE respectively induced an increase and decrease in pCO_2^{sw} at the same locations. However, the continuous rise in A_T in this basin doesn't appear to have a decreasing effect on pCO_2^{sw}.

The increasing Eastward trend of A_T was mainly driven by the salinity changes (Figure 7a) between the Western and Eastern Basins (Hassoun et al., 2015). Salinity affects pCO_2 by the change in the CO_2 solubility and the dissociation constants of carbonic acid in seawater (Takahashi et al., 1993). In the Western basin, contrary to the temperature, a strong correlation between salinity and pCO_2^{sw} ($r = 0.72$) is detected (Figure 7b) and the accuracy of the fit is significant with $r^2 = 0.51$. In this basin, the considerable salinity increase of 1.72 units between the Strait of Gibraltar and the Strait of Sicily is one of the main factors driving the observed pCO_2^{sw} increase. In the Eastern basin, the salinity contributes to 47% of the pCO_2^{sw} variability, but the accuracy of the fit is very low with $r^2 = 0.23$ (Table 3). The effect of salinity on pCO_2^{sw} changes in the Eastern basin (Figure 7c) is similar in magnitude to the effect of temperature on pCO_2^{sw} changes in the Western basin.

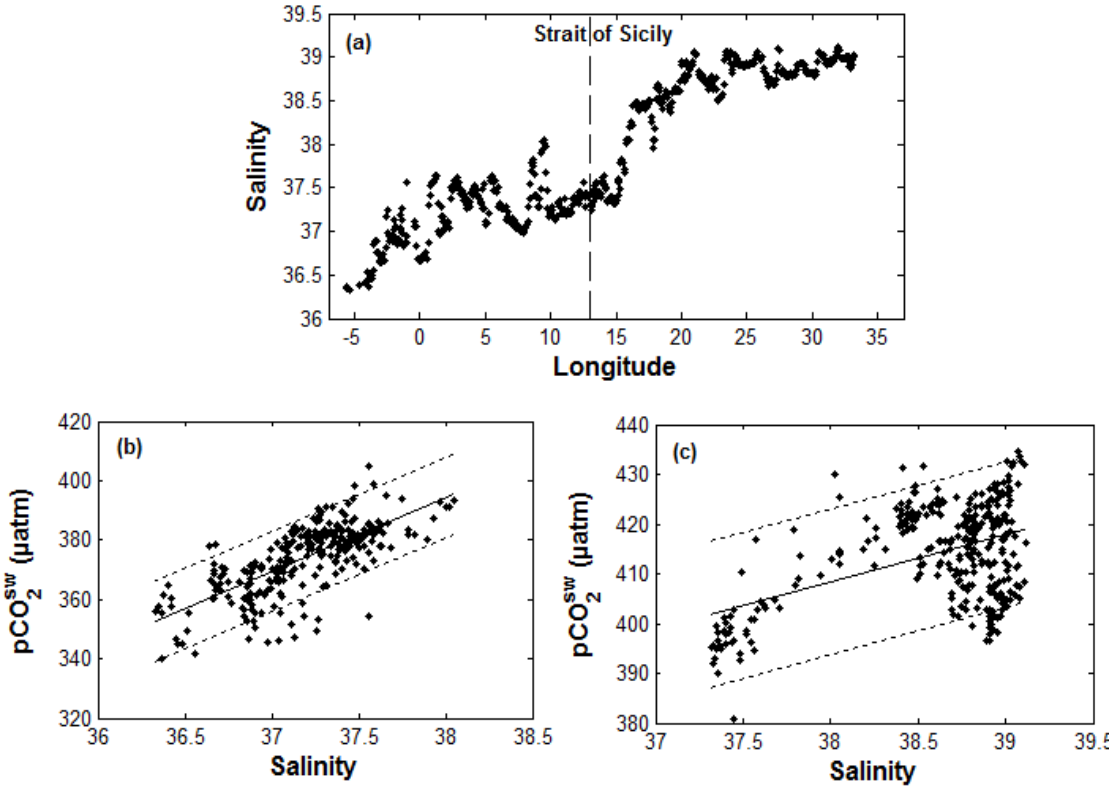

Figure 7. Diagrams showing (a) the surface salinity longitudinal variation during the 2013 MedSeA cruise and the pCO_2^{sw}-salinity dependence in (b) the Western basin and (c) the Eastern basin

Photosynthetic activity could also be a driver of pCO_2^{sw} during the spring period. The continuous fluorescence records (in arbitrary unit) follow the oligotrophic to ultra-oligotrophic gradient that marks the two basins (Figure 8a). Surface Chl*a* concentrations ranged from 0.234 to 0.014 µg/L and the highest phytoplanktonic biomasses were found in the Westernmost part of the Mediterranean Sea particularly in the Strait of Gibraltar and the Alboran sub-basin (Figure 8b). The peaks in Chl*a* concentrations indicate the biological uptake of CO_2 by photosynthesis and mark these regions with the lowest pCO_2^{sw}. The pCO_2^{sw} under equilibrium is only found in the Alboran sub-basin where inflowing AW is significantly modified as it mixes with resident Mediterranean Waters. In this area, the turbulent mixing that results from the interaction of these opposing flows is largely responsible for the enhanced biological variability (Arnone, 1995).

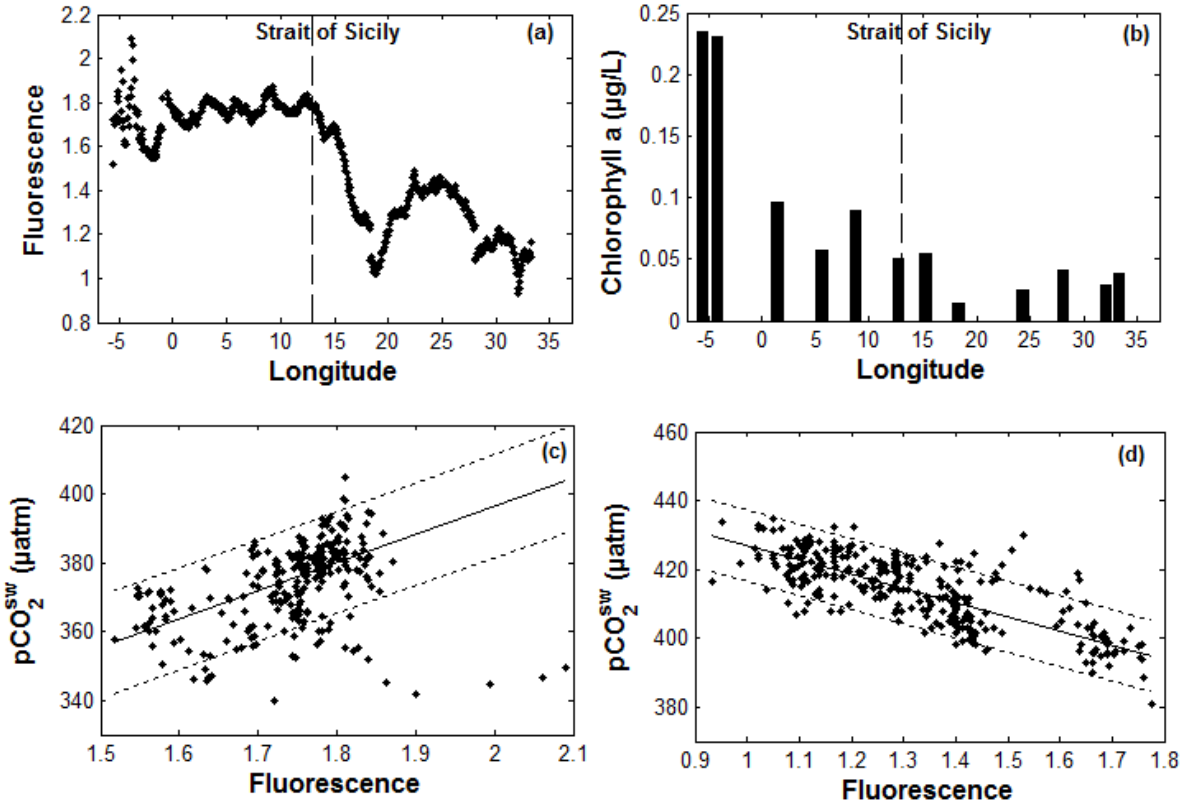

Figure 11. Diagrams showing spatial variation of (a) the fluorescence and (b) the surface Chlorophyll_a samples during the 2013 MedSeA cruise. The pCO_2^{sw}-fluorescence dependence is also presented for (c) the Western basin and (d) the Eastern basin

For the rest of the Western basin, the pCO_2^{sw} drawdown due to the photosynthetic activity was not observed, on the contrary a weak postive correlation was detected between pCO_2^{sw} and fluorescence ($r = 0.32$; Figure 8c). Eastward of the Alboran sub-basin, other processes are potentially masking the CO_2 drawdown by photosynthesis. The increase of pCO_2^{sw} for Chl*a* concentrations lower than 0.1 µg/L suggests that the spring bloom was ending, and the Chl*a* could be lost by grazing or sinking (Sasaki et al., 1998). In this case, a net increase in pCO_2^{sw} could be observed and hence positively correlating with the fluorescence. Another important consideration is that heterotrophic communities prevail in the oligotrophic waters

of the Mediterranean Sea (Duarte et al., 2013). In such environments where net carbon fixation rates are low, respiration exceeds photosynthesis, therefore leaving the system with an organic carbon deficit (Williams, 1998).

In the Eastern basin, the very low biomass in late spring is in good agreement with the temporal changes in phytoplankton concentrations (D'Ortenzio and Ribera d'Alcalà, 2009). The sharp decrease in fluorescence was accompagnied by an increase in pCO_2^{sw}, marked by a negative correrlation (r = -0.62; Figure 8d). However the low Chlorophyll_a concentrations coincided with high temperatures (Figures 5a and 8a) which imply that the pCO_2^{sw} increase due to increasing temperature was not counteracted by photosynthesis. The temperature stratification usually develops during high air temperatures and inhibits the flux of nutrients towards the surface layer, preventing the autotrophic biomass accumulation (Stambler, 2013).

The pCO_2^{sw} enrichment of the upper surface layer could also be influenced by transport processes driving a net upward flux of inorganic carbon (Sarmiento and Gruber, 2013). Between 22ºE and 27ºE a sudden temperature drop (Figure 5a) was observed. It was associated with a pCO_2^{sw} decrease, a C_T decrease and a fluorescence increase (Figure 4a, 6 and 8a). The surface water cooling could be driven by the high wind speed event that occurred simultaneously in the same region (section 3.1; Figure 2a). The induced heat loss increases surface salinity which in turn could enhance the vertical transport of dissolved CO_2 in the mixed layer (Figure 7a). For the intermediate to high wind speeds encountered in this region (9 to 17 $m.s^{-1}$) a wind stress-induced mixing could also be dominating (Rutgersson et al., 2011). This could explain the upward flux of phytoplankton - marked by an increase in fluorescence - which consumed the $[CO_2^*]$ and hence decreased the C_T and the pCO_2^{sw}.

3.4. Air-sea disequilibrium and CO_2 fluxes

During the MedSeA cruise, the air-sea disequilibrium (ΔpCO_2) shifted from under to over equilibrium with the atmosphere in the same direction as the pCO_2^{sw} longitudinal increase. The ΔpCO_2 varied from - 31 µatm in the Strait of Gibraltar to + 57 µatm in the Levantine sub-basin, with an average of 12.23 µatm. The CO_2 sink/source variability observed during the short time of the cruise is determined by the atmospheric CO_2 concentration. Negative ΔpCO_2 are observed in the Western basin that is acting as a sink of CO_2 for the atmosphere. The opposite is seen in the Eastern basin that can be considered as a net source of CO_2 for the atmosphere

The daily and climatological air-sea CO_2 fluxes computed from the two wind speed sources and the different gas transfer formulations revealed important differences (Table 4). The results show that the CO_2 fluxes calculation is dependent upon both of the parameterization and the wind speed source choice. The computed daily CO_2 fluxes show that the Mediterranean Sea releases CO_2 at a rate ranging from 1.35 (Nightingale et al., 2000) to 2 $mmol.m^{-2}.day^{-1}$ (Wanninkhof, 1992). However the climatological CO_2 fluxes are significantly lower, ranging from 0.97 (Ho et al., 2006) to 1.18 $mmol.m^{-2}.day^{-1}$ (Wanninkhof, 1992).

Moreover, the Wanninkhof (1992) yields higher CO_2 fluxes compared to the parameterizations of Nightingale et al. (2000) and Ho et al. (2006). This is due to the rough sea conditions that were encountered South of Crete where wind speed reached as high as 17 $m.s^{-1}$. The Wanninkhof (1992) parameterization can reasonably describe the relationship between wind speed and gas exchange in the 5 to 11 $m.s^{-1}$ wind speed range but may overestimates the gas transfer velocity at wind speeds between 6 and 12 $m.s^{-1}$ (Ho et al., 2011).

Table 4. Daily [FCO_2(day)] and climatological [FCO_2(clim)] CO_2 fluxes ($mmol.m^{-2}.day^{-1}$) calculated from the Aanderaa and ASCAT wind sources respectively, and from three different wind speed parameterizations.

	Wanninkhof (1992)		Nightingale et al. (2000)		Ho et al. (2006)	
	FCO_2(day)	FCO_2(clim)	FCO_2(day)	FCO_2(clim)	FCO_2(day)	FCO_2(clim)
Western Basin	-0.13 ± 0.35	-0.36 ± 0.84	-0.12 ± 0.31	-0.30 ± 0.70	-0.11 ± 0.29	-0.29 ±0.69
Eastern Basin	3.27 ± 2.30	2.55 ± 1.01	2.67 ± 1.76	2.15 ± 0.85	2.68 ± 1.88	2.09 ± 0.82
Med Sea	1.66 ± 2.38	1.18 ± 1.71	1.35 ± 1.89	0.99 ± 1.44	1.36 ± 1.95	0.97 ± 1.40

In the Western basin, the wind speeds derived from the ASCAT (climatological winds) were higher than those derived from the Aanderaa weather station (daily winds). Hence the daily CO_2 fluxes [FCO_2(day)] were on average 71 % lower than the climatological CO_2 fluxes [FCO_2(clim)]. In the Eastern basin, and during the high speed wind event, the ASCAT wind speeds were significantly lower than the Aanderaa. Consequently the FCO_2(day) during this period were 42 % higher than the FCO_2(clim). This implies that throughout the month of May 2013 the onboard recorded wind speeds were affected by local weather events and were not representative of the climatological conditions prevailing in the study area.

The climatological CO_2 net flux calculated from the parameterization of Wanninkhof (1992) varied from - 5.28 to 5.79 $mmol.m^{-2}.day^{-1}$. With the smooth variations of the ASCAT winds, the CO_2 fluxes are regulated by the ΔpCO_2 Eastward variations. The largest daily sinks for atmospheric CO_2 are found in the Strait of Gibraltar and the Alboran sub-basin, whereas the largest sources cover the entire Eastern basin (Figure 9). A similar CO_2 flux of -5.5 $mmol.m^{-2}.day^{-1}$ was calculated during May 1998 over the Strait of Gibraltar (Santana-Casiano et al., 2002), that acts as a net sink of atmospheric CO_2 on an annual basis (de la Paz et al., 2009).

Within the upper mixed layer, the summer heating is associated with an outflux of CO_2 to the atmosphere while winter cooling is associated with an influx of CO_2 into the ocean. For example, the daily CO_2 fluxes calculated at the DYFAMED time-series and the Aegean Sea show that during winter these areas act a as net sink of atmospheric CO_2 with a calculated rate of -3.8 and -5.5 $mmol.m^{-2}.day^{-1}$ respectively (Copin-Montégut and Bégovic, 2002; Krasakopoulou et al., 2009). The late spring CO_2 fluxes calculated in this study fall within the seasonal cycle and agree with the previously simulated - October to May - seasonal CO_2 fluxes where the Western basin was under equilibrium and the Eastern basin was a permanent source of CO_2 to the atmosphere (D'Ortenzio et al., 2008; Taillandier et al., 2012).

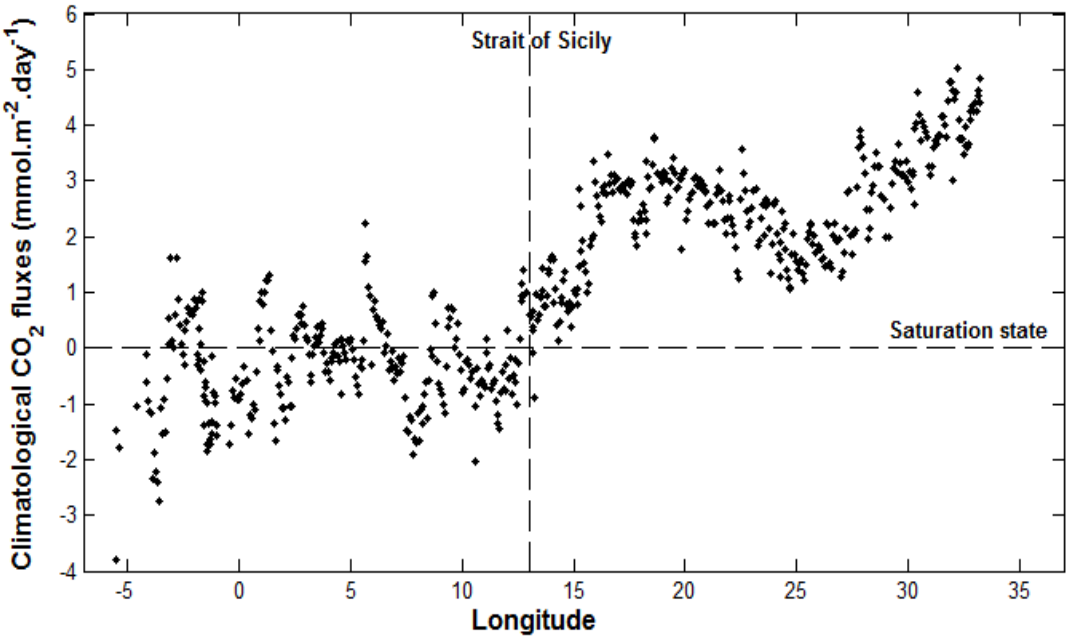

Figure 9. Diagram showing the spatial variability of the climatological CO_2 fluxes calculated from the wind parameterization of Wanninkhof (1992)

Concluding remarks

This study presents a recent survey of surface carbonate system parameters that crosses the entire Mediterranean Sea from the Strait of Gibraltar to the Levantine sub-basin during May 2013. A quality data set is provided describing the pCO_2^{sw} distributions within a time month scale on a large longitudinal band, with emphasis on the contrasts between the Western and Eastern basins. The results suggest that within May 2013, two pCO_2^{sw} regimes can be identified due to the different thermodynamic and biological properties of the Western and Eastern basin. Salinity and temperature variations were the main drivers of the pCO_2^{sw} variability in the Western and Eastern basins respectively, whereas the low Chlorophyll_a concentrations did not seem to counteract these effects. Also the pCO_2^{sw} variations were affected by local effects such as the inflow of cold Atlantic Waters through the Strait of Gibraltar and the high wind speeds encountered in the Eastern Basin. The daily air-sea CO_2 fluxes were forced by the meteorological conditions and were not representative of the climatological CO_2 exchange rate.

The basin scale approach covered during this study on a large longitudinal band of the Mediterranean Sea helps to better resolve the monthly sources of variability in pCO_2^{sw} and air-sea CO_2 fluxes. However in order to better determine the seasonal and interannual cycle, we recommend installing a pCO_2 continuous measuring system such as the AFT-CO_2 aboard the ships of opportunity monitoring the Mediterranean Sea surface waters and to add the pCO_2 to the recommended measurements of the carbonate system in the Med-SHIP initiative for repeated oceanographic surveys.

Acknowledgments

This work was funded by the EC "Mediterranean Sea Acidification in a changing climate" project (MedSeA; grant agreement 265103). Atmospheric CO_2 data were obtained from the World Data Center for Greenhouse Gases Web site and we acknowledge the use of these data sets for broad scientific use. The ASCAT on Metop-A Level 4 monthly gridded mean wind fields in 0.25° geographical grid were obtained from the Centre de Recherche et d' Exploitation Satellitaire (CERSAT), at IFREMER, Plouzané (France). The NCEP_Reanalysis 2 data was provided by the NOAA/OAR/ESRL PSD, Boulder, Colorado, USA, from their Web site at *http://www.esrl.noaa.gov/psd/*. We wish to thank the Spanish crew members of the R/VAngeles Alvarino, for their upmost support in the cruise and FALCO Cedric and GUGLIELMI Véronique for their help and guidance with the A_T/C_T measurements and the setup of the pCO_2 continuous system. We are genuinely grateful to the National Council for Scientific Research (CNRS) in Lebanon for the PhD thesis scholarship granted to Miss GEMAYEL Elissar.

References

Álvarez, M., 2012. The CO_2 system observations in the Mediterranean Sea: past, present and future, in: Briand, F. (Ed.), Designing Med-SHIP: a Program for repeated oceanographic surveys. CIESM Monaco, p. 164.

Álvarez, M., Sanleón-Bartolomé, H., Tanhua, T., Mintrop, L., Luchetta, A., Cantoni, C., Schroeder, K., Civitarese, G., 2014. The CO_2 system in the Mediterranean Sea: a basin wide perspective. Ocean Sci. 10, 69-92. 10.5194/os-10-69-2014

Arnone, R., 1995. The temporal and spatial variability of chlorophyll in the Western Mediterranean, in: La Violette, P. (Ed.), Seasonal and interannual variability of the Western Mediterranean Sea. American Geophysical Union, Washington, DC, p. 228.

Bakker, D.C.E., Pfeil, B., Smith, K., Hankin, S., Olsen, A., Alin, S.R., Cosca, C., Harasawa, S., Kozyr, A., Nojiri, Y., O'Brien, K.M., Schuster, U., Telszewski, M., Tilbrook, B., Wada, C., Akl, J., Barbero, L., Bates, N.R., Boutin, J., Bozec, Y., Cai, W.J., Castle, R.D., Chavez, F.P., Chen, L., Chierici, M., Currie, K., de Baar, H.J.W., Evans, W., Feely, R.A., Fransson, A., Gao, Z., Hales, B., Hardman-Mountford, N.J., Hoppema, M., Huang, W.J., Hunt, C.W., Huss, B., Ichikawa, T., Johannessen, T., Jones, E.M., Jones, S.D., Jutterström, S., Kitidis, V., Körtzinger, A., Landschützer, P., Lauvset, S.K., Lefèvre, N., Manke, A.B., Mathis, J.T., Merlivat, L., Metzl, N., Murata, A., Newberger, T., Omar, A.M., Ono, T., Park, G.H., Paterson, K., Pierrot, D., Ríos, A.F., Sabine, C.L., Saito, S., Salisbury, J., Sarma, V.V.S.S., Schlitzer, R., Sieger, R., Skjelvan, I., Steinhoff, T., Sullivan, K.F., Sun, H., Sutton, A.J., Suzuki, T., Sweeney, C., Takahashi, T., Tjiputra, J., Tsurushima, N., van Heuven, S.M.A.C., Vandemark, D., Vlahos, P., Wallace, D.W.R., Wanninkhof, R., Watson, A.J., 2014. An update to the Surface Ocean CO_2 Atlas (SOCAT version 2). Earth Syst. Sci. Data 6, 69-90. 10.5194/essd-6-69-2014

Bégovic, M., 2001. Contribution á l'étude du système des carbonates en Méditerranée. Distribution et variation spatio-temporelle de la pression partielle de CO_2 dans les eaux superficielles du bassin Liguro-Provencal. Thèse, Université Paris 6, p. 303.

Bégovic, M., Copin-Montégut, C., 2002. Processes controlling annual variations in the partial pressure of CO_2 in surface waters of the central northwestern Mediterranean Sea

(Dyfamed site). Deep-Sea Res. Part II Top. Stud. Oceanogr. 49, 2031-2047. http://dx.doi.org/10.1016/S0967-0645(02)00026-7

Bonanno, A., Placenti, F., Basilone, G., Mifsud, R., Genovese, S., Patti, B., Di Bitetto, M., Aronica, S., Barra, M., Giacalone, G., Ferreri, R., Fontana, I., Buscaino, G., Tranchida, G., Quinci, E., Mazzola, S., 2014. Variability of water mass properties in the Strait of Sicily in summer period of 1998–2013. Ocean Sci. 10, 759-770. 10.5194/os-10-759-2014

Calleja, M.L., Duarte, C.M., Álvarez, M., Vaquer-Sunyer, R., Agustí, S., Herndl, G.J., 2013. Prevalence of strong vertical CO_2 and O_2 variability in the top meters of the ocean. Global Biogeochem. Cycles 27, 941-949. 10.1002/gbc.20081

Cantoni, C., Luchetta, A., Celio, M., Cozzi, S., Raicich, F., Catalano, G., 2012. Carbonate system variability in the Gulf of Trieste (North Adriatic Sea). Estuar. Coast. Shelf Sci. 115, 51-62. http://dx.doi.org/10.1016/j.ecss.2012.07.006

CIESM, 2012. Designing Med-SHIP: a Program for repeated oceanographic surveys, in: Briand, F. (Ed.), N°43 CIESM Workshop Monographs. CIESM, Monaco, p. 164.

Copin-Montégut, C., 1988. A new formula for the effect of temperature on the partial pressure of CO_2 in seawater. Mar. Chem. 25, 29-37. http://dx.doi.org/10.1016/0304-4203(88)90012-6

Copin-Montégut, C., Bégovic, M., 2002. Distributions of carbonate properties and oxygen along the water column (0–2000m) in the central part of the NW Mediterranean Sea (Dyfamed site): influence of winter vertical mixing on air–sea CO_2 and O_2 exchanges. Deep-Sea Res. Part II Top. Stud. Oceanogr. 49, 2049-2066. http://dx.doi.org/10.1016/S0967-0645(02)00027-9

Copin-Montégut, C., Bégovic, M., Merlivat, L., 2004. Variability of the partial pressure of CO_2 on diel to annual time scales in the Northwestern Mediterranean Sea. Mar. Chem. 85, 169-189. http://dx.doi.org/10.1016/j.marchem.2003.10.005

D'Ortenzio, F., Ribera d'Alcalà, M., 2009. On the trophic regimes of the Mediterranean Sea: a satellite analysis. Biogeosciences 6, 139-148. 10.5194/bg-6-139-2009

D'Ortenzio, F., Antoine, D., Marullo, S., 2008. Satellite-driven modeling of the upper ocean mixed layer and air–sea CO_2 flux in the Mediterranean Sea. Deep-Sea Res. Part I Oceanogr. Res. Pap. 55, 405-434. http://dx.doi.org/10.1016/j.dsr.2007.12.008

De Carlo, E., Mousseau, L., Passafiume, O., Drupp, P., Gattuso, J.-P., 2013. Carbonate chemistry and air–sea CO_2 flux in a NW Mediterranean Bay over a four-year period: 2007–2011. Aquat. Geochem. 19, 399-442. 10.1007/s10498-013-9217-4

de la Paz, M., Gómez-Parra, A., Forja, J., 2009. Seasonal variability of surface fCO_2 in the Strait of Gibraltar. Aquat. Sci. 71, 55-64. 10.1007/s00027-008-8060-y

de la Paz, M., Huertas, E.M., Padín, X.-A., Gónzalez-Dávila, M., Santana-Casiano, M., Forja, J.M., Orbi, A., Pérez, F.F., Ríos, A.F., 2011. Reconstruction of the seasonal cycle of air–sea CO_2 fluxes in the Strait of Gibraltar. Mar. Chem. 126, 155-162. http://dx.doi.org/10.1016/j.marchem.2011.05.004

DeGrandpre, M.D., Baehr, M.M., Hammar, T.R., 1999. Calibration-free optical chemical sensors. Anal. Chem. 71, 1152-1159. 10.1021/ac9805955

Duarte, C.M., Regaudie-de-Gioux, A., Arrieta, J.M., Delgado-Huertas, A., Agustí, S., 2013. The oligotrophic ocean is heterotrophic. Ann. Rev. Mar. Sci. 5, 551-569. doi:10.1146/annurev-marine-121211-172337

Gazeau, F., Duarte, C.M., Gattuso, J.P., Barrón, C., Navarro, N., Ruiz, S., Prairie, Y.T., Calleja, M., Delille, B., Frankignoulle, M., Borges, A.V., 2005. Whole-system metabolism and CO_2 fluxes in a Mediterranean Bay dominated by seagrass beds (Palma Bay, NW Mediterranean). Biogeosciences 2, 43-60. 10.5194/bg-2-43-2005

Goyet, C., Millero, F.J., Poisson, A., Shafer, D.K., 1993. Temperature dependence of CO_2 fugacity in seawater. Mar. Chem. 44, 205-219. http://dx.doi.org/10.1016/0304-4203(93)90203-Z

Goyet, C., Poisson, A., 1989. New determination of carbonic acid dissociation constants in seawater as a function of temperature and salinity. Deep-Sea Res. Part A Oceanogr. Res. Pap. 36, 1635-1654. http://dx.doi.org/10.1016/0198-0149(89)90064-2

Hassoun, A.E.R., Gemayel, E., Krasakopoulou, E., Goyet, C., Abboud-Abi Saab, M., Ziveri, P., Touratier, F., Guglielmi, V., Falco, C., 2015. Modeling of the total alkalinity and the total inorganic carbon in the Mediterranean Sea. J. Water Resource Ocean Sci. 4, 24-32. doi: 10.11648/j.wros.20150401.14

Ho, D.T., Law, C.S., Smith, M.J., Schlosser, P., Harvey, M., Hill, P., 2006. Measurements of air-sea gas exchange at high wind speeds in the Southern Ocean: Implications for global parameterizations. Geophys. Res. Lett. 33, L16611. 10.1029/2006gl026817

Ho, D.T., Wanninkhof, R., Schlosser, P., Ullman, D.S., Hebert, D., Sullivan, K.F., 2011. Toward a universal relationship between wind speed and gas exchange: Gas transfer velocities measured with $^3He/SF_6$ during the Southern Ocean Gas Exchange Experiment. J. Geophys. Res. 116, C00F04. 10.1029/2010jc006854

Hood, E.M., Merlivat, L., 2001. Annual to interannual variations of fCO_2 in the northwestern Mediterranean Sea: Results from hourly measurements made by CARIOCA buoys, 1995-1997. J. Mar. Res. 59, 113-131. http://dx.doi.org/10.1357/002224001321237399

Krasakopoulou, E., Rapsomanikis, S., Papadopoulos, A., Papathanassiou, E., 2009. Partial pressure and air–sea CO_2 flux in the Aegean Sea during February 2006. Cont. Shelf. Res. 29, 1477-1488. http://dx.doi.org/10.1016/j.csr.2009.03.015

Krasakopoulou, E., Souvermezoglou, E., Goyet, C., 2011. Anthropogenic CO_2 fluxes in the Otranto Strait (E. Mediterranean) in February 1995. Deep-Sea Res. Part I Oceanogr. Res. Pap. 58, 1103-1114. http://dx.doi.org/10.1016/j.dsr.2011.08.008

Lefèvre, N., Taylor, A., 2002. Estimating pCO_2 from sea surface temperatures in the Atlantic gyres. Deep-Sea Res. Part I Oceanogr. Res. Pap. 49, 539-554. http://dx.doi.org/10.1016/S0967-0637(01)00064-4

Liss, P., Merlivat, L., 1986. Air-sea gas exchange rates: Introduction and synthesis, in: Buat-Ménard, P. (Ed.), The role of air-sea exchange in geochemical cycling. Springer Netherlands, pp. 113-127. 10.1007/978-94-009-4738-2_5 978-94-010-8606-6

Luchetta, A., Cantoni, C., Catalano, G., 2010. New observations of CO_2 induced acidification in the northern Adriatic Sea over the last quarter century. Chem. Ecol. 26, 1-17. 10.1080/02757541003627688

Nightingale, P.D., Malin, G., Law, C.S., Watson, A.J., Liss, P.S., Liddicoat, M.I., Boutin, J., Upstill-Goddard, R.C., 2000. In situ evaluation of air-sea gas exchange parameterizations using novel conservative and volatile tracers. Global Biogeochem. Cycles 14, 373-387. 10.1029/1999gb900091

Rivaro, P., Messa, R., Massolo, S., Frache, R., 2010. Distributions of carbonate properties along the water column in the Mediterranean Sea: Spatial and temporal variations. Mar. Chem. 121, 236-245. http://dx.doi.org/10.1016/j.marchem.2010.05.003

Robbins, L.L., Hansen, M.E., Kleypas, J.A., Meylan, S.C., 2010. CO_2calc—A user-friendly seawater carbon calculator for Windows, Max OS X, and iOS (iPhone), U.S. Geological Survey Open-File Report 2010-1280, p. 17.

Rutgersson, A., Smedman, A., Sahlée, E., 2011. Oceanic convective mixing and the impact on air-sea gas transfer velocity. Geophys. Res. Lett. 38, L02602. 10.1029/2010gl045581

Santana-Casiano, J.M., Gonza

lez-Davila, M., Laglera, L.M., 2002. The carbon dioxide system in the Strait of Gibraltar. Deep-Sea Res. Part II Top. Stud. Oceanogr. 49, 4145-4161. http://dx.doi.org/10.1016/S0967-0645(02)00147-9

Sarmiento, J., Gruber, N., 2013. Ocean biogeochemical dynamics. Princeton University Press, Princeton.

Sasaki, K., Ono, T., Tanaka, K., Kawasaki, K., Saito, H., 1998. Variation of the partial pressure of CO_2 in surface water from Kuroshio to Oyashio and the relation between environmental factors and the partial pressure at 144°E off Sanriku, northwestern North Pacific in May, 1997. J. Oceanogr. 54, 593-603. 10.1007/bf02742461

Schneider, A., Wallace, D.W.R., Körtzinger, A., 2007. Alkalinity of the Mediterranean Sea. Geophys. Res. Lett. 34, L15608. 10.1029/2006gl028842

Stambler, N., 2013. Mediterranean Sea - primary productivity, in: Goffredo, S., Dubinsky, Z. (Eds.), The Mediterranean Sea: its history and present challenges. Springer, p. 678. ISBN 978-94-007-6703-4

Taillandier, V., D'Ortenzio, F., Antoine, D., 2012. Carbon fluxes in the mixed layer of the Mediterranean Sea in the 1980s and the 2000s. Deep-Sea Res. Part I Oceanogr. Res. Pap. 65, 73-84. http://dx.doi.org/10.1016/j.dsr.2012.03.004

Takahashi, T., Olafsson, J., Goddard, J.G., Chipman, D.W., Sutherland, S.C., 1993. Seasonal variation of CO_2 and nutrients in the high-latitude surface oceans: A comparative study. Global Biogeochem. Cycles 7, 843-878. 10.1029/93gb02263

Takahashi, T., Sutherland, S.C., Kozyr, A., 2014. Global ocean surface water partial pressure of CO_2 database: Measurements performed during 1957-2013 (Version 2013). Carbon Dioxide Information Analysis Center. Oak Ridge National Laboratory, U.S. Department of Energy, Oak Ridge, Tennessee. 10.3334/CDIAC/OTG.NDP088(V2013)

Takahashi, T., Sutherland, S.C., Sweeney, C., Poisson, A., Metzl, N., Tilbrook, B., Bates, N., Wanninkhof, R., Feely, R.A., Sabine, C., Olafsson, J., Nojiri, Y., 2002. Global sea–air CO_2 flux based on climatological surface ocean pCO_2, and seasonal biological and temperature effects. Deep-Sea Res. Part II Top. Stud. Oceanogr. 49, 1601-1622. http://dx.doi.org/10.1016/S0967-0645(02)00003-6

Touratier, F., Guglielmi, V., Goyet, C., Prieur, L., Pujo-Pay, M., Conan, P., Falco, C., 2012. Distributions of the carbonate system properties, anthropogenic CO_2, and acidification during the 2008 BOUM cruise (Mediterranean Sea). Biogeosci. Discuss. 9, 2709-2753. 10.5194/bgd-9-2709-2012

Turk, D., Malačič, V., DeGrandpre, M.D., McGillis, W.R., 2010. Carbon dioxide variability and air-sea fluxes in the northern Adriatic Sea. J. Geophys. Res. 115, C10043. 10.1029/2009jc006034

Wanninkhof, R., 1992. Relationship between wind speed and gas exchange over the ocean. J. Geophys. Res. 97, 7373-7382. 10.1029/92jc00188

Wanninkhof, R., Asher, W.E., Ho, D.T., Sweeney, C., McGillis, W.R., 2009. Advances in quantifying air-sea gas exchange and environmental forcing. Ann. Rev. Mar. Sci. 1, 213-244. doi:10.1146/annurev.marine.010908.163742

Weiss, R.F., 1974. Carbon dioxide in water and seawater: the solubility of a non-ideal gas. Mar. Chem. 2, 203-215. http://dx.doi.org/10.1016/0304-4203(74)90015-2

Weiss, R.F., Price, B.A., 1980. Nitrous oxide solubility in water and seawater. Mar. Chem. 8, 347-359. http://dx.doi.org/10.1016/0304-4203(80)90024-9

Williams, P.J.l.B., 1998. The balance of plankton respiration and photosynthesis in the open oceans. Nature 394, 55-57.

Article III: Estimates of pCO_2 and air-sea CO_2 fluxes in the Mediterranean Sea in May 2007 and 2013 from satellite data

Gemayel, E., et al. (2015)

Submitted to Remote sensing of Environment

Estimates of pCO_2 and air-sea CO_2 fluxes in the Mediterranean Sea in May 2007 and 2013 from satellite data

Elissar GEMAYEL[1,2,3], Mohamed Anis BENALLAL[1,2], Catherine GOYET[1,2], Maria CALLEJA[4], Abed El Rahman HASSOUN[3], Marta ALVAREZ[5], Carlos DUARTE[6], Marie ABBOUD-ABI SAAB[3], Franck TOURATIER[1,2] and Véronique GUGLIELMI[1,2]

[1] Université de Perpignan Via Domitia, IMAGES_ESPACE-DEV, 52 avenue Paul Alduy, 66860 Perpignan Cedex 9, France
[2] ESPACE-DEV, UG UA UR UM IRD, Maison de la télédétection, 500 rue Jean-François Breton, 34093 Montpellier Cedex 5, France
[3] National Council for Scientific Research, National Center for Marines Sciences, P.O Box 534, Batroun, Lebanon
[4] King Abdullah University of Science and Technology (KAUST), Red Sea Research Center, Thuwal 23955-6900, Saudi Arabia
[5] IEO – Instituto Español de Oceanografía, Apd. 130, A Coruña, 15001, Spain
[6] Mediterranean Institute of Advanced Studies, Department of Global Change Research, CSIC-UIB, 07190 Esporles, Spain;

Abstract

This study presents a first attempt to retrieve air-sea CO_2 fluxes in the Mediterranean Sea from direct measurements of surface water pCO_2 (pCO_2^{sw}) and satellite derived parameters of Sea Surface Temperature (SST), Chlorophyll_a (Chla) and Chromophoric Dissolved Organic Matter index (CDOMi). The dataset consists of direct pCO_2^{sw} measurements conducted along two cruises in May 2007 and 2013, and their correspondent monthly composites of different parameters at 4 km resolution derived from the Moderate Resolution Imaging Spectroradiometer on board the Aqua Satellite (MODIS-A). For each cruise, we conducted a comparison of three different combinations that include fitting pCO_2^{sw} from SST alone or SST with Chla or CDOMi. In May 2007 and 2013 the best relationships were found by fitting pCO_2^{sw} to SST and CDOMi with RMSE (Root Mean Square Error) of ± 9 µatm and pCO_2^{sw} to SST and Chla with RMSE of ± 10 µatm respectively. The addition of a biological parameter such as CDOMi or Chla to SST significantly reduced the uncertainty of the fits. For instance in May 2007, SST and CDOMi contributed to 50 % of the pCO_2^{sw} variability, compared to only 34 % for SST alone. The equation developed for May 2013 showed a temporal limitation but it captured 96 % of the in situ pCO_2^{sw} range and was hence used to map the pCO_2^{sw} and air-sea CO_2 fluxes on the scale of the Mediterranean Sea. The mapped pCO_2^{sw} and air-sea CO_2 fluxes show that this equation can capture the sink/source behavior of the Western and Eastern basins respectively with an Eastward pCO_2^{sw} range of 120 µatm. These results indicate that satellite products provide an excellent source of data that can be used to map the air-sea CO_2 fluxes from direct pCO_2^{sw} measurements with a high resolution and on a large scale in the Mediterranean Sea.

Keywords: Mediterranean Sea; pCO_2; regressions; satellite images; CO_2 fluxes

1. Introduction

The Mediterranean Sea represents only 0.8 % of the global oceanic surface, but is capable of absorbing more CO_2 from the atmosphere than the near oceanic regions (Schneider *et al.*, 2010; Hassoun *et al.*, 2015). This semi-enclosed basin is characterized by warm, high alkalinity waters, with a fast overturning circulation that absorbs CO_2 from the atmosphere and transports it to the deep waters (Schneider *et al.*, 2010; Touratier and Goyet, 2011; Touratier *et al.*, 2012; Cossarini *et al.*, 2015). The Mediterranean Sea also impacts the global thermohaline circulation by the export of intermediate waters to the Atlantic Ocean. Due to the limited exchange with the world ocean it can be considered as a "laboratory basin", representing processes that take place at a larger scale in the world ocean (Béthoux *et al.*, 1999; Bergamasco and Malanotte-Rizzoli, 2010; Malanotte-Rizzoli *et al.*, 2014).

Despite the importance of the Mediterranean Sea in improving our understanding of the mechanisms and feedbacks controlling the Earth's climate (Turley, 1999); the measurements of the carbonate system parameters in particular those of the partial pressure of CO_2 (pCO_2) are still limited both in time and in space (Hood *et al.*, 1999; Bégovic and Copin-Montégut, 2002; Álvarez, 2012). The direct measurements of surface water pCO_2 (pCO_2^{sw}) is important to estimate global and regional air-sea CO_2 fluxes. As such an effort should be done to introduce pCO_2^{sw} data from the Mediterranean Sea and other non-inspected areas to the actual climatological mean distributions of the air–sea CO_2 flux based on ~ 3 million measurements of pCO_2^{sw}, mostly from the open ocean (Takahashi *et al.*, 2009; Takahashi *et al.*, 2014).

Due to the scarcity of the pCO_2^{sw} measurements, the Mediterranean Sea has been included only in a few global air-sea CO_2 fluxes schemes (Valsala and Maksyutov, 2010; Rödenbeck *et al.*, 2013; Zeng *et al.*, 2014). Generally the CO_2 fluxes on the scale of the entire basin were calculated either from the DYFAMED time-series monthly fluxes (Hood and Merlivat, 2001; Bégovic and Copin-Montégut, 2002; Copin-Montégut *et al.*, 2004) or from coupled-models (D'Ortenzio *et al.*, 2008; Louanchi *et al.*, 2009; Taillandier *et al.*, 2012).

In areas of limited data availability such as the Mediterranean Sea, the use of remote sensing products with high temporal and spatial resolutions provides a useful tool to interpret the pCO_2^{sw} variability (Boutin *et al.*, 1999). Because of the strong thermodynamic effect of Sea Surface Temperature (SST) on pCO_2^{sw} (Copin-Montégut, 1988; Goyet *et al.*, 1993; Takahashi *et al.*, 1993), remotely sensed SST is often used to generate surface water pCO_2^{sw} maps (Stephens *et al.*, 1995; Lee *et al.*, 1998; Boutin *et al.*, 1999; Nelson *et al.*, 2001; Olsen *et al.*, 2003; Olsen *et al.*, 2004). However these algorithms did not account for the important role of the biological pump on pCO_2^{sw} that could directly drive the air-sea CO_2 fluxes even in the open ocean (Calleja *et al.*, 2005). In more recent works Chlorophyll_a (Chla) concentration derived from ocean color satellites have been included to improve the interpolation of pCO_2^{sw} (Ono *et al.*, 2004; Rangama *et al.*, 2005; Jamet *et al.*, 2007; Padin *et al.*, 2009; Moussa *et al.*, 2015). A few numbers of studies have also included in their algorithms parameters other than SST or Chla, in an attempt to improve their satellite-retrieve

pCO_2^{sw} estimates. For instance, Lohrenz and Cai (2006) added the Chromophoric Dissolved Organic Matter index (CDOMi), Sarma *et al.* (2006) included the climatological sea surface salinity (SSS), and Else *et al.* (2008) integrated the Mixed Layer Depth (MLD).

The use of remote sensing products over the Mediterranean Sea remains very rare. To the best of our knowledge only few studies referred to these products for the estimation of the CO_2 fluxes or any other carbonate system parameter (D'Ortenzio *et al.*, 2008; Taillandier *et al.*, 2012; D'Ortenzio *et al.*, 2014). In particular, D'Ortenzio *et al.* (2008) applied a satellite-driven modeling approach to estimate the seven years average (1998-2004) CO_2 fluxes from SST, wind speed and Chla satellite data retrieved from the Pathfinder Sea Surface Temperature, QuikSCAT and SeaWifs respectively. Then, Taillandier *et al.* (2012) simulated the mixed-layer CO_2 fluxes in the 1980s and the 2000s from an array of one-dimensional physical–biological–chemical model, using the ocean color satellite products of the CZCS and the SeaWifs respectively.

In this study, we introduce a comparison between different empirical algorithms intended to retrieve the pCO_2^{sw} during two cruises in the Mediterranean Sea conducted in May 2007 and 2013, from satellite imagery of SST, SST and Chla or SST and CDOMi retrieved from MODIS-Aqua. Then we evaluate the performance and application of the selected relationships using another dataset of pCO_2^{sw} discrete samples measured in June 2006 (Calleja *et al.*, 2013). Finally we generate on the scale of the entire Mediterranean Sea, high resolution maps of pCO_2^{sw} and air-sea CO_2 fluxes for the month of May 2007 and 2013.

2. Methods

2.1. In situ pCO_2 measurements

Continuous underway measurements of surface water pCO_2^{sw} were conducted in May 2007 and 2013 during the Thresholds and MedSeA cruises respectively (Figure 1).

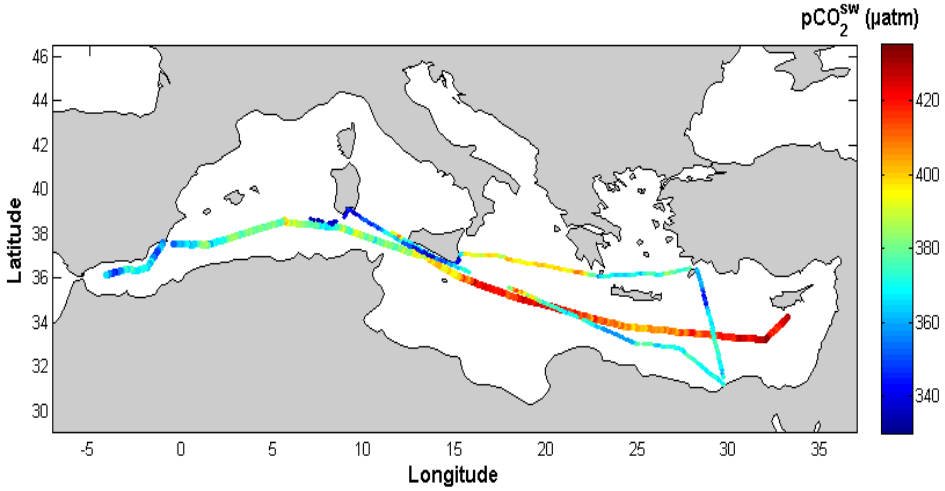

Figure 1. pCO_2^{sw} measurements conducted during the Thresholds cruise in May 2007 (thin line) and the MedSeA cruise in May 2013 (thick line)

During the Thresholds 2007 cruise (5 to 31 May 2007), the pCO_2^{sw} was measured at 5 m depth using a high-precision (± 2 ppm) non-dispersive infrared gas analyzer (EGM-4, from PP-Systems) averaging measurements at 1 min recording interval. Before entering the gas analyzer, the gas stream was circulated through a calcium sulfate column to avoid interferences from water vapor, and through a gas exchange column connected to the research vessel seawater flow, for air-sea water equilibration, as described in Calleja *et al.* (2005). During the MedSeA 2013 cruise, the pCO_2^{sw} was also measured (3 to 17 May 2013) at 5m depth and at a 20 min interval using an AFT-CO_2 (Autonomous Flow Thru; spectrophotometry based on the optical absorbance of the pH indicator solution of bromothymol blue diluted in seawater [DeGrandpre *et al.*, 1999]) sensor (± 3 µatm) connected to the seawater line (Gemayel *et al.*, 2015; Goyet *et al.*, 2015).

2.2. Satellite derived properties

For May 2007 and 2013 monthly composites of Sea Surface Temperature (SST), Chlorophyll_a (Chla) and Chromophoric Dissolved Organic Matter (CDOM) index, were retrieved from the Moderate Resolution Imaging Spectroradiometer aboard the Aqua satellites (MODIS-A). We used the Level 3 Standard Mapped Images (L3 SMI) at 4 km resolution generated from the MODIS-A product available from the Ocean Color Web (http://oceancolor.gsfc.nasa.gov/ftp.html).

The CDOM index (CDOMi) product is defined according to Morel and Gentili (2009) where two ratios of spectral reflectance R(412)/R(443) and R(490)/R(555) are computed as a function of Chla. The CDOMi is defined upon the existence of a mean relationship between the CDOM content and the Chla concentration (Morel, 2009). If CDOM is in "excess" compared to its mean value as expected from the Chla value, then CDOMi is > 1. If the CDOM content is below its expected average value, the CDOMi is < 1.

Level 4 gridded mean monthly wind fields in 0.25º geographical grid were also retrieved for May 2007 and 2013, from the Advanced SCATterometer (ASCAT) carried onboard of the Meteorological Operational Polar (Metop-A) satellites (http://cersat.ifremer.fr/).

2.3. Linear and multiple linear regressions

The two datasets used in this study have very different sample size due to the difference in the measurements frequency: 20000 compared to 621 data points for the Thresholds and MedSeA cruises respectively. In order to develop comparable regressions, the sample size should be roughly equal. In this manner, the measurements of the Thresholds cruise were averaged at the same recording interval of the MedSeA cruise. Then, the satellite derived composites of SST, Chla and CDOMi were extracted at the nearest neighboring position of the in situ pCO_2^{sw} measurements. From each image, single pixels were spatially and temporally matched with the respective cruise (Thresholds and MedSeA) and disregarded when any pixel was located at a distance greater than the image resolution (4 km). The mean,

standard deviation (Std), minimum (min) and maximum (max) of the different parameters for each cruise is presented in Table 1.

Several linear and multiple linear regressions (MLR) were tested to estimate pCO_2^{sw} from the derived SST alone or SST combined with Chla or CDOMi. The best relationship was chosen according to highest coefficient of determination (r^2) and the lowest Root Mean Square Error (RMSE).

Measurements of discrete water samples of pCO_2^{sw} taken in June 2006 (Calleja *et al.*, 2013) were used as another dataset in order to evaluate the performance of the selected relationships. For this cruise we also extracted the associated satellite derived composites of SST, Chla and CDOMi.

Table 1. Mean, standard deviation (Std), minimum and maximum of the different parameters in May 2007 and 2013. The pCO_2^{sw} is measured in situ, whereas SST, Chla and CDOMi are retrieved from the correspondent monthly composites of MODIS-A at 4km resolution

	pCO_2^{sw} (µatm)	SST (ºC)	Chla ($mg.m^{-3}$)	CDOMi
May 2007 (Thresholds)				
Mean	369	19.6	0.12	4
Std	± 17	± 0.7	± 0.05	± 1
Min	330	17.3	0.06	2
Max	420	21.5	0.48	9
May 2013 (MedSeA)				
Mean	395	19.2	0.15	5
Std	± 22	± 1.6	± 0.13	± 1
Min	342	16.7	0.04	2
Max	435	22.6	0.99	9

2.4. Maps of pCO_2^{sw} and air-sea CO_2 fluxes

In order to generate for May 2007 and 2013 maps of pCO_2^{sw} on the scale of the entire Mediterranean Sea, the selected relationships were applied to the respective maps of SST, Chla and CDOMi (section 2.2). In order to avoid the extrapolation of pCO_2^{sw} values outside the validity range of the different input parameters, the pCO_2^{sw} was only mapped where all input parameters were within the range of the respective database (Table 1).

The CO_2 air–sea fluxes ($mol.m^{-2}.month^{-1}$) were computed according to equation 1 using the "CO_2calc 1.2.0" software (Robbins *et al.*, 2010).

$$F = \beta o \times k \times \Delta pCO_2 \qquad (1)$$

where F is the monthly air–sea flux of CO_2; βo is the solubility of CO_2 in seawater, k is the gas exchange coefficient and ΔpCO_2 is the gradient between the ocean and the atmosphere ($\Delta pCO_2 = pCO_2^{sw} - pCO_2^{air}$) .

The calculation of solubility requires measurements of SST and SSS (Weiss, 1974). Solubility maps for May 2007 and 2013 were created by combining for a given year the correspondent SST from the MODIS-A imagery and SSS retrieved from the Mediterranean Sea physical reanalysis (1987-2013) product (http://www.myocean.eu/). The latter consists of a hydrodynamic model at a 1/16° grid resolution, supplied by the Nucleus for European Modeling of the Ocean (NEMO), with a variational data assimilation scheme (OceanVar) for temperature and salinity vertical profiles and satellite sea level anomaly.

The ASCAT wind speed retrievals for May 2007 and 2013 were used to calculate the transfer velocity (k) according to equation 2 (Wanninkhof, 1992):

$$k = 0.31 \times U_{10}^2 \times (Sc/660)^{-0.5} \qquad (2)$$

where Sc and 660 are the Schmidt number of CO_2 in seawater as function of in situ SST and SSS; and at 20 ºC and SSS = 35 respectively; U_{10} is the wind speed at 10 m above sea level derived by the ASCAT ($m.s^{-1}$). We computed the average U_{10}^2 using the instantaneous coefficient for wind speed as suggested by Olsen *et al.* (2004) and Wanninkhof *et al.* (2013).

The atmospheric pCO_2 (pCO_2^{air}) was computed from equation 3:

$$pCO_2^{air} = xCO_2(p_{atm} - pH_2O) \qquad (3)$$

Where xCO_2 is the average mixing ratio of CO_2 in air, p_{atm} is the atmospheric pressure (generally close to 1 atm), and pH_2O is the partial pressure of water vapor at 100% humidity saturation computed from the SSS and SST maps (Weiss and Price, 1980). We assumed a constant mean of xCO_2 of 386 and 399 ppm for May 2007 and 2013 respectively as measured at the Lampedusa Island station (Italy) and downloaded from the World Data Center for Greenhouse Gases (http://ds.data.jma.go.jp/gmd/wdcgg/).

The wind fields and salinity maps at 1/4º and 1/16º resolution respectively, were resized into 4 km grids using the nearest neighboring position interpolation method. This allowed us to produce pCO_2^{sw} and air-sea CO_2 fluxes maps at a 4 km resolution.

3. Results and discussion

3.1. Comparison of equations

The two cruises were conducted during a month of May; however there is a clear inter-annual variability in the physico-bio-chemical parameters because of the 7 years gap between them. This was especially noticed for pCO_2^{sw} where values of 360 µatm and 400 µatm were recorded at the same geographical location (33 ºN; 29 ºE) for the Thresholds and MedSeA cruises respectively (Figure 1). Also, the range of pCO_2^{sw} in May 2007 was smaller than that

in May 2013. This was also the case for SST, Chla and CDOMi (Table 1). The observed inter-annual variability between the two periods, lead us to study each cruise separately. For each cruise we will present equations that estimate pCO_2^{sw} from the correspondent satellite data of May 2007 or 2013.

Previous studies suggested that the use of SST alone could be used to provide reliable extrapolations of pCO_2^{sw} (Stephens *et al.*, 1995; Hood *et al.*, 1999; Nelson *et al.*, 2001; Olsen *et al.*, 2004). However, the different equations presented in Table 2, show that for both cruises using SST as the only predictor of pCO_2^{sw} yields the lowest r^2 and the highest RMSE (Eqs 4 and 7). In fact, the addition of Chla or CDOMi, along with SST as independent variables, significantly improved the performance of the fits (Table 2).

Table 2. Test of different equations intended to derive pCO_2^{sw} from satellite retrievals of SST alone or SST combined with Chla or CDOMi

Datasets	Equations	N	r^2	RMSE (µatm)
May 2007 (Thresholds)	(4): $pCO_2^{sw} = 8.56(SST) + 200.2$	660	0.34	± 9
	(5): $pCO_2^{sw} = 6.85(SST) – 52.59(Chla) + 239.4$	660	0.37	± 9
	(6): $pCO_2^{sw} = 4.93(SST) – 5.11(CDOMi) + 294.2$	681	0.50	± 9
May 2013 (MedSeA)	(7): $pCO_2^{sw} = 10.32(SST) + 197.8$	546	0.73	± 10
	(8): $pCO_2^{sw} = 7.83(SST) – 49.09(Chla) + 253.3$	552	0.76	± 10
	(9): $pCO_2^{sw} = 11.34(SST) + 2.92(CDOMi) + 162.6$	547	0.75	± 10

The two datasets have comparable slopes for SST, or SST and Chla. In equations (5) and (8), the pCO_2^{sw} was positively correlated with SST and negatively correlated with Chla. The thermodynamic effect of temperature on pCO_2^{sw} (at constant salinity, alkalinity and dissolved inorganic carbon) is about 4%/ºC (Copin-Montégut, 1988; Goyet *et al.*, 1993; Takahashi *et al.*, 1993). However, photosynthetic activity consumes the dissolved CO_2 which lowers the pCO_2^{sw} (Takahashi *et al.*, 2002). In the Mediterranean Sea, the Eastward increasing gradient of SST (Lionello *et al.*, 2012) and the decreasing Eastward trophic gradient in productivity (Bosc *et al.*, 2004; D'Ortenzio and Ribera d'Alcalà, 2009) could explain the opposite signs in the slopes of SST and Chla.

For the Thresholds cruise, the combination SST and CDOMi (Eq 6) improved significantly the accuracy of the fit compared to the combination of SST and Chla (Eq 5). It also maintained a good r^2 for the MedSeA cruise (Eq 9). However the relationships are very different when the independent variables were SST and CDOMi. In equation 6, pCO_2^{sw} was positively correlated with SST and negatively correlated with CDOMi, whereas in equation 9 pCO_2^{sw} was positively correlated with both SST and CDOMi.

The distance of the stations to the shore could affect the CDOM dynamics, as the dissolved organic carbon (DOC) concentrations in coastal areas are mostly delivered by river discharges (Bates and Hansell, 1999; Hung *et al.*, 2007). We noticed that in many instances the track of the Threshold cruise was closer to the coast than that of the MedSeA cruise. To

test the effect of coastal inputs, we combined both datasets (Thresholds and MedSeA) and calculated the distance of each data point to the nearest coast and then defined two subsets corresponding to coastal (distance to the coast < 1 km) and open waters (distance to the coast > 1 km) stations (Table 3). The analysis revealed that in open waters (Eq 11) the accumulation of CDOM is significantly more pronounced than in coastal stations (Eq 10). The stations that are closer to the coast tend to be marked by higher primary production than those in open waters, where more fresh and labile CDOM might be produced and then consumed by heterotrophs. On the other hand, in open waters, CDOM are essentially controlled by modifications of the water column physical structure and by the balance between production and degradation processes (Coble, 2007). Hence, the DOC concentrations in the upper open are relatively high in warm seasons because the water column is stratified and regenerated production dominates (Hansell, 2002). Thus CDOM accumulates while other organic compounds are being respired. That could also explain why equation 5 has a higher slope than equation 8. The potentially high productivity in coastal stations could drive an accentuated change of pCO_2^{sw} with Chla.

The repartitions of the stations between the Western and Eastern basins could also explain the different signs of the CDOMi slopes between equations 6 and 9. The MedSeA sampling scheme covered the entire Eastward transect of the Mediterranean Sea, whereas the stations of the Threshold cruise where more concentrated in the Eastern basin. If we divide the MedSeA cruise data into two subsets, we find that the CDOMi slope is positive in the Western Basin (Eq 12) and negative in the Eastern Basin (Eq 13). The CDOMi slope in equation 13 is also comparable to that of equation 6 for the Threshold cruise data that represents the Eastern Basin. The difference in the CDOMi slope between equations 6 and 9 is then influenced by the CDOM content in each basin. In fact, the near surface absorption coefficients of CDOM in the Western Basin exceed those of the Eastern Basin by 50 % (Morel and Gentili, 2009a). This was later confirmed by Xing *et al.* (2012) who noted considerable differences between the two basins at all depths with a marked photobleaching in the summer especially in the Eastern Mediterranean.

Table 3. Subsets to test the different CDOMi drivers. The first subset divides the data from both the Thresholds and MedSeA cruises into coastal and open water stations. The second subset divides the MedSeA cruise data in Western and Eastern basins

Cruise	Subsets		N	r^2	RMSE (µatm)
Thresholds and MedSeA	Coastal water	(10): pCO_2^{sw} = 1.40SST + 1.09CDOMi + 336.9	600	0.03	± 9
	Open water	(11): pCO_2^{sw} = 11.53SST + 7.31CDOMi + 127.2	628	0.57	± 13
MedSeA	Western basin	(12): pCO_2^{sw} = 10.15SST + 3.86CDOMi + 174.3	260	0.57	± 6
	Eastern basin	(13): pCO_2^{sw} = 2.65SST – 4.35CDOMi + 380.8	287	0.60	± 6

3.2. Selection of equations

Equations 6 and 8 were derived from in situ pCO_2^{sw} measurements and satellite data in May 2007 and 2013 respectively. In the following we will test whether these equations can be applied beyond their respective time period. In that order we computed the pCO_2^{sw} residuals (pCO_2^{sw} residuals = measured pCO_2^{sw} – estimated pCO_2^{sw}) from equations 6 and 8 applied to the datasets of May 2007 or May 2013 respectively. Then we calculated the pCO_2^{sw} residuals from equation 8 applied to the May 2007 dataset and vice-versa the pCO_2^{sw} residuals from equation 6 applied to the May 2013 dataset.

By applying equation 6 to the dataset of May 2007, the pCO_2^{sw} residuals yielded a maximum of ± 18 µatm. However, by applying equation 8 to the same dataset of May 2007, pCO_2^{sw} residuals reached up to – 56 µatm (Figure 2a). By applying equation 8 to the dataset of May 2013, pCO_2^{sw} residuals yielded a maximum of ± 20 µatm. This was not the case when we applied equation 6 to the dataset of May 2013, where pCO_2^{sw} residuals reached up to 68 µatm (Figure 2b). The negative pCO_2^{sw} residuals indicate that equation 8 tends to overestimate the pCO_2^{sw} in May 2007, whereas the opposite is seen in equation 6 that tends to underestimate the pCO_2^{sw} in May 2013. This clearly shows that equations 6 and 8 are confined to the months of May 2007 and May 2013 respectively. Their application beyond their respective time periods could lead to significant deviations.

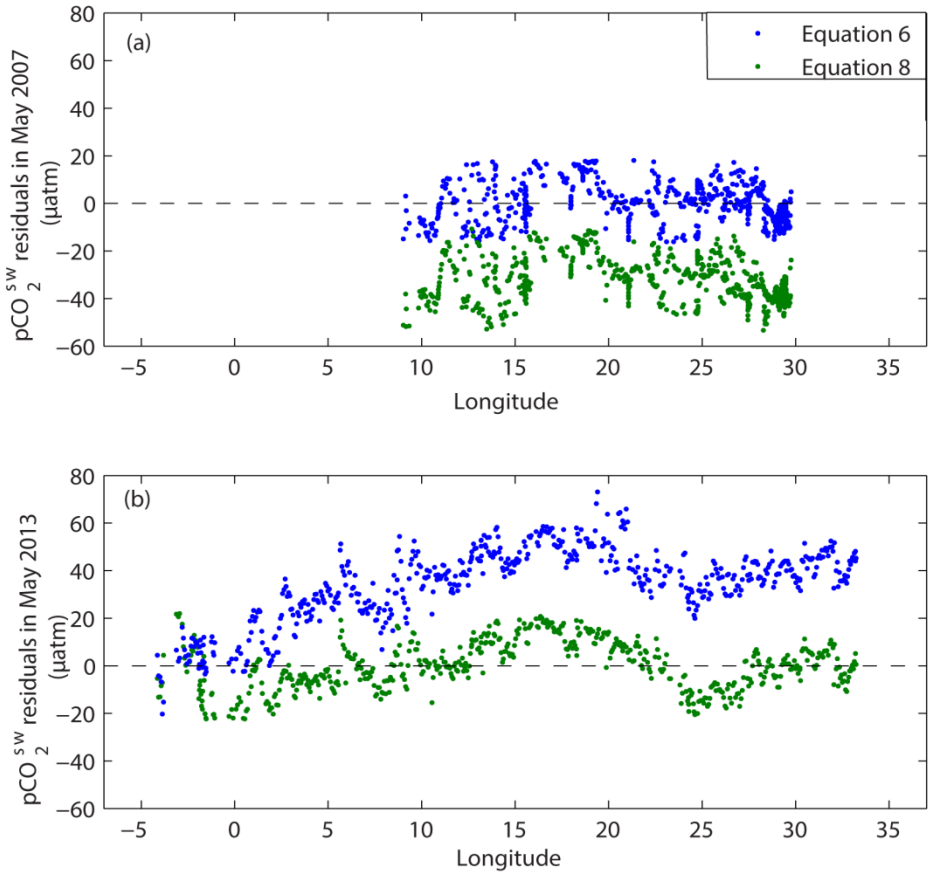

Figure 2. (a) pCO_2^{sw} residuals of equation 6 and 8 applied to the dataset of May 2007, (b) pCO_2^{sw} residuals of equations 6 and 8 applied to the dataset of May 2013

Taking each time period separately, the relationships determined for May 2007 and 2013 were SST and CDOMi (Eq 6) and SST and Chla (Eq 8) respectively. In equation 6, SST and CDOMi explained 50 % of the pCO_2^{sw} variability whereas in equation 8, SST and Chla contributed to 75 % of the pCO_2^{sw} variability. The RMSE of ± 9 and ± 10 µatm for equations 6 and 8 respectively show that for both time periods the algorithms are performing well (Table 3). The calculated RMSE are comparable with other studies that have added Chla or CDOMi to account for the role of the biological pump on pCO_2^{sw}. In the North Pacific, Ono *et al.* (2004) reported an RMSE value of ± 14 µatm using the combination SST and Chla. In the Hudson Bay (Canada), Else *et al.* (2008) reported a RMSE of ± 12 µatm with an r^2 of 0.90 using in situ SST and CDOMi. The uncertainties in equations 6 and 8 are also within the range of the usual thermodynamic calculations used to estimate the pCO_2^{sw} in case of lack of measurements. For instance, the estimated probable errors in calculating pCO_2^{sw} from A_T and C_T can vary from ± 5.7 µatm (Millero, 2007) to reach as high as ± 26 µatm (Lee *et al.*, 2000). Also a recent inter-laboratory comparison study showed that the uncertainty of the A_T and C_T measurements can reach as high as ± 10 µmol.kg^{-1} (Bockmon and Dickson, 2015), which would provide a calculated pCO_2^{sw} with an uncertainty higher than ± 20 µatm.

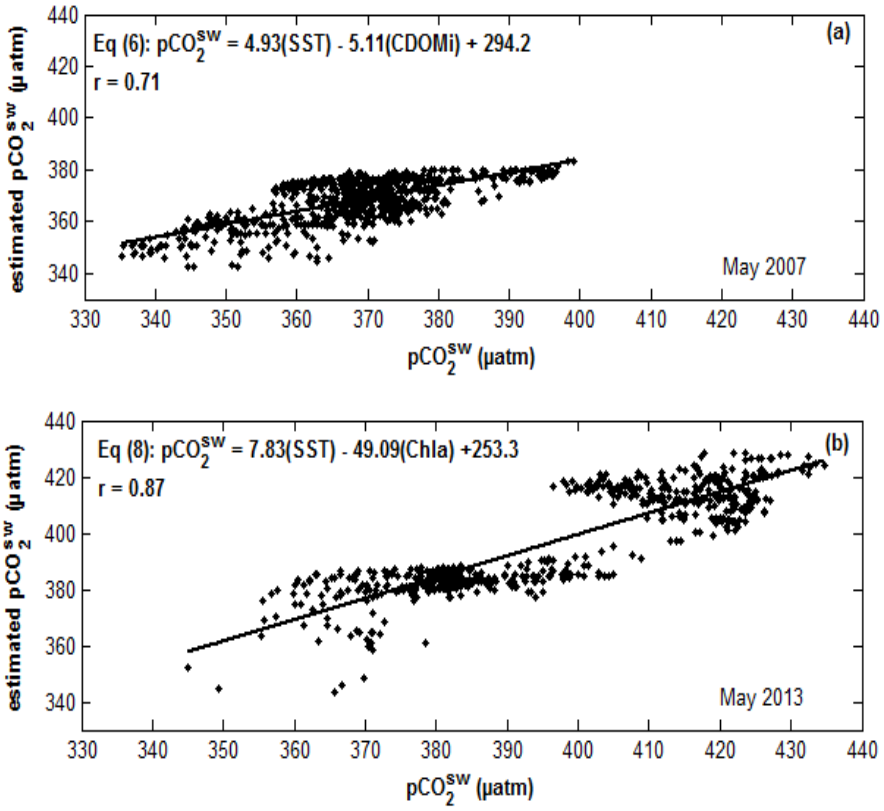

Figure 3. Correlations between the estimated pCO_2^{sw} and the measured pCO_2^{sw}, (a) from SST and CDOMi for May 2007 (Eq 6; Eastern Mediterranean) and (b) pCO_2^{sw} from SST and Chla for May 2013 (Eq 8; Whole Mediterranean)

For equation 8, the correlation coefficient (r) between the estimated and the measured pCO_2^{sw} (r = 0.87) was significantly higher than that of equation 6 (r = 0.71). Also the pCO_2^{sw} estimation range of equation 8 (85 µatm) was twice as high as that of equation 6 (42 µatm).

Consequently, the pCO_2^{sw} estimation range formed 64 % and 94 % of the in situ pCO_2^{sw} range for May 2007 and 2013 respectively (Figure 3). Hence equation 8 has better estimation skills than equation 6, since it can estimate the pCO_2^{sw} with a low uncertainty and on a wide range.

The low range of estimated pCO_2^{sw} captured by equation 6 could be explained by the temporal displacement between daily and monthly averages of the different parameters. In fact to directly apply equations 6 or 8, there should be no systematic bias between in situ and remotely sensed data (Olsen et al., 2004). This can only be done for SST since in situ measurements of CDOM and Chla are not available for both cruises. The mean difference between in situ and satellite derived SST (ΔSST = SST in situ – SST satellite) is -0.49 ± 0.60 ºC and 0.23 ± 0.81 ºC for the MedSeA and Thresholds cruises respectively. However the range of ΔSST was higher in the Threshold cruise compared to that of the MedSeA cruise. The ΔSST was up to ± 2 ºC for the Threshold cruise, whereas the maximum ΔSST was 0.73 ºC for the MedSeA cruise. In equation 6, the ability of the MODIS-A to adequately measure the absorbance of CDOM at 412 nm should also be considered (Else *et al.*, 2008). Xing *et al.* (2014) showed that at the surface, the subsurface maxima and seasonal enhancement of CDOM cannot be detected by satellite data in the Mediterranean Sea.

The use of daily instead of monthly satellite products would have probably increased the r^2 of the fits. However the use of daily products will reduce significantly the retrieved SST, Chla and CDOMi data because of the cloud coverage and the revisiting time of the MODIS-A. In other words, the revisiting time of the MODIS-A was not synchronous with the cruise transects, leaving many areas with no data records. We are then assuming that the daily pCO_2^{sw} measurements are representative of the monthly pCO_2^{sw} variations that would occur in May 2007 and May 2013. Several studies such as Ono *et al.* (2004), Rangama *et al.* (2005), Jamet *et al.* (2007), Zhu *et al.* (2009), Jo *et al.* (2012) and Parard *et al.* (2014) have made the same assumption, by collocating monthly satellite derived data with daily in situ pCO_2^{sw} measurements.

3.3. Testing the equations on an another dataset

As previously described by Calleja *et al.* (2013), several discrete pCO_2^{sw} measurements were performed in June 2006 at different stations located in the Mediterranean Sea (Figure 4a). The pCO_2^{sw} residuals (pCO_2^{sw} – estimated pCO_2^{sw}) were computed at 15 stations from equations 6 and 8 using collocated monthly composite satellite data corresponding to June 2006 of SST and CDOMi or SST and Chla respectively.

For most of the stations the estimated pCO_2^{sw} from equation 6 was in a close agreement with the in situ pCO_2^{sw}. Most of the residuals computed from equation 6 were within a range of 1 to 6 µatm which is close the uncertainty of the in situ pCO_2^{sw} measurements. However, for stations 19 to 21 residuals reached up to 94 µatm. The large residuals observed for these three stations are probably due to the seasonal variation of pCO_2^{sw}, as the sampling was performed towards the end of the month (24 to 26 June), whereas other stations were sampled during the

first two weeks of June 2006. The other few punctual deviations observed are probably due to the interannual variation of pCO_2^{sw}, the sampling depth and the influence of riverine and coastal inputs. For example, stations 10, 17 and 18 located in the northern part of the Aegean Sea could be affected by the inflows of the Black Sea (Figure 4b).

The estimated pCO_2^{sw} from equation 8 are significantly different from the in situ pCO_2^{sw} (Figure 4c). For instance, equation 8 overestimates pCO_2^{sw} which lead to negative residuals as high as - 41 µatm for station 4 compared to only - 3 µatm as computed from equation 6. Also for stations 10, 17 and 18 located in the Aegean Sea, the mean residual of pCO_2^{sw} for equation 8 was ± 24 µatm. The high residuals computed from equation 8 can be explained by the 7 years differences between the cruises in June 2006 and May 2013. This shows that equation 8 is temporally confined to the month of May 2013 and its application beyond that period can lead to significant deviations.

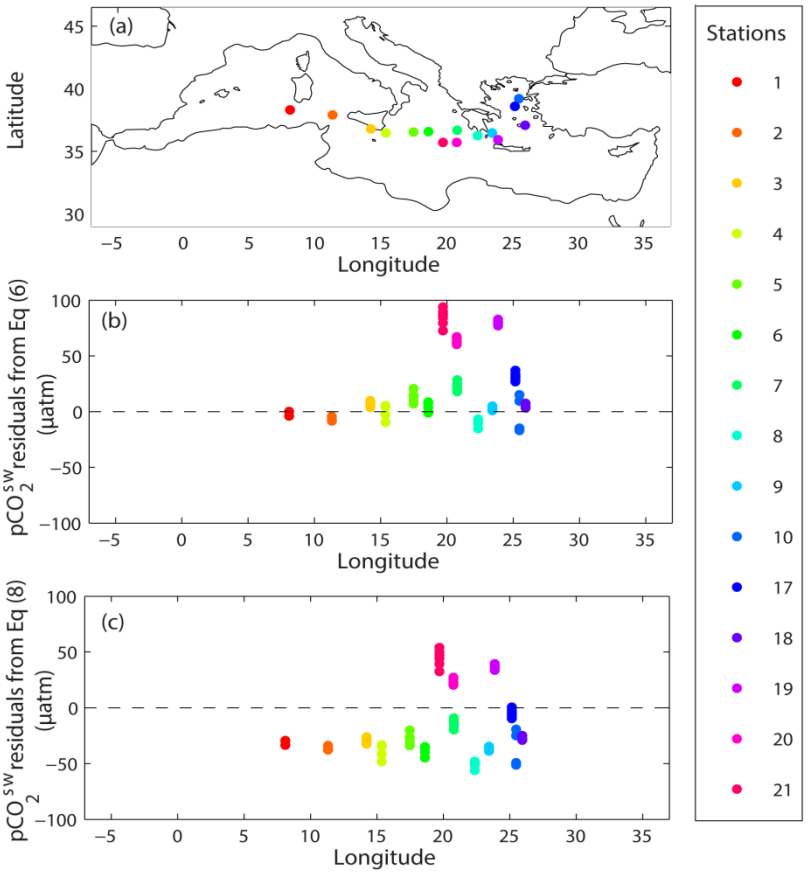

Figure 4. (a) Repartition of the in situ pCO_2^{sw} measurement in June 2006, and (b) the pCO_2^{sw} residuals when applying equation 6 and (c) equation 8 on the validation dataset

3.4. Estimates of pCO_2^{sw} in May 2007 and 2013

The pCO_2^{sw} in May 2007 is mapped by applying equation 6 to the May 2007 satellite data of SST and CDOMi. The pCO_2^{sw} in in May 2013 is mapped by applying equation 8 to the May 2013 satellite data of SST and Chla. In order to map the pCO_2^{sw} on the spatial scale of the entire Mediterranean Sea, the selected equation should have a low uncertainty and a wide

estimation range. As previously shown, equation 6 might work locally since it showed good estimation skills when applied to the dataset of June 2006. However, it represented only 64 % (estimation range = 60 µatm) of the in situ pCO_2^{sw} range which limits its application on a large spatial scale.

As shown in Figure 5a, the estimated pCO_2^{sw} from equation 6 is somewhat uniform and does not represent the high variability encountered in the Mediterranean Sea. On the other hand, equation 8 can estimate pCO_2^{sw} within a range of about 90 µatm (94 % of the in situ pCO_2^{sw} range in May 2013). Hence equations 8 with a dataset covering a larger Eastward transect and a higher representation of the in situ pCO_2^{sw} range than equation 6; is more appropriate to extrapolate pCO_2^{sw} on the scale of the entire Mediterranean Sea than equation 6. But equation 8 cannot be applied in the areas of Gulf of Lyon, the North Balearic Sea and the northernmost part of the Levantine Sea, because the SST and Chla concentrations in these areas are outside its validity range (section 2.3; Table 1).

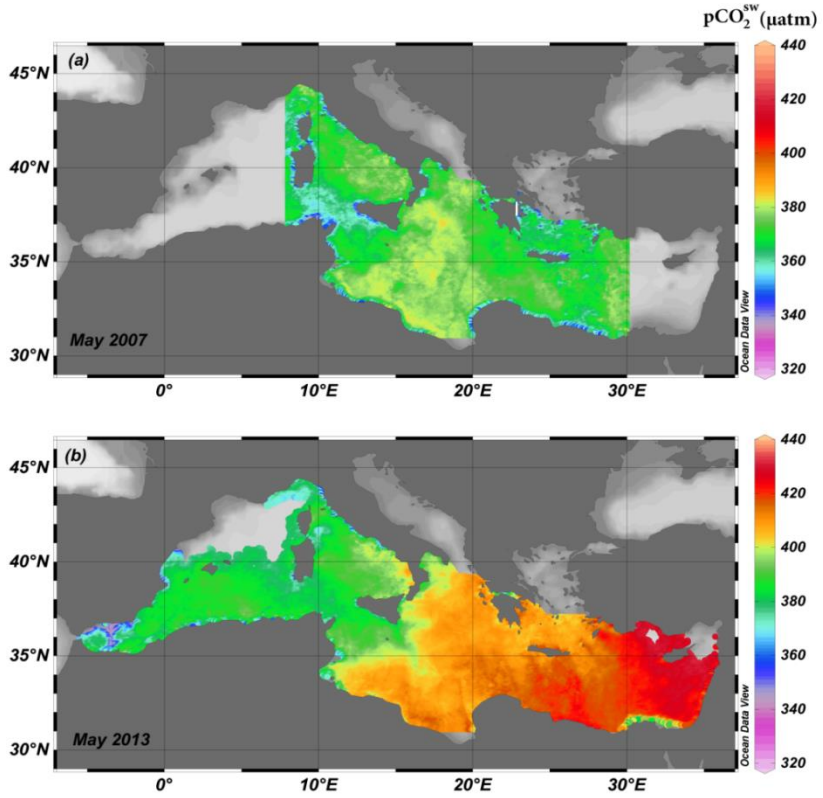

Figure 5. pCO_2^{sw} during (a) May 2007 (Equation 6) and (b) May 2013 (Equation 8)

The estimated pCO_2^{sw} during May 2013 from equation 8 show a clear Eastward gradient with a minimum of 318 µatm to a maximum of 431 µatm in the areas of the Alboran Sea and the Levantine sub-basin respectively (Figure 5b). The low values encountered in the Strait of Gibraltar can be explained by the inflow of surface Atlantic Water that is significantly modified as it mixes with Mediterranean Waters, causing strong phytoplankton blooms (Bosc *et al.*, 2004). Then a shift is observed just after the Strait of Sicily, where pCO_2^{sw} are always higher than 400 µatm. During the last month of spring (May), the Eastward increase in SST along with the evaporation, is one of the main drivers of the pCO_2^{sw} surface variability. The SST increase induces an enhanced density stratification which inhibits the flux of nutrients

towards the surface layer and prevents the biomass accumulation (Longhurst, 1998). Hence the high pCO_2^{sw} values are favored by low biomass values during the summer period (May to September) and by the grazing activities that fasten the bloom decay (D'Ortenzio and Ribera d'Alcalà, 2009; Lazzari *et al.*, 2012).

3.5. Estimates of air-sea CO_2 fluxes in May 2013

Because of the spatial limitation of equation 6, the CO_2 fluxes across the air-sea interface were only computed for May 2013. In order to apply equation 8 on the spatial scale of the Mediterranean Sea, it is important to quantify the errors of the estimated pCO_2^{sw} from equation 8 on the calculated air-sea CO_2 fluxes during May 2013. The errors are expressed as the difference between the CO_2 fluxes calculated from the in situ pCO_2^{sw} measurements of the MedSeA cruise and the CO_2 fluxes calculated from the pCO_2^{sw} estimated in equation 8.

The results show that the air-sea CO_2 fluxes calculated from the in situ pCO_2^{sw} measurements of the MedSeA cruise varied between -0.1 to 0.17 $mol.m^{-2}.month^{-1}$, with a clear increasing Eastward trend (Figure 6a). The mean error on the air-sea CO_2 fluxes was close to 0 $mol.m^{-2}.month^{-1}$ ($-2x10^{-4}$ $mol.m^{-2}.month^{-1}$) with a standard error of ± 0.03 $mol.m^{-2}.month^{-1}$ (Figure 6b). Hence we obtain an error of 11 % on the CO_2 fluxes calculated from the estimated pCO_2^{sw} (Equation 8), which we will consider acceptable in order to map the CO_2 fluxes throughout the whole Mediterranean Sea.

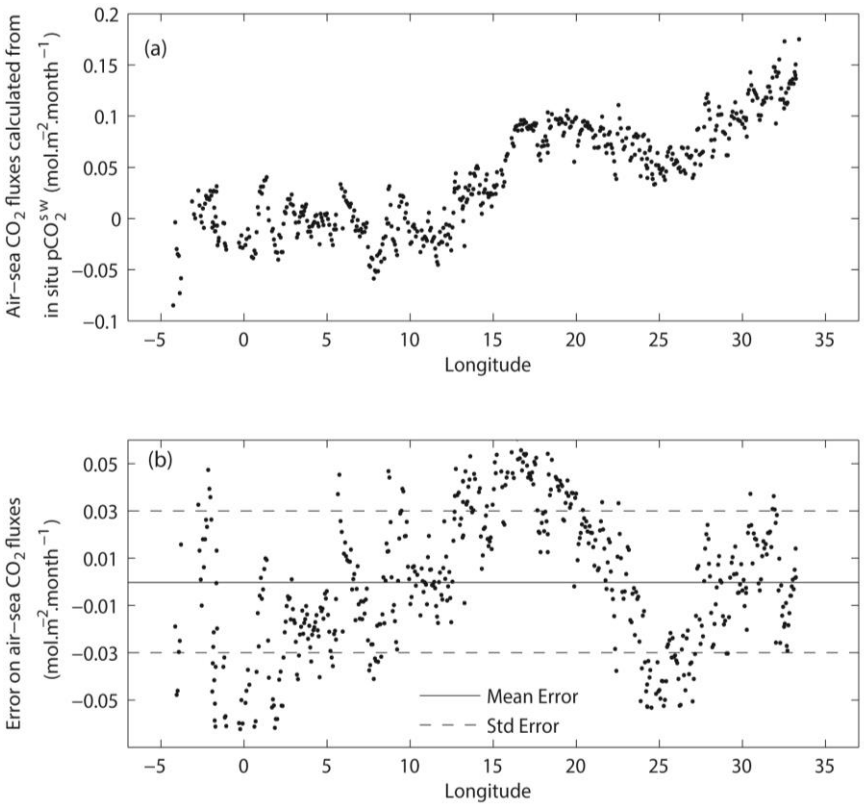

Figure 6. (a) Air-sea CO_2 fluxes calculated from the in situ pCO_2^{sw} measurements of the MedSeA cruise and (b) error on the air-sea CO_2 fluxes by considering the pCO_2^{sw} estimated from equation 8

Considering a constant atmospheric CO_2 of 399 ppm (section 2.4), the air-sea CO_2 fluxes are mainly affected by the pCO_2^{SW} spatial variations and with the wind speed regime. During May 2013, the CO_2 fluxes varied between – 0.25 to 0.06 $mol.m^{-2}.month^{-1}$. The strongest sinks for atmospheric CO_2 are located in the Alboran, Ligurian and South Tyrrhenian sub-basins, whereas the strongest sources are found in the Levantine sub-basin (Figure 7). In the Western basin, the negative CO_2 fluxes reflect the under equilibrium with the atmospheric CO_2, whereas the opposite is seen in the Eastern basin reflecting the over equilibrium with the atmosphere. The sink/source behavior of the Western and Eastern Mediterranean respectively is in agreement with the previous CO_2 fluxes simulations of D'Ortenzio et al. (2008) and Taillandier et al. (2012).

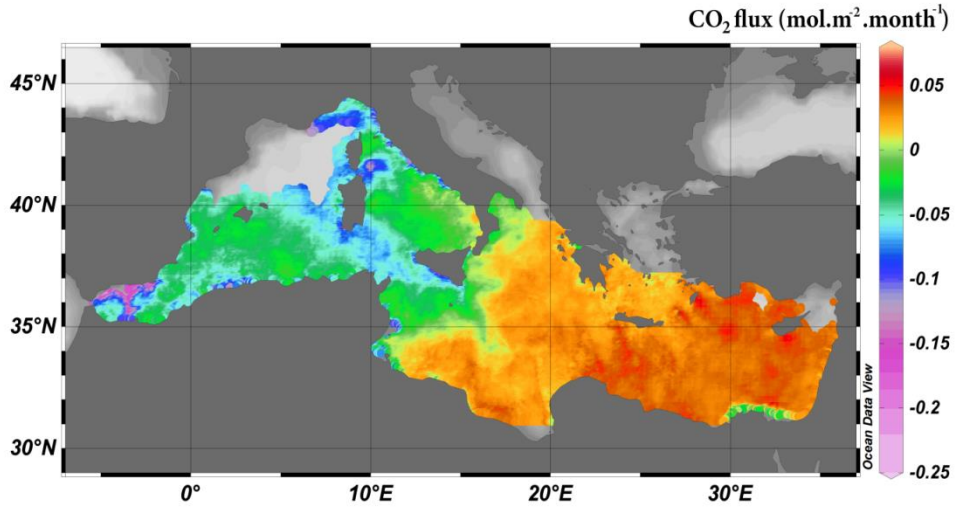

Figure 7. Air-sea CO_2 fluxes during May 2013 (using equations 1 and 2 and 3 and 8)

Conclusion

In reference to two recent cruises conducted in May 2007 and 2013, this study present the first estimate of air-sea CO_2 fluxes in May over the whole Mediterranean Sea based on local in situ pCO_2^{SW} measurements and satellite derived parameters of SST, Chla and CDOMi. In order to estimate surface water pCO_2^{SW}, we tested different combinations of parameters and selected the relationships that have the lowest uncertainties. The results show that the uncertainty of the fits is significantly reduced when the biological contribution to the pCO_2^{SW} variability is accounted for. For the Thresholds cruise, CDOMi and SST contributed to 50 % of the pCO_2^{SW} variability (Equation 6), whereas SST alone contributed only to 34 %. For the MedSeA cruise, the best regression was found when fitting pCO_2^{SW} with SST and Chla which contributed to 76 % of the variability (Equation 8).

The accuracy of equations 6 and 8 showed good prediction skills with RMSE of ± 9 and ± 10 µatm for May 2007 and 2013 respectively. However when we switched the application of equation 6 to the dataset of May 2013 and equation 8 to the dataset of May 2007, the pCO_2^{SW} residuals reached up to ± 70 µatm. Hence equations 6 and 8 are temporally confined to the months of May 2007 and May 2013 respectively, and their application beyond that time period can lead to significant deviations. The mapping of pCO_2^{SW} in May 2007 from equation

3 was somewhat uniform and did not represent the high variability encountered in the Mediterranean Sea. For equation 8, the pCO_2^{sw} estimation range was 90 µatm which formed 94 % of the in situ pCO_2^{sw} range. Hence equation 8 can be used during May 2013 to map the pCO_2^{sw} and air-sea CO_2 fluxes in the Mediterranean Sea, except the regions of the Gulf of Lyon, the North Balearic Sea and the northernmost part of the Levantine Sea.

The results of this study show that over the Mediterranean Sea, satellite products provide a reliable source of physical and biological data that can be used to estimate the air-sea CO_2 fluxes. Thus we provide a method to estimate the CO_2 fluxes with a high spatial resolution and with a reduced uncertainty since it relies on direct pCO_2^{sw} measurements. This is particularly important since the previous simulated CO_2 fluxes in the Mediterranean Sea were calculated from measurements of total alkalinity, total inorganic carbon or pH which could add a significant error to the results.

The scarcity of pCO_2^{sw} measurements in the Mediterranean Sea does not allow us to test this method on a larger dataset, thus the results of this study might/or not be generalized. Hence a more comprehensive study on newly acquired pCO_2^{sw} datasets would bring more insights on which satellite data products are adequate to estimate the pCO_2^{sw} in the Mediterranean Sea. A pCO_2^{sw} database for this area will allow to develop a global relationship that encompass the temporal limitations encountered in this study as well as to work towards integrating the Mediterranean Sea into future global CO_2 fluxes climatologies.

Acknowledgments

The research leading to these results has received funding from the European Community's Seventh Framework programme under grant agreement 265103 (Project MedSeA). It is also part of SOERE MOOSE.
The monthly composites of SST, Chla and CDOMi were retrieved from the L3SMI product of the MODIS-A available at the ocean color website (http://oceancolor.gsfc.nasa.gov/). NASA Ocean Biology (OB). Moderate Resolution Imaging Spectroradiometer (MODIS) Ocean Color Data, 2014.0. Reprocessing. NASA OB.DAAC, Greenbelt, MD, USA. doi: 10.5067/AQUA/MODIS_OC.2014.0. Accessed 2015/03/05. Maintained by NASA Ocean Biology Distibuted Active Archive Center (*OB.DAAC*), Goddard Space Flight Center, Greenbelt MD.
The ASCAT on Metop-A Level 4 monthly gridded mean wind fields in 0.25° geographical grid were obtained from the Centre de Recherche et d' Exploitation Satellitaire (CERSAT) website (http://cersat.ifremer.fr/), IFREMER, Plouzané (France). The atmospheric CO_2 data were obtained from the World Data Center for Greenhouse Gases Web site (http://ds.data.jma.go.jp/gmd/wdcgg/) and we acknowledge the use of these data sets for broad scientific use. The sea surface salinity was retrieved from the Mediterranean Sea physical reanalysis (1987-2013) MyOcean product supported by the FP7 EU projects MyOcean2 (grant agreement 283367). A special thanks to Cédric FALCO and Jean-Philippe SAVY for their technical help to set up the underway system for pCO_2^{sw} measurements during the MedSeA cruise 2013

References

Álvarez, M., 2012. The CO_2 system observations in the Mediterranean Sea: past, present and future. In: Briand, F. (Ed.), Designing Med-SHIP: a Program for repeated oceanographic surveys. CIESM Monaco, p. 164.

Bates, N.R., Hansell, D.A., 1999. A high resolution study of surface layer hydrographic and biogeochemical properties between Chesapeake Bay and Bermuda. Mar. Chem. 67 (1–2), 1-16. http://dx.doi.org/10.1016/S0304-4203(99)00045-6

Bégovic, M., Copin-Montégut, C., 2002. Processes controlling annual variations in the partial pressure of CO_2 in surface waters of the central northwestern Mediterranean Sea (Dyfamed site). Deep Sea Res. Part II Top. Stud. Oceanogr. 49 (11), 2031-2047. http://dx.doi.org/10.1016/S0967-0645(02)00026-7

Bergamasco, A., Malanotte-Rizzoli, P., 2010. The circulation of the Mediterranean Sea: a historical review of experimental investigations. Adv. Oceanogr. Limnol. 1 (1), 11-28. 10.1080/19475721.2010.491656

Béthoux, J.P., Gentili, B., Morin, P., Nicolas, E., Pierre, C., Ruiz-Pino, D., 1999. The Mediterranean Sea: a miniature ocean for climatic and environmental studies and a key for the climatic functioning of the North Atlantic. Prog. Oceanogr. 44 (1–3), 131-146. http://dx.doi.org/10.1016/S0079-6611(99)00023-3

Bockmon, E.E., Dickson, A.G., 2015. An inter-laboratory comparison assessing the quality of seawater carbon dioxide measurements. Mar. Chem. 171 (0), 36-43. http://dx.doi.org/10.1016/j.marchem.2015.02.002

Bosc, E., Bricaud, A., Antoine, D., 2004. Seasonal and interannual variability in algal biomass and primary production in the Mediterranean Sea, as derived from 4 years of SeaWiFS observations. Global Biogeochem. Cycles 18 (1). 10.1029/2003gb002034

Boutin, J., Etcheto, J., Dandonneau, Y., Bakker, D.C.E., Feely, R.A., Inoue, H.Y., Ishii, M., Ling, R.D., Nightingale, P.D., Metzl, N., Wanninkhof, R., 1999. Satellite sea surface temperature: a powerful tool for interpreting in situ pCO_2 measurements in the equatorial Pacific Ocean. Tellus B 51 (2), 490-508. 10.1034/j.1600-0889.1999.00025.x

Calleja, M.L., Duarte, C.M., Álvarez, M., Vaquer-Sunyer, R., Agustí, S., Herndl, G.J., 2013. Prevalence of strong vertical CO_2 and O_2 variability in the top meters of the ocean. Global Biogeochem. Cycles 27 (3), 941-949. 10.1002/gbc.20081

Calleja, M.L., Duarte, C.M., Navarro, N., Agustí, S., 2005. Control of air-sea CO_2 disequilibria in the subtropical NE Atlantic by planktonic metabolism under the ocean skin. Geophys. Res. Lett. 32 (8). 10.1029/2004gl022120

Coble, P.G., 2007. Marine Optical Biogeochemistry: The Chemistry of Ocean Color. Chem. Rev. 107 (2), 402-418. 10.1021/cr050350+

Copin-Montégut, C., 1988. A new formula for the effect of temperature on the partial pressure of CO_2 in seawater. Mar. Chem. 25 (1), 29-37. http://dx.doi.org/10.1016/0304-4203(88)90012-6

Copin-Montégut, C., Bégovic, M., Merlivat, L., 2004. Variability of the partial pressure of CO_2 on diel to annual time scales in the Northwestern Mediterranean Sea. Mar. Chem. 85 (3–4), 169-189. http://dx.doi.org/10.1016/j.marchem.2003.10.005

Cossarini, G., Lazzari, P., Solidoro, C., 2015. Spatiotemporal variability of alkalinity in the Mediterranean Sea. Biogeosciences 12 (6), 1647-1658. 10.5194/bg-12-1647-2015

D'Ortenzio, F., Lavigne, H., Besson, F., Claustre, H., Coppola, L., Garcia, N., Laës-Huon, A., Le Reste, S., Malardé, D., Migon, C., Morin, P., Mortier, L., Poteau, A., Prieur, L., Raimbault, P., Testor, P., 2014. Observing mixed layer depth, nitrate and chlorophyll concentrations in the northwestern Mediterranean: A combined satellite and NO_3

profiling floats experiment. Geophys. Res. Lett. 41 (18), 6443-6451. 10.1002/2014gl061020

D'Ortenzio, F., Ribera d'Alcalà, M., 2009. On the trophic regimes of the Mediterranean Sea: a satellite analysis. Biogeosciences 6 (2), 139-148. 10.5194/bg-6-139-2009

D'Ortenzio, F., Antoine, D., Marullo, S., 2008. Satellite-driven modeling of the upper ocean mixed layer and air–sea CO_2 flux in the Mediterranean Sea. Deep Sea Res. Part I Oceanogr. Res. Pap. 55 (4), 405-434. http://dx.doi.org/10.1016/j.dsr.2007.12.008

DeGrandpre, M.D., Baehr, M.M., Hammar, T.R., 1999. Calibration-free optical chemical sensors. Anal. Chem. 71 (6), 1152-1159. 10.1021/ac9805955

Else, B.G.T., Yackel, J.J., Papakyriakou, T.N., 2008. Application of satellite remote sensing techniques for estimating air–sea CO_2 fluxes in Hudson Bay, Canada during the ice-free season. Remote Sens. Environ. 112 (9), 3550-3562. http://dx.doi.org/10.1016/j.rse.2008.04.013

Gemayel, E., Hassoun, A.E.R., Benallal, M.A., Goyet, C., Krasakopoulou, E., Abboud-Abi Saab, M., Touratier, F., 2015. Distribution of surface water pCO_2 and air-sea fluxes in the Mediterranean Sea during May 2013. Submitted to Deep Sea Research Part I.

Goyet, C., Gemayel, E., Hassoun, A.E.R., 2015. Underway pCO_2 in surface water during the 2013 MedSeA cruise. Pangaea. Dataset #841928 (DOI registration in progress)

Goyet, C., Millero, F.J., Poisson, A., Shafer, D.K., 1993. Temperature dependence of CO_2 fugacity in seawater. Mar. Chem. 44 (2–4), 205-219. http://dx.doi.org/10.1016/0304-4203(93)90203-Z

Hansell, D.A., 2002. DOC in the global ocean carbon cycle. In: Hansell, D.A., Carlson, D.A. (Eds.), Biogeochemistry of Marine Dissolved Organic Matter. Elsevier, San Diego, pp. 685-715.

Hassoun, A.E.R., Gemayel, E., Krasakopoulou, E., Goyet, C., Abboud-Abi Saab, M., Guglielmi, V., Touratier, F., Falco, C., 2015. Acidification of the Mediterranean Sea from anthropogenic carbon penetration. Deep Sea Res. Part I Oceanogr. Res. Pap. 102 (0), 1-15. http://dx.doi.org/10.1016/j.dsr.2015.04.005

Hood, E.M., Merlivat, L., 2001. Annual to interannual variations of fCO_2 in the northwestern Mediterranean Sea: Results from hourly measurements made by CARIOCA buoys, 1995-1997. J. Mar. Res. 59 (1), 113-131. http://dx.doi.org/10.1357/002224001321237399

Hood, E.M., Merlivat, L., Johannessen, T., 1999. Variations of fCO_2 and air-sea flux of CO_2 in the Greenland Sea gyre using high-frequency time series data from CARIOCA drift buoys. J. Geophys. Res. 104 (C9), 20571-20583. 10.1029/1999jc900130

Hung, J.J., Wang, S.M., Chen, Y.L., 2007. Biogeochemical controls on distributions and fluxes of dissolved and particulate organic carbon in the Northern South China Sea. Deep Sea Res. Part II Top. Stud. Oceanogr. 54 (14–15), 1486-1503. http://dx.doi.org/10.1016/j.dsr2.2007.05.006

Jamet, C., Moulin, C., Lefèvre, N., 2007. Estimation of the oceanic pCO_2 in the North Atlantic from VOS lines in-situ measurements: parameters needed to generate seasonally mean maps. Ann. Geophys. 25 (11), 2247-2257. 10.5194/angeo-25-2247-2007

Jo, Y.-H., Dai, M., Zhai, W., Yan, X.-H., Shang, S., 2012. On the variations of sea surface pCO_2 in the northern South China Sea: A remote sensing based neural network approach. J. Geophys. Res. 117 (C8). 10.1029/2011jc007745

Lazzari, P., Solidoro, C., Ibello, V., Salon, S., Teruzzi, A., Béranger, K., Colella, S., Crise, A., 2012. Seasonal and inter-annual variability of plankton chlorophyll and primary production in the Mediterranean Sea: a modelling approach. Biogeosciences 9 (1), 217-233. 10.5194/bg-9-217-2012

Lee, K., Millero, F.J., Byrne, R.H., Feely, R.A., Wanninkhof, R., 2000. The recommended dissociation constants for carbonic acid in seawater. Geophys. Res. Lett. 27 (2), 229-232. 10.1029/1999gl002345

Lee, K., Wanninkhof, R., Takahashi, T., Doney, S.C., Feely, R.A., 1998. Low interannual variability in recent oceanic uptake of atmospheric carbon dioxide. Nature 396 (6707), 155-159.

Lionello, P., Abrantes, F., Congedi, L., Dulac, F., Gacic, M., Gomis, D., Goodess, C., Hoff, H., Kutiel, H., Luterbacher, J., Planton, S., Reale, M., Schröder, K., Vittoria Struglia, M., Toreti, A., Tsimplis, M., Ulbrich, U., Xoplaki, E., 2012. Introduction: Mediterranean Climate—Background Information. In: Lionello, P. (Ed.), The Climate of the Mediterranean Region. Elsevier, Oxford, pp. xxxv-xc. http://dx.doi.org/10.1016/B978-0-12-416042-2.00012-4

Lohrenz, S.E., Cai, W.-J., 2006. Satellite ocean color assessment of air-sea fluxes of CO_2 in a river-dominated coastal margin. Geophys. Res. Lett. 33 (1). 10.1029/2005gl023942

Longhurst, A.R., 1998. Ecological Geography of the Sea. Elsevier Science, New York.

Louanchi, F., Boudjakdji, M., Nacef, L., 2009. Decadal changes in surface carbon dioxide and related variables in the Mediterranean Sea as inferred from a coupled data-diagnostic model approach. ICES J. Mar. Sci. 66 (7), 1538-1546. 10.1093/icesjms/fsp049

Malanotte-Rizzoli, P., Artale, V., Borzelli-Eusebi, G.L., Brenner, S., Crise, A., Gacic, M., Kress, N., Marullo, S., Ribera d'Alcalà, M., Sofianos, S., Tanhua, T., Theocharis, A., Alvarez, M., Ashkenazy, Y., Bergamasco, A., Cardin, V., Carniel, S., Civitarese, G., D'Ortenzio, F., Font, J., Garcia-Ladona, E., Garcia-Lafuente, J.M., Gogou, A., Gregoire, M., Hainbucher, D., Kontoyannis, H., Kovacevic, V., Kraskapoulou, E., Kroskos, G., Incarbona, A., Mazzocchi, M.G., Orlic, M., Ozsoy, E., Pascual, A., Poulain, P.M., Roether, W., Rubino, A., Schroeder, K., Siokou-Frangou, J., Souvermezoglou, E., Sprovieri, M., Tintoré, J., Triantafyllou, G., 2014. Physical forcing and physical/biochemical variability of the Mediterranean Sea: a review of unresolved issues and directions for future research. Ocean Sci. 10 (3), 281-322. 10.5194/os-10-281-2014

Millero, F.J., 2007. The Marine inorganic carbon cycle. Chem. Rev. 107 (2), 308-341. 10.1021/cr0503557

Morel, A., 2009. Are the empirical relationships describing the bio-optical properties of case 1 waters consistent and internally compatible? J. Geophys. Res. 114 (C1). 10.1029/2008jc004803

Morel, A., Gentili, B., 2009. A simple band ratio technique to quantify the colored dissolved and detrital organic material from ocean color remotely sensed data. Remote Sens. Environ. 113 (5), 998-1011. http://dx.doi.org/10.1016/j.rse.2009.01.008

Moussa, H., Goyet, C., Benallal, M.A., Lefèvre, N., 2015. Satellite-derived CO_2 fugacity in surface seawater of the tropical Atlantic Ocean using Feedforward Neural Network: Current status and perspectives. To be submitted to Remote sensing of environement

Nelson, N.B., Bates, N.R., Siegel, D.A., Michaels, A.F., 2001. Spatial variability of the CO_2 sink in the Sargasso Sea. Deep Sea Res. Part II Top. Stud. Oceanogr. 48 (8–9), 1801-1821. http://dx.doi.org/10.1016/S0967-0645(00)00162-4

Olsen, A., Bellerby, R.G.J., Johannessen, T., Omar, A.M., Skjelvan, I., 2003. Interannual variability in the wintertime air–sea flux of carbon dioxide in the northern North Atlantic, 1981–2001. Deep Sea Res. Part I Oceanogr. Res. Pap. 50 (10–11), 1323-1338. http://dx.doi.org/10.1016/S0967-0637(03)00144-4

Olsen, A., Triñanes, J.A., Wanninkhof, R., 2004. Sea–air flux of CO_2 in the Caribbean Sea estimated using in situ and remote sensing data. Remote Sens. Environ. 89 (3), 309-325. http://dx.doi.org/10.1016/j.rse.2003.10.011

Ono, T., Saino†, T., Kurita, N., Sasaki, K., 2004. Basin-scale extrapolation of shipboard pCO_2 data by using satellite SST and Chla. Int. J. Remote Sens. 25 (19), 3803-3815. 10.1080/01431160310001657515

Padin, X.A., Navarro, G., Gilcoto, M., Rios, A.F., Pérez, F.F., 2009. Estimation of air–sea CO_2 fluxes in the Bay of Biscay based on empirical relationships and remotely sensed observations. J. Mar. Syst. 75 (1–2), 280-289. http://dx.doi.org/10.1016/j.jmarsys.2008.10.008

Parard, G., Charantonis, A.A., Rutgerson, A., 2014. Remote sensing algorithm for sea surface CO_2 in the Baltic Sea. Biogeosci. Discuss. 11 (8), 12255-12294. 10.5194/bgd-11-12255-2014

Rangama, Y., Boutin, J., Etcheto, J., Merlivat, L., Takahashi, T., Delille, B., Frankignoulle, M., Bakker, D.C.E., 2005. Variability of the net air–sea CO_2 flux inferred from shipboard and satellite measurements in the Southern Ocean south of Tasmania and New Zealand. J. Geophys. Res. 110 (C9). 10.1029/2004jc002619

Robbins, L.L., Hansen, M.E., Kleypas, J.A., Meylan, S.C., 2010. CO_2calc—A user-friendly seawater carbon calculator for Windows, Max OS X, and iOS (iPhone). U.S. Geological Survey Open-File Report 2010-1280, 17

Rödenbeck, C., Keeling, R.F., Bakker, D.C.E., Metzl, N., Olsen, A., Sabine, C., Heimann, M., 2013. Global surface-ocean pCO_2 and sea–air CO_2 flux variability from an observation-driven ocean mixed-layer scheme. Ocean Sci. 9 (2), 193-216. 10.5194/os-9-193-2013

Sarma, V.V.S.S., Saino, T., Sasaoka, K., Nojiri, Y., Ono, T., Ishii, M., Inoue, H.Y., Matsumoto, K., 2006. Basin-scale pCO_2 distribution using satellite sea surface temperature, Chla, and climatological salinity in the North Pacific in spring and summer. Global Biogeochem. Cycles 20 (3). 10.1029/2005gb002594

Schneider, A., Tanhua, T., Körtzinger, A., Wallace, D.W.R., 2010. High anthropogenic carbon content in the Eastern Mediterranean. J. Geophys. Res. 115 (C12), C12050. 10.1029/2010jc006171

Stephens, M.P., Samuels, G., Olson, D.B., Fine, R.A., Takahashi, T., 1995. Sea-air flux of CO_2 in the North Pacific using shipboard and satellite data. J. Geophys. Res. 100 (C7), 13571-13583. 10.1029/95jc00901

Taillandier, V., D'Ortenzio, F., Antoine, D., 2012. Carbon fluxes in the mixed layer of the Mediterranean Sea in the 1980s and the 2000s. Deep Sea Res. Part I Oceanogr. Res. Pap. 65 (0), 73-84. http://dx.doi.org/10.1016/j.dsr.2012.03.004

Takahashi, T., Olafsson, J., Goddard, J.G., Chipman, D.W., Sutherland, S.C., 1993. Seasonal variation of CO_2 and nutrients in the high-latitude surface oceans: A comparative study. Global Biogeochem. Cycles 7 (4), 843-878. 10.1029/93gb02263

Takahashi, T., Sutherland, S.C., Chipman, D.W., Goddard, J.G., Ho, C., Newberger, T., Sweeney, C., Munro, D.R., 2014. Climatological distributions of pH, pCO_2, total CO_2, alkalinity, and $CaCO_3$ saturation in the global surface ocean, and temporal changes at selected locations. Mar. Chem. 164 (0), 95-125. http://dx.doi.org/10.1016/j.marchem.2014.06.004

Takahashi, T., Sutherland, S.C., Sweeney, C., Poisson, A., Metzl, N., Tilbrook, B., Bates, N., Wanninkhof, R., Feely, R.A., Sabine, C., Olafsson, J., Nojiri, Y., 2002. Global sea–air CO_2 flux based on climatological surface ocean pCO_2, and seasonal biological and temperature effects. Deep Sea Res. Part II Top. Stud. Oceanogr. 49 (9–10), 1601-1622. http://dx.doi.org/10.1016/S0967-0645(02)00003-6

Takahashi, T., Sutherland, S.C., Wanninkhof, R., Sweeney, C., Feely, R.A., Chipman, D.W., Hales, B., Friederich, G., Chavez, F., Sabine, C., Watson, A., Bakker, D.C.E., Schuster, U., Metzl, N., Yoshikawa-Inoue, H., Ishii, M., Midorikawa, T., Nojiri, Y., Körtzinger, A., Steinhoff, T., Hoppema, M., Olafsson, J., Arnarson, T.S., Tilbrook, B., Johannessen, T., Olsen, A., Bellerby, R., Wong, C.S., Delille, B., Bates, N.R., de Baar, H.J.W., 2009. Climatological mean and decadal change in surface ocean pCO_2, and net sea–air CO_2 flux over the global oceans. Deep Sea Res. Part II Top. Stud. Oceanogr. 56 (8–10), 554-577. http://dx.doi.org/10.1016/j.dsr2.2008.12.009

Touratier, F., Goyet, C., 2011. Impact of the Eastern Mediterranean Transient on the distribution of anthropogenic CO_2 and first estimate of acidification for the Mediterranean Sea. Deep Sea Res. Part I Oceanogr. Res. Pap. 58 (1), 1-15. http://dx.doi.org/10.1016/j.dsr.2010.10.002

Touratier, F., Guglielmi, V., Goyet, C., Prieur, L., Pujo-Pay, M., Conan, P., Falco, C., 2012. Distributions of the carbonate system properties, anthropogenic CO_2, and acidification during the 2008 BOUM cruise (Mediterranean Sea). Biogeosci. Discuss. 9 (3), 2709-2753. 10.5194/bgd-9-2709-2012

Turley, C.M., 1999. The changing Mediterranean Sea — a sensitive ecosystem? Prog. Oceanogr. 44 (1–3), 387-400. http://dx.doi.org/10.1016/S0079-6611(99)00033-6

Valsala, V., Maksyutov, S., 2010. Simulation and assimilation of global ocean pCO_2 and air–sea CO_2 fluxes using ship observations of surface ocean pCO_2 in a simplified biogeochemical offline model. Tellus B 62 (5), 821-840. 10.1111/j.1600-0889.2010.00495.x

Wanninkhof, R., 1992. Relationship between wind speed and gas exchange over the ocean. J. Geophys. Res. 97 (C5), 7373-7382. 10.1029/92jc00188

Wanninkhof, R., Doney, S.C., Takahashi, T., McGillis, W.R., 2013. The Effect of Using Time-Averaged Winds on Regional Air-Sea CO_2 Fluxes. Gas Transfer at Water Surfaces. American Geophysical Union, pp. 351-356. 10.1029/GM127p0351

Weiss, R.F., 1974. Carbon dioxide in water and seawater: the solubility of a non-ideal gas. Mar. Chem. 2 (3), 203-215. http://dx.doi.org/10.1016/0304-4203(74)90015-2

Weiss, R.F., Price, B.A., 1980. Nitrous oxide solubility in water and seawater. Mar. Chem. 8 (4), 347-359. http://dx.doi.org/10.1016/0304-4203(80)90024-9

Xing, X., Claustre, H., Wang, H., Poteau, A., D'Ortenzio, F., 2014. Seasonal dynamics in colored dissolved organic matter in the Mediterranean Sea: Patterns and drivers. Deep Sea Res. Part I Oceanogr. Res. Pap. 83 (0), 93-101. http://dx.doi.org/10.1016/j.dsr.2013.09.008

Zeng, J., Nojiri, Y., Landschützer, P., Telszewski, M., Nakaoka, S., 2014. A Global Surface Ocean fCO_2 Climatology Based on a Feed-Forward Neural Network. J. Atmos. OceanicTechnol. 31 (8), 1838-1849. 10.1175/jtech-d-13-00137.1

Zhu, Y., Shang, S., Zhai, W., Dai, M., 2009. Satellite-derived surface water pCO_2 and air–sea CO_2 fluxes in the northern South China Sea in summer. Prog. Nat. Sci. 19 (6), 775-779. http://dx.doi.org/10.1016/j.pnsc.2008.09.004

Article IV: Modeling of the total alkalinity and the total inorganic carbon in the Mediterranean Sea

Hassoun, A.E.R., **Gemayel, E.,** et al**.** (2015).

Journal of Water Resources and Ocean Science, 4 (1), 24-32. doi: 10.11648/j.wros.20150401.14

Modeling of the total alkalinity and the total inorganic carbon in the Mediterranean Sea

Abed El Rahman HASSOUN[1], Elissar GEMAYEL[1,2,3], Evangelia KRASAKOPOULOU[4,5], Catherine GOYET[2,3], Marie ABBOUD-ABI SAAB[1], Patrizia ZIVERI[6], Franck TOURATIER[2,3], Véronique GUGLIELMI[2,3], Cédric FALCO[2, 3]

[1]National Council for Scientific Research, National Center for Marine Sciences, Batroun, Lebanon
[2]IMAGES_ESPACE-DEV, Université de Perpignan Via Domitia, Perpignan, France
[3]ESPACE-DEV, UG UA UR UM IRD, Maison de la télédétection, 500 rue Jean-François Breton, Montpellier, France
[4]Institute of Oceanography, Hellenic Centre for Marine Research, Anavyssos, Greece
[5]University of the Aegean, Department of Marine Sciences, University Hill, Mytilene, Greece
[6]Universitat Autònoma de Barcelona (UAB), Institute of Environmental Science and Technology (ICTA), Edifici Cn, Campus UAB, Bellaterra, Barcelona, Spain

Abstract

Measurements of the CO_2 system parameters in the Mediterranean Sea are relatively scarce and not representative for all its sub-basins. High quality data collected on May 2013 during the 2013 MedSeA cruise covering the whole basin were used to provide for the first time linear relationships estimating the total alkalinity (A_T) and the total dissolved inorganic carbon (C_T) from salinity in each Mediterranean basin and sub-basin at different depth layers. These correlations show that a substantial quantity of alkalinity is added to the seawater during its residence time in the Mediterranean Sea, whereas the biological processes, the air-sea exchange and the high remineralization rate are responsible of the high C_T concentrations in this sea. Moreover, these fits could be used to estimate the A_T and C_T from salinity where there are not available measurements of the carbonate system parameters.

Keywords: Carbonate System; Total Alkalinity; Total Dissolved Inorganic Carbon; Fits; Mediterranean Sea

1. Introduction

Aiming to understand and quantify the carbonate system in the Mediterranean Sea, several studies have been realized (e.g. [1], [2], [3], [4], [5], [6], [7]). However, the amount of high quality measurements of the carbonate system properties, particularly the total alkalinity (A_T) and the total dissolved inorganic carbon (C_T), through the whole Mediterranean Sea remained scarce. Recently, during several oceanographic cruises carried out from 2001 until now, the measurement of carbonate system parameters was included [5] [8] [9] [10] [11]. However, many Mediterranean sub-basins remain out of coverage and need to be studied in order to have a better understanding of the carbonate system in this enclosed sea. The measurement of the A_T and C_T parameters could be furthermore used to calculate the carbon budget in the Mediterranean and to estimate the acidification variation and the concentrations of the anthropogenic carbon dioxide sequestered in this sea.

The present paper is based on A_T and C_T data measured during the 2013 MedSeA cruise which covered during the same month almost the entire Mediterranean Sea from the West to the East and from the South to the North. In this study, we present and discuss, for the first time, the A_T-Salinity and C_T-Salinity relationships in each Mediterranean basin and sub-basin at different depth layers. These correlations could be used to estimate the A_T and C_T from salinity data where there is a lack in the measurements of the carbonate system parameters.

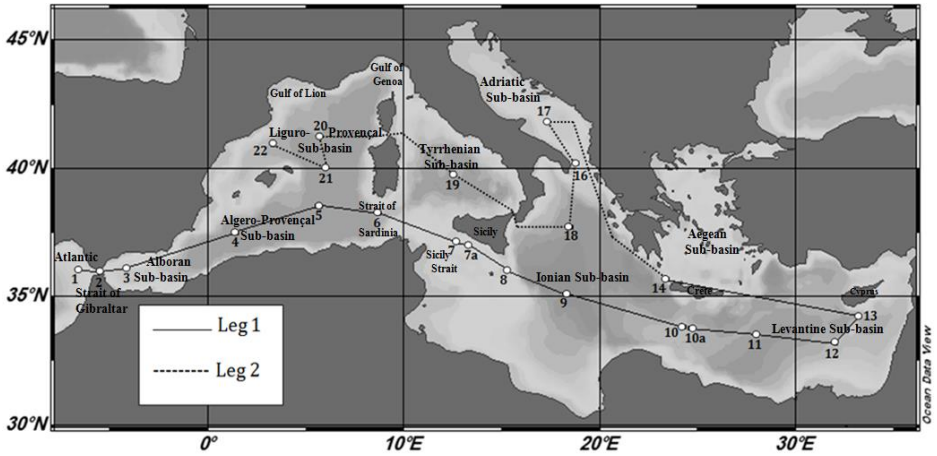

Figure 1. Tracks of the 2013 MedSeA cruise in the Mediterranean Sea. The numbers from 1 to 22 correspond to the sampled stations.

2. Study Area and Methodology

2.1.MedSeA Cruise

During the MedSeA (Mediterranean Sea Acidification In A Changing Climate) cruise realized on board of the Spanish R/V Angeles Alvariño, from May 2nd to June 2nd 2013, 23 stations along the Mediterranean Sea were sampled throughout the water column. The overall goal and scientific objectives of the MedSeA project are well described in the following links [12 and 13]. The full cruise track (more than 8000 km long) consisted of two almost longitudinal legs. During the first leg, samples were collected from Atlantic waters off Cadiz harbor, Spain to the Levantine Sub-basin in the Eastern Mediterranean Sea [3879 km long, 15 stations, 279 sampled points, maximum sampled depth = 3720 m]. The second leg was conducted in the Northern part of the Mediterranean from the Western Cretan Straits in the Eastern Mediterranean basin to Barcelona, Spain in the North Western Mediterranean basin, passing through the South of the Adriatic Sub-basin [3232.5 km long, 8 stations, 183 sampled points, maximum sampled depth = 3000 m] (Figure 1).

2.2. Sampling and Measurement

The salinity (S) was measured *in situ* using a Sea-Bird Electronics CTD system (SBE 911 plus) associated with a General Oceanic rosette sampler, equipped with twenty four 12 L Niskin bottles. The precision of salinity measurements is ± 0.0003.

For the determination of A_T and C_T, seawater samples were collected, at all stations and depths, into washed 500 ml borosilicate glass bottles, according to standard operational protocol. A small headspace (< 1 %) was adjusted to prevent pressure build-up and loss of CO_2 during storage. Few drops of a saturated solution of $HgCl_2$ were added to the samples in order to avoid any biological activity. Then, the samples were stored in the dark at constant temperature (~ 4 ºC) until their analysis on shore (IMAGES laboratory, Perpignan, France). The measurement of these two parameters was performed simultaneously by potentiometric acid titration using a closed cell. The principle and procedure of measurements, as well as a complete description of the system used to perform accurate analysis can be found in [14]. The precision of A_T and C_T analysis was determined to be ± 2 μmol kg^{-1} for A_T and ± 4 μmol kg^{-1} for C_T, by titration of 261 samples, collected at the same conditions of temperature and S, from Banyuls Sur Mer, South France. The accuracy of A_T and C_T measurements was determined to be ± 1 μmol kg^{-1} for A_T and ± 4 μmol kg^{-1} for C_T by analyzing a total of 26 bottles of three different batches of Certified Reference Material (Andrew Dickson, CA, USA, batches 85, 86 and 128). More information about the carbonate system measurements and precisions are detailed by [15]. The carbonate system and hydrographic data of the 2013 MedSeA cruise are available in Pangaea data repository [16, 17, 18, 19 and 20].

3. Results and Discussion

3.1. A_T-S Relationships in the Mediterranean Sea, its Basins and Sub-Basins

Termed as "evaporation basin", the Mediterranean Sea is characterized by elevated salinities in relation to the adjacent Atlantic Ocean. As a consequence of the surface heat loss and the excessive evaporation [21] [22], the general pattern of salinity in the Mediterranean is an Eastward global increase (Fig.2). The highest salinity values were measured in the Eastern Mediterranean basin (Max. 39.18 in front of Nile Delta, at ~ 5 m), while the lowest salinities were detected at the surface of both the Western Mediterranean basin and the Strait of Gibraltar (Min. 36.29 at the surface of the Strait of Gibraltar, ~ 20 m). High total alkalinity concentrations were recorded in the Mediterranean Sea (Mean = 2588 ± 46 μmol kg^{-1}). The highest A_T concentrations were measured in the Eastern Mediterranean basin (Max. A_T = 2666.0 μmol kg^{-1}, at 300 m in the area of Western Cretan Straits, whereas the lowest A_T concentrations were measured in both the Strait of Gibraltar and the surface waters of the Western Mediterranean basin (Min. A_T = 2377.0 μmol kg^{-1} at 25 m in the Strait of Gibraltar). An Eastward increasing tendency for the total alkalinity was also well noticeable, likewise the salinity trend (Fig.3).

Based on the carbonate system parameters data collected during the 2013 MedSeA cruise, an Eastward increasing trend of A_T was remarked in parallel with the salinity one [15]. Our results indicate the presence of significant correlations between A_T and S in the Mediterranean Sea globally, its main basins and many of its sub-basins as well. Table 1 presents the Model II linear regression between these two parameters in each basin and sub-basin and at different depth layers (surface, intermediate and deep layers). These equations were obtained using the Excel Microsoft Office program (2007). For all the equations derived

in this study, the root mean square deviation (RMSD), which is a good measure of the accuracy of the fit, the coefficient of correlation (Pearson coefficient ; r), and the number of data pairs (n) used to derive each correlation, are also mentioned in the Table 1 for each A_T-S fit.

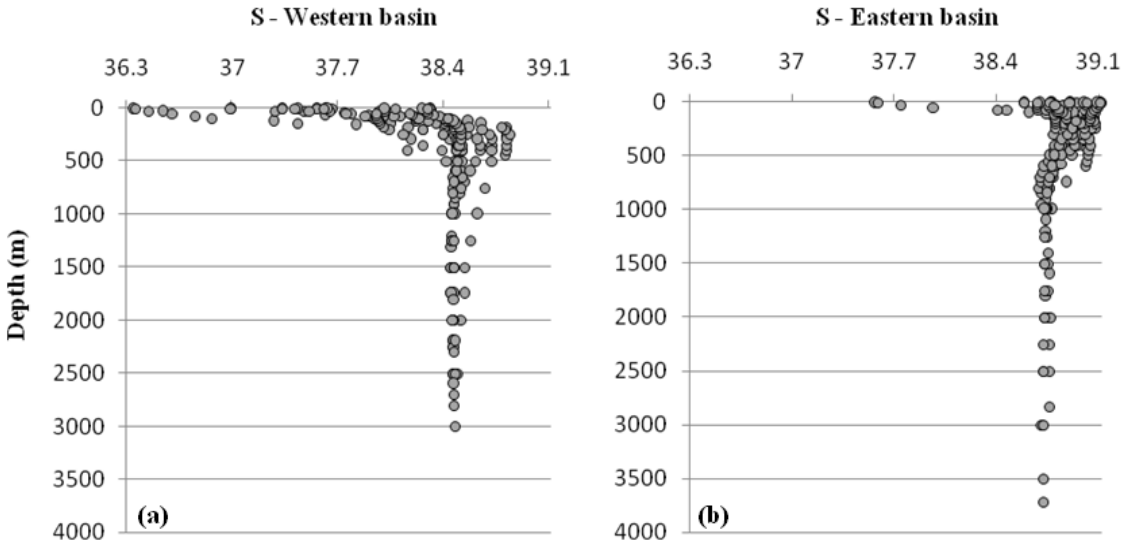

Figure 2. Salinity (S) as a function of depth in the Western (a) and in the Eastern (b) Mediterranean basins.

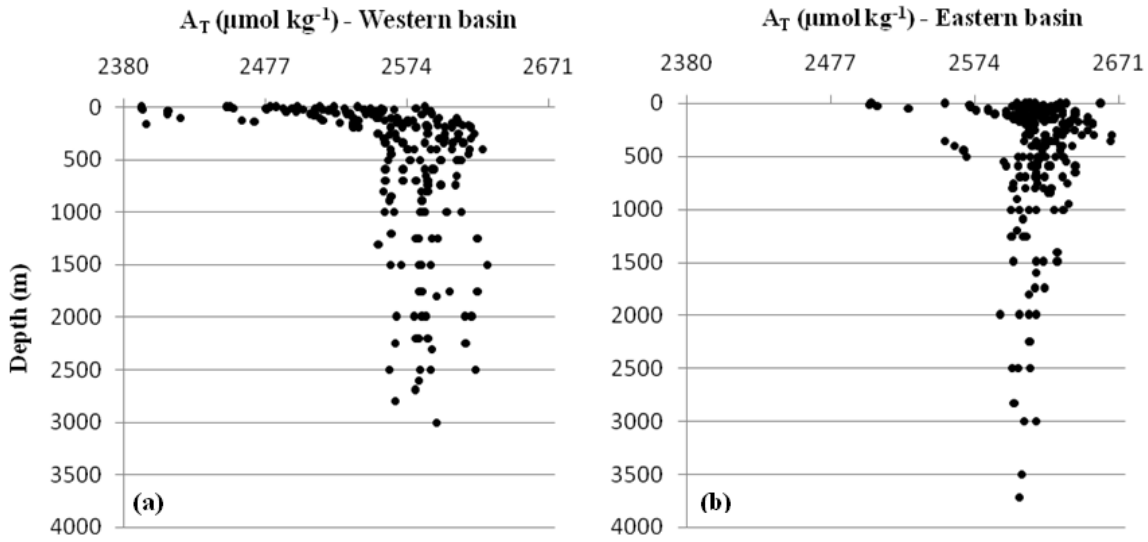

Fig. 3. Total alkalinity (µmol kg^{-1}) as a function of depth in the Western (a) and in the Eastern (b) Mediterranean basins

Evaporation would drive a steady increase in salinity and total alkalinity during the propagation of surface waters toward the Eastern part of the Mediterranean Sea. Therefore, the negative intercepts obtained in most A_T-S fits (Table 1) may be explained by the high evaporation in the sea along with the influence of high A_T inputs by freshwater contributions from the local rivers and the Black Sea. These two systems carry very high total alkalinities (between 2000 µmol kg^{-1} and 6500 µmol kg^{-1}), at low or zero salinity, to shelf areas, especially in the Eastern basin, where surface S and A_T tend to be higher due to the

cumulative effects of evaporation [5]. Moreover, our results indicate the absence of a significant A_T-S correlation in the intermediate and deep layers of the Eastern basin, especially in the Levantine Sub-basin in which we detected no significant A_T-S relationship at all depth layers (Table1).

Table 1. The A_T-S relationships in the different layers of the main basins and sub-basins in the Mediterranean Sea during May 2013 (R.M.S.D. = root mean square deviation, r = coefficient of correlation (Pearson's coefficient), n = number of data pairs used to derive each relationship, [-] means that no significant relationship was found).

Basin/Sub-basin	Depth	A_T-S relationships	R.M.S.D	r	n	Number of equation
Mediterranean	All	$A_T = 98.48*S - 1208$	± 19	0.9	428	Eq. 1
	Surface (0-25 m)	$A_T = 89*S - 845$	± 18	0.96	58	Eq. 2
	Intermediate (>25-400 m)	$A_T = 98*S - 1191$	± 18.5	0.91	208	Eq. 3
	Deep (> 400 m)	$A_T = 134*S - 2578$	± 17	0.57	160	Eq. 4
Western basin	All	$A_T = 99*S – 1225.5$	± 15.6	0.94	215	Eq. 5
	Surface (0-25 m)	$A_T = 92*S - 956$	± 12.5	0.97	30	Eq. 6
	Intermediate (>25-400 m)	$A_T = 101.5*S - 1322$	± 15.6	0.94	105	Eq. 7
	Deep (> 400 m)	-	-	-	-	-
Eastern basin	All	$A_T = 111.42*S - 1713$	± 19	0.54	212	Eq.8
	Surface (0-25 m)	$A_T = 89*S - 846$	± 19	0.86	27	Eq. 9
	Intermediate (>25-400 m)	-	-	-	-	-
	Deep (> 400 m)	-	-	-	-	-
Alboran Sub-basin	All	$A_T = 81.15*S – 567.7$	± 4.4	0.99	23	Eq. 10
	Surface (0-25 m)	$A_T = 10.65*S + 2005$	± 0.07	0.98	3	Eq. 11
	Intermediate (>25-400 m)	$A_T = 82*S – 605.6$	± 5	0.99	11	Eq. 12
	Deep (> 400 m)	$A_T = 171*S – 4020$	± 2	0.7	8	Eq. 13
Algero-Provencal Sub-basin	All	$A_T = 98*S – 1190$	± 11.7	0.95	73	Eq. 14
	Surface (0-25 m)	$A_T = 100.72*S – 1282.6$	± 14	0.89	9	Eq. 15
	Intermediate (>25-400 m)	$A_T = 119.38*S – 2009.7$	± 11.8	0.92	33	Eq. 16
	Deep (> 400 m)	-	-	-	-	-
Liguro-Provencal Sub-basin	All	$A_T = 126*S – 2252$	± 15	0.84	71	Eq. 17
	Surface (0-25 m)	$A_T = 93.33*S – 1008$	± 12.5	0.9	9	Eq. 18
	Intermediate (>25-400 m)	$A_T = 128*S – 2327$	± 11.6	0.89	31	Eq. 19
	Deep (> 400 m)	-	-	-	-	-
Tyrrhenian Sub-basin	All	$A_T = 95.4*S – 1084.5$	± 5.4	0.97	21	Eq. 20
	Surface (0-25 m)	$A_T = 339.73*S – 10384$	± 3	-0.96	3	Eq. 21
	Intermediate (>25-400 m)	$A_T = 96.72*S – 1139$	± 4	0.98	11	Eq. 22
	Deep (> 400 m)	-	-	-	-	-
Ionian Sub-basin	All	$A_T = 112*S – 1730$	± 15	0.88	57	Eq. 23
	Surface (0-25 m)	$A_T = 97.56*S – 1173.5$	± 17	0.95	8	Eq. 24
	Intermediate (>25-400 m)	$A_T = 140*S – 2818$	± 16	0.82	27	Eq. 25
	Deep (> 400 m)	-	-	-	-	-
Adriatic Sub-basin	All	-	-	-	-	-
	Surface (0-25 m)	$A_T = 239.5*S – 6653.7$	± 8	-0.84	6	Eq. 26
	Intermediate (>25-400 m)	-	-	-	-	-
	Deep (> 400 m)	-	-	-	-	-
Western Cretan Straits	All	-	-	-	-	-
	Surface (0-25 m)	$A_T = 81.28*S – 569$	± 0.13	0.99	3	Eq. 27
	Intermediate (>25-400 m)	-	-	-	-	-
	Deep (> 400 m)	$A_T = 1236.95*S – 45690$	± 6.3	-0.88	4	Eq. 28
Levantine Sub-basin	All	-	-	-	-	-
	Surface (0-25 m)	-	-	-	-	-
	Intermediate (>25-400 m)	-	-	-	-	-
	Deep (> 400 m)	-	-	-	-	-

In addition, our results reveal the presence of a very strong positive A_T-S correlation (Eq.27) in the surface layer of the Western Cretan Straits, whereas in the deep layer a significant negative A_T-S correlation is observed (Eq.28). It is also shown the presence of a negative and significant A_T-S fit exclusively in the surface layer of the Adriatic Sub-basin (Eq.26; Table 1). These remarks demonstrate that the relationship between S and A_T does not follow the Eastward strict evaporation trend. However, it reflects the mixture of waters characterized by

high A_T concentrations with low salinity waters in the Eastern part of the Eastern Sub-basins and in the Adriatic Sub-basin. This fact is explained by the mixing, between high salinity surface water in the Eastern Sub-basins with waters from rivers flowing through carbonate-dominated terrains and/or the Black Sea, that change the characteristics of surface waters which become less saline with higher A_T concentrations.

Our A_T-S equation (Eq.1), that takes into account all available data pairs of both parameters in the entire Mediterranean basin, is very similar to the one published by [23]: $A_T = 99.6*S - 1238.4 \pm 4.5 \mu mol\ kg^{-1}$ (Eq.I), obtained using all the available data in the DYFAMED site in the North-Western basin of the Mediterranean Sea from 1998 to 2005. The reason for the slightly less steep slope and the less negative intercept in our correlation (Eq.1) compared to the other one (Eq.I) could be attributed to the difference of sampling locations (different specific total alkalinities between the Western and the Eastern basins). Located in the North-Western Mediterranean basin (43º 25'N, 07º52'E), the DYFAMED site is more influenced by the contributions of waters coming from the continents than most of the stations of the 2013 MedSeA cruise (Fig.1). In the coastal zone, total alkalinity inputs by rivers (ex. the nearby Rhone has an $A_T = 2885\ \mu mol\ kg^{-1}$ [5]) and potentially by sediments, may induce the steep slope of the regression line.

In the Alboran Sub-basin, a positive and highly significant A_T-S correlation was detected (Table 1). This is attributed firstly to the parallel increase of salinity and A_T of the surface Atlantic waters incoming towards the Mediterranean Sea, and secondly, to the high S and A_T in the outgoing Mediterranean waters toward the Atlantic at the deepest layers. In addition, it was noted that the A_T-S fit (Eq.10) obtained based on all the data collected in the Alboran Sub-basin, is different from the one mentioned by [4] in the same sub-basin: $A_T = 94.85*S - 1072.6\ \mu mol\ kg^{-1}$ (Eq.II). This may be due to the large difference in the number of sampled points (23 in our study *vs.* 440 in [4]) and the time difference of ~25 years between the sampling dates of the two studies. Therefore, the observed differences between Eq.10 and the equation of [4] could also be attributed to the temporal variability of the temperature and S, related to the climate change, in the Mediterranean Sea [24] [25] [26] [27].

Similarly, a positive and highly significant A_T-S correlation was noted in the deepest and most isolated sub-basin of the Western basin, the Tyrrhenian Sub-basin. The circulation patterns of the Mediterranean Sea show generally that most of the saline and high-A_T water, coming from the East to the Western basin, enters the Tyrrhenian Sub-basin [28]. Below the surface modified Atlantic waters, the Tyrrhenian Sub-basin is the first Western Sub-basin reached by the Levantine Intermediate Waters (LIW), coming from the Eastern basin through the Sicily Channel. The LIW enters the Tyrrhenian Sub-basin along the slope of Sicily and leaves it along the Sardinian coast [29]. The fact that the intermediate layer of this sub-basin is occupied by the LIW explains the positive and very significant correlation between A_T and S in the intermediate depths of the Tyrrhenian. Our A_T-S fit (Eq.20), obtained by all the available data of the Tyrrhenian Sub-basin, is similar to the one recorded by [8]: $A_T = 96.62*S - 1139.1\ \mu mol\ kg^{-1}$ (Eq.III). The slight differences in the slopes and intercepts between the two equations are due firstly to the different number of stations and sampled

points (one station and n = 21 in our study *vs.* six stations and n = 320 in the other one), and secondly to the date of sampling (May 2013 in our study, November 2006, February, April and July 2007 and February 2008 in the other one).

The A_T-S correlation (Eq.2) for the surface layer of the entire Mediterranean Sea differs from the regression reported by [5]: $A_T = 73.7*S - 285.7 \pm 8.20$ μmol kg^{-1} (Eq. IV). The reason for the steeper slope and the more negative intercept in Eq.2 compared to Eq.IV, could be attributed to the different sampling locations : our track passed through the Strait of Gibraltar toward the Eastern part of the Mediterranean Sea and the stations were equally distributed between the two main Mediterranean basins, while the track covered in the other study was conducted from the South-East of Sardinia toward the Levantine Sub-basin and the sampled stations were concentrated mainly in the Eastern basin. In addition, the sampling periods were different: the data of the present study were collected in May 2013, whereas the data of [5] were sampled in October/November 2001. The differentiation in Eq.2 and Eq.IV could thus be attributed to the temporal variability of temperature and S in the Mediterranean Sea, which is in part associated to the climate change (as mentioned above for the Alboran Sub-basin). Equation 2 also differs from the recently reported A_T-S fit (Eq.V) for Mediterranean surface waters reported by [30]: $A_T = 79.84*S - 510$ (Eq.V) that was based exclusively on measurements made at 5m below the sea surface. Furthermore, the A_T-S relationships noted for the surface waters of the entire Mediterranean Sea (Eq.2) and specifically for the surface waters of the Western basin (Eq.6), are very close to the relationship: $A_T = 93.996*S - 1038.1 \pm 2.5$ μmol kg^{-1} (Eq.VI), calculated for samples located between the surface and the maximum of salinity (LIW horizon) at the DYFAMED site [31].

The abovementioned similarities of A_T-S correlations in the different Mediterranean areas, imply that the A_T could considered to be conservative in the Mediterranean Sea, as previously was stated by [32]. The conservative behavior of A_T with respect to salinity occurs because HCO_3^- (which is, together with CO_3^{2-} and $B(OH)_4^-$, one of the most important bases for seawater) is a major constituent of seawater and the ratio of HCO_3^- to the salinity or the chlorinity is nearly constant [8]. Equations 5 and 8 describing the A_T-S relationship in the Western and Eastern Mediterranean basins, respectively, are considerably different although both have negative intercepts. The slope and the absolute intercept values are higher in the Eastern basin, indicating that the salinity-specific alkalinity (i.e. A_T/S ratio) increases with salinity. The specific alkalinity of the Eastern Mediterranean waters is therefore higher than that of less saline Western ones. As the regression lines do not pass through the origin, the different values of the intercept between the different A_T-S equations (Table 1) reflect the different specific total alkalinities of the Eastern and Western Mediterranean water masses due to the contributions to A_T besides the salinity. However, excessive inputs of A_T from rivers in the Adriatic Sub-basin [33] result in the absence of a significant correlation between A_T and S at all the depths of this sub-basin, except on the surface layer where a significant but negative A_T-S fit was detected. The mixing of saline surface water, coming from the Eastern Sub-basins with local waters discharged by the nearby rivers and characterized by very high A_T concentrations, shaping the specific fit.

3.2. C_T-S Relationships in the Mediterranean Sea, its Basins and Sub-Basins

Total dissolved inorganic carbon (C_T) varied between a minimum of 2095 µmol kg^{-1} at the surface layers (~ 5 m) of the Alboran Sub-basin in the Western Mediterranean basin and a maximum of 2359.0 ± 0.4 µmol kg^{-1} in the intermediate waters (~ 350 m) of the Eastern Mediterranean basin (Mean = 2308.5 ± 22 µmol kg^{-1}, Fig.4). However, it is obvious that the intermediate, deep and bottom layers of the Western basin are characterized by the highest C_T concentrations (2321 ± 12 µmol kg^{-1} in the intermediate layers of the Algero-Provencal Sub-basin and 2322.0 ± 0.0 µmol kg^{-1} in the deep layers of the Liguro-Provencal Sub-basin) compared to the Eastern basin.

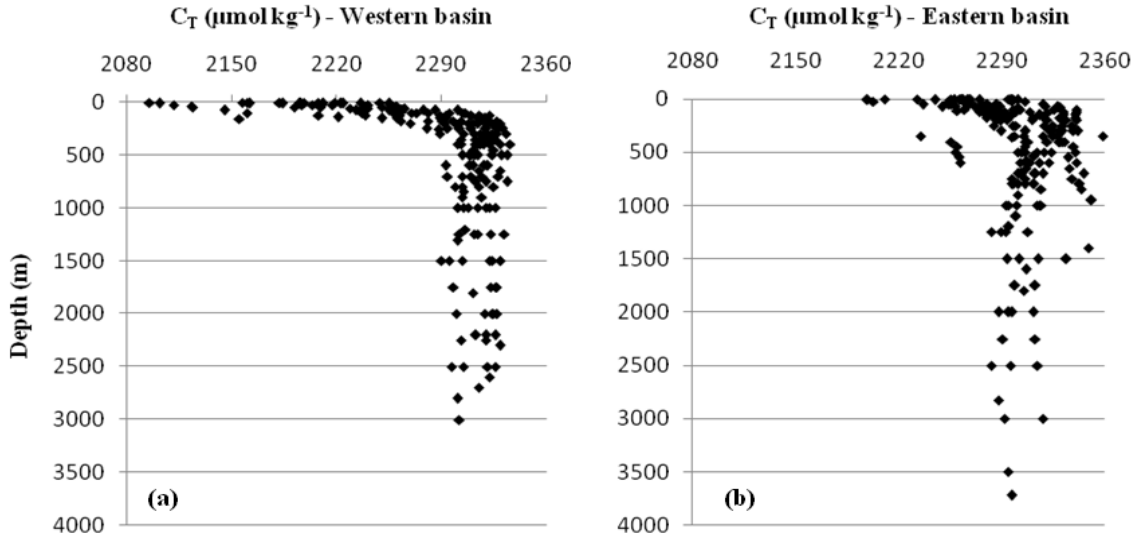

Figure 4. Total inorganic carbon (µmol kg^{-1}) as a function of depth in the Western (a) and in the Eastern (b) Mediterranean Basins.

The presence of high C_T concentrations in conjunction with high salinities (Fig.2 and 4) in both the Eastern and the Western Mediterranean basins explains the general significant correlation obtained between these two parameters in the entire Mediterranean Sea. Up to our knowledge, the C_T-S equations are not assessed for all the Mediterranean basins and sub-basins and at different depth layers (surface, intermediate and deep). The Table 3 presents the C_T-S fits in the different layers of the main basins and sub-basins in the Mediterranean Sea obtained by linear regression of Model II, using the data of the 2013 MedSeA cruise. The variability of C_T, apart of salinity, is also controlled by biological processes (i.e. precipitation and dissolution of calcium carbonate, photosynthesis, oxidation of organic matters), and the air-sea exchange of carbon dioxide. Due to the additional impact of these non-conservative processes on C_T, significant C_T-S correlations are not obtained at all depth layers. In the Eastern basin, there is no significant relationship between these two parameters in the intermediate layer, but we have noted a significant and negative C_T-S fit (Eq.8) in the deep layers. The deep waters of this basin are characterized by high C_T concentrations and relatively low salinities in relation to the overlying layers, which explain the negative C_T-S correlation. In the Mediterranean Sea, the convective processes and the consequent advection of dense waters assume a relevant role in sustaining the amount of remineralization in deep

layers and appear to be more important than the sinking of particulate matter from the upper layers [34]. It is evident that the active overturning circulation of the Mediterranean Sea fuels the deep layers with labile carbon entrained in the newly formed deep waters inducing enhanced production of respiratory CO_2. The involvement of remineralization explains the high C_T concentrations measured in the deep layers of both the Eastern and the Western basins and the absence of a significant C_T-S correlation in the deep layers of many Mediterranean sub-basins (Table 2).

Table 2. The C_T-S relationships in the different layers of the main basins and sub-basins in the Mediterranean Sea during May 2013 (R.M.S.D. = root mean square deviation, r = coefficient of correlation (Pearson's coefficient), n = number of data pairs used to derive each relationship, [-] means that no significant relationship was found).

Basin/Sub-basin	Depth	C_T-S correlation	R.M.S	r	n	Number of equation
Mediterranean	All	$C_T = 90.91*S - 1213$	± 29	0.72	428	Eq. 1
	Surface (0-25 m)	$C_T = 63.65*S - 198$	± 18	0.93	58	Eq. 2
	Intermediate (>25-400 m)	$C_T = 80.75*S - 822$	± 26.5	0.69	207	Eq. 3
	Deep (> 400 m)	-	-	-	-	-
Western basin	All	$C_T = 107.68*S – 1836.6$	± 19	0.93	215	Eq. 4
	Surface (0-25 m)	$C_T = 74*S – 583.5$	± 14	0.94	30	Eq. 5
	Intermediate (>25-400 m)	$C_T = 99.3*S - 1515$	± 18	0.91	105	Eq. 6
	Deep (> 400 m)	-	-	-	-	-
Eastern basin	All	-	-	-	-	-
	Surface (0-25 m)	$C_T = 66*S – 292.6$	± 20	0.68	28	Eq. 7
	Intermediate (>25-400 m)	-	-	-	-	-
	Deep (> 400 m)	$C_T = 269.6*S – 8145.8$	± 16	-0.53	81	Eq. 8
Alboran Sub-basin	All	$C_T = 97.84*S – 1456.5$	± 7.6	0.99	23	Eq. 9
	Surface (0-25 m)	$C_T = 148*S - 3282$	± 4	0.83	3	Eq. 10
	Intermediate (>25-400 m)	$C_T = 102*S – 1611$	± 5	0.99	11	Eq. 11
	Deep (> 400 m)	$C_T = 244*S – 7083$	± 2	0.87	8	Eq. 12
Algero-Provencal Sub-basin	All	$C_T = 123.78*S – 2445.5$	± 13.7	0.95	73	Eq. 13
	Surface (0-25 m)	$C_T = 85.61*S – 1012$	± 12	0.88	9	Eq. 14
	Intermediate (>25-400 m)	$C_T = 136.62*S – 2934.5$	± 12	0.93	32	Eq. 15
	Deep (> 400 m)	-	-	-	-	-
Liguro-Provencal Sub-basin	All	$C_T = 143*S – 2904$	± 18	0.83	70	Eq. 16
	Surface (0-25 m)	$C_T = 56.89*S + 66$	± 5.6	0.95	8	Eq. 17
	Intermediate (>25-400 m)	$C_T = 113.5*S – 2059$	± 13.6	0.8	33	Eq. 18
	Deep (> 400 m)	-	-	-	-	-
Tyrrhenian Sub-basin	All	$C_T = 126.6*S – 2285$	± 8	0.96	21	Eq. 19
	Surface (0-25 m)	$C_T = 335.17*S – 10537$	± 3	-0.95	3	Eq. 20
	Intermediate (>25-400 m)	$C_T = 103.24*S – 1683.5$	± 5.26	0.97	11	Eq. 21
	Deep (> 400 m)	-	-	-	-	-
Ionian Sub-basin	All	$C_T = 111*S – 2003$	± 21	0.77	57	Eq. 22
	Surface (0-25 m)	$C_T = 72.71*S – 540$	± 16	0.91	8	Eq. 23
	Intermediate (>25-400 m)	$C_T = 149*S – 3481$	± 23.6	0.61	27	Eq. 24
	Deep (> 400 m)	-	-	-	-	-
Adriatic Sub-basin	All	-	-	-	-	-
	Surface (0-25 m)	-	-	-	-	-
	Intermediate (>25-400 m)	-	-	-	-	-
	Deep (> 400 m)	-	-	-	-	-
Western Cretan Straits	All	-	-	-	-	-
	Surface (0-25 m)	-	-	-	-	-
	Intermediate (>25-400 m)	-	-	-	-	-
	Deep (> 400 m)	$C_T = 104.18*S – 1805$	± 0.8	-0.68	4	Eq. 25
Levantine Sub-basin	All	-	-	-	-	-
	Surface (0-25 m)	$C_T = 39.22*S + 1082$	± 4	-0.54	4	Eq. 26
	Intermediate (>25-400 m)	-	-	-	-	-
	Deep (> 400 m)	-	-	-	-	-

Our C_T-S correlations at the surface (Eq.17) and intermediate (Eq.18) layers of the Liguro-Provencal Sub-basin are different from the ones reported by [32]. However, it has to be mentioned that the C_T-S relationships obtained by the two studies are not totally comparable. The differences could be attributed to the different sampling strategy ; the equations of [32] are based on data collected in one fixed station in a coastally-influenced area (DYFAMED site) that was sampled monthly for a 2-years period, whereas the equations of the present study derived from data collected in May 2013 in three sampling stations. In addition, the data used in the study of [32] are originating from different depth intervals than ours: the relationship [C_T = 74.53*S-555.2 μmol kg^{-1}] corresponds to depths below the salinity maximum (LIW horizon) down to the bottom and the equation [C_T =155.17*S – 3662.6 μmol kg^{-1}] was calculated for samples located between the surface and the maximum of salinity in wintertime.

Our results showed that the total alkalinity and total inorganic carbon were higher in the Mediterranean outflow than in the Atlantic inflow, in agreement with [35]. It seems that there is an important flux of C_T from the Mediterranean to the Atlantic (at the Strait of Gibraltar, C_T is equal to 2327 ± 2μmol kg^{-1} in the outflowing Mediterranean waters vs. 2123 ± 7 μmol kg^{-1} in the inflowing Atlantic waters). This is probably due to the supply of carbon by the rivers and the Black Sea, to the transformation of 40% of the organic carbon entering the Mediterranean to inorganic carbon [4] and to the high remineralization rates in the Mediterranean deep layers [34]. Moreover, our results confirm that the Mediterranean Sea exports C_T to the Atlantic Ocean. These findings are in agreement with those of [36] whom estimated that there is a net export of inorganic carbon from the Mediterranean Sea to the Atlantic Ocean varying from 0.02 to 0.07 pg C yr^{-1}, whereas [37] estimated that this export amounted to 0.025 $PgCyr^{-1}$.

4. Conclusion

Based on high quality and recent carbonate system data collected on May 2013 during the MedSeA cruise, this paper provides for the first time A_T-S and C_T-S fits in each Mediterranean basin and sub-basin and at different depth layers. These equations could be used to estimate, based on salinity data, the carbonate system parameters in cases where there is a lack in this kind of measurements. This study show that a substantial quantity of alkalinity is added to the seawater during its residence time in the Mediterranean Sea, whereas the biological processes, the air-sea exchange and the high remineralization rate are responsible of the high C_T concentrations in this sea.

A continuous monitoring of the CO_2 system parameters in the main sub-basins of the Mediterranean Sea is recommended to evaluate the spatial and temporal evolution of this system in the context of climate change and ocean acidification.

Acknowledgements

This work is an essential part of the European project "Mediterranean Sea Acidification in a changing climate – MedSeA" (http://medsea-project.eu/), funded by the EC FP7 Cooperation program (grant agreement 265103). The authors are pleased to thank the captain and the crew of the Spanish research vessel R/V Ángeles Alvariño. Authors are grateful to the National Council for Scientific Research (CNRS) in Lebanon for the PhD thesis scholarship granted to A.E.R. HASSOUN and E. GEMAYEL.

References

[1] Alekin O.A., 1972. Saturation of Mediterranean Sea water with calcium carbonate. *Geochemistry*, 206, 239–242.

[2] Chernyakova A.M., 1976. Elements of the carbonate system in the Straits of Sicily (Tunis Strait) area. *Oceanology*, 16, 36–39.

[3] Millero F.J., Morse J., Chen C.-T.,1979. The carbonate system in the western Mediterranean Sea. *Deep Sea Research Part A : Oceanographic Research Papers*, 26 (12), 1395–1404.

[4] Copin-Montégut C., 1993. Alkalinity and carbon budgets in the Mediterranean Sea. *Global Biogeochemical Cycles,* 7 (4), 915–925, doi:10.1029/93GB01826.

[5] Schneider A., Wallace D.W.R., and Körtzinger A., 2007. Alkalinity of the Mediterranean Sea. *Geophysical Research Letters,* 34, L15608, doi:10.1029/2006GL028842.

[6] Schneider A., Tanhua T., Körtzinger A., Wallace D.W.R., 2010. High anthropogenic carbon content in the eastern Mediterranean. *Journal of Geophysical Research*, 115, C12050, doi:10.1029/2010JC006171.

[7] De Carlo E.H., Mousseau L., Passafiume O., Drupp P.S., Gattuso J., 2013. Carbonate chemistry and air-sea CO_2 flux at a fixed point in a NW Mediterranean bay over a four-year period: 2007-2011. *Aquatic Geochemistry*, 19, 399–442.

[8] Rivaro P., Messa R., Massolo S., Frache R., 2010. Distributions of carbonate properties along the water column in the Mediterranean Sea: Spatial and temporal variations. *Marine Chemistry*, 121, 236–245.

[9] Touratier F. and Goyet C., 2011. Impact of the Eastern Mediterranean Transient on the distribution of anthropogenic CO_2 and first estimate of acidification for the Mediterranean Sea. *Deep Sea Research Part I: Oceanographic Research Papers*, 58,1–15.

[10] Pujo-Pay M., Conan P., Oriol L., Cornet-Barthaux V., Falco C., Ghiglione J.F., Goyet C., Moutin T., and Prieur L., 2011. Integrated survey of elemental stoichiometry (C, N, P) from the western to eastern Mediterranean Sea. *Biogeosciences*, 8, 883–899.

[11] Álvarez M., Sanleón-Bartolomé H., Tanhua T., Mintrop L., Luchetta A., Cantoni C., Schroeder K., and Civitarese G., 2014. The CO_2 system in the Mediterranean Sea : a basin wide perspective. *Ocean Science*, 10, 69–92.

[12] MedSeA (Mediterranean Sea Acidification in a changing climate) project, 2015 : http://medsea-project.eu/

[13] 2013 MedSeA research cruise on ocean acidification and warming : http://medseaoceancruise.wordpress.com/

[14] DOE, 1994. Handbook of methods for the analysis of the various parameters of the carbon dioxide system in sea water ; version 2, A. G. Dickson & C. Goyet, eds., ORNL/CDIAC-74.

[15] Hassoun A.E.R., 2014. Analyse et Modélisation de l'Acidification en Mer Méditerranée.

Thèse de doctorat soutenue le 29 septembre 2014 à l'Université de Perpignan Via Domitia, laboratoire IMAGES : https://tel.archives-ouvertes.fr/tel-01083406.

[16] Goyet C., Hassoun A.E.R., Gemayel E., 2015. Carbonate system during the May 2013 MedSeA cruise. Dataset #841933 (DOI registration in progress).

[17] Goyet C., Gemayel E., Hassoun A.E.R., 2015. Underway pCO_2 in surface water during the 2013 MedSEA cruise. Dataset #841928 (DOI registration in progress).

[18] Ziveri P., and Grelaud M., 2013. Continuous thermosalinograph oceanography along Ángeles Alvariño cruise track MedSeA2013. Universitat Autònoma de Barcelona, doi:10.1594/PANGAEA.822153.

[19] Ziveri P., and Grelaud M., 2013. Physical oceanography during Ángeles Alvariño cruise MedSeA2013. Universitat Autònoma de Barcelona, doi:10.1594/PANGAEA.822162.

[20] Ziveri P., and Grelaud M., 2013. Physical oceanography measured on water bottle samples during Ángeles Alvariño cruise MedSeA2013. Universitat Autònoma de Barcelona, doi:10.1594/PANGAEA.822163.

[21] Mariotti A., Struglia M.V., Zeng N., Lau K.-M., 2002. The Hydrological Cycle in the Mediterranean Region and Implications for the Water Budget of the Mediterranean Sea. *Journal of Climate,* 15, 1674–1690.

[22] Bergamasco A. and Malanotte-Rizzoli P., 2010. The circulation of the Mediterranean Sea: a historical review of experimental investigations. *Advances in Oceanography and Limnology*, 1 (1), 11–28.

[23] Touratier F. and Goyet C., 2009. Decadal evolution of anthropogenic CO_2 in the northwestern Mediterranean Sea from the mid-1990s to the mid-2000s. *Deep Sea Research Part I: Oceanographic Research Papers*, 56 (10), 1708–1716.

[24] Béthoux J. P., Gentili B., Raunet J., and Tailliez D., 1990. Warming trend in the western Mediterranean deep water. *Nature*, 347, 660–662, doi: 10.1038/347660a0.

[25] Cacho I., Grimalt J.O., Canals M., Sbaffi L., Shackleton N.J., Schönfeld J., and Zahn R., 2001. Variability of the western Mediterranean Sea surface temperature during the last 25,000 years and its connection with the Northern Hemisphere climatic changes. *Paleoceanography*, 16 (1), 40–52, doi:10.1029/2000PA000502.

[26] Tsimplis M.N., and Rixen M., 2002. Sea level in the Mediterranean Sea -The contribution of temperature and salinity changes. *Geophysical Research Letters*, 0094-8276.

[27] Skliris N., Sofianos S., Gkanasos A., Mantziafou A., Vervatis V., Axaopoulos P. and Lascaratos A., 2011. Decadal scale variability of sea surface temperature in the Mediterranean Sea in relation to atmospheric variability. *Ocean Dynamics*, 62 (1), 13–30, doi: 10.1007/s10236-011-0493-5.

[28] Sparnocchia S., Gasparini G.P., Astraldi M., Borghini M., Pistek P., 1999. Dynamics and mixing of the Eastern Mediterranean outflow in the Tyrrhenian Sea. *Journal of Marine Systems*, 20, 301–317.

[29] Budillon G., Gasparini G.P. and Schröder K., 2009. Persistence of an eddy signature in the central Tyrrhenian basin. *Deep Sea Research Part II: Topical Studies in Oceanography*, 56, 713–724.

[30] Jiang Z.-P., Tyrrell T., Hydes D.J., Dai M., and Hartman S.E., 2014. Variability of alkalinity and the alkalinity-salinity relationship in the tropical and subtropical surface ocean, *Global Biogeochemical Cycles*, 28, doi:10.1002/2013GB004678.

[31] Copin-Montégut C. and Bégovic M., 2002. Distributions of carbonate properties and oxygen along the water column (0 – 2000 m) in the central part of the NW Mediterranean Sea (Dyfamed site). Influence of winter vertical mixing on air – sea CO_2 and O_2 exchanges. *Deep-Sea Research, II. Topical studies in oceanography*, 49 (11), 2049–2066.

[32] Bégovic M. and Copin-Montégut C., 2002. Processes controlling annual variations in the

partial pressure of CO_2 in surface waters of the central northwestern Mediterranean Sea (Dyfamed site). *Deep Sea Research Part II: Topical Studies in Oceanography*, 49 (11), 2031–2047.

[33] Cantoni C., Luchetta A., Celio M., Cozzi S., Raicich F., and Catalano G., 2012. Carbonate system variability in the Gulf of Trieste (North Adriatic Sea). *Estuarine. Coastal and Shelf Science*, 115, 51–62.

[34] La Ferla R., Azzaro M., Civitarese G., and Ribera d'Alcalà M., 2003. Distribution patterns of carbon oxidation in the eastern Mediterranean Sea: Evidence of changes in the remineralization processes. *Journal of Geophysical Research*, 108 (C9), 8111, doi:10.1029/2002JC001602, C9.

[35] Santana-Casiano J.M., Gonzalez-Davila M. and Laglera L.M., 2002. The carbon dioxide system in the Strait of Gibraltar. *Deep-Sea Research, II. Topical studies in oceanography,* 49, 4145–4161.

[36] Aït-Ameur N. and Goyet C., 2006. Distribution and transport of natural and anthropogenic CO_2 in the Gulf of Cadiz. *Deep Sea Research Part II: Topical Studies in Oceanography*, 53 (11-13), 1329–1343.

[37] Huertas I.E., Ríos A.F., García-Lafuente J., Makaoui A., Rodríguez-Gálvez S., Sánchez-Román A., Orbi A., Ruíz J., and Pérez F.F., 2009. Anthropogenic and natural CO_2 exchange through the Strait of Gibraltar. Biogeosciences Discussion, 6, 1021–1067.

Article V: Climatological variations of total alkalinity and total inorganic carbon in the Mediterranean Sea surface waters

Gemayel et al. (2015)

Earth System Dynamics Discussions, 6 (2), 1499-1533. doi: 10.5194/esdd-6-1499-2015

Climatological variations of total Alkalinity and total inorganic carbon in the Mediterranean Sea surface waters

Elissar GEMAYEL[1,2,3], Abed El Rahman HASSOUN[3], Mohamed Anis BENALLAL[1,2], Catherine GOYET[1,2], Paola RIVARO[4], Marie ABBOUD-ABI SAAB[3], Evangelina KRASAKOPOULOU[5], Franck TOURATIER[1,2] and Patrizia ZIVERI[6,7]

[1] Université de Perpignan Via Domitia, IMAGES_ESPACE-DEV, 52 avenue Paul Alduy, 66860 Perpignan Cedex 9, France
[2] ESPACE-DEV, UG UA UR UM IRD, Maison de la télédétection, 500 rue Jean-François Breton, 34093 Montpellier Cedex 5, France
[3] National Council for Scientific Research, National Center for Marines Sciences, P.O Box 534, Batroun, Lebanon
[4] University of Genova, Department of Chemistry and Industrial Chemistry, via Dodecaneso 31, 16146 Genova, Italy
[5] University of the Aegean, Department of Marine Sciences, University Hill, Mytilene 81100, Greece
[6] Universitat Autònoma de Barcelona, Institute of Environmental Science and Technology, Barcelona, Spain
[7] Universiteit Amsterdam, Earth & Climate Cluster, Department of Earth Sciences, Faculty of Earth and Life Sciences, Amsterdam, The Netherlands

Abstract

A compilation of several cruises data from 1998 to 2013 was used to derive polynomial fits that estimate total alkalinity (A_T) and total inorganic carbon (C_T) from measurements of salinity and temperature in the Mediterranean Sea surface waters. The optimal equations were chosen based on the 10-fold cross validation results and revealed that a second and third order polynomials fit the A_T and C_T data respectively. The A_T surface fit showed an improved root mean square error (RMSE) of ± 10.6 µmol.kg^{-1}. Furthermore we present the first annual mean C_T parameterization for the Mediterranean Sea surface waters with a RMSE of ± 14.3 µmol.kg^{-1}. Excluding the marginal seas of the Adriatic and the Aegean, these equations can be used to estimate A_T and C_T in case of the lack of measurements. The seven years averages (2005-2012) mapped using the quarter degree climatologies of the World Ocean Atlas 2013 showed that in surface waters A_T and C_T have similar patterns with an increasing Eastward gradient. The surface variability is influenced by the inflow of cold Atlantic waters through the Strait of Gibraltar and by the oligotrophic and thermohaline gradient that characterize the Mediterranean Sea. The summer-winter seasonality was also mapped and showed different patterns for A_T and C_T. During the winter, the A_T and C_T concentrations were higher in the Western than in the Eastern basin, primarily due to the deepening of the mixed layer and upwelling of dense waters. The opposite was observed in the summer where the Eastern basin was marked by higher A_T and C_T concentrations than in winter**.** The strong evaporation that takes place in this season along with the ultra-oligotrophy of the Eastern basin determines the increase of both A_T and C_T concentrations.

Keywords: Mediterranean Sea; Carbonate System; Surface Waters; Empirical Modeling; Seasonal Variations

1. Introduction

The role of the ocean in mitigating climate change is well known as it absorbs about 2 Pg C yr^{-1} of anthropogenic CO_2 (Wanninkhof *et al.*, 2013). Worldwide measurements of surface seawater CO_2 properties are being conducted as they are important for advancing our understanding of the carbon cycle and the underlying processes controlling it. For instance, the buffer capacity of the CO_2 system varies with temperature, the distribution of total inorganic carbon and total alkalinity (Omta *et al.*, 2011).

Our understanding of the open-ocean CO_2 dynamics has drastically improved over the years (Watson and Orr, 2003; Sabine *et al.*, 2004; Takahashi *et al.*, 2009; Rödenbeck *et al.*, 2013). However our understanding of marginal seas such as the Mediterranean remains poor due to the limited measurements combined with the enhanced complexity of the land-ocean interactions. In the Mediterranean Sea, available measurements of the carbonate system are still scarce and only available in specific regions such as the Alboran sea (Copin-Montégut, 1993), the Gibraltar Strait (Santana-Casiano *et al.*, 2002), the Dyfamed time-series in the Ligurian Sea (Bégovic and Copin-Montégut, 2002; Copin-Montégut and Bégovic, 2002; Touratier and Goyet, 2009) and the Otranto Strait (Krasakopoulou *et al.*, 2011). Large geographical repartition of CO_2 data are often confined to cruises with a short sampling period (Schneider *et al.*, 2007; Rivaro *et al.*, 2010; Touratier *et al.*, 2012; Álvarez *et al.*, 2014; Goyet *et al.*, 2015). Numerical models have provided some insights of the carbon dynamics in the Mediterranean Sea (D'Ortenzio *et al.*, 2008; Louanchi *et al.*, 2009; Cossarini *et al.*, 2015), but it remains important to constrain the system from in situ measurements to validate their output.

The scarcity of the CO_2 system measurements in the Mediterranean Sea make it difficult to constrain the CO_2 uptake in this landlocked area and also limits our understanding of the magnitude and mechanisms driving the natural variability on the ocean carbon system (Touratier and Goyet, 2009). Empirical modeling has been successfully used to study the marine carbon biogeochemical processes such as the estimation of biologically produced O_2 in the mixed layer (Keeling *et al.*, 1993), estimation of global inventories of anthropogenic CO_2 (Sabine *et al.*, 2004) and estimation of the $CaCO_3$ cycle (Koeve *et al.*, 2014). Empirical algorithms were also used to relate limited A_T and C_T measurements to more widely available physical parameters such as salinity and temperature (Bakker *et al.*, 1999; Ishii *et al.*, 2004; Lee *et al.*, 2006). The A_T and C_T fields can then be used to calculate pCO_2 fields and thus predict the CO_2 flux across the air-sea interface (McNeil *et al.*, 2007).

Previous empirical approaches to constrain A_T in the Mediterranean Sea have only covered selected cruises (Schneider *et al.*, 2007; Touratier and Goyet, 2009) or local areas such as the Dyfamed time-series station or the Strait of Gibraltar (Copin-Montégut, 1993; Santana-Casiano *et al.*, 2002). As for C_T, empirical models have only been applied to data below the mixed layer depth (MLD) following the equation of Goyet and Davis (1997) at the Dyfamed time series station (Touratier and Goyet, 2009) or using the composite dataset from Meteor 51/2 and Dyfamed (Touratier and Goyet, 2011). Also Lovato and Vichi (2015) proposed an

optimal multiple linear model for C_T using the Meteor 84/3 full water colum data. To the best of our knowledge the reconstruction of C_T in surface waters has not been yet performed in the Mediterranean Sea. This is probably due to the lack of measurements available for previous studies to capture the more complex interplay of biological, physical and solubility processes that drive C_T variability in the surface waters.

In this study we have compiled CO_2 system measurements from 14 cruises between 1995 and 2013, that allowed us to constrain an improved and new empirical algorithms for A_T and C_T in the Mediterranean Sea surface waters. We also evaluated the spatial and seasonal variability of the carbon system in the Mediterranean Sea surface waters, by mapping the 2005-2012 annual and seasonal averages of surface A_T and C_T using the quarter degree climatologies of salinity and temperature from the World Ocean Atlas 2013 (WOA13).

2. Methods

2.1. Surface A_T and C_T data in the Mediterranean Sea

Between 1998 and 2013, there have been multiple research cruises sampling the seawater properties throughout the Mediterranean Sea. This includes parameters of the carbonate system more specifically A_T, pH and C_T and physico-chemical properties of in situ salinity, and temperature. However, the number of the nutrients concentrations was very limited. In this study we have compiled surface water samples between 0 and 10 m depth, totaling 490 and 426 measurements for A_T and C_T respectively (Table 1).

Table 1. List of available carbonate system datasets for the Mediterranean Sea

Dataset	Period	Carbonate system parameters	Reference
Prosope	Sep-Oct 1999	A_T and pH	Bégovic and Copin (2013)
Meteor 51/2	Oct-Nov 2001	A_T and C_T	Schneider and Roether (2007)
Meteor 84/3	Apr 2004	A_T, C_T and pH	Tanhua *et al.* (2012)
Carbogib 2-6	2005-2006	A_T and pH	(Huertas, 2007a, b, c, d, e)
Gift 1-3	2005-2006	A_T and pH	(Huertas, 2007f, g, h)
Transmed	Jun 2007	A_T and pH	Rivaro *et al.* (2010)
Sesame IT-4	Mar - Apr 2008	A_T and C_T	SeaDataNet
Boum	Jun-Jul 2008	A_T and C_T	Touratier *et al.* (2012)
Pacific-Celebes	2007-2009	A_T and C_T	Hydes *et al.* (2012)
Moose-GE	May 2010	A_T and C_T	SeaDataNet
Hesperides	May 2013	A_T	Perez *et al.* (2013)
MedSEA	May 2013	A_T and C_T	Goyet *et al.* (2015)
Dyfamed time-series	1998-2013	A_T and C_T	Oceanological Observatory of Villefranche-sur-Mer

2.2. Polynomial model for fitting A_T and C_T data

Two polynomial equations for fitting A_T or C_T from salinity (S) alone or combined with sea surface temperature (T) in the surface waters (0 – 10 m) of the Mediterranean Sea were chosen from the results of the 10-fold cross validation method (Stone, 1974; Breiman, 1996). This type of analysis was previously performed by Lee *et al.* (2006) for global relationships of A_T with salinity and temperature. This model validation technique is performed by retaining a single subsample used for testing and training the algorithm on the 9 remaining subsamples. The cross validation process is then repeated 10 times. The best fit is chosen by computing the residuals from each regression model, and computing independently the performance of the selected optimal polynomial on the remaining subsets. The analysis was applied for polynomials of order 1 to 3, and the optimal equation was chosen based on the lowest Root Mean Square Error (RMSE) and the highest coefficient of determination (r^2).

To ensure the same spatial and temporal distribution of A_T and C_T polynomial fits we only selected stations where A_T and C_T were simultaneously measured (Table 1; Figure 1). To validate the general use of the proposed parameterizations we tested the algorithms with measurements which are not included in the fits (Testing dataset). Hence for the A_T, 375 and 115 data points are used for the training and testing datasets respectively. For the C_T the training dataset is formed from 381 data points and the validation dataset is the same as the testing subset of the 10th fold (45 data points).

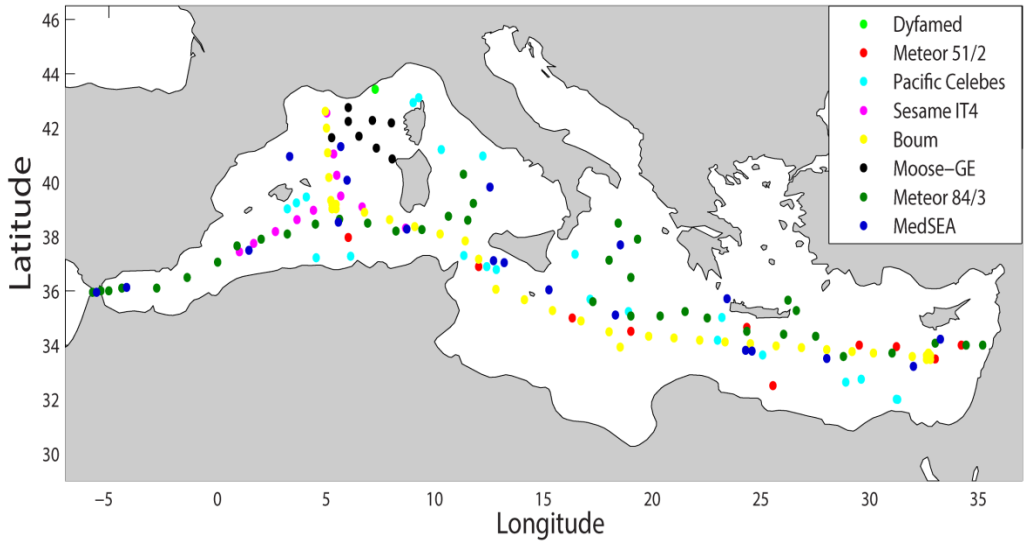

Figure 1. Spatial distribution of data points used to initiate the fits of A_T and C_T

2.3. Climatological and seasonal mapping of A_T and C_T

The climatological and seasonal averages of salinity (Zweng *et al.*, 2013) and temperature (Locarnini *et al.*, 2013) in 1/4*1/4 degree grid cells were downloaded from the World Ocean Atlas 2013 (WOA13). The seven years averages (2005-2012) and the summer-winter seasonality of A_T and C_T fields were mapped at 5 m depth by applying the respective derived algorithms in their appropriate ranges of S and T.

3. Results and Discussion

3.1. Fitting A_T in the Mediterranean Sea surface waters

In the surface ocean the A_T variability is controlled by freshwater addition or the effect of evaporation, and salinity contributes to more than 80% of the A_T variability (Millero *et al.*, 1998). In the Mediterranean Sea, several studies have shown that the relationship between A_T and S is linear (Copin-Montégut, 1993; Copin-Montégut and Bégovic, 2002; Schneider *et al.*, 2007; Rivaro *et al.*, 2010; Hassoun *et al.*, 2015b). In other studies, the sea surface temperature (T) has been included as an additional proxy for changes in surface water A_T related to convective mixing (Lee *et al.*, 2006; Touratier and Goyet, 2011).

The results of the 10-fold cross validation analysis revealed that the optimal model for A_T is a second order polynomial in which A_T is fitted to both S and T (Table 2, Eq 1). A linear relationship between A_T and S yields a higher RMSE (14.5 µmol.kg^{-1}) and a lower r^2 (0.91) than Eq (1). In a semi-enclosed basin such as the Mediterranean Sea, the insulation and high evaporation as well as the input of rivers and little precipitation leads to a negative freshwater balance (Rohling *et al.*, 2009). The resulting anti-estuarine thermohaline circulation could explain the contribution of temperature to the A_T variability (Touratier and Goyet, 2011).

Table 2. Second order polynomial fit to derive A_T from salinity and temperature in the Mediterranean Sea surface waters

Polynomial fit	N	r^2	RMSE (µmol.kg^{-1})
Eq (1): $A_T = 2558.4 + 49.83(S) - 3.89(T) - 3.12(S)^2 - 1.06(T)^2$ $T > 13$ ºC and $36.30 < S < 39.65$	375	0.96	10.6

The residuals of training dataset used to generate the second order polynomial fit for A_T are presented in Figure 2a. Most of the A_T residuals (340 over 375) were within a range of ± 15 µmol.kg^{-1} (1 σ). However 35 residuals over were high up to ± 30 µmol.kg^{-1} (1 σ). Applying the A_T algorithm to the testing dataset (Figure 2b), yields a mean residual of 0.91 ± 10.30 µmol.kg^{-1} (1 σ), and only 6 data points have residuals higher than ± 15 µmol.kg^{-1} (1 σ).

The comparison of the RMSE as reported by other studies with that of Eq (1) does not indicate if the parameterization developed here has advanced or not on previous attempts in the Mediterranean Sea. In that order, we independently applied each of the previous equations on the same training dataset used to develop Eq (1) and then computed the RMSE and r^2 for every one (Table 3). The results show that Eq (1) has a lower RMSE and a higher r^2 than all of the parameterizations presented in Table 3. For instance, the global relationship of Lee et al. (2006) applied to the dataset of this study yields an RMSE as high as ± 40.50 µmol.kg^{-1}. The RMSE of other studies developed strictly in the Mediterranean Sea varied from ± 13.81 to ± 26.11 µmol.kg^{-1} using the equations of Touratier and Goyet (2011) and Schneider *et al.* (2007) respectively.

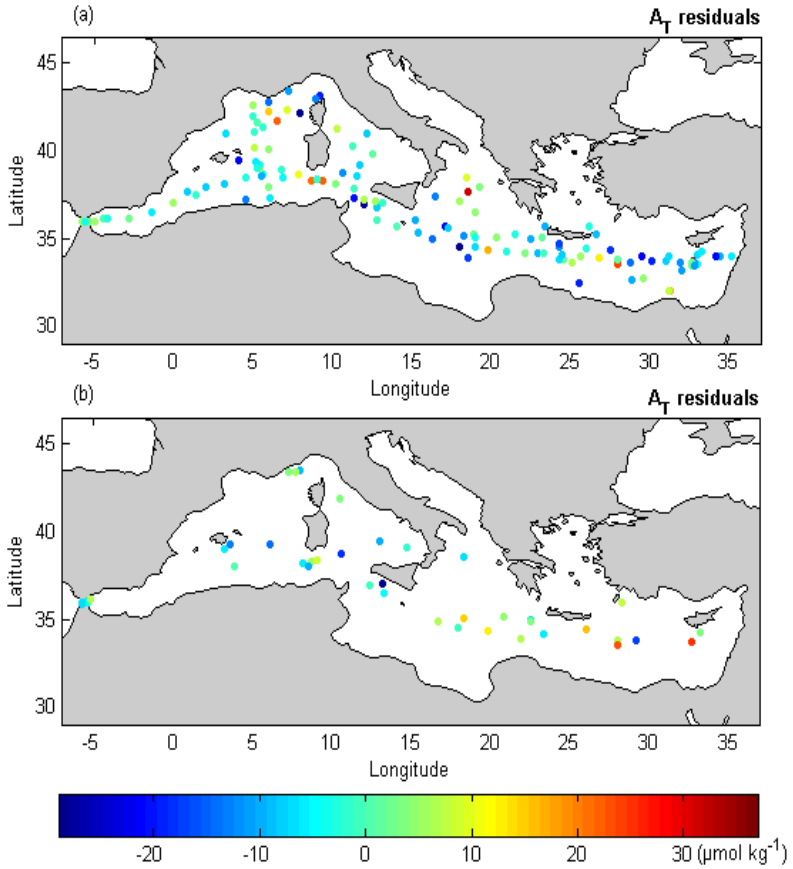

Figure 2. Map of the residuals of the A_T algorithm (Table 1; Eq 1) applied the (a) training and (b) testing datasets

By applying directly the previous parameterizations to our training dataset, the calculated RMSE are significantly higher than the ones reported in their respective studies. For instance the reported RMSE in Lee *et al.* (2006) for sub-tropical oceanic regions is ± 8 µmol.kg^{-1} and that of Schneider *et al.* (2007) for the Meteor 51/2 cruise is ± 4.2 µmol.kg^{-1}. This shows that previous models were constrained by their spatial coverage, time span and used datasets. In fact the previous equations were calculated in local areas such as the Alboran Sea (Copin-Montégut, 1993), the Strait of Gibraltar (Santana-Casiano *et al.*, 2002) or the Dyfamed Site (Copin-Montégut and Bégovic, 2002; Touratier and Goyet, 2009). On a large scale, equations were applied using limited datasets such as the Meteor 51/2 cruise in October-November 2001 (Schneider *et al.*, 2007), the Transmed cruise in May-June 2007 (Rivaro *et al.*, 2010) or the Meteor 51/2 and the Dyfamed time series station (Touratier and Goyet, 2011).

The proposed algorithm including surface data from multiple cruises, and on a large time span, presents a more global relationship to estimate A_T from S and T than the previously presented equations (Table 3). In equation 1, T and S contribute to 96% of the A_T variability and the RMSE of ± 10.6 µmol.kg^{-1} presents a significant improvement of the spatial and temporal estimations of A_T in the Mediterranean Sea surface waters.

Table 3. Performance of the different parameterizations for the estimation of A_T applied independently to the training dataset of this study

Region	Parameterization	RMSE ($\mu mol.kg^{-1}$)	r^2	Reference
Alboran Sea	$A_T = 94.85(S) - 1072.6$	± 16.61	0.92	Copin-Montégut (1993)
Dyfamed site	$A_T = 93.99(S) - 1038.1$	± 16.31	0.92	Copin-Montégut and Bégovic (2002)
Strait of Gibraltar	$A_T = 92.28(S) - 968.7$	± 16.48	0.92	Santana-Casiano *et al.* (2002)
Mediterranean Sea	$A_T = 73.7(S) - 285.7$	± 26.11	0.68	Schneider *et al.* (2007)
Dyfamed site	$A_T = 99.26(S) - 1238.4$	± 18.53	0.91	Touratier and Goyet (2009)
Western Mediterranean	$A_T = 95.25(S) - 1089.3$	± 16.97	0.92	Rivaro *et al.* (2010)
Eastern Mediterranean	$A_T = 80.04(S) - 499.8$	± 14.58	0.91	
Mediterranean Sea	$A_T = 1/(6.57*10^{-5}+1.77\text{-}10^{-2})/S - (5.93 - 10^{-4}(\ln\theta))/\theta^2)$	± 13.81	0.92	Touratier and Goyet (2011)
Global relationship (Sub-tropics)	$A_T = 2305 + 58.66\ (S - 35) + 2.32\ (S - 35)^2 + 1.41\ (T - 20) + 0.04\ (T - 20)^2$	± 40.50	0.26	Lee *et al.* (2006)

3.2. Fitting C_T in the Mediterranean Sea surface waters

The surface C_T concentrations are influenced by lateral and vertical mixing, photosynthesis, oxidation of organic matter and changes in temperature and salinity (Poisson *et al.*, 1993; Takahashi *et al.*, 1993). All these processes are directly or indirectly correlated with sea-surface temperature (Lee *et al.*, 2000). Hence, the parameterization of C_T in surface waters includes both physical (S and T) and/or biological parameters (Bakker *et al.*, 1999; Lee *et al.*, 2000; Bates *et al.*, 2006; Koffi *et al.*, 2010; Sasse *et al.*, 2013).

The results of the 10-fold cross validation analysis showed that a first order polynome fits C_T to S and T with an RMSE of 16.25 $\mu mol.kg^{-1}$ and $r^2 = 0.87$. These values are comparable to the RMSE and r^2 found by previous empirical approaches applied in the Eastern Atlantic (Bakker *et al.*, 1999; Koffi *et al.*, 2010). However we found that a third order polynome improved the RMSE and r^2 of the equation compared to the first order fit (Table 4, Eq 2). Hence we will retain the large dataset used to develop Eq (2), where temperature and salinity contribute to 90% of the C_T variability encountered in the Mediterranean Sea surface waters. The remaining 10% could be attributed to the biological and air-sea exchange contributions to the C_T variability.

Table 4. Third order polynomial fit to derive C_T from salinity and temperature in the Mediterranean Sea surface waters

Polynomial fit	N	r^2	RMSE ($\mu mol.kg^{-1}$)
Eq (2): $C_T = 2234 + 38.15(S) - 14.38(T) - 4.48(S)^2 + 9.62(T)^2 - 1.10(S)^3 + 3.53(T)(S)^2 + 1.47(S)(T)^2 - 4.61(T)^3$ $T > 13$ ºC and $36.30 < S < 39.65$	381	0.90	14.3

The C_T parameterization developed in this study (Table 4; Eq 2) showed a higher uncertainty than that of A_T regarding both RMSE and r^2. In fact, the interpolation of C_T in the mixed layer adds a high uncertainty due to the seasonal variability. Also in surface waters the C_T are directly affected by air-sea exchange, and their concentrations will increase in response to the oceanic uptake of anthropogenic CO_2.

Previous models accounted for the anthropogenic biases in the C_T measurements by calculating the C_T rate of increase (Lee *et al.*, 2000; Bates, 2007; Sasse *et al.*, 2013; Takahashi *et al.*, 2014). However in a study, Lee *et al.* (2000) also did not correct the C_T concentrations for regions above 30º latitude such as the Mediterranean Sea. In the following we will assess the importance of accounting or not for anthropogenic biases in the C_T measurements. In that order we dowloaded the monthly atmospheric pCO_2 concentrations measured from 1999 to 2013 at the Lampedusa Island Station (Italy) from the World Data Center for Green House Gases (http://ds.data.jma.go.jp/gmd/wdcgg/). Following the method described by Sasse *et al.* (2013), we corrected the C_T measurements to the nominal year of 2005 and applied the same 10-fold cross validation analysis using data with and without anthropogenic C_T corrections. We found that the RMSE of the C_T model trained using measurements with anthropogenic corrections is 13.9 $\mu mol.kg^{-1}$, which is not significantly different from the model trained using measurements without anthropogenic corrections (Eq 2; RMSE = 14.3 $\mu mol.kg^{-1}$).

The yearly increase of C_T concentrations is difficult to assess due to the wide spatial distribution of the training dataset used to generate Eq (2). Hence we will refer to the monthly C_T concentrations measured between 1998 and 2013 at the Dyfamed time-series station. We found that the rate of increase in C_T concentrations at the Dyfamed site was 0.99 $\mu mol.kg^{-1}.yr^{-1}$ (Figure 3), which is consistent with the anthropogenic C_T correction rate used in the previous studies of Lee *et al.* (2000), Bates (2007) and Sasse *et al.* (2013).

The rate of increase in C_T concentrations of 0.99 $\mu mol.kg^{-1}.yr^{-1}$ as well as the RMSE difference of ± 0.4 $\mu mol.kg^{-1}$ between the two models (with or without anthropogenic corrections) are both smaller than the uncertainty of the C_T measurements of at least ± 2 $\mu mol.kg^{-1}$ (Millero, 2007). A recent study also showed that the uncertainty of the C_T measurements can be significantly higher than ± 2 $\mu mol.kg^{-1}$, as most laboratories reported values of C_T for the measures that were within a range of ± 10 $\mu mol.kg^{-1}$ of the stated value (Bockmon and Dickson, 2015).

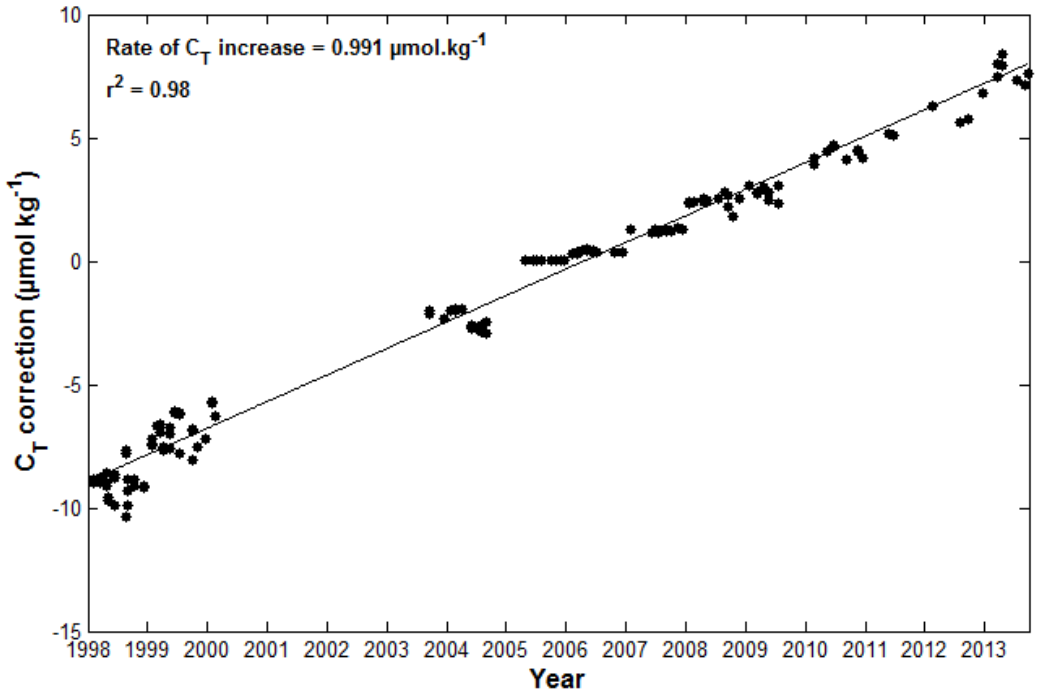

Figure 12. Rate of increase applied to correct the C_T measurements in reference to the year 2005

Between 1998 and 2013, the C_T concentrations measured at the Dyfamed time-series station showed a slightly increasing trend (r^2 = 0.05). The increase in C_T concentrations in response to elevated atmospheric CO_2, was masked by the high seasonal variations. For example, during the year 1999 the variation in C_T concentrations reached as high as 100 µmol.kg^{-1} (Figure 4a). Also there is a clear seasonal cycle of surface waters C_T in the Dyfamed station (Figure 4b). In the summer, the C_T starts to increase gradually to reach a maximum of 2320 µmol.kg^{-1} during the winter season, after which a gradual decrease is observed to reach a minimum of 2200 µmol.kg^{-1} by the end of spring. The seasonal cycle can be explained by the counter effect of temperature and biology on the C_T variations. During the spring, the increasing effect of warming of pCO_2 is counteracted by the photosynthetic activity that lowers the C_T. During the winter, the decreasing effect of cooling on pCO_2 is counteracted by the upwelling of deep waters rich in C_T (Takahashi *et al.*, 1993; Hood and Merlivat, 2001). This shows that the C_T concentrations in surface waters were more affected by the seasonal variations than by anthropogenic forcing.

Considering the small differences in RMSE obtained by the two models, the uncertainties in the C_T measurements and the clear signal of the seasonal variations; no corrections were made to account for the rising atmospheric CO_2 concentrations. In regions above 30º latitude such as the Mediterranean Sea, the corrections of C_T are small considering that the outcropping of deep isopycnal surfaces dilutes the anthropogenic CO_2 throughout the water column (Lee *et al.*, 2000). Also the dynamic overturning circulation in the Mediterranean Sea plays an effective role in absorbing the anthropogenic CO_2 and transports it from the surface to the interior of the basins (Lee *et al.*, 2011; Hassoun *et al.*, 2015a).

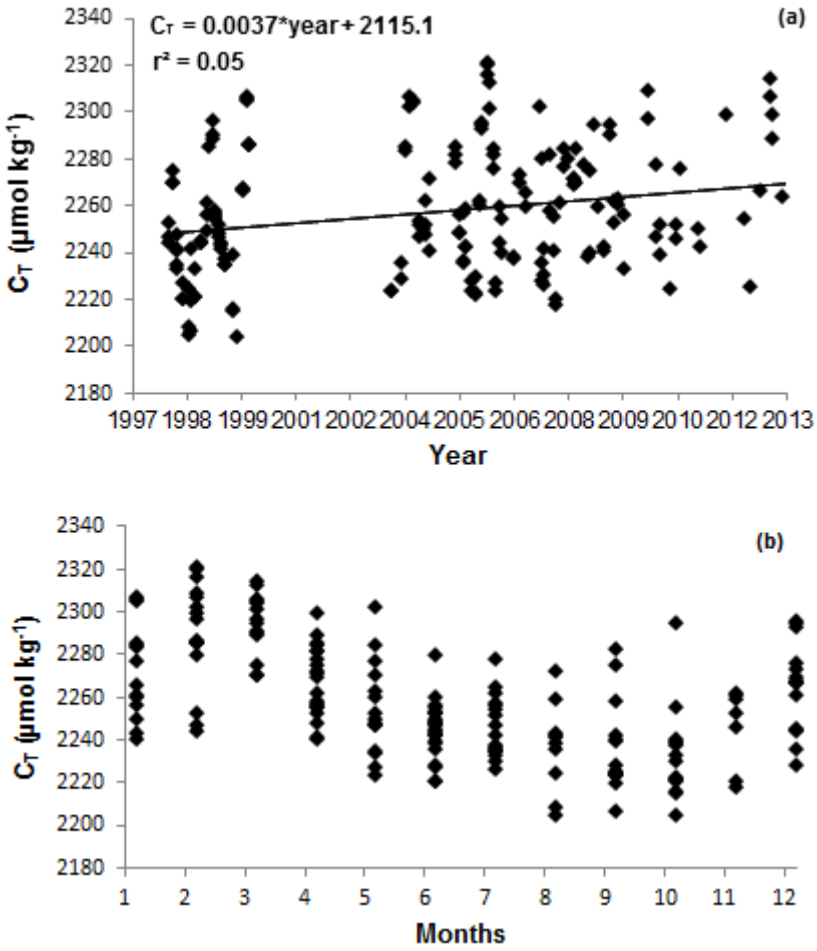

Figure 4. (a) Temporal and (b) seasonal variations of C_T measured at the Dyfamed time-series station between 1998 and 2013

The residuals of the dataset used to generate the third order polynomial fit for C_T are presented in Figure 5a. Most of the C_T residuals (330 over 381) were within a range of ± 18 µmol.kg^{-1} (1 σ). In contrast only few residuals (12 over 381) reached up to ± 50 µmol.kg^{-1} (1 σ). Applying the C_T algorithm to the testing dataset (Figure 5b), yields a mean residual of 1.48 ± 19.80 µmol.kg^{-1} (1 σ) which is close to the uncertainties of our C_T relationship. The high residuals observed in this study are consistent with the results of the optimal multiple linear regression performed by Lovato and Vichi (2015), where the largest discrepancies between observations and reconstructed data were detected at the surface layer with RMSE higher than ± 20 µmol.kg^{-1}.

Considering the high uncertainties of the C_T measurements, the seasonal variations and the anthropogenic forcing; Eq (2) presents the first parametrization for C_T in the Mediterranean Sea surface waters, with an RMSE of ± 14.3 µmol.kg^{-1} (1 σ) and a r^2 = 0.90 (Table 4, Eq 2).

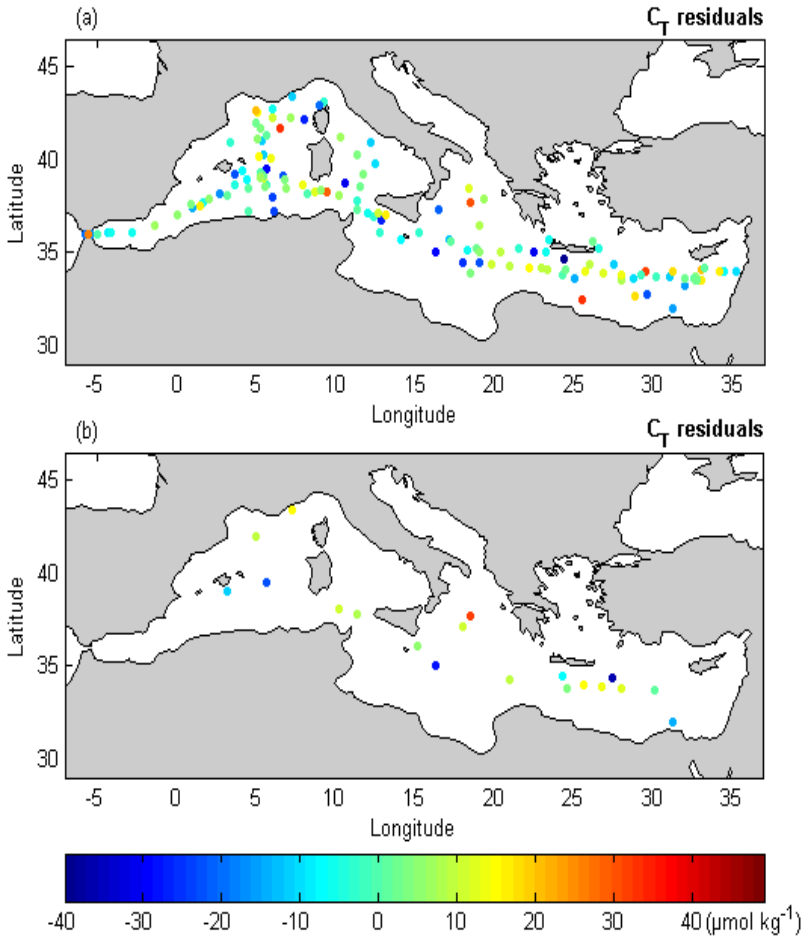

Figure 5. Comparison of the predicted C_T values from the C_T algorithm given in Table 1 - Eq (2) with measurements which are (a) included or (b) excluded when deriving the fit

3.3. Spatial and seasonal variability of A_T and C_T in surface waters

The ranges of the 2005-2012 average annual climatologies of the World Ocean Atlas 2013 (WOA13) are from 35.91 to 39.50 for S and from 16.50 ºC to 23.57 ºC for T (Locarnini *et al.*, 2013; Zweng *et al.*, 2013). However a wider range is observed for the seasonal climatologies, especially during the winter season where T ranges from 9.05 ºC to 18.43 ºC. The estimations of A_T and C_T in surface waters from Eq (1) and (2) respectively are only applicable in the appropriate ranges of $T > 13$ ºC and $36.3 < S < 39.65$. Hence the surface waters A_T and C_T concentrations were mapped only where T and S were within the validity range of Eq (1) and (2) respectively (Table 2 and 4). Excluding few near-shore areas and the influence of cold Atlantic Waters in winter, the ranges in which Eq (1) and Eq (2) can be applied are within those of the climatological products of T and S of the WOA13.

The mapped climatologies for 2005-2012 at 5m depth show a strong increase in the Eastward gradient for both A_T and C_T with the highest concentrations always found in the Eastern Mediterranean (Figure 6). The minimum values of 2400 µmol.kg^{-1} for A_T and 2100 µmol.kg^{-1} for C_T are found near the Strait of Gibraltar and the maximum values of 2650 µmol.kg^{-1} and 2300 µmol.kg^{-1} are found in the Levantine and Aegean sub-basin for A_T and C_T respectively.

The A_T parameterization of this study detects a clear signature of the alkaline waters entering through the Strait of Gibraltar that remains traceable to the Strait of Sicily as also shown by Cossarini *et al.* (2015). In the Eastern basin the positive balance between evaporation and precipitation contributes to the increasing surface A_T. Local effects from some coastal areas such as the Gulf of Gabes and riverine inputs from the Rhone and Po River are also detected.

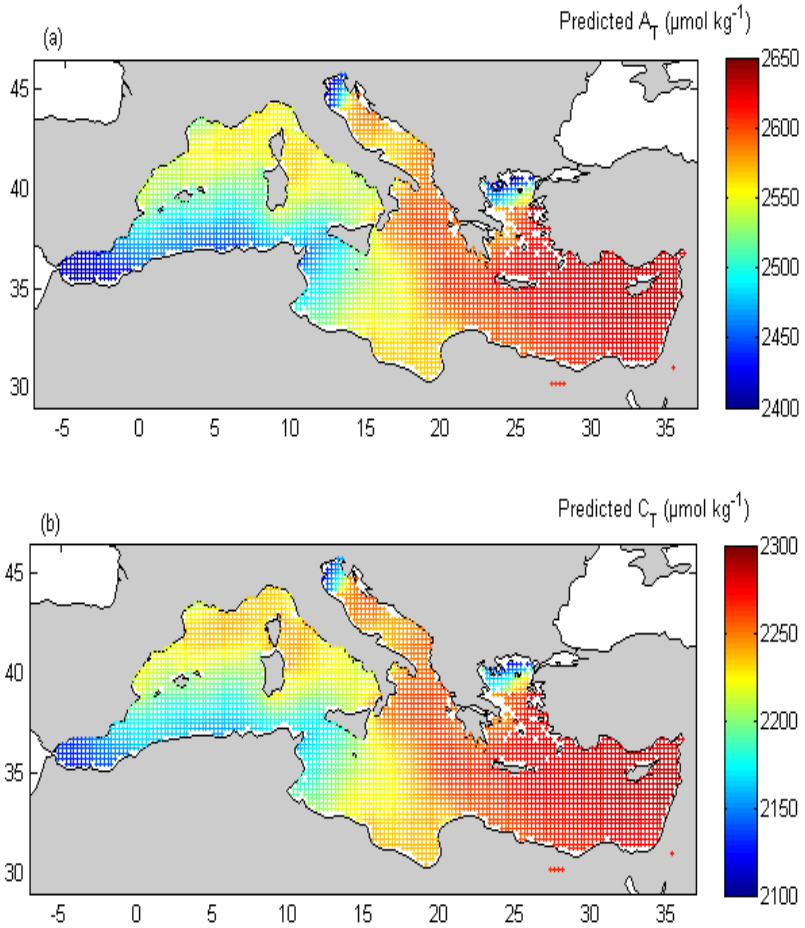

Figure 6. The seven years averages spatial variability of (a) surface A_T predicted from Eq (1) and (b) surface C_T predicted from Eq (2), applied to the 2005-2012 climatological fields of S and T from the WOA13

Our results for surface A_T have a similar spatial pattern and range as the annual climatology of Cossarini *et al.* (2015) which simulates surface A_T values from 2400 to 2700 µmol.kg^{-1}. The main difference is marked in the upper ends of the Adriatic and Aegean sub-basins where our algorithm predicts A_T values around 2400-2500 µmol.kg^{-1}, whereas the analysis of Cossarini *et al.* (2015) yields a maximum of 2700 µmol.kg^{-1} in these regions. Regressions in regions of river input indicate a negative correlation between alkalinity and salinity (Luchetta *et al.*, 2010); hence Eastern marginal seas are expected to have high A_T due to the freshwater inputs (Souvermezoglou *et al.*, 2010; Cantoni *et al.*, 2012). This shows the sensitivity of our algorithms to temperature and salinity especially in areas that are more influenced by continental inputs such as the Po River and inputs of the Dardanelle in the northern Adriatic and northern Aegean respectively (Figure 6a).

At the surface, the basin wide distributions of C_T are affected by physical processes and their gradient is similar to that of A_T (Figure 6b). The lowest C_T concentrations are found in the zone of the inflowing Atlantic water and increases toward the East in part due to evaporation as also shown by Schneider *et al.* (2010). Our results for surface C_T have a similar range as the optimal linear regression performed by Lovato and Vichi (2015) which estimates surface C_T values from 2180 to 2260 µmol.kg^{-1}. Moreover, the results show that the Mediterranean Sea is characterized by C_T values that are much higher (100–200 µmol.kg^{-1} higher) than those observed in the Atlantic Ocean at the same latitude (Key *et al.*, 2004).

As a consequence of uptake of atmospheric CO_2, the Eastward pCO_2 increase is parallel to that of C_T (D'Ortenzio *et al.*, 2008). For example the Ionian and Levantine sub-basin are characterized by a pCO_2 as high as 470 µatm (Bégovic, 2001), whereas the Algerian sub-basin is characterized by a much lower pCO_2 of 310 µatm (Calleja *et al.*, 2013). The high pCO_2 and C_T encountered in the Eastern basin make it a permanent source of atmospheric CO_2 (D'Ortenzio *et al.*, 2008; Taillandier *et al.*, 2012). Overall the Western basin has a lower surface C_T content than the Eastern basin which could be explained by the Eastward decrease of the Mediterranean Sea trophic gradient (Lazzari *et al.*, 2012). The higher rate of inorganic carbon consumption by photosynthesis in the Western basin can lead to the depletion of C_T in the surface waters, whereas the ultra-oligotrophic state in the Eastern basin can lead to a high remineralization rate that consumes oxygen and enriches surface waters with C_T (Moutin and Raimbault, 2002).

The magnitude of the seasonal variability between summer and winter for A_T and C_T is shown in Figure 7. Unlike the seven years averages, the seasonal climatological variations (2005-2012) of A_T have different spatial patterns than those of C_T. Overall the summer-winter time differences for A_T have an increasing Eastward gradient (Figure 7a). The largest magnitudes are marked in the Alboran Sea with differences reaching up to - 80 µmol.kg^{-1}; the negative difference implies that during the winter inflowing surface Atlantic water has higher A_T concentrations than in summer. Higher winter than summer time A_T concentrations are also observed in the Balearic, Ligurian and the South-Western Ionian sub-basins but with a less pronounced seasonality (~ -30 µmol.kg^{-1}). For these three sub-basins, the C_T has a higher summer-winter magnitude than A_T (~ -70 µmol.kg^{-1}). The winter cooling of surface waters increases their density and promotes a mixing with deeper water. Thus, the enrichment in winter time likely reflects the upwelling of deep waters that have accumulated A_T and C_T from the remineralization of organic matter, respiration and the dissolution of $CaCO_3$. The seasonality is more pronounced for C_T, which likely reflects the stronger response of C_T to biological processes than A_T (Takahashi *et al.*, 1993).

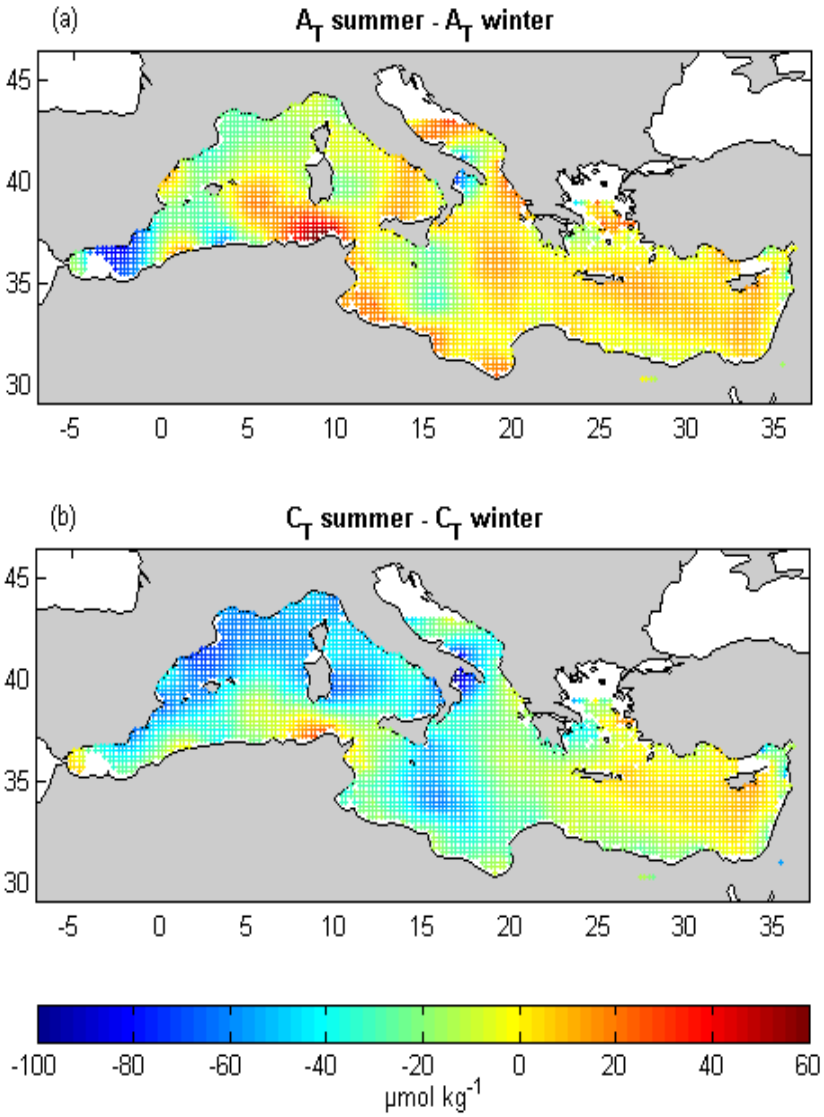

Figure 7. Distribution of the summer-winter differences of (a) surface A_T predicted from Eq (1) and (b) surface C_T predicted from Eq (2), applied to the 2005-2012 climatological fields of S and T from the WOA13

In the Algerian sub-basin and along the coasts of Tunisia and Libya, the seasonality is inversed with higher A_T and C_T concentrations prevailing in the summer. The African coast is an area of coastal downwelling during the winter season. However, during summer the coastal upwelling appears in response to turning of the wind near the coast toward the West (Bakun and Agostini, 2001). In general, the magnitude of the A_T seasonal variability is higher in summer than in winter for the Eastern basin and more particularly in the Ionian and Levantine sub-basins. During this season strong evaporation takes place and induce an increase of A_T concentrations (Schneider *et al.*, 2007). In the Eastern basin, the high evaporation during the summer has a smaller effect on the C_T, and magnitudes reach their maxima in the Levantine sub-basin (~ + 20 µmol.kg^{-1}). During winter time the Western basin and South East of Sicily appear to be dominated by higher C_T concentrations than the rest of the Eastern basin, where the summer C_T concentrations are prevailing (Figure 7b). During winter the high C_T concentrations that coincide with low SST in the Western basin, could

result from the deepening of the mixed layer and could be enhanced by the upwelling associated with the Tramontane-Mistral winds that blow from the southern of France and reach the Balearic Islands and the Spanish coast.

Summary

The A_T and C_T algorithms are derived from a compilation of 490 and 426 quality controlled surface measurements respectively, collected between 1999 and 2013 in the Mediterranean Sea. A second order polynomial relating A_T to both S and T yielded a lower RMSE (± 10.4 $\mu mol.kg^{-1}$) and a higher r^2 (0.96) than a linear fit deriving A_T from S alone. This confirmed the important contribution of temperature to the A_T variability. Hence, temperature should be included in future algorithms to help better constrain the surface A_T variations. The proposed second order polynomial had a lower RMSE than other studies when we applied their respective algorithms to the same training dataset. In this study we propose an improved and more global relationship to estimate the A_T spatial and temporal variations in the Mediterranean Sea surface waters.

The C_T parameterization is a first attempt to estimate the surface variations in the Mediterranean Sea. A third order polynomial is suggested to fit the C_T to T and S with a RMSE of ± 14.3 $\mu mol.kg^{-1}$. The biological contributions to the C_T variations were less pronounced than the physical processes. The contributions of to the physical processes and biology to the C_T variability were 90 and 10 % respectively. In terms of anthropogenic forcing, the C_T rate of increase of 0.99 $\mu mol.kg^{-1}.yr^{-1}$ was significantly lower than the uncertainty of the measurements than can reach ± 10 $\mu mol.kg^{-1}$ between different laboratories. Moreover the C_T concentrations were more affected by the seasonal variations than the increase of atmospheric CO_2.

We propose to use Equations (1) and (2) for the estimation of surface A_T and C_T in the Mediterranean Sea when salinity and temperature of the area are available and are in the appropriate ranges of the equations. However in the Eastern marginal seas especially the northern Adriatic and northern Aegean there is a need to develop a more specific equation that minimizes the errors in these areas. Hence, it is important to enrich the existing dataset by an extensive sampling program such as the Med-SHIP initiative (CIESM, 2012) in order to improve the modeling of the carbonate system over the whole Mediterranean Sea.

Acknowledgments

The authors would like to thank all parties that have contributed to the data provision in particular:

- The Sesame IT4 and Moose-GE cruise data were provided through SeaDataNet - Pan-European infrastructure for ocean and marine data management (http://www.seadatanet.org).

- The DYFAMED time series have been provided by the Oceanological Observatory of Villefranche-sur-Mer (L.Coppola). This project is funded by CNRS-INSU and ALLENVI through the MOOSE observing network".
- The Transmed cruise data were provided by Dr. Rivaro, P., Dr. Russo, A. and Dr. Kovacevic, V. The Transmed cruise is part of the VECTOR Project, funded by: the Ministry of Education, University and Research, the Ministry of Economy and Finance, the Ministry of the Environment and Protection of Natural Resources and the Ministry of Agriculture and Forestry with an Integrated Special Fund for Research (FISR).
- The MedSEA 2013 cruise data were provided by the University of Perpignan Via Domitia: 'Institut de Modélisation et d'Analyse en Géo-Environnements et Santé, ESPACE-DEV' (Goyet, C. and Hassoun, A.E.R.). This project was funded by the EC "Mediterranean Sea Acidification in a changing climate" project (MedSeA; grant agreement 265103).

Authors are also grateful to the National Council for Scientific Research (CNRS) in Lebanon for the PhD thesis scholarship granted to Miss Gemayel Elissar.

References

Álvarez, M., Sanleón-Bartolomé, H., Tanhua, T., Mintrop, L., Luchetta, A., Cantoni, C., Schroeder, K., Civitarese, G., 2014. The CO_2 system in the Mediterranean Sea: a basin wide perspective. Ocean Sci. 10 (1), 69-92. 10.5194/os-10-69-2014

Bakker, D.C.E., de Baar, H.J.W., de Jong, E., 1999. The dependence on temperature and salinity of dissolved inorganic carbon in East Atlantic surface waters. Mar. Chem. 65 (3–4), 263-280. http://dx.doi.org/10.1016/S0304-4203(99)00017-1

Bakun, A., Agostini, V.N., 2001. Seasonal patterns of wind-induced upwelling/downwelling in the Mediterranean Sea. Sci. Mar. 65 (3), 243-257.

Bates, N.R., 2007. Interannual variability of the oceanic CO_2 sink in the subtropical gyre of the North Atlantic Ocean over the last 2 decades. J. Geophys. Res. 112 (C9), C09013. 10.1029/2006jc003759

Bates, N.R., Pequignet, A.C., Sabine, C.L., 2006. Ocean carbon cycling in the Indian Ocean: 1. Spatiotemporal variability of inorganic carbon and air-sea CO_2 gas exchange. Global Biogeochem. Cycles 20 (3), GB3020.

Bégovic, M., 2001. Contribution á l'étude du système des carbonates en Méditerranée. Distribution et variation spatio-temporelle de la pression partielle de CO_2 dans les eaux superficielles du bassin Liguro-Provencal, Thèse, Université Paris 6.

Bégovic, M., Copin-Montégut, C., 2002. Processes controlling annual variations in the partial pressure of CO_2 in surface waters of the central northwestern Mediterranean Sea (Dyfamed site). Deep Sea Res. Part II Top. Stud. Oceanogr. 49 (11), 2031-2047. http://dx.doi.org/10.1016/S0967-0645(02)00026-7

Bégovic, M., Copin, C., 2013. Alkalinity and pH measurements on water bottle samples during THALASSA cruise PROSOPE. doi:10.1594/PANGAEA.805265

Bockmon, E.E., Dickson, A.G., 2015. An inter-laboratory comparison assessing the quality of seawater carbon dioxide measurements. Mar. Chem. 171 (0), 36-43. http://dx.doi.org/10.1016/j.marchem.2015.02.002

Breiman, L., 1996. Stacked regressions. Mach. Learn. 24 (1), 49-64. 10.1007/bf00117832

Calleja, M.L., Duarte, C.M., Álvarez, M., Vaquer-Sunyer, R., Agustí, S., Herndl, G.J., 2013. Prevalence of strong vertical CO_2 and O_2 variability in the top meters of the ocean. Global Biogeochem. Cycles 27 (3), 941-949. 10.1002/gbc.20081

Cantoni, C., Luchetta, A., Celio, M., Cozzi, S., Raicich, F., Catalano, G., 2012. Carbonate system variability in the Gulf of Trieste (North Adriatic Sea). Estuar. Coast. Shelf Sci. 115 (0), 51-62. http://dx.doi.org/10.1016/j.ecss.2012.07.006

CIESM, 2012. Designing Med-SHIP: a Program for repeated oceanographic surveys. CIESM. N°43 CIESM Workshop Monographs, 164

Copin-Montégut, C., 1993. Alkalinity and carbon budgets in the Mediterranean Sea. Global Biogeochem. Cycles 7 (4), 915-925. 10.1029/93gb01826

Copin-Montégut, C., Bégovic, M., 2002. Distributions of carbonate properties and oxygen along the water column (0–2000m) in the central part of the NW Mediterranean Sea (Dyfamed site): influence of winter vertical mixing on air–sea CO_2 and O_2 exchanges. Deep Sea Res. Part II Top. Stud. Oceanogr. 49 (11), 2049-2066. http://dx.doi.org/10.1016/S0967-0645(02)00027-9

Cossarini, G., Lazzari, P., Solidoro, C., 2015. Spatiotemporal variability of alkalinity in the Mediterranean Sea. Biogeosciences 12 (6), 1647-1658. 10.5194/bg-12-1647-2015

D'Ortenzio, F., Antoine, D., Marullo, S., 2008. Satellite-driven modeling of the upper ocean mixed layer and air–sea CO_2 flux in the Mediterranean Sea. Deep Sea Res. Part I Oceanogr. Res. Pap. 55 (4), 405-434. http://dx.doi.org/10.1016/j.dsr.2007.12.008

Goyet, C., Davis, D., 1997. Estimation of total CO_2 concentration throughout the water column. Deep Sea Res. Part I Oceanogr. Res. Pap. 44 (5), 859-877. http://dx.doi.org/10.1016/S0967-0637(96)00111-2

Goyet, C., Hassoun, A.E.R., Gemayel, E., 2015. Carbonate system during the May 2013 MedSeA cruise. Pangaea. Dataset #841933 (DOI registration in progress)

Hassoun, A.E.R., Gemayel, E., Krasakopoulou, E., Goyet, C., Abboud-Abi Saab, M., Guglielmi, V., Touratier, F., Falco, C., 2015a. Acidification of the Mediterranean Sea from anthropogenic carbon penetration. Deep Sea Res. Part I Oceanogr. Res. Pap. 102 (0), 1-15. http://dx.doi.org/10.1016/j.dsr.2015.04.005

Hassoun, A.E.R., Gemayel, E., Krasakopoulou, E., Goyet, C., Abboud-Abi Saab, M., Ziveri, P., Touratier, F., Guglielmi, V., Falco, C., 2015b. Modeling of the total alkalinity and the total inorganic carbon in the Mediterranean Sea. J. Water Resource Ocean Sci. 4 (1), 24-32. doi: 10.11648/j.wros.20150401.14

Hood, E.M., Merlivat, L., 2001. Annual to interannual variations of fCO_2 in the northwestern Mediterranean Sea: Results from hourly measurements made by CARIOCA buoys, 1995-1997. J. Mar. Res. 59 (1), 113-131. http://dx.doi.org/10.1357/002224001321237399

Huertas, E., 2007a. Hydrochemistry measured on water bottle samples during Al Amir Moulay Abdallah cruise CARBOGIB-2. Unidad de Tecnología Marina - Consejo Superior de Investigaciones Científicas. doi:10.1594/PANGAEA.618899

Huertas, E., 2007b. Hydrochemistry measured on water bottle samples during Al Amir Moulay Abdallah cruise CARBOGIB-3. Unidad de Tecnología Marina - Consejo Superior de Investigaciones Científicas. doi:10.1594/PANGAEA.618898

Huertas, E., 2007c. Hydrochemistry measured on water bottle samples during Al Amir Moulay Abdallah cruise CARBOGIB-4. Unidad de Tecnología Marina - Consejo Superior de Investigaciones Científicas. doi:10.1594/PANGAEA.618897

Huertas, E., 2007d. Hydrochemistry measured on water bottle samples during Al Amir Moulay Abdallah cruise CARBOGIB-5. Unidad de Tecnología Marina - Consejo Superior de Investigaciones Científicas. doi:10.1594/PANGAEA.618896

Huertas, E., 2007e. Hydrochemistry measured on water bottle samples during Al Amir Moulay Abdallah cruise CARBOGIB-6. Unidad de Tecnología Marina - Consejo Superior de Investigaciones Científicas. doi:10.1594/PANGAEA.618895

Huertas, E., 2007f. Hydrochemistry measured on water bottle samples during Garcia del Cid cruise GIFT-1. Unidad de Tecnología Marina - Consejo Superior de Investigaciones Científicas. doi:10.1594/PANGAEA.618916

Huertas, E., 2007g. Hydrochemistry measured on water bottle samples during Garcia del Cid cruise GIFT-2. Unidad de Tecnología Marina - Consejo Superior de Investigaciones Científicas. doi:10.1594/PANGAEA.618915

Huertas, E., 2007h. Hydrochemistry measured on water bottle samples during Garcia del Cid cruise GIFT-3. Unidad de Tecnología Marina - Consejo Superior de Investigaciones Científicas. doi:10.1594/PANGAEA.618914

Hydes, D., Jiang, Z., Hartman, M.C., Campbell, J.M., Hartman, S.E., Pagnani, M.R., B.A., K.-G., 2012. Surface DIC and TALK measurements along the M/V Pacific Celebes VOS Line during the 2007-2012 cruises. http://cdiac.ornl.gov/ftp/oceans/VOS_Pacific_Celebes_line/. Carbon Dioxide Information Analysis Center, Oak Ridge National Laboratory, US Department of Energy, Oak Ridge, Tennessee. doi: 10.3334/CDIAC/OTG.VOS_PC_2007-2012.

Ishii, M., Saito, S., Tokieda, T., Kawano, T., Matsumoto, K., Inoue, H.Y., 2004. Variability of surface layer CO_2 parameters in the Western and Central Equatorial Pacific. In: Shiyomi M., K.H., Koizumi H., Tsuda A., Awaya Y. (Ed.), Global Environmental Change in the Ocean and on Land. TERRAPUB, Tokyo.

Keeling, R.F., Najjar, R.P., Bender, M.L., Tans, P.P., 1993. What atmospheric oxygen measurements can tell us about the global carbon cycle. Global Biogeochem. Cycles 7 (1), 37-67. 10.1029/92gb02733

Key, R.M., Kozyr, A., Sabine, C.L., Lee, K., Wanninkhof, R., Bullister, J.L., Feely, R.A., Millero, F.J., Mordy, C., Peng, T.H., 2004. A global ocean carbon climatology: Results from Global Data Analysis Project (GLODAP). Global Biogeochem. Cycles 18 (4), GB4031. 10.1029/2004gb002247

Koeve, W., Duteil, O., Oschlies, A., Kähler, P., Segschneider, J., 2014. Methods to evaluate $CaCO_3$ cycle modules in coupled global biogeochemical ocean models. Geosci. Model. Dev. 7 (5), 2393-2408. 10.5194/gmd-7-2393-2014

Koffi, U., Lefèvre, N., Kouadio, G., Boutin, J., 2010. Surface CO_2 parameters and air–sea CO_2 flux distribution in the Eastern Equatorial Atlantic Ocean. J. Mar. Syst. 82 (3), 135-144. http://dx.doi.org/10.1016/j.jmarsys.2010.04.010

Krasakopoulou, E., Souvermezoglou, E., Goyet, C., 2011. Anthropogenic CO_2 fluxes in the Otranto Strait (E. Mediterranean) in February 1995. Deep Sea Res. Part I Oceanogr. Res. Pap. 58 (11), 1103-1114. http://dx.doi.org/10.1016/j.dsr.2011.08.008

Lazzari, P., Solidoro, C., Ibello, V., Salon, S., Teruzzi, A., Béranger, K., Colella, S., Crise, A., 2012. Seasonal and inter-annual variability of plankton chlorophyll and primary production in the Mediterranean Sea: a modelling approach. Biogeosciences 9 (1), 217-233. 10.5194/bg-9-217-2012

Lee, K., Sabine, C.L., Tanhua, T., Kim, T.-W., Feely, R.A., Kim, H.-C., 2011. Roles of marginal seas in absorbing and storing fossil fuel CO_2. Energy Environ. Sci. 4 (4), 1133-1146. 10.1039/c0ee00663g

Lee, K., Tong, L.T., Millero, F.J., Sabine, C.L., Dickson, A.G., Goyet, C., Park, G.-H., Wanninkhof, R., Feely, R.A., Key, R.M., 2006. Global relationships of total alkalinity with salinity and temperature in surface waters of the world's oceans. Geophys. Res. Lett. 33 (19), L19605. 10.1029/2006gl027207

Lee, K., Wanninkhof, R., Feely, R.A., Millero, F.J., Peng, T.-H., 2000. Global relationships of total inorganic carbon with temperature and nitrate in surface seawater. Global Biogeochem. Cycles 14 (3), 979-994. 10.1029/1998gb001087

Locarnini, R.A., Mishonov, A.V., Antonov, J.I., Boyer, T.P., Garcia, H.E., Baranova, O.K., Zweng, M.M., Paver, C.R., Reagan, J.R., Johnson, D.R., Hamilton, M., Seidov, D., 2013. World Ocean Atlas 2013, Volume 1: Temperature. NOAA Atlas NESDIS 73. 40

Louanchi, F., Boudjakdji, M., Nacef, L., 2009. Decadal changes in surface carbon dioxide and related variables in the Mediterranean Sea as inferred from a coupled data-diagnostic model approach. ICES J. Mar. Sci. 66 (7), 1538-1546. 10.1093/icesjms/fsp049

Lovato, T., Vichi, M., 2015. An objective reconstruction of the Mediterranean sea carbonate system. Deep Sea Res. Part I Oceanogr. Res. Pap. 98 (0), 21-30. http://dx.doi.org/10.1016/j.dsr.2014.11.018

Luchetta, A., Cantoni, C., Catalano, G., 2010. New observations of CO_2 induced acidification in the northern Adriatic Sea over the last quarter century. Chem. Ecol. 26 (sup1), 1-17. 10.1080/02757541003627688

McNeil, B.I., Metzl, N., Key, R.M., Matear, R.J., Corbiere, A., 2007. An empirical estimate of the Southern Ocean air-sea CO_2 flux. Global Biogeochem. Cycles 21 (3), GB3011. 10.1029/2007gb002991

Medar-Group, 2002. MEDATLAS 2002. Mediterranean and Black Sea database of temperature, salinity and biochemical parameters. Climatological Atlas.

Millero, F.J., 2007. The Marine inorganic carbon cycle. Chem. Rev. 107 (2), 308-341. 10.1021/cr0503557

Millero, F.J., Lee, K., Roche, M., 1998. Distribution of alkalinity in the surface waters of the major oceans. Mar. Chem. 60 (1–2), 111-130. http://dx.doi.org/10.1016/S0304-4203(97)00084-4

Moutin, T., Raimbault, P., 2002. Primary production, carbon export and nutrients availability in Western and Eastern Mediterranean Sea in early summer 1996 (MINOS cruise). J. Mar. Syst. 33–34 (0), 273-288. http://dx.doi.org/10.1016/S0924-7963(02)00062-3

Omta, A.W., Dutkiewicz, S., Follows, M.J., 2011. Dependence of the ocean-atmosphere partitioning of carbon on temperature and alkalinity. Global Biogeochem. Cycles 25 (1), GB1003. 10.1029/2010gb003839

Perez, F.F., Rios, A.F., Pelegri, J.L., de la Paz, M., Alonso, F., Royo, E., Velo, A., Garcia-Ibanez, M., Padin, X.A., 2013. Carbon Data Obtained During the R/V Hesperides Cruise in the Atlantic Ocean on CLIVAR Repeat Hydrography Section A17, FICARAM XV, (March 20 - May 2, 2013). http://cdiac.ornl.gov/ftp/oceans/CLIVAR/A17_FICARAM_XV_2013/. Carbon Dioxide Information Analysis Center, Oak Ridge National Laboratory, US Department of Energy, Oak Ridge, Tennessee. doi: 10.3334/CDIAC/OTG.CLIVAR_FICARAM_XV

Poisson, A., Metzl, N., Brunet, C., Schauer, B., Bres, B., Ruiz-Pino, D., Louanchi, F., 1993. Variability of sources and sinks of CO_2 in the western Indian and southern oceans during the year 1991. J. Geophys. Res. 98 (C12), 22759-22778. 10.1029/93jc02501

Rivaro, P., Messa, R., Massolo, S., Frache, R., 2010. Distributions of carbonate properties along the water column in the Mediterranean Sea: Spatial and temporal variations. Mar. Chem. 121 (1–4), 236-245. http://dx.doi.org/10.1016/j.marchem.2010.05.003

Rödenbeck, C., Keeling, R.F., Bakker, D.C.E., Metzl, N., Olsen, A., Sabine, C., Heimann, M., 2013. Global surface-ocean pCO_2 and sea–air CO_2 flux variability from an observation-driven ocean mixed-layer scheme. Ocean Sci. 9 (2), 193-216. 10.5194/os-9-193-2013

Rohling, E.J., Abu-Zied, R.H., Casford, J.S.L., Hayes, A., Hoogakker, B.A.A., 2009. The marine environment: Present and past. In: Woodward, J.C. (Ed.), The physical geography of the Mediterranean. Oxford University Press, pp. 33-67.

Sabine, C.L., Feely, R.A., Gruber, N., Key, R.M., Lee, K., Bullister, J.L., Wanninkhof, R., Wong, C.S., Wallace, D.W.R., Tilbrook, B., Millero, F.J., Peng, T.-H., Kozyr, A., Ono, T., Rios, A.F., 2004. The oceanic sink for anthropogenic CO_2. Science 305 (5682), 367-371. 10.1126/science.1097403

Santana-Casiano, J.M., Gonzalez-Davila, M., Laglera, L.M., 2002. The carbon dioxide system in the Strait of Gibraltar. Deep Sea Res. Part II Top. Stud. Oceanogr. 49 (19), 4145-4161. http://dx.doi.org/10.1016/S0967-0645(02)00147-9

Sasse, T.P., McNeil, B.I., Abramowitz, G., 2013. A novel method for diagnosing seasonal to inter-annual surface ocean carbon dynamics from bottle data using neural networks. Biogeosciences 10 (6), 4319-4340. 10.5194/bg-10-4319-2013

Schneider, A., Tanhua, T., Körtzinger, A., Wallace, D.W.R., 2010. High anthropogenic carbon content in the Eastern Mediterranean. J. Geophys. Res. 115 (C12), C12050. 10.1029/2010jc006171

Schneider, A., Wallace, D.W.R., Körtzinger, A., 2007. Alkalinity of the Mediterranean Sea. Geophys. Res. Lett. 34 (15), L15608. 10.1029/2006gl028842

Schneider, B., Roether, W., 2007. Meteor 06MT20011018 cruise data from the 2001 cruises, CARINA Data Set. http://cdiac.ornl.gov/ftp/oceans/CARINA/Meteor/06MT512/. Carbon Dioxide Information Analysis Center, Oak Ridge National Laboratory, US Department of Energy, Oak Ridge, Tennessee. doi: 10.3334/CDIAC/otg.CARINA 06MT20011018.

Souvermezoglou, E., Krasakopoulou, E., Goyet, C., 2010. Total inorganic carbon and total alkalinity distribution in the Aegean Sea. CIESM. Rapp. Comm. int. Mer Médit. 39, 312

Stone, M., 1974. Cross validatory choice and assessment of statistical predictions. J. R. Stat. Soc. Series B Stat. Methodol. 36 (2), 111-147.

Taillandier, V., D'Ortenzio, F., Antoine, D., 2012. Carbon fluxes in the mixed layer of the Mediterranean Sea in the 1980s and the 2000s. Deep Sea Res. Part I Oceanogr. Res. Pap. 65 (0), 73-84. http://dx.doi.org/10.1016/j.dsr.2012.03.004

Takahashi, T., Olafsson, J., Goddard, J.G., Chipman, D.W., Sutherland, S.C., 1993. Seasonal variation of CO_2 and nutrients in the high-latitude surface oceans: A comparative study. Global Biogeochem. Cycles 7 (4), 843-878. 10.1029/93gb02263

Takahashi, T., Sutherland, S.C., Chipman, D.W., Goddard, J.G., Ho, C., Newberger, T., Sweeney, C., Munro, D.R., 2014. Climatological distributions of pH, pCO_2, total CO_2, alkalinity, and $CaCO_3$ saturation in the global surface ocean, and temporal changes at selected locations. Mar. Chem. 164 (0), 95-125. http://dx.doi.org/10.1016/j.marchem.2014.06.004

Takahashi, T., Sutherland, S.C., Wanninkhof, R., Sweeney, C., Feely, R.A., Chipman, D.W., Hales, B., Friederich, G., Chavez, F., Sabine, C., Watson, A., Bakker, D.C.E., Schuster, U., Metzl, N., Yoshikawa-Inoue, H., Ishii, M., Midorikawa, T., Nojiri, Y., Körtzinger, A., Steinhoff, T., Hoppema, M., Olafsson, J., Arnarson, T.S., Tilbrook, B., Johannessen, T., Olsen, A., Bellerby, R., Wong, C.S., Delille, B., Bates, N.R., de Baar, H.J.W., 2009. Climatological mean and decadal change in surface ocean pCO_2, and net sea–air CO_2 flux over the global oceans. Deep Sea Res. Part II Top. Stud. Oceanogr. 56 (8–10), 554-577. http://dx.doi.org/10.1016/j.dsr2.2008.12.009

Tanhua, T., Alvarez, M., Mintrop, L., 2012. Carbon dioxide, hydrographic, and chemical data obtained during the R/V Meteor MT84_3 Mediterranean Sea cruise (April 5. - April 28, 2011). http://cdiac.ornl.gov/ftp/oceans/CLIVAR/Met_84_3_Med_Sea/. Carbon Dioxide

Information Analysis Center, Oak Ridge National Laboratory, US Department of Energy, Oak Ridge, Tennessee. doi: 10.3334/CDIAC/OTG.CLIVAR_06MT20110405.

Touratier, F., Goyet, C., 2009. Decadal evolution of anthropogenic CO_2 in the northwestern Mediterranean Sea from the mid-1990s to the mid-2000s. Deep Sea Res. Part I Oceanogr. Res. Pap. 56 (10), 1708-1716. http://dx.doi.org/10.1016/j.dsr.2009.05.015

Touratier, F., Goyet, C., 2011. Impact of the Eastern Mediterranean Transient on the distribution of anthropogenic CO_2 and first estimate of acidification for the Mediterranean Sea. Deep Sea Res. Part I Oceanogr. Res. Pap. 58 (1), 1-15. http://dx.doi.org/10.1016/j.dsr.2010.10.002

Touratier, F., Guglielmi, V., Goyet, C., Prieur, L., Pujo-Pay, M., Conan, P., Falco, C., 2012. Distributions of the carbonate system properties, anthropogenic CO_2, and acidification during the 2008 BOUM cruise (Mediterranean Sea). Biogeosci. Discuss. 9 (3), 2709-2753. 10.5194/bgd-9-2709-2012

Wanninkhof, R., Park, G.H., Takahashi, T., Sweeney, C., Feely, R., Nojiri, Y., Gruber, N., Doney, S.C., McKinley, G.A., Lenton, A., Le Quéré, C., Heinze, C., Schwinger, J., Graven, H., Khatiwala, S., 2013. Global ocean carbon uptake: magnitude, variability and trends. Biogeosciences 10 (3), 1983-2000. 10.5194/bg-10-1983-2013

Watson, A., Orr, J., 2003. Carbon Dioxide Fluxes in the Global Ocean. In: Fasham, M.R. (Ed.), Ocean Biogeochemistry. Springer Berlin Heidelberg, pp. 123-143. 10.1007/978-3-642-55844-3_6

Zweng, M.M., Reagan, J.R., Antonov, J.I., Locarnini, R.A., Mishonov, A.V., Boyer, T.P., Garcia, H.E., Baranova, O.K., Johnson, D.R., Seidov, D., Biddle, M.M., 2013. World Ocean Atlas 2013, Volume 2: Salinity. In: Levitus, S., Ed., Mishonov, A., Technical Ed (Eds.). NOAA Atlas NESDIS 74, p. 39.

Article VI: Acidification of the Mediterranean Sea from anthropogenic carbon penetration

Hassoun, A.E.R., **Gemayel, E.**, et al. (2015)

Deep Sea Research Part I Oceanographic Research Papers, 102 (0), 1-15. http://dx.doi.org/10.1016/j.dsr.2015.04.005

Acidification of the Mediterranean Sea from anthropogenic carbon penetration[6]

Abed El Rahman HASSOUN[1,2], Elissar GEMAYEL[1,2,3], Evangelia KRASAKOPOULOU[4], Catherine GOYET[2,3], Marie ABBOUD-ABI SAAB[1], Véronique GUGLIELMI[2,3], Franck TOURATIER[2,3], Cédric FALCO[2,3]

[1]National Council for Scientific Research, National Center for Marine Sciences, P.O.Box 534, Batroun, Lebanon
[2]IMAGES_ESPACE-DEV, Université de Perpignan Via Domitia, 52 avenue Paul Alduy, 66860 Perpignan Cedex 9, France
[3]ESPACE-DEV, UG UA UR UM IRD, Maison de la télédétection, 500 rue Jean-François Breton, 34093 Montpellier Cedex 5, France
[4]University of the Aegean, Department of Marine Sciences, University Hill, Mytilene 81100, Greece.

Abstract

This study presents an estimation of the anthropogenic CO_2 (C_{ANT}) concentrations and acidification ($\Delta pH = pH_{2013} - pH_{pre\text{-}industrial}$) in the Mediterranean Sea, based upon hydrographic and carbonate chemistry data collected during the May 2013 MedSeA cruise. The concentrations of C_{ANT} were calculated using the composite tracer TrOCA. The C_{ANT} distribution shows that the most invaded waters (> 60 µmol kg^{-1}) are those of the intermediate and deep layers in the Alboran, Liguro- and Algero-Provencal Sub-basins in the Western basin, and in the Adriatic Sub-basin in the Eastern basin. Whereas the areas containing the lowest C_{ANT} concentrations are the deep layers of the Eastern basin, especially those of the Ionian Sub-basin, and those of the northern Tyrrhenian Sub-basin in the Western basin. The acidification level in the Mediterranean Sea reflects the excessive increase of atmospheric CO_2 and therefore the invasion of the sea by C_{ANT}. This acidification varies between -0.055 and -0.156 pH unit and it indicates that all Mediterranean Sea waters are already acidified, especially those of the Western basin where ΔpH is rarely less than -0.1 pH unit. Both C_{ANT} concentrations and acidification levels are closely linked to the presence and history of the different water masses in the intermediate and deep layers of the Mediterranean basins. Despite the high acidification levels, both Mediterranean basins are still highly supersaturated in calcium carbonate minerals.

Keywords: Anthropogenic CO_2; acidification; carbonate system; Mediterranean Sea.

1. Introduction

The Mediterranean Sea is a land-locked relatively small marine ecosystem that represents approximately 0.8% of the world's ocean surface area (EEA, 2002 ; UNEP/MAP-Plan Bleu, 2009). It is connected to the Atlantic Ocean via the Strait of Gibraltar ; it receives surface Atlantic waters (AW) flowing Eastwards and exports intermediate waters to the Atlantic contributing thus to the global overturning circulation (Bergamasco and Malanotte-Rizzoli,

[6] Authors preprint. Deep Sea Research Part I: Oceanographic Research Papers, 102, Acidification of the Mediterranean Sea from anthropogenic carbon penetration, 15 p, Copyright (2015), License number 3640261058167, with permission from Elsevier (Annexes)

2010). The Mediterranean Sea is considered a small-scale ocean with high environmental variability and steep physicochemical gradients within a relatively limited region (Béthoux *et al.*, 1999). The circulation is characterized by the presence of sub-basin gyres, intense mesoscale activity and a strong seasonal variability related to highly variable atmospheric forcing strongly affected by orographic constraints (Malanotte-Rizzoli *et al.*, 1997 ; Millot, 1999).

The Mediterranean Sea is very special in terms of CO_2 dynamics, global carbon cycle and anthropogenic CO_2 drawdown and storage. Its waters are characterized by high alkalinity (~ 2600 µmol kg^{-1} ; Schneider *et al.*, 2007 ; Hassoun *et al.*, 2015b) compared to other oceans. In addition, the Mediterranean waters are slightly more basic (less than a quarter of a pH unit) than the Atlantic waters at corresponding depths (Millero *et al.*, 1979 ; CARINA project data collection—version 1.2, http://odv.awi.de/en/data/ocean/carina_bottle_data/). Thus, through the simple acid-base reaction, CO_2 is attracted more easily in a slightly more basic seawater than in a slightly less basic seawater. Moreover, its warm and high alkalinity waters, characterized thus by low Revelle factor, are prone to absorb CO_2 from the atmosphere and be transported to the interior by the active overturning circulation (Álvarez *et al.*, 2011). The anthropogenic CO_2 inventory for the Mediterranean has been estimated to be 1.7 PgC, thus indicating that this marginal sea has higher C_{ANT} concentrations than the global average, mainly determined by the surprisingly high anthropogenic carbon content of the Eastern Mediterranean Sea (Sabine and Tanhua, 2010 ; Schneider *et al.*, 2010). However the role of marginal seas (like the Mediterranean) as a sink of atmospheric CO_2 has been understudied because they have been considered to play a minor role in absorbing and storing anthropogenic CO_2 due to their small surface area (Lee *et al.*, 2011). Several scientists from various research institutes have recently measured the carbonate system properties (pH ; total alkalinity, A_T ; total dissolved inorganic carbon, C_T ; and partial pressure of CO_2, pCO_2) in the Mediterranean Sea. The majority of these studies have been performed in the Western Mediterranean basin (Alekin, 1972 ; Millero *et al.*, 1979 ; Copin-Montégut, 1993 ; Bégovic and Copin-Montégut, 2002 ; Copin-Montégut and Bégovic, 2002 ; Copin-Montégut *et al.*, 2004 ; De Carlo *et al.*, 2013), in the Catalano-Balearic region (Delgado and Estrada, 1994), in the Strait of Gibraltar and the Gulf of Cadiz (Dafner *et al.*, 2001 ; Santana-Casiano *et al.*, 2002 ; Huertas *et al.*, 2006 ; De la Paz *et al.*, 2008 ; De la Paz *et al.*, 2009 ; Ribas-Ribas *et al.*, 2011). Whereas fewer ones have been achieved in the other Mediterranean Sea areas : Sicily strait (Chernyakova, 1976) ; Eastern basin (Schneider *et al.*, 2007 ; Pujo-Pay *et al.*, 2011). Moreover, few attempts have been dedicated to estimate the C_{ANT} penetration in the Mediterranean and the C_{ANT} exchanges with the Atlantic (Aït-Ameur and Goyet, 2006 ; Huertas *et al.*, 2009 ; Flecha *et al.*, 2012). Data attained in the Strait of Gibraltar and the Gulf of Cadiz by the abovementioned studies have indicated that a net export of total inorganic carbon occurs from the Mediterranean to the Atlantic, while there have been contradicting results about the sign of the net C_{ANT} that is exchanged between both basins with the exchange being markedly sensitive to the interface definition between the inflowing and the outflowing water bodies and the method considered for C_{ANT} estimation. However, the role of the Mediterranean outflowing waters as an important contributor of the North Atlantic C_{ANT} inventories has been well recognized (Ríos *et al.*, 2001 ; Álvarez *et al.*, 2005 ; Aït-

Ameur and Goyet, 2006 ; Huertas *et al.*, 2009 ; Flecha *et al.*, 2012). To date, studies devoted to the estimation of the C_{ANT} in the Eastern basin are still very scarce (Schneider *et al.*, 2010 ; Rivaro *et al.*, 2010 ; Krasakopoulou *et al.*, 2011).

In order to quantify the ocean capacity to sequester C_{ANT} as well as the increase of acidification, the C_{ANT} should be accurately known. Since anthropogenic CO_2 cannot be measured directly, as it cannot be chemically discriminated from the bulk of dissolved inorganic carbon, several independent approaches for its indirect estimation have been developed. Using a common and a high quality dataset available for the Atlantic, the Antarctic, and the Arctic Oceans, Vázquez Rodríguez *et al.* (2009) performed an inter-comparison exercise of the C_{ANT} concentrations estimated by the five most recent models (ΔC^*, Gruber *et al.*, 1996 ; C^0_{IPSL}, Lo Monaco *et al.*, 2005 ; TTD, Waugh *et al.*, 2006 ; TrOCA, Touratier *et al.*, 2007 ; and the φC^0_T, Vázquez Rodríguez *et al.*, 2009). They concluded that all methods give similar spatial distributions and magnitude of C_{ANT} between latitude 60°N–40°S, and that some differences are found among the methods in the Southern Ocean and the Nordic Seas. The C_{ANT} total inventories computed with the TrOCA approach for the whole Atlantic Ocean is 51 PgC ; this clearly shows that this approach does not over- or underestimate C_{ANT} since it is well in the range of the inventories computed by the four other methods (from 47 to 67 PgC). Several studies have estimated the C_{ANT} using the TrOCA approach in the Mediterranean Sea (Touratier and Goyet, 2011), in the Otranto Strait (Krasakopoulou *et al.*, 2011), in the Bay of Biscay (Castaño Carrera *et al.*, 2012) and in the Iberian Sub-basin (Fajar *et al.*, 2012). The differences between the C_{ANT} estimations from the φC^0_T method and those from the TrOCA method are very small (-0.77 ± 4.4 µmol kg^{-1}, n = 301), and both C_{ANT} estimates present the same spatial variations (Castaño Carrera *et al.*, 2012). Thus, these recent comparisons testify that the TrOCA method provides similar spatial variations as other models and a reasonable upper limit of C_{ANT} estimates (within the uncertainty of the results). Therefore, here this simple and accurate method is chosen to estimate the C_{ANT}.

Although there are already some quantifications of the C_{ANT} in the Mediterranean Sea and some estimations of the acidification evolution in its waters (Touratier and Goyet, 2009 ; Rivaro *et al.*, 2010 ; Schneider *et al.*, 2010 ; Touratier and Goyet 2011 ; Palmiéri *et al.*, 2015), there is still a lack of data to get a complete picture of the evolution of the C_{ANT} and the acidification in this semi-enclosed sea. Thus, the present study has the following objectives: 1 - to quantify the C_{ANT} and to examine its trends in the Mediterranean Sea based on the new data of the MedSeA (Mediterranean Sea Acidification In A Changing Climate) cruise collected during May 2013 ; 2 - to characterize the different Mediterranean water masses based on the C_{ANT}, and 3 - to assess the acidification state of the Mediterranean waters.

1.1. Oceanographic features of the Mediterranean Sea

At the Strait of Gibraltar, the AW inflows at the surface layer of the Mediterranean Sea. This water mass flows Eastwards at shallow depth into the Tyrrhenian Sub-basin, then into the

Eastern Mediterranean basin via the Strait of Sicily. The salinity of the AW increases along its pathway from 36.5 to > 38 due to net evaporation and is then described as Modified Atlantic Water (MAW ; Wüst, 1961). The surface water in the Western Mediterranean basin is supplied by less dense AW through the Strait of Gibraltar (Stöven and Tanhua, 2014).

The heat loss of the MAW during winter time along with evaporation leads to a sufficient increase of density to form the Levantine Intermediate Water (LIW) in the Eastern Mediterranean basin (Wüst, 1961 ; Brasseur *et al.,* 1996). The main volume of the LIW flows back Westwards over the shallow sill between Sicily and Tunisia entering the Tyrrhenian Sub-basin along the continental slope of Italy forming a maximum-salinity layer in a few hundred meters depth (Wüst, 1961). Moreover, the mid-depth waters are also fed by the warm and saline waters (Cretan Intermediate Waters, CIW) formed in the Aegean Sub-basin. These waters outflow through the Western Cretan Straits and circulate in the major part of the intermediate layers of the Ionian Sub-basin. The LIW is a dominant water mass which circulates through both the Eastern and Western basins and is the principal component of the efflux from Gibraltar to the Atlantic Ocean (Roether *et al.,* 1998) with weak contribution of other Mediterranean deep waters [Tyrrhenian Deep Waters (TDW) and Western Mediterranean Deep Waters (WMDW)].

The Mediterranean Sea is a site for deep water mass formation processes. These processes take place in both the Eastern and Western basins ; the deep water renewal time has been estimated to be 20–40 years in the Western basin (Stratford *et al.,* 1998) and about 100 years in the Eastern basin (Roether *et al.,* 1996 ; Stratford and Williams, 1997 ; Stratford *et al.,* 1998). In the Eastern basin, parts of the LIW enter the Adriatic Sub-basin via the Strait of Otranto, where it serves as an initial source of the $EMDW_{Adr}$ (Stöven and Tanhua, 2014). The formation of $EMDW_{Adr}$ in the Adriatic Sub-basin is based on interactions between the LIW and water masses coming from its northern part as well as the natural preconditioning factors, e.g. wind stress and heat loss (Artegiani *et al.,* 1996 a, b; Astraldi *et al.,* 1999; Lascaratos *et al.,* 1999). The $EMDW_{Adr}$ flows then over the sill of Otranto into the Ionian Sub-basin intruding the bottom layer and thus representing a main source of the Eastern Mediterranean Deep Water (EMDW) (Schlitzer *et al.,* 1991; Roether and Schlitzer, 1991). However, in the 1990's, the "engine" of the closed thermohaline cell switched to the Aegean Sub-basin (Bergamasco and Malanotte-Rizzoli, 2010). This latter, which previously had only been a minor contributor to the EMDW, became more effective than the Adriatic Sub-basin as a new source of deep and bottom waters (Eastern Mediterranean Deep Waters originated from the Aegean Sub-basin, $EMDW_{Aeg}$) in the Eastern Mediterranean basin (Robinson *et al.,* 2001). In the Western Mediterranean basin, deep water mass formation occurs in two areas: 1) in the Gulf of Lion (the Northwestern part of the Western basin) where the Western Mediterranean Deep Waters (WMDW) are formed and 2) the Tyrrhenian Sub-basin where the Tyrrhenian Deep Waters (TDW) are formed from a mixing between Eastern waters and WMDW. The acronyms of the abovementioned water masses are used thereafter and thus summarized in the Table 1.

Table 1. The water masses detected in the Mediterranean Sea, their acronyms and the stations numbers used in their characterization in this study.

Water Masses	Acronyms	Stations
Atlantic Waters	AW	1, 2, 3, 4, 8
Cretan Intermediate Waters	CIW	10, 14
Eastern Mediterranean Deep Waters, Adriatic origin	$EMDW_{Adr}$	16, 17
Eastern Mediterranean Deep Waters, Aegean origin	$EMDW_{Aeg}$	9, 10, 11, 12, 13, 18
Levantine Intermediate Waters	LIW	9, 10, 11, 12, 13, 14, 17, 19
Levantine Surface Waters	LSW	9, 10, 11, 12, 13
Modified Atlantic Waters	MAW	5, 6, 7, 7a
Tyrrhenian Deep Waters	TDW	19
Western Mediterranean Deep Waters	WMDW	20, 21, 22

2. Methodology

2.1. Study area

During the 2013 MedSeA cruise realized on board of the Spanish vessel R/V Angeles Alvariño, from May 2nd to June 2nd 2013, 23 stations along the Mediterranean Sea were sampled throughout the water column. The major cruise objective is to study, at the basin scale, the impact of elevated CO_2 on the Mediterranean Sea biogeochemistry by conducting a comprehensive water column sampling from each of the main Mediterranean basins. The overall goal and scientific objectives of this cruise are further described at the following links: http://medsea-project.eu/; http://medseaoceancruise.wordpress.com/.

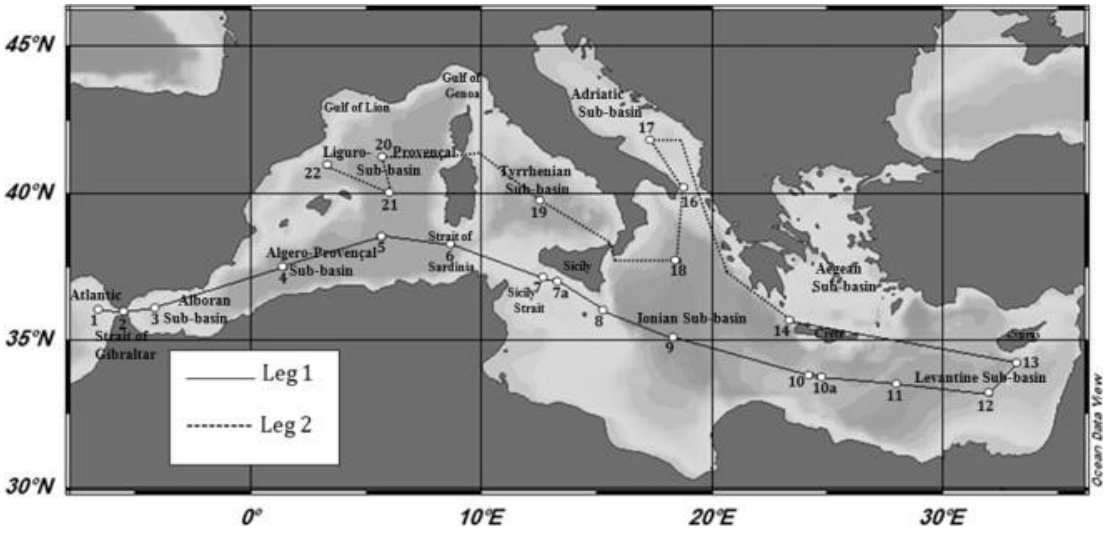

Fig.1. Map of the 2013 MedSeA cruise in the Mediterranean Sea. The numbers from 1 to 22 refer to the sampled stations.

The full cruise track (more than 8000 km long) consisted of two almost latitudinal legs. During the first leg, samples were collected from Atlantic waters off Cadiz harbor, Spain to the Levantine Sub-basin in the Eastern Mediterranean Sea (3879 km long, 15 stations, 279

sampled points, maximum sampled depth = 3720 m). The second leg was conducted in the Northern part of the Mediterranean from the Western Cretan Straits in the Eastern Mediterranean basin to Barcelona, Spain in the North Western Mediterranean basin passing through the South of the Adriatic Sub-basin (3232.5 km long, 8 stations, 183 sampled points, maximum sampled depth = 3000 m ; Fig.1).

2.2. Measured properties

Hydrographic properties [Salinity, S and Temperature, T (ºC)] were measured *in situ* using a Sea-Bird Electronics CTD system (SBE 911plus) associated with a General Oceanic rosette sampler, equipped with twenty four 12 L Niskin bottles. The precision of measurements is ± 0.001 ºC for T and ± 0.0003 for S.

On board, seawater samples for the dissolved oxygen determination were drawn first from the Niskin bottles followed by the C_T/A_T samples taking the precautions recommended to prevent any biological activity and gas exchanges with the atmosphere. Water samples for dissolved oxygen (O_2) determination were collected in calibrated BOD 60 mL bottles. Oxygen concentrations were measured using a Winkler iodometric titration (Hansen, 1999) with a Mettler-Toledo DL-21 potentiometric titrator with a Pt ring redox electrode for the determination of the equivalence point (Outdot *et al*.,1988). The analytical precision and accuracy of O_2 measurements are ± 1.5 µmol kg^{-1}.

For A_T and C_T, seawater samples were collected, at all stations and depths, into pre-washed 500 mL borosilicate glass bottles, according to standard operational protocol. A small headspace (< 1 %) was adjusted to prevent pressure build-up and loss of CO_2 during storage. The samples were poisoned with a saturated solution of $HgCl_2$ and stored in the dark at constant temperature (~ 4 ºC) until their analysis on shore (at the University of Perpignan, IMAGES, France). The measurement of these two parameters was performed by potentiometric acid titration using a closed cell. The principle and procedure of measurements, as well as a complete description of the system used to perform accurate analysis can be found in the DOE handbook of methods for CO_2 analysis (DOE, 1994).

Table 2. A_T and C_T concentrations (± standard deviation) of the titrated batches of CRM and of the seawater samples. The certified A_T and C_T concentrations of the 3 batches are also mentioned.

Measurements	Number of titrated bottles	Certified A_T (µmol kg^{-1})	Certified C_T (µmol kg^{-1})	Average A_T (µmol kg^{-1})	Average C_T (µmol kg^{-1})
Batch 85	5	2184.03 ± 0.79	2000.44 ± 0.43	2185.79± 9	1998.61± 10
Batch 86	13	2175.56 ± 0.67	1998.37 ± 0.54	2175.9± 1	1997.66± 4
Batch 128	8	2240.28 ± 0.76	2013.54 ± 0.66	2242± 4	2014± 6
Seawater samples (Banyuls Sur Mer)	261	-	-	2565.64± 2	2287.85± 4

The precision of A_T and C_T analysis was determined to be ± 2 µmol kg^{-1} for A_T and ± 4 µmol kg^{-1} for C_T, by titrating 261 samples with the same T and S, collected during May 2013 off Banyuls Sur Mer, South France. Whereas the accuracy of A_T and C_T measurements was determined to be ± 1 µmol kg^{-1} for A_T and ± 4 µmol kg^{-1} for C_T by analyzing a total of 26 bottles of three different batches of Certified Reference Material (CRM, batches 85, 86 and 128, Andrew Dickson, CA, USA) in order to test the sensitivity of the electrodes to the various A_T and C_T concentrations and the precision of the analysis (Table 2).

2.3. Computed properties

In order to estimate accurately the anthropogenic carbon dioxide concentration (C_{ANT}) by the TrOCA approach, four parameters were used: potential temperature (θ), dissolved oxygen, total dissolved inorganic carbon and total alkalinity. Since this approach has been previously described in details (Touratier and Goyet, 2004; Touratier *et al.*, 2007), only the basic equations are presented hereafter.

The TrOCA approach is based on the "semi-conservative" tracer TrOCA, which is defined by:

$$TrOCA = O_2 + a\,(C_T - 0.5A_T) \qquad (I)$$

Similarly to all other approaches, the TrOCA tracer is based upon the Redfield equation and is derived in the same manner as tracers NO and PO defined by Broecker (1974). The conservative tracer $TrOCA^0$ is defined as:

$$TrOCA^0 = O_2^0 + a\,(C_T^0 - 0.5A_T^0) \qquad (II)$$

where $TrOCA^0$ is tracer TrOCA but without any anthropogenic contribution and O_2^0, C_T^0 and A_T^0 are the "pre-industrial" concentrations of O_2, C_T and A_T. By definition, the A_T is not affected by the increase of atmospheric CO_2, thus $A_T^0 = A_T$. Furthermore, we assume that oxygen is not substantially perturbed by anthropogenic effects (Manning and Keeling, 2006), i.e. $O_2^0 \approx O_2$. Consequently, the concentration of anthropogenic CO_2 (C_{ANT}) can be estimated as:

$$C_{ANT} = \frac{(TrOCA - TrOCA^0)}{a} \qquad (III)$$

For the estimation of the conservative property $TrOCA^0$, Touratier *et al.* (2007) established the following equation (IV) and defined the optimal set of parameters a, b, c and d for the world ocean:

$$TrOCA^0 = e^{(b + C\theta + d/A_T^2)} \qquad (IV)$$

The concentration of C_{ANT} is then estimated using the four parameters (θ, O_2, A_T and C_T) required to implement the TrOCA approach by applying the following equation via the Ocean Data View [ODV] program (Schlitzer, 2014):

$$C_{ANT} = \frac{O_2 + 1.279[C_T - 0{,}5A_T] - e^{(7.511 - (1.087\times10^{-2})\theta - (7.81\times10^5)/(A_T)^2)}}{1.279} \qquad (V)$$

In our study, below 300 m, the accuracy of the estimated C_{ANT} concentrations using the TrOCA approach is ± 8.7 µmol kg^{-1}.

The pre-industrial C_T, used afterwards to calculate the pre-industrial pH ($pH_{pre\text{-}industrial}$), was computed by subtracting the 2013 C_{ANT} concentrations from the measured 2013 C_T (Eq. VI):

$$C_{Tpre\text{-}industrial} = C_{T\,2013} - C_{ANT\,2013} \quad \text{(VI)}$$

The modern pH (pH_{2013}) was calculated from the modern C_T (C_{T2013}) and A_T (A_{T2013}). This calculation was fulfilled at the seawater scale, via the "CO2SYS" program configured for Excel by Pierrot *et al.* (2006), according to the *in situ* temperature, salinity and pressure conditions, based on A_T-C_T combination and choosing the set of apparent constants (K_1 and K_2) of Goyet and Poisson (1989), the sulfate constants of Dickson (1990), and the borate constants of Uppström (1974). Whereas, the $pH_{pre\text{-}industrial}$ was estimated from the $C_{Tpre\text{-}industrial}$ and the 2013 A_T since this property is not affected by the accumulation of the C_{ANT} in seawater (Touratier and Goyet, 2004).

The acidification level (ΔpH) is computed from the difference between the 2013 distribution of pH and the $pH_{pre\text{-}industrial}$:

$$\Delta pH = pH_{2013} - pH_{pre\text{-}industrial} \quad \text{(VII)}$$

The saturation degree of calcite (ΩCa) and aragonite (ΩAr) were also computed by using the "CO2SYS" program. The calculation was done according to the same *in situ* conditions and constants used for the aforementioned computed variables.

The hydrographic and carbonate system data of the 2013 MedSeA cruise are available on Pangaea data repository (Goyet *et al.*, 2015a, b; Ziveri and Grelaud, 2013a, b, c).

3. Results and discussion

3.1. Distribution of C_{ANT} concentrations in the Mediterranean Sea

Since today, all the various approaches used to estimate C_{ANT} in seawater are based upon the Redfield concept which is valid only below the wintertime mixed layer depth. None are reliable for the upper ocean where there are biological processes and gas exchanges across the air–sea interface. Therefore, these approaches could not distinguish the C_{ANT} from the bulk of CO_2 in surface layer. Subsequently, we will exclusively consider the estimations located below the winter mixed layer (> 300 m).

3.1.1. General Distribution of the C_{ANT}

In the layers deeper than 300 m down to the bottom, the calculated C_{ANT} concentrations vary between 35.2 and 101.9 µmol kg^{-1} (Fig.2) and the corresponding mean C_{ANT} concentration is equal to 63 µmol kg^{-1} showing that all the Mediterranean waters are invaded by anthropogenic CO_2, in agreement with Touratier and Goyet (2011). The fast overturning

circulation in the Mediterranean Sea has led to an overall invasion of the anthropogenic CO_2 in the basin. The general profile of C_{ANT} shows that its concentration decreases gradually with depth in the Eastern basin to reach its lowest values in the deepest layers (35.55 - 48 µmol kg^{-1}). Contrariwise, the C_{ANT} concentrations are always greater than 70 µmol kg^{-1} in the Western basin even in the deepest water masses. Rivaro *et al.* (2010) reported the presence of a slight increase from 300 to 1000 m, and constant values in deep waters of the Mediterranean (29-75 µmol kg^{-1}).

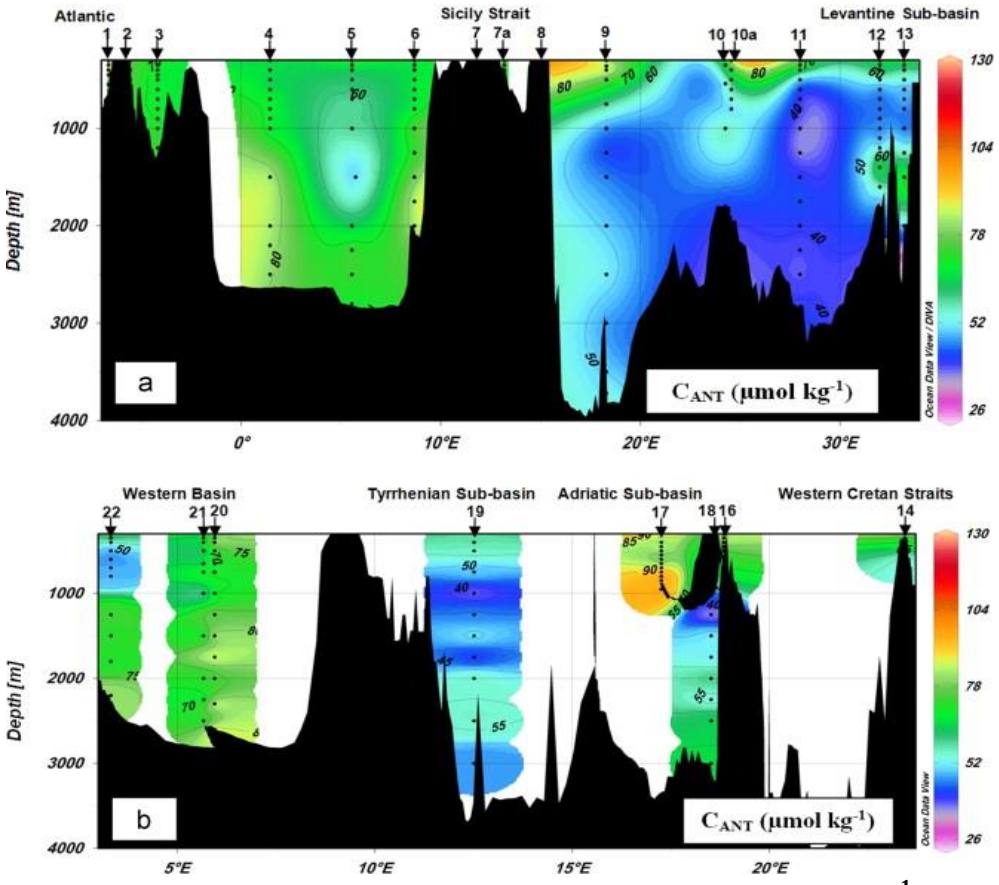

Fig.2. Distribution of anthropogenic CO_2 concentrations (C_{ANT} ; µmol kg^{-1}) along (a) the southern and (b) the northern sections of the 2013 MedSeA cruise.

In general, the open ocean C_{ANT} concentrations are much lower than those of the Mediterranean Sea. Anthropogenic CO_2 generally penetrates to shallower depths in the tropical oceans but to deeper depths in the subtropical ocean (30°–40°). The symmetry of vertical penetration of anthropogenic CO_2 about the equator breaks down toward the poles (latitudes > 50° ; Lee *et al.*, 2003). In the Western basin of the North Atlantic Ocean between 40°N and 50°N, the penetration of anthropogenic CO_2 based on data collected in 1994, was all the way to the bottom of the water column (Kortzinger *et al.*, 1998), and a C_{ANT} mean of 10.4 µmol kg^{-1} was calculated for the deepest waters. In the Eastern basin of the North Atlantic, the penetration was shallower and C_{ANT} concentrations of ~5 µmol kg^{-1} were detected at ~3500 m depth. Estimations based on data collected between 1990 and 1998 have shown that in the Northern high-latitude regions, the penetration of anthropogenic CO_2, as defined by a 5 µmol kg^{-1} contour, is greater than 3000 m (Lee *et al.*, 2003). Moderate

anthropogenic CO_2 concentrations (~10 µmol kg^{-1}) were found below 4000 m between 30°S and 50°S in the South Atlantic western basin for the year 1994 (Ríos *et al.*, 2010), while previous estimates for that region showed zero and negative values beneath this depth (Lee *et al.*, 2003 ; Sabine *et al.*, 2004). South of 50°S in the South Atlantic, the value of C_{ANT} falls sharply to below 5 µmol kg^{-1} at a depth of only 500 m (Lee *et al.*, 2003). It is thus evident that the atmospheric CO_2, among which the anthropogenic CO_2, is efficiently transferred from the atmosphere to the Mediterranean waters, thereby it is well disseminated in this sea, even in the deepest layers. The main reason of the higher uptake and vertical penetration of CO_2 in relation to other oceanic regions seems to be the fast deep water formation processes in the Mediterranean Sea combined with surface waters having a relatively low Revelle factor (Schneider *et al.*, 2010), which means that Mediterranean waters are prone to absorb and have the ability to store more C_{ANT} than the oceanic ones.

3.1.2. Distribution of the C_{ANT} in the Western and Eastern Mediterranean basins

Between 300 to 1000 m depth, the C_{ANT} varies from 45 to 93 µmol kg^{-1} in the Western basin and from 37 to 101.9 µmol kg^{-1} in the Eastern basin. However, it decreases below 1000 m, ranging between 48 and 84 µmol kg^{-1} and between 35 and 80 µmol kg^{-1} in the Western and Eastern basins, respectively. These results show that the Western basin of the Mediterranean Sea is more invaded by C_{ANT} than the Eastern one, especially in deep layers. Several factors could explain the observed differences: 1- the renewal time of deep waters is considerably different varying between 20 and 40 years in the Western basin (Stratford *et al.*, 1998) and approximately 100 years in the Eastern basin (Roether *et al.*,1996 ; Stratford *et al.*, 1998), 2 - the high surface temperature and salinity may reduce the solubility and penetration of atmospheric CO_2 in the Eastern basin. In this latter, using the Transit Time Distribution (TTD) method, Schneider *et al.* (2010) estimated the minimum C_{ANT} concentration of about 20.5 µmol kg^{-1} in the intermediate layer which is 15 µmol kg^{-1} lower than the minimum C_{ANT} obtained in the present study using the TrOCA approach.

Within a study of the decadal (from the mid-1990s to the mid-2000s) evolution of anthropogenic CO_2 at the DYFAMED site, in the Northwestern Mediterranean Sea, Touratier and Goyet (2009) reported a decreasing temporal trend of C_{ANT}, especially in intermediate and deep layers. They have found a significant correlation between the decrease in C_{ANT} and a decrease in the dissolved oxygen that was accompanied by an increase in both salinity and temperature. This latter increase has been related to an enhanced vertical mixing of intermediate waters, coming from the Eastern basin, into the deep waters of the Tyrrhenian Sub-basin, that has been noted and associated with the Eastern Mediterranean Transient (EMT) signal (Gasparini *et al.*, 2005 ; Schröder *et al.*, 2006 ; Roether and Lupton, 2011). The EMT has played an important role in the intrusion of old water masses characterized by low C_{ANT} concentrations, since the waters overflowing in the Sicily Strait have long subsurface travel times from their formation regions (Roether and Lupton, 2011). Using the anthropogenic tracer CFC-12, Roether *et al.* (1998) estimated that the age of the LIW increased by 6 years from 1987 to 1995 as a result of enhanced incorporation of older deep waters into the LIW layer. They also suggested that because of the EMT, the older EMDW of

Adriatic origin (low CFC-12 concentration) was uplifted by the newly formed EMDW of Aegean origin (characterized by a higher concentration of CFC-12 since they are much younger). However, the maximum Mediterranean C_{ANT} estimation of the current study (101.9 µmol kg^{-1}) is higher than the one earlier provided by Touratier and Goyet (2011; 65 µmol kg^{-1}) after the EMT. The increasing trend of the C_{ANT} concentrations between 2001 and 2013, could be attributed to the new deep water masses formation occurred during the intervening period in the Western basin. Actually, Schröder *et al.* (2008) have confirmed that between 2004 and 2006 almost the whole deep Western basin has been filled with highly saline and warm new deep water, which substantially renewed the resident deep water. On the other hand, the salt content of the LIW, that is an important factor controlling the deep water formation in the Northwestern Mediterranean basin, can explain the high heat and salt contents of the new deep water formed during the severe weather conditions of winter 2004/2005 (Schröder *et al.*, 2008). The newly formed deep waters replaced the old deep ones by uplifting them, which explains the high C_{ANT} concentrations in the intermediate and deep layers of the Western sub-basins. In the same direction are also the findings of the CASCADE cruise, conducted during March 2011 in the Northwest part of this basin, that pointed out the key role of the dense shelf waters in the formation of the Western deep waters under determined atmospheric conditions (Durrieu de Madron *et al.*, 2013 ; Puig *et al.*, 2013). Coastal surface waters over the wide shelf of the Gulf of Lion become denser than the underlying waters and cascade downslope, usually through submarine canyons, until reaching their equilibrium depth (Durrieu de Madron *et al.*, 2005). These cold coastal waters which were directly in contact with the atmosphere, thus accumulating high C_{ANT} concentrations, are cascading downward to participate in the deep water mass formation. These findings could also explicate the high C_{ANT} concentrations recorded in the deep layers of the Western basin.

3.1.3. Distribution of the C_{ANT} at sub-basin scale

In the Northern part of the Mediterranean Sea, C_{ANT} concentrations are higher than 50 µmol kg^{-1} in the Western basin with relatively low estimates (> 38 µmol kg^{-1}) in the Tyrrhenian Sub-basin (Fig.2). Furthermore, the lowest C_{ANT} concentrations were observed in the deep layers of the Ionian Sub-basin (35 µmol kg^{-1}). A study of the evolution of the water mass circulation in the Mediterranean Sea, between 2008 and 2013 (Hassoun *et al.*, 2015a), has proved that the deep layers of the Ionian Sub-basin are still dominated by the EMDW of Aegean origin. This explains the low C_{ANT} concentrations noted in this old deep water body where low concentrations of O_2 were similarly measured (Fig.4). In the Tyrrhenian Sub-basin, the relatively low dynamics and the presence of gyre structures are favorable conditions for vertical exchanges (Astraldi and Gasparini, 1994), resulting in the creation of a peculiar water type, the Tyrrhenian Deep Water (TDW), a product of the mixing between LIW and WMDW (Sparnocchia *et al.*, 1999). Based on ^{3}He and tritium data from the period 1987-2009, a downward cascading of inflowing waters from the Eastern basin to the Southern Tyrrhenian Sub-basin has been detected, showing a reduced impact of WMDW on the TDW during the period of enhanced mixing (Roether and Lupton, 2011). Our results are in agreement with Povero *et al.* (1990) findings, showing that the intermediate and deep

waters of this sub-basin have low O_2 concentrations (Fig.4). The previous facts indicate that the Tyrrhenian Sub-basin is filled with old waters, which explains its relatively low C_{ANT} concentrations. These results are in a good agreement with the recent findings of Schneider *et al.* (2014) who, in spite of the detection of a massive input of recently ventilated waters in the Western Mediterranean deep basin, they have found that the ventilation in the Tyrrhenian Sub-basin seemed to be fairly constant since the EMT. The highest C_{ANT} concentrations are found in the deep layers of the Adriatic Sub-basin (100 µmol kg^{-1}). This indicates that the waters filling the deep layers of this sub-basin have been recently in contact with the atmosphere as it is confirmed by the relatively high concentrations of O_2 (Fig.4). These results are consistent with the findings of Schneider *et al.* (2014) who have detected in the Ionian Sub-basin an evidence of increased ventilation after year 2001, indicating the restart of deep water formation in the nearby Adriatic Sub-basin. Moreover, Schneider *et al.* (2010) hypothesized that waters of the Eastern deep water mass formation sites with high CO_2 uptake capacity, which are preconditioned for deep water formation, quickly cool during winter and transfer anthropogenic CO_2 into the deep basin.

3.1.4. Could we characterize the water masses based on the C_{ANT} concentrations?

Based on the composite θ/S diagram where the C_{ANT} concentrations are superimposed (Fig.3), we noticed that water masses in the Mediterranean Sea can be easily characterized using the C_{ANT} concentrations that differ from one water mass to another (Fig. 3 ; Table 3).

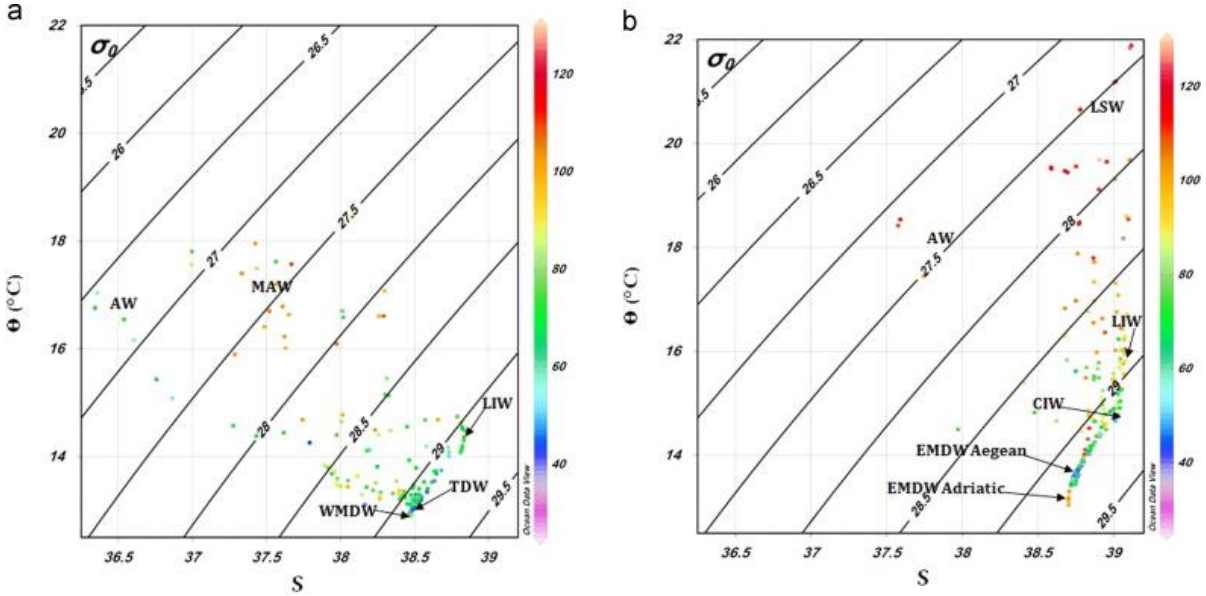

Fig.3. Anthropogenic CO_2 concentrations superimposed on θ/S diagrams for the Western basin (a) and the Eastern basin (b). Abbreviations on the figures correspond to the following water masses : AW, Atlantic Water ; MAW, Modified Atlantic Water ; LSW, Levantine Surface Water ; LIW, Levantine Intermediate Water ; CIW, Cretan Intermediate Water ; EMDW-Aegean, Eastern Mediterranean Deep Water originated from the Aegean Sub-basin ; EMDW-Adriatic, Eastern Mediterranean Deep Water originated from the Adriatic Sub-basin ; TDW, Tyrrhenian Deep Water ; WMDW, Western Mediterranean Deep Water.

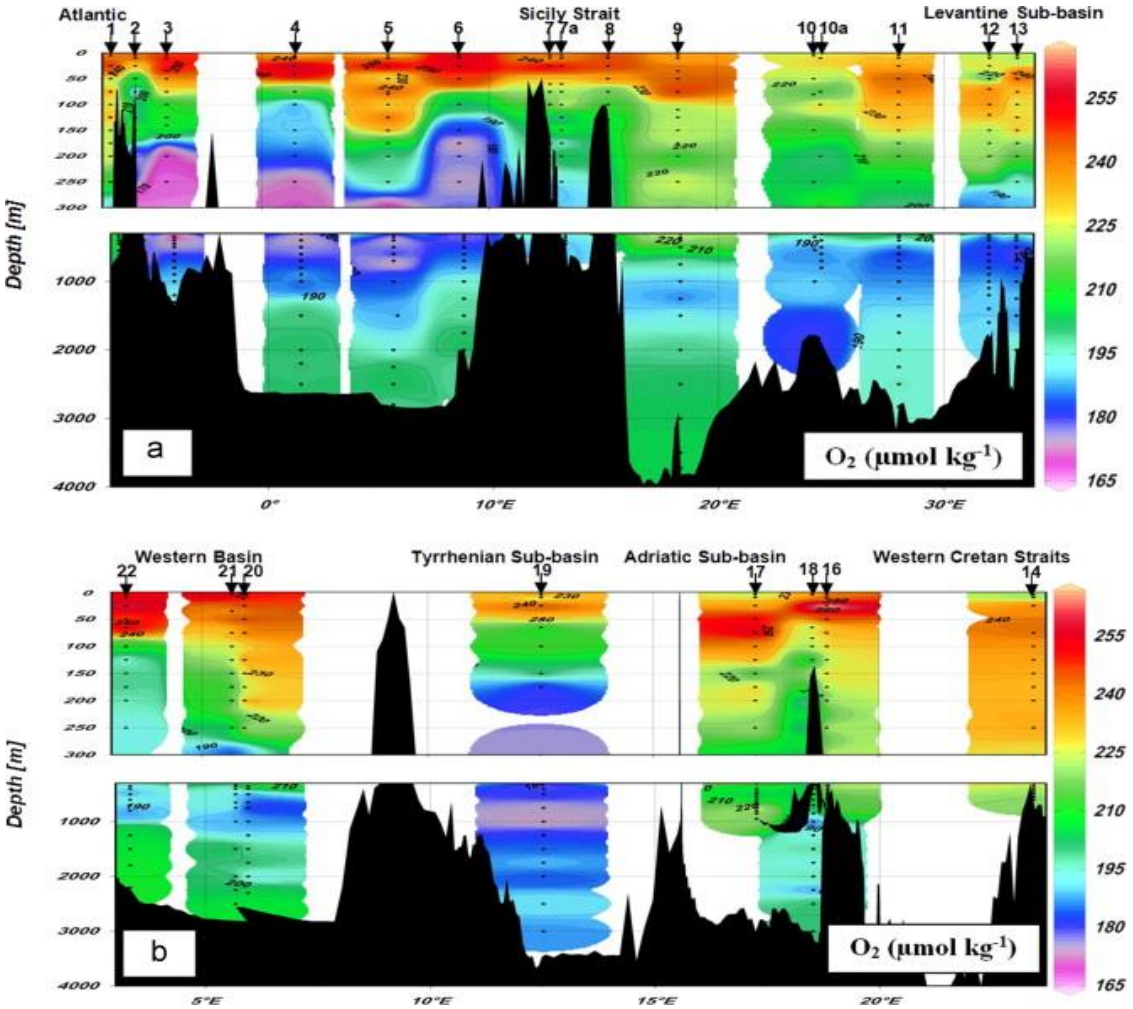

Fig.4. Distribution of the dissolved oxygen (O_2 ; µmol kg^{-1}) along (a) the southern and (b) the northern sections of the 2013 MedSeA cruise.

The characterization of the water masses mentioned in Table 3 was realized based on their hydrographic features and the isopycnals. For example, in the Eastern basin, the newly formed EMDW in the Adriatic Sub-basin could be discriminated from the EMDW of Aegean origin by its higher C_{ANT} concentrations. Similarly in the Western basin, the WMDW has higher C_{ANT} concentrations than those recorded in the relatively old TDW. Although TrOCA approach is not reliable to estimate the C_{ANT} concentrations in the upper mixed layer, the surface water masses which are in direct contact with the atmosphere could also be distinguished from the bulk of the Mediterranean intermediate and deep water masses by their extremely high concentrations of C_{ANT} (i.e. MAW, LSW).

3.2.Estimation of acidification in the Mediterranean Sea

3.2.1. The pH

The average pH of the Mediterranean Sea, during the 2013 MedSeA cruise, is equal to 8.074 ± 0.034. It ranges from a minimum of 7.962 and a maximum of 8.148 (Fig.5). During May, within the upper part of the water column (0-25 m), pH varies between a minimum of 8.049

and a maximum of 8.148. CO_2 uptake by phytoplankton increases seawater pH and shifts the dissolved inorganic carbon equilibrium toward carbonate ions. Therefore, the highest pH values have been calculated in the surface layer. The exchange of CO_2 with the atmosphere can also cause a change in pH. On a decadal time scale, the accumulation of C_{ANT} resulted in a significant reduction of pH compared to the preindustrial era, as mentioned by Touratier and Goyet (2009) from the data of the DYFAMED site.

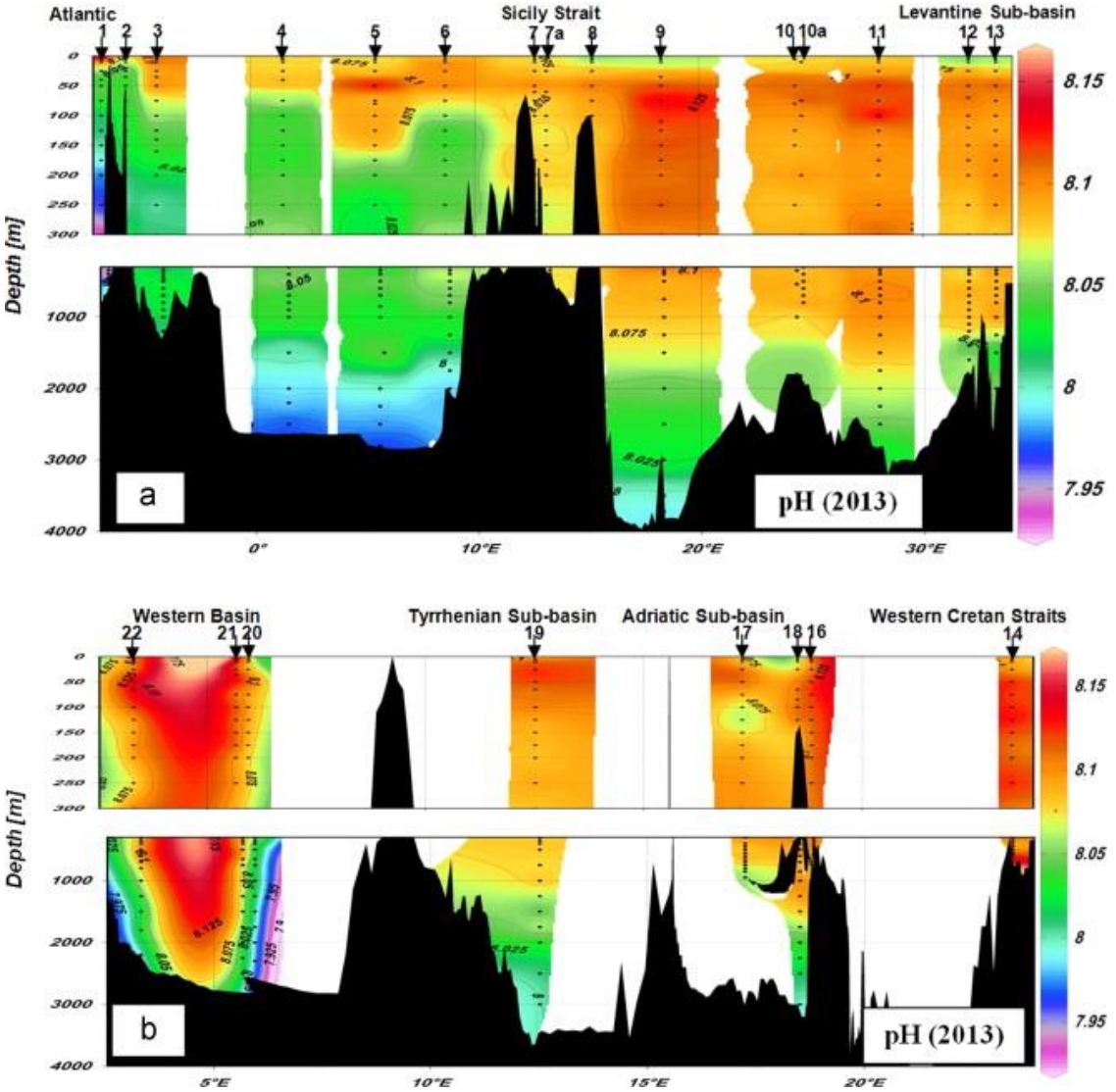

Fig.5. Distribution of pH along (a) the southern and (b) the northern sections of the 2013 MedSeA cruise.

The pH increases Eastward, especially below the surface mixed layer (Fig.5). In other words, the waters of the Western basin (average pH = 8.061 ± 0.033) are more acidic than those of the Eastern basin (average pH = 8.087 ± 0.024). The lowest pH values were recorded in the intermediate and deep layers of the Western basin. Particularly, they correspond to the layer occupied by the Levantine Intermediate Waters (250 m) in the Alboran Sub-basin, where a zone of minimum oxygen was also detected (Fig.4), as well as to the deep water mass filling the deepest parts of the Western basin (WMDW). However, the maximum pH values correspond to the Ionian surface water flowing into the Adriatic Sub-basin.

Table 3. Range (Min., Max.), average and standard deviations (S.D.) of the hydrological and carbonate system parameters in the Mediterranean Sea water masses detected in both the Western and the Eastern basins during the 2013 MedSeA cruise.

Parameters		**Western basin**				**Eastern basin**			
Water masses		LIW	WIW	TDW	WMDW	LIW	CIW	$EMDW_{Aeg}$	$EMDW_{Adr}$
Number of measurements		16	3	29	44	18	8	39	19
θ (°C)	Mean ± S.D.	13.38 ± 0.32	13.30 ± 0.06	13.18 ± 0.19	12.92 ± 0.03	14.53 ± 0.55	14.39 ± 0.33	13.62 ± 0.11	13.46 ± 0.21
	Min.-Max.	13.07 - 14.13	13.22 - 13.36	12.92 - 13.75	12.89 - 13.01	13.80 - 15.57	13.87 - 14.78	13.42 - 13.88	13.04 - 13.87
S	Mean ± S.D.	38.559 ± 0.080	38.363 ± 0.070	38.517 ± 0.083	38.470 ± 0.007	38.912 ± 0.087	38.924 ± 0.091	38.753 ± 0.022	38.732 ± 0.024
	Min.-Max.	38.492 - 38.733	38.266 - 38.431	38.166 - 38.682	38.458 - 38.484	38.775 - 39.045	38.800 - 39.027	38.717 - 38.804	38.701 - 38.789
O_2 (µmol kg^{-1})	Mean ± S.D.	176.9 ± 9.5	202.0 ± 19.1	186.4 ± 6.9	197.5 ± 1.5	201.1 ± 15.7	199.9 ± 17.2	189.8 ± 6.5	205.7 ± 16.6
	Min. - Max.	164.0 - 195.4	178.2 - 224.8	173.2 - 199.4	182.8 - 209.2	174.9 - 224.4	178.9 - 220.9	177.8 - 203.8	175.5 - 228.1
A_T (µmol kg^{-1})	Mean ± S.D.	2588.3 ± 20.1	2576.3 ± 5.0	2594.7 ± 15.2	2584.0 ± 17.9	2613.2 ± 26.8	2611.0 ± 23.2	2608.5 ± 8.2	2619.0 ± 11.9
	Min.-Max.	2560 - 2626	2571 - 2583	2572 - 2619	2555 - 2629	2554 - 2665	2568 - 2633	2591 - 2630	2599 - 2637
C_T (µmol kg^{-1})	Mean ± S.D.	2321.6 ± 8.5	2317.0 ± 11.0	2310.2 ± 9.3	2314.4 ± 11.5	2307.7 ± 30.4	2300.7 ± 33.6	2302.1 ± 12.4	2318.2 ± 17.9
	Min. – Max.	2310 - 2336	2303 - 2330	2293 - 2327	2290 - 2332	2235 - 2359	2259 - 2330	2283 - 2349	2283 - 2351
C_{ANT} (µmol kg^{-1})	Mean ± S.D.	66.5 ± 6.0	87.1 ± 6.4	55.8 ± 10.3	72.6 ± 0.3	69.7 ± 13.5	61.5 ± 10.1	47.4 ± 8.9	67.6 ± 20.1
	Min. – Max.	55.2 - 73.5	78.3 – 93.2	37.9 – 74.2	48.0 – 89.0	49.6 – 92.8	49.9 – 78.3	35.3 – 80.4	35.9 - 101.9
pH_{2013}	Mean ± S.D.	8.048 ± 0.026	8.041 ± 0.015	8.059 ± 0.028	8.016 ± 0.032	8.088 ± 0.012	8.097 ± 0.018	8.067 ± 0.028	8.068 ± 0.029
	Min. – Max.	8.007 - 8.093	8.024 - 8.062	8.000 - 8.104	7.962 - 8.081	8.061 - 8.107	8.080 - 8.124	7.987 - 8.104	7.996 - 8.102
ΔpH (pH_{2013}- $pH_{pre-ind}$)	Mean ± S.D.	0.110 ± 0.012	0.142 ± 0.008	0.090 ± 0.018	0.119 ± 0.000	0.106 ± 0.019	0.093 ± 0.016	0.074 ± 0.014	0.104 ± 0.030
	Min. – Max.	0.087 - 0.124	0.130 - 0.149	0.060 - 0.123	0.078 - 0.146	0.076 - 0.136	0.074 - 0.119	0.055 - 0.126	0.056 - 0.156

3.2.2. Acidification variations (ΔpH)

Despite the knowledge of its potential impacts on biological and chemical processes by the scientific community, estimations of the acidification in the Mediterranean Sea are still scarce. Variations of the acidification ($\Delta pH = pH_{2013} - pH_{pre\text{-}industrial}$) in the Mediterranean Sea waters for the two sections of the 2013 MedSeA cruise are presented in Figure 6.

The results show that the Mediterranean Sea water masses are already acidified. A pH decrease ranging between -0.055 and -0.156 pH unit is noted below 300 m. This range is close to the one reported by Touratier and Goyet (2011 ; -0.05_-0.14 pH unit from pre-industrial period till 2001) and Touratier *et al.* (2012 ; -0.061_-0.148 pH unit from pre-industrial period till 2008). As the atmospheric CO_2 has increased by 371.13 ppm in 2001 to

385.59 ppm in 2008 and to 396.48 ppm in 2013 (http://www.climate.gov/ ; http://co2now.org/), the aggravation of the acidification, during the twelve years (between 2001 and 2013), is attributed to the amount of the absorbed anthropogenic CO_2 related to the rapid increase of the atmospheric CO_2 concentrations emitted by human activities. Moreover, the acidification of the Mediterranean waters is directly associated with its active overturning circulation and the high A_T and temperature prevailing throughout the water column. An additional factor could be the fact that only surface anthropogenic CO_2-loaded waters are inflowing from the Atlantic to the Mediterranean Sea. The ΔpH values of the present study (as well as by Touratier and Goyet, 2011; Touratier et *al.*, 2012) are higher than those mentioned by Palmiéri *et al.* (2015), although they have the same pattern. This is attributed to the different methods (TrOCA *vs.* TTD) used in each study to estimate the anthropogenic CO_2 and then to calculate the pre-industrial C_T and the pre-industrial pH.

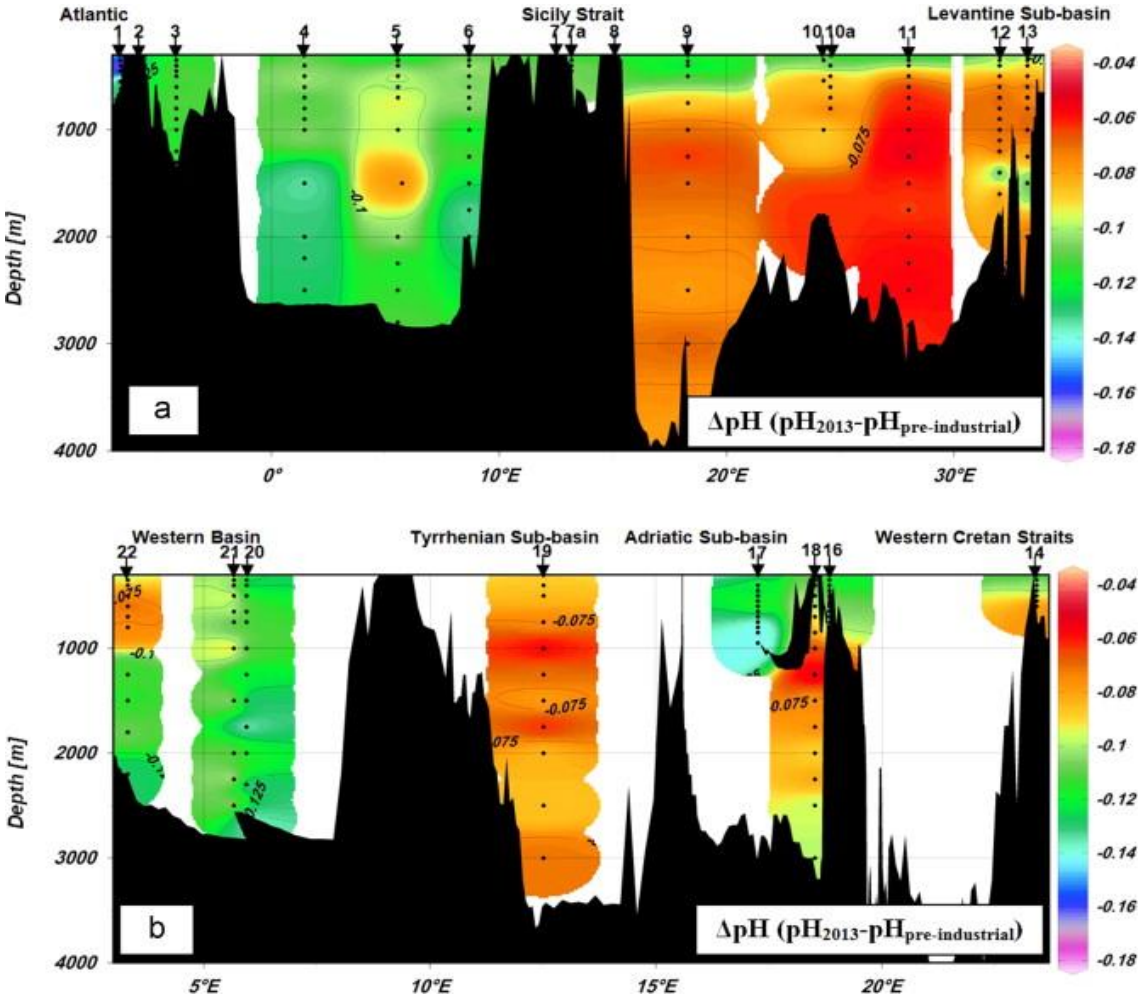

Fig.6. Acidification (ΔpH) below 300m, along (a) the southern and (b) the northern sections of the 2013 MedSeA cruise.

Generally, the waters of the Eastern basin are less acidified than those of the Western basin where the ΔpH is always greater than -0.1 pH unit (except in the deep layers of the Adriatic Sub-basin where ΔpH is ~ -0.156 unit ; Fig.6). This finding is related to the difference of the renewal time in each Mediterranean basin, i.e. the renewal time of the Western deep waters is

shorter than the Eastern one [20–40 years in the Western basin (Stratford *et al.*, 1998) and about 100 years in the Eastern basin (Roether *et al.*, 1996; Stratford and Williams, 1997; Stratford *et al.*, 1998)]. This fact also explains the higher accumulation of C_{ANT} in the Western basin which is more invaded by C_{ANT} than the Eastern basin (i.e. low concentrations of C_{ANT} in the deep layers of Ionian and Tyrrhenian Sub-basins are highly correlated with the weak levels of acidification, Fig.2 and 6).

3.3. Impact of the acidification on the formation of biogenic carbonate in the Mediterranean Sea

Ocean uptake of anthropogenic CO_2 increases the concentration of hydrogen ions (H^+), thereby it decreases the seawater pH. This reduction in ocean pH has some direct effects on marine organisms (Seibel and Walsh, 2001 ; Ishimatsu *et al.*, 2005) and decreases carbonate ion concentrations (Cao *et al.*, 2007 ; Wolf-Gladrow and Rost, 2014), making it more difficult for calcifying marine organisms to form their shells and skeletons (Kroeker *et al.*, 2013 and references therein ; Sanford *et al.*, 2014 and references therein ; Collins *et al.*, 2014 and references therein ; Hilmi *et al.*, 2014 and references therein).

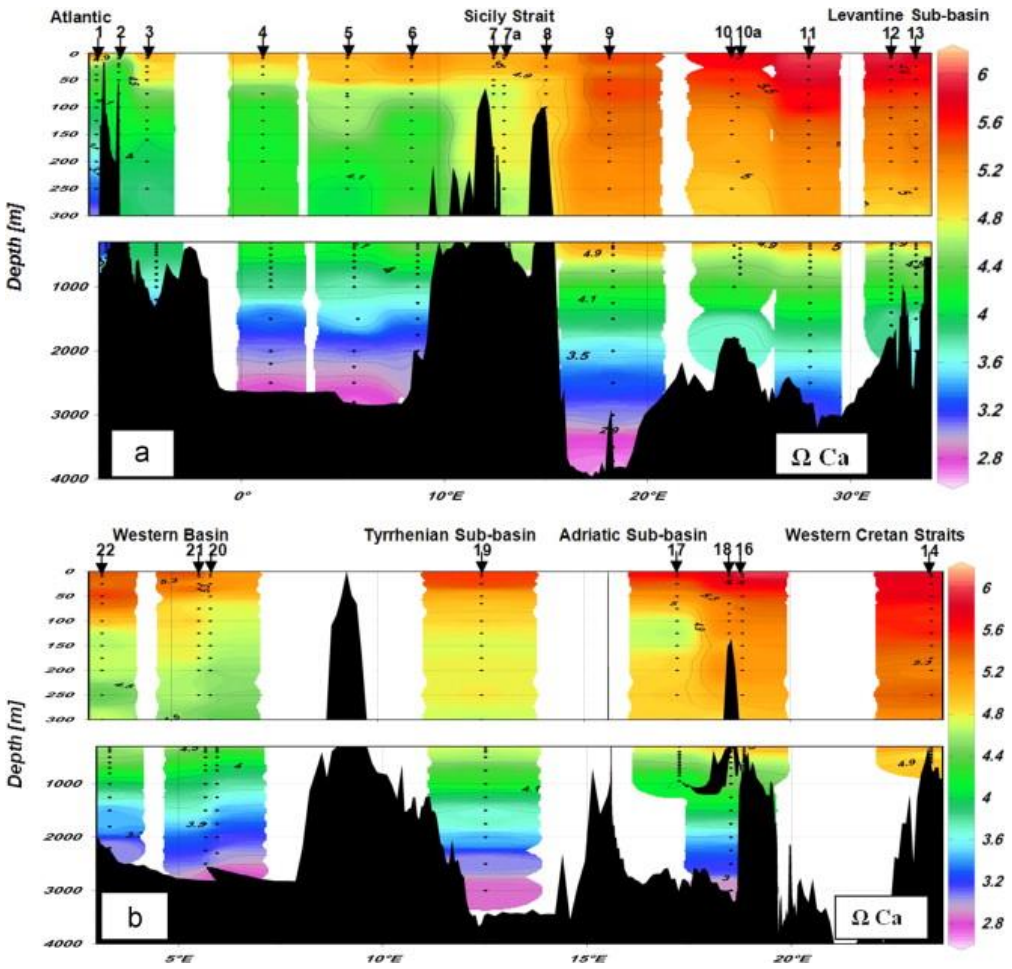

Fig.7. Degree of calcite saturation along (a) the southern and (b) the northern sections of the 2013 MedSeA cruise.

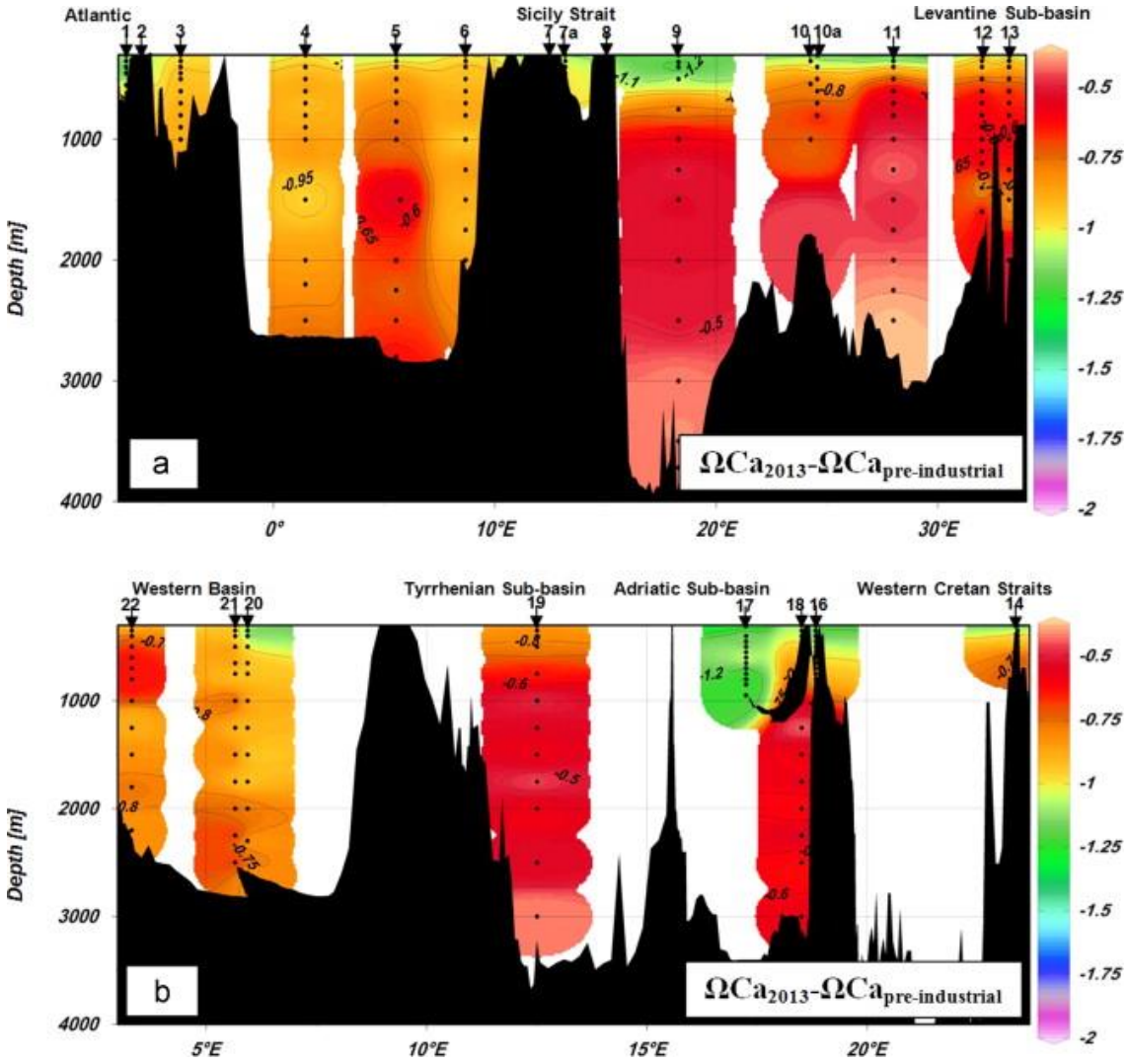

Fig.8. The variation of calcite saturation between 2013 and the pre-industrial period along (a) the southern and (b) the northern sections of the 2013 MedSeA cruise.

In agreement with previous Mediterranean studies (Alekin, 1972 ; Millero *et al.*, 1979 ; Schneider *et al.*, 2007 ; Álvarez *et al.*, 2014), our results show that all Mediterranean waters are strongly saturated with respect to both calcite and aragonite (Ω>> 1 ; Fig.7 and 8). Figures 7a and 9a indicate that the saturation state of both minerals exhibit a clear longitudinal gradient with increasing values eastward at all depths. The intermediate and deep Mediterranean waters appear more saturated with respect to both calcium carbonate minerals than the Atlantic waters at the same depth. The Eastern basin, which accumulates less C_{ANT}, has higher saturation levels for calcite and aragonite (Fig.7, 9) than those of the Western basin. Based on both sections (the northern and southern ones) conducted along the Mediterranean Sea, it is evident that the upper layers are characterized by higher Ω values than the deeper ones reflecting the effect of pressure on the solubility of the calcium carbonate.

Figures 8 and 10 show the variations of calcite and aragonite (ΩCa_{2013} - $\Omega Ca_{Pre\text{-}industrial}$ and ΩAr_{2013} - $\Omega Ar_{Pre\text{-}industrial}$), in the Mediterranean Sea, between the pre-industrial period and 2013. These figures indicate that their levels decreased in the Mediterranean waters within a

range from -0.37 to -2 for ΩCa and from -0.24 to -1.3 for ΩAr. This phenomenon reflects the aggravated effect of the excessive anthropogenic CO_2 penetration, and thus of the ocean acidification on the calcium carbonate states, particularly in the sub-basins invaded by high C_{ANT} concentrations (i.e. the Western basin and the Adriatic Sub-basin).

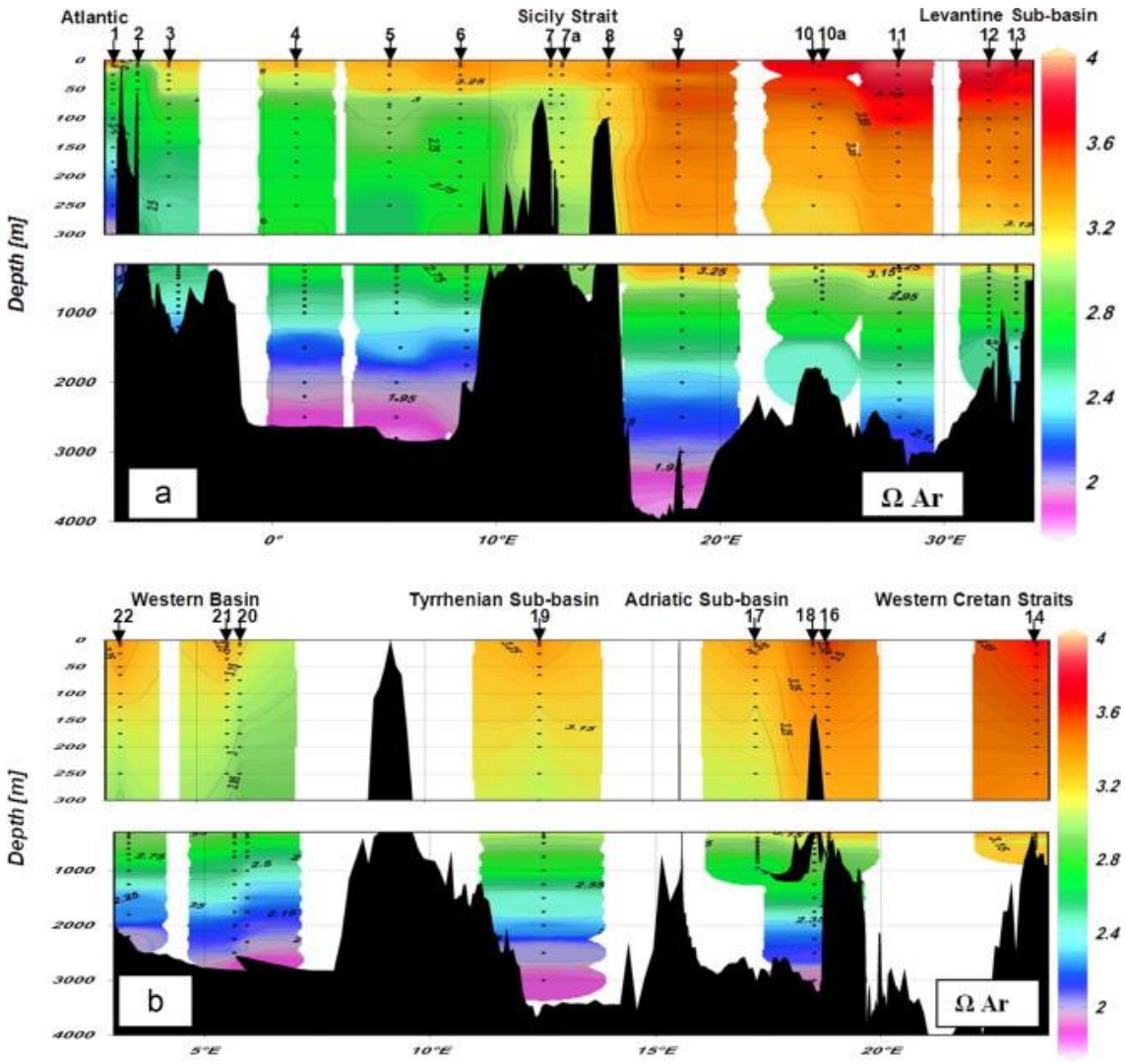

Fig.9. Degree of aragonite saturation along (a) the southern and (b) the northern sections of the 2013 MedSeA cruise.

Time-series studies conducted in the North Pacific Ocean between 1988 and 2007 (Dore *et al.*, 2009) and in the North Atlantic Subtropical gyre between 1983 and 2011 (Bates *et al.*, 2012) have documented a significant long-term decreasing trend of -0.05 pH unit (-0.0019 and -0.0017 unit yr^{-1} in the North Pacific and the North Atlantic respectively). Comparing the acidification levels in the Mediterranean Sea ranging between -0.055 and -0.156 pH unit with values found in the ocean surface water, this semi-enclosed sea appears as one of the most affected regions by acidification. Notwithstanding, it is still remaining highly supersaturated in both calcite (ΩCa ~ 2.63-6.17 ; Fig.7) and aragonite (ΩAr ~ 1.77-4.02 ; Fig.8). Therefore, carbonate ions depletion in this area is not an anticipated problem, at least in the near future. However, the high ability of Mediterranean waters to uptake the atmospheric CO_2 which is

then rapidly transported to the sea interior with the overturning circulation, has the potential to alter the carbonate saturation conditions, with consequences not yet clearly defined for the well adapted organisms. In addition, high acidification levels can influence the microbial nutrient cycling and the speciation of nutrients in the Mediterranean Sea. There is a high probability that the decreasing pH may increase its oligotrophic nature and the degree of phosphorus limitation by changing the N:P stoichiometry due to reductions in phosphate concentrations and shifts in the nitrogen speciation (CIESM, 2008 and references therein). During a mesocosm experiment off Corsica performed in the frame of MedSeA project, the nitrogen fixation rates were seen to increase approximately 10-fold for pH levels predicted after ~2100 (pH<7.73) (Rees *et al.*, 2013), implying future changes of the nitrogen cycle within the Mediterranean with likely consequences on ecosystem functioning due to changes in community structure.

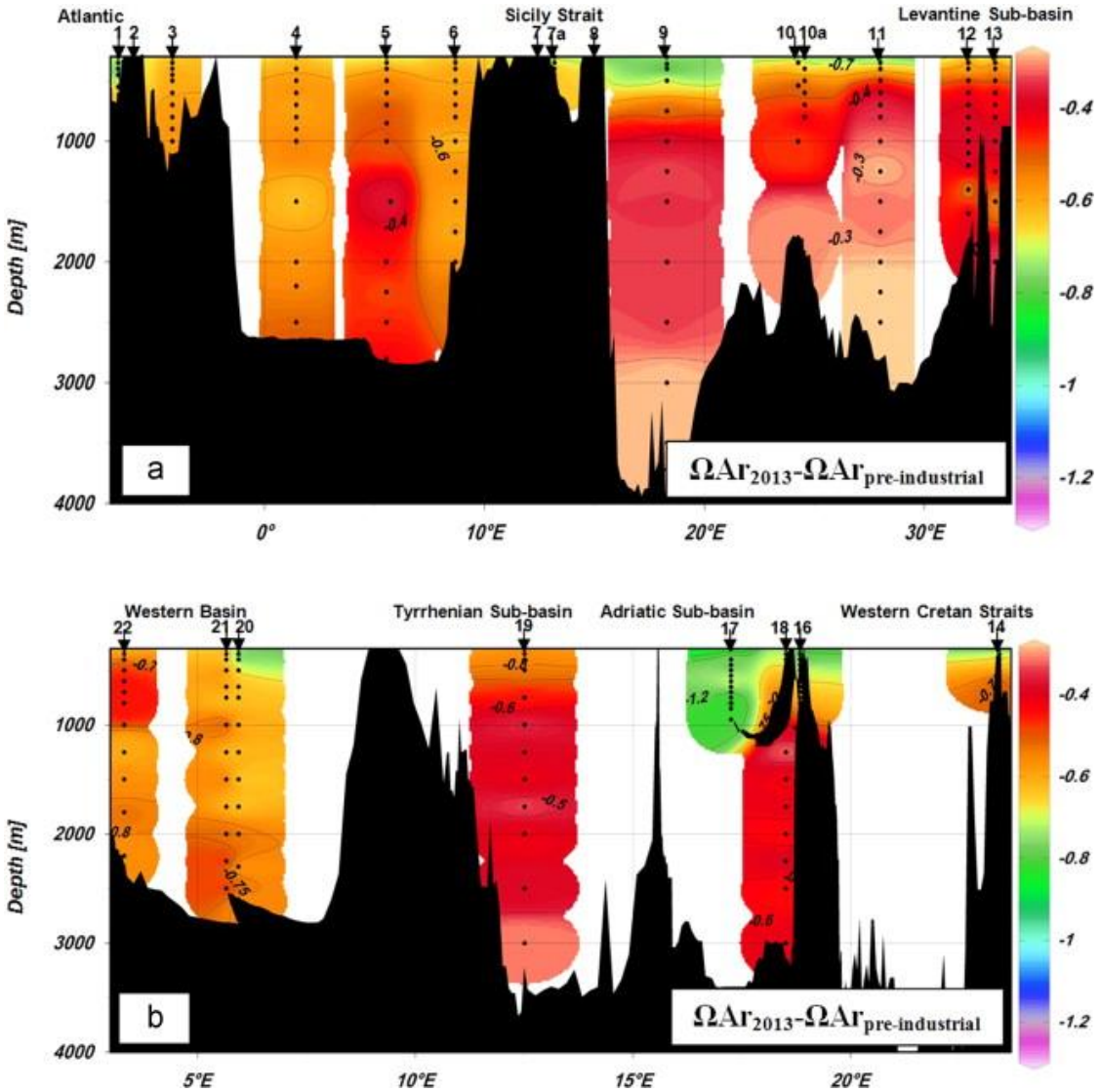

Fig.10. The variation of aragonite saturation between 2013 and the pre-industrial period along (a) the southern and (b) the northern sections of the 2013 MedSeA cruise.

4. Conclusions

In this paper, the distributions of anthropogenic CO_2, pH_{2013} and acidification (between pre-industrial period and 2013) in the Mediterranean Sea, have been presented and discussed. All Mediterranean waters are invaded by anthropogenic CO_2 with concentrations much higher than those recorded in other oceanic areas. This fact is attributed to the effective atmospheric CO_2 absorption at the surface and to the short deep water renewal time in this sea. In general, the Eastern basin accumulates less C_{ANT} than the Western basin. Moreover, the most invaded waters by C_{ANT} (> 60 µmol kg^{-1}) have been detected in the intermediate (300-500 m) and deep (> 500 m) layers :1- of the Alboran, Liguro and Algero-Provencal Sub-basins in the Western basin, and 2- of the Adriatic Sub-basin in the Eastern basin. This fact shows that these waters have recently been in contact with the atmosphere. Whereas the areas containing the lowest C_{ANT} concentrations are the deep layers of the Eastern basin, especially those of the Ionian Sub-basin and those of the northern Tyrrhenian Sub-basin in the Western basin where the concomitant low O_2 concentrations indicate that the prevailing waters are very old.

The acidification (ΔpH between 2013 and the pre-industrial period) of the Mediterranean Sea reflects the excessive increase of atmospheric CO_2 and therefore the invasion of the sea by C_{ANT}. This acidification ranges from -0.055 to -0.156 pH unit. It indicates that all Mediterranean Sea waters are already acidified, especially those of the Western basin where ΔpH is rarely less than -0.1 pH unit.

Although both basins are supersaturated with calcite and aragonite, respectively, the Western basin is characterized by carbonate ions concentrations and saturation degrees lower than those in the other basin. This shows that, at a large time scale, the pH decrease can influence the dissolution of carbonate ions and then the biological activity of several marine organisms, especially the calcifying ones.

Acknowledgment

This work was funded by the EC FP7 “Mediterranean Sea Acidification in a changing climate” project (MedSeA ; grant agreement 265103 ; medsea-project.eu). The authors are pleased to thank the captain, the crew of the Spanish research vessel R/V Ángeles Alvariño and the chief scientists of the 2013 MedSeAcruise: Patrizia Ziveri (the coordinator of the MedSeA project) and Jordi Garcia-Orellana, for their excellent cooperation during and after the campaign. Authors are grateful to the National Council for Scientific Research (CNRS) in Lebanon for the PhD thesis scholarships granted to Mr. Abed El Rahman HASSOUN and to Miss Elissar GEMAYEL.

References

Aït-Ameur N. and Goyet C., 2006. Distribution and transport of natural and anthropogenic CO2 in the Gulf of Cadiz. *Deep Sea Research Part II: Topical Studies in Oceanography*, **53** (11-13), 1329-1343.

Alekin O.A., 1972. Saturation of Mediterranean Sea water with calcium carbonate. *Geochemistry*, **206**, 239-242.

Álvarez M., Perez F.F., Shoosmith D.R., and Bryden H.L., 2005. Unaccounted role of Mediterranean Water in the drawdown of anthropogenic carbon. *Journal of Geophysical Research-Oceans*, **110**, C09S03, doi:10.1029/2004JC002633.

Álvarez M., 2011. The CO2 system observations in the Mediterranean sea: Past, present and future. *In: Designing Med-SHIP: a Program for repeated oceanographic surveys.* N°43 in CIESM Workshop Monographs [F. Briand Ed.], 164, Monaco.

Álvarez M., Sanleón-Bartolomé H., Tanhua T., Mintrop L., Luchetta A., Cantoni C., Schroeder K., and Civitarese G., 2014. The CO2 system in the Mediterranean Sea: a basin wide perspective. *Ocean Science*, **10**, 69–92.

Artegiani A., Bregant D., Paschini E., Pinardi N., Raicich F., and Russo A., 1996a. The Adriatic Sea General Circulation, Part I: air-sea interactions and water mass structure. *Journal of Physical Oceanography*, **27**, 1492–1514.

Artegiani A., Bregant D., Paschini E., Pinardi N., Raicich F., and Russo A., 1996b. The Adriatic Sea General Circulation, Part II: baroclinic circulation structure. *Journal of Physical Oceanography*, **27**, 1515–1532.

Astraldi M. and Gasparini G.P., 1994. The seasonal characteristics of the circulation in the Tyrrhenian Sea. *In La Violette*, P. E., editor, Seasonal and Interannual Variability of the Western Mediterranean Sea, p. 115-134. American Geophysical Union.

Astraldi M., Balopoulos S., Candela J., Font J., Gacic M., Gasparini G.P., Manca B., Theocharis A., and Tintoré J., 1999. The role of straits and channels in understanding the characteristics of Mediterranean circulation. *Progress in Oceanography*, **44** (1–3), 65–108.

Bates N.R., Best M.H.P., Neely K., Garley R. , Dickson A.G., and Johnson R.J., 2012. Detecting anthropogenic carbon dioxide uptake and ocean acidification in the North Atlantic Ocean. *Biogeosciences*, **9**, 2509–2522, doi:10.5194/bg-9-2509-2012.

Bégovic M. and Copin-Montégut C., 2002. Processes controlling annual variations in the partial pressure of CO2 in surface waters of the central northwestern Mediterranean Sea (Dyfamed site). *Deep Sea Research Part II: Topical Studies in Oceanography*, **49** (11), 2031–2047.

Bergamasco A. and Malanotte-Rizzoli P., 2010. The circulation of the Mediterranean Sea: a historical review of experimental investigations. *Advances in Oceanography and Limnology*, **1** (1), 11–28.

Béthoux J.P., Gentili B., Morin P., Nicolas E., Pierre C. and Ruiz-Pino D., 1999. The Mediterranean Sea: a miniature ocean for climatic and environmental studies and a key for the climatic functioning of the North Atlantic. *Progress in Oceanography*, **44** (1–3), 131–146.

Brasseur P., Beckers J.-M., Brankart J.-M., and Schoenauen R., 1996. Seasonal temperature and salinity fields in the Mediterranean Sea: Climatological analyses of an historical data set. *Deep Sea Research Part I: Oceanographic Research Papers*, **43** (2), 159–192.

Broecker W.S., 1974. "NO", a conservative water-mass tracer. *Earth and Planetary Science Letters*, **23** (1), 100–107.

Cao L., Caldeira K., and Jain A.K., 2007. Effects of carbon dioxide and climate change on ocean acidification and carbonate mineral saturation. *Geophysical Research Letters*, **34** (L05607), doi:10.1029/2006GL028605.

Castaño-Carrera M., Pardo P.C., Alvarez M., Lavín A., Rodríguez C., Carballo R., Ríos A.F., and Pérez F.F., 2012. Anthropogenic carbon and water masses in the Bay of Biscay. *Ciencias Marinas*, **38** (1B), 191–207.
http://rcmarinas.ens.uabc.mx/index.php/cmarinas/article/viewArticle/1820.

Chernyakova A.M., 1976. Elements of the carbonate system in the Straits of Sicily (Tunis Strait) area. *Oceanology*, **16**, 36-39.

CIESM, 2008. Impacts of acidification on biological, chemical and physical systems in the Mediterranean and Black Seas. In: F. Briand (Ed.), No.36 in CIESM Workshop Monographs, Monaco, 124.

Collins S., Rost B., and Rynearson T.A., 2014. Evolutionary potential of marine phytoplankton under ocean acidification. *Evolutionary Applications*, **7**, 140–155, doi: 10.1111/eva.12120.

Copin-Montégut C., 1993. Alkalinity and carbon budgets in the Mediterranean Sea. *Global Biogeochemical Cycles*, **7** (4), 915–925, doi:10.1029/93GB01826.

Copin-Montégut C. and Bégovic M., 2002. Distributions of carbonate properties and oxygen along the water column (0-2000 m) in the central part of the NW Mediterranean Sea (Dyfamed site). Influence of the winter vertical mixing on air-sea CO2 and O2 exchanges. *Deep Sea Research Part II: Topical Studies in Oceanography*, **49** (11), 2049–2066.

Copin-Montégut C., Bernard A., and Claire C., 2004. Continuous pCO2 measurements in surface water during transect EUM4LPEU, doi:10.1594/PANGAEA.139915.

Dafner E., González Dávila M., Santana Casiano J.M., and Semperé R., 2001. Total organic and inorganic carbon exchange through Strait of Gibraltar in September 97. *Deep-Sea Research Part I: Oceanographic Research Papers*, **48** , 1217–1235.

De Carlo E.H., Mousseau L., Passafiume O., Drupp P.S., and Gattuso J.-P., 2013. Carbonate Chemistry and Air–Sea CO2 Flux in a NW Mediterranean Bay Over a Four-Year Period: 2007–2011. *Aquatic Geochemistry*, **19**, 399–442, doi:10.1007/s10498-013-9217-4.

De la Paz M., Debelius B., Macias D., Gomez-Parra A., and Forja J., 2008. Inorganic carbon dynamic and the influence of tidal mixing processes on the Strait of Gibraltar (SW Spain). *Continental Shelf Research*, **38**, 1827–1837.

De la Paz M., Gomez-Parra A., and Forja J., 2009. Seasonal variability of surface fCO2 in the Strait of Gibraltar. *Aquatic Sciences*, **71**, 55–64.

Delgado O. and Estrada M., 1994. CO2 system in a Mediterranean frontal zone. *Scientia Marina*, **58** (3), 237-250.

Dickson A.G., 1990. Standard potential of the reaction: AgCl(s) + 1/2H2 = Ag(s) + HCl(aq), and the standard acidity constant of the ion HSO4 in synthetic sea water from 273.15 to 318.15 K. *Journal of Chemical Thermodynamics*, **22**, 113–127.

DOE, 1994. Handbook of methods for the analysis of the various parameters of the carbon dioxide system in sea water. Version 2, A. G. Dickson & C. Goyet, eds., *ORNL/CDIAC-74*.

Dore J.E., Lukas R., Sadler D.W., Church M.J., and Karl D.M., 2009. Physical and biogeochemical modulation of ocean acidification in the central North Pacific. *Proceedings of the National Academy of Sciences of the United States of America*, **106** (30), 12235–12240, doi: 10.1073/pnas.0906044106.

Durieu de Madron X., Zervakis V., Theocharis A., and Georgopoulos D., 2005. Comments on "Cascades of dense water around the world". *Progress in Oceanography*, **64**, 83–90.

Durrieu de Madron X., Houpert L., Puig P., Sanchez-Vidal A., Testor P., Bosse A., Estournel C., Somot S., Bourrin F., Bouin M.N, Beauverger M., Beguery L., Calafat A., Canals M., Coppola L., Dausse D., D'Ortenzio F., Font J., Heussner S., Kunesch S., Lefevre D., Le Goff H., Martín J., Mortier L., Palanques A., and Raimbault P., 2013. Interaction of dense dense shelf water cascading and open-sea convection in the Northwestern Mediterranean during winter 2012. *Geophysical Research Letters*, **40**, 1379–1385, doi:10.1002/grl.50331.

EEA, 2002. Europe's biodiversity—biogeographical regions and seas. Seas around Europe. The Mediterranean Sea—blue oxygen-rich, nutrient poor waters.

Fajar N.M., Pardo P.C., Carracedo L., Vázquez-Rodríguez M., Ríos A.F., and Pérez F.F., 2012. Trends of the anthropogenic CO2 along 20ºW in the Iberian basin. *Ciencias Marinas*, **38** (1B), 287–306. http://rcmarinas.ens.uabc.mx/index.php/cmarinas/article/view/1810.

Flecha S., Pérez F.F., Navarro G., Ruiz J., Olivé I., Rodríguez-Gálvez S., Costas E., and Huertas I.E., 2012. Anthropogenic carbon inventory in the Gulf of Cádiz. *Journal of Marine Systems*, **92**, 67–75.

Gasparini G.P., Ortona A., Budillon B., Astraldi M., and Sansone E., 2005. The effect of the Eastern Mediterranean Transient on the hydrographic characteristics in the Strait of Sicily and in the Tyrrhenian Sea. *Deep Sea Research Part I: Oceanographic Research Papers*, **52**, 915–935.

Goyet C. and Poisson A., 1989. New determination of carbonic-acid dissociation-constants in seawater as a function of temperature and salinity. *Deep Sea Research Part A. Oceanographic Research Papers*, **36** (11), 1635-1654.

Goyet C., Hassoun A.E.R., and Gemayel E., 2015a. Carbonate system during the May 2013 MedSeA cruise., doi:10.1594/PANGAEA.841933.

Goyet C., Gemayel E., and Hassoun A.E.R., 2015b. Underway pCO2 in surface water during the 2013 MedSEA cruise, doi:10.1594/PANGAEA.841928.

Gruber N., Sarmiento J.L., and Stocker T.F., 1996. An improved method for detecting anthropogenic CO2 in the oceans. *Global Biogeochemical Cycles*, **10**, 809–837, doi:199610.1029/96GB01608.

Hansen H.P., 1999. Determination of oxygen. Methods of Seawater Analysis, K. Grasshoff, K. Kremling, and M. Ehrhardt, Eds., *VerlagChemie*, Weinheim, 75–89.

Hassoun A.E.R., Guglielmi V., Gemayel E., Goyet C., Abboud-Abi Saab M., Giani M., Ziveri P., Ingrosso G., and Touratier F., 2015 a. Is the Mediterranean Sea Circulation in a Steady State. *Journal of Water Resources and Ocean Science*, **4** (1), 6–17, doi: 10.11648/j.wros.20150401.12.

Hassoun A.E.R., Gemayel E., Krasakopoulou E., Goyet C., Abboud-Abi Saab M., Ziveri P., Touratier F., Guglielmi V. and Falco C., 2015 b. Modeling of the Total Alkalinity and the Total Inorganic Carbon in the Mediterranean Sea. *Journal of Water Resources and Ocean Science*, **4** (1), 24–32, doi: 10.11648/j.wros.20150401.14.

Hilmi N., Allemand D., Haraldsson G., Reynaud S., Cinar M., Jeffree R.A., Cooley S., Hattam C., Safa A., and Dupont S., 2014. Exposure of Mediterranean Countries to Ocean Acidification. *Water*, **6**, 1719–1744, doi:10.3390/w6061719.

Huertas I.E., Navarro G., Rodriguez-Galvez S., and Lubian L.M., 2006. Temporal patterns of carbon dioxide in relation to hydrological conditions and primary production in the northeastern shelf of the Gulf of Cadiz (SW Spain). *Deep Sea Research Part II: Topical Studies in Oceanography*, **53**, 1344–1362.

Huertas I.E., Rios A.F., Garcia-Lafuente J., Makaoui A., Rodriguez-Galvez S., Sanchez-Roman A., Orbi A., Ruiz J., and Pérez F.F., 2009. Anthropogenic and natural CO2 exchange through the Strait of Gibraltar. *Biogeosciences*, **6**, 647–662.

Ishimatsu A., Hayashi M., Lee K.-S., Kikkawa T., and Kita J., 2005. Physiological effects of fishes in a high-CO2 world. *Journal of Geophysical Research*, **110** (10), 1029/2004JC002564.

Kortzinger A., Mintrop L., and Duinker J.C., 1998. On the penetration of anthropogenic CO2 into the North Atlantic Ocean. *Journal of Geophysical Research*, **103** (C9), 18681–18689.

Krasakopoulou E., Souvermezoglou E., and Goyet C., 2011. Anthropogenic CO2 fluxes in the Otranto Strait (E. Mediterranean) in February 1995. *Deep-Sea Research Part I: Oceanographic Research Papers*, **58**, 1103–1114.

Kroeker K.J., Kordas R. L., Crim R., Hendriks I.E., Ramajo L., Singh G.S., Duarte C.M., and Gattuso J.-P., 2013. Impacts of ocean acidification on marine organisms: quantifying sensitivities and interaction with warming. *Global Change Biology*, **19**, 1884–1896. doi: 10.1111/gcb.12179.

Lascaratos A., Roether W., Nittis K., and Klein B., 1999. Recent changes in deep water formation and spreading in the eastern Mediterranean Sea: a review. *Progress in Oceanography*, **44**, 5–36.

Lee K., Choi S.-D., Park G.-H., Wanninkhof R., Peng T.H., Key R.M., Sabine C.L., Feely R.A., Bullister J.L., Millero F.J., 2003. An updated anthropogenic CO2 inventory in the Atlantic Ocean. *Global Biogeochemical Cycles*, **17** (4), 1116, doi:10.1029/2003GB002067.

Lee K., Sabine C.L., Tanhua T., Kim T.W., Feely R.A., and Kim H.C., 2011. Roles of marginal seas in absorbing and storing fossil fuel CO2. *Energy and Environmental Science*, **4**, 1133–1146, doi:10.1039/C0EE00663G.

Lo Monaco C., Goyet C., Metzl N., Poisson A., and Touratier F., 2005. Distribution and inventory of anthropogenic CO2 in the Southern Ocean : comparison of three data-based methods. *Journal of Geophysical Research*, **110**, C09S02. doi:10.1029/2004JC002571.

Malanotte-Rizzoli P., Manca B.B., Ribera d'Alcalà M., Theocharis A., Bergamasco A., Bregant D., Budillon G., Civitarese G., Georgopoulos D., Michelato A., Sansone E., Scarazzato P. and Souvermezoglou E., 1997. A synthesis of the Ionian Sea hydrography, circulation and water mass pathways during POEM-Phase I. *Progress in Oceanography*, **39**, 153–204.

Manning A.C. and Keeling R.F., 2006. Global oceanic and land biotic carbon sinks from the Scripps atmospheric oxygen flask sampling network. *Tellus*, **58B**, 95–116.

Millero F.J., Morse J., and Chen C.-T., 1979. The carbonate system in the western Mediterranean sea. *Deep Sea Research Part A, Oceanographic Research Papers*, **26** (12), 1395–1404.

Millot C., 1999. Circulation in the Western Mediterranean Sea. *Journal of Marine Systems*, **20** (1–4), 423–442.

Oudot C., Gerard R., Morin P., and Gningue I., 1988. Precise shipboard determination of dissolved oxygen (Winkler procedure) for productivity studies with commercial system. *Limnology and Oceanography*, **33**, 146–150.

Palmiéri J., Orr J.C., Dutay J.-C., Béranger K., Schneider A., Beuvier J., and Somot S., 2015. Simulated anthropogenic CO2 uptake and acidification of the Mediterranean Sea. *Biogeosciences*, **12,** 781–802, doi:10.5194/bg-12-781-2015.

Pierrot D., Lewis E., and Wallace D.W.R., 2006. MS Excel Program Developed for CO2 System Calculations.,*ORNL/CDIAC-105*. Carbon Dioxide Information Analysis Center, Oak Ridge National Laboratory, U.S. Department of Energy, Oak Ridge, Tennessee.

Povero P., Hopkins T.S., and Fabiano M., 1990. Oxygen and nutrient observations in the Southern Tyrrhenian Sea. *Oceanologica Acta*, **13** (3), 299–305.

Puig. P., Durrieu de Madron X., Salat J., Schroeder K., Martín J., Karageorgis A.P., Palanques A., Roullier F., Lopez-Jurado J.L., Emelianov M., Moutin T., and Houpert L., 2013. Thick bottom nepheloid layers in the western Mediterranean generated by deep dense shelf water cascading. *Progress in Oceanography*, **111**, 1–23.

Pujo-Pay M., Conan P., Oriol L., Cornet-Barthaux V., Falco C., Ghiglione J.-F., Goyet C., Moutin T., and Prieur L., 2011. Integrated survey of elemental stoichiometry (C, N, P) from the western to eastern Mediterranean Sea. *Biogeosciences*, **8**, 883–899, doi:10.5194/bg-8-883-2011.

Rees A.P., Clark D.R., Turk-Kubo K.A., Zehr J.P., and Al-Moosawi L., 2013. Acidification of the marine nitrogen cycle. *ASLO 2013 Aquatic Sciences Meeting*, 17-22 February 2013, New Orleans Louisiana, USA. http://www.sgmeet.com/aslo/neworleans2013/viewabstract2.asp?AbstractID=10910.

Ribas-Ribas M., Gómez-Parra A., and Forja J.M., 2011. Air–sea CO2 fluxes in the northeastern shelf of the Gulf of Cádiz (southwest Iberian Peninsula). *Marine Chemistry*, **123**, 56–66.

Ríos A.F., Pérez F.F., and Fraga F., 2001. Long-term (1977–1997) measurements of carbon dioxide in the Eastern North Atlantic: evaluation of anthropogenic input. *Deep Sea Research Part II: Topical Studies in Oceanography*, **48**, 2227–2239.

Ríos A.F., Vázquez-Rodríguez M., Padín X.A. and Pérez F.F., 2010. Anthropogenic carbon dioxide in the South Atlantic western basin. *Journal of Marine Systems*, **83**, 38–44.

Rivaro P., Messa R., Massolo S., and Frache R., 2010. Distributions of carbonate properties along the water column in the Mediterranean Sea: Spatial and temporal variations. *Marine Chemistry*, **121**, 236–245.

Robinson A.R., Leslie W.G., Theocharis A., and Lascaratos A., 2001. Mediterranean Sea circulation. *In Encyclopedia of Ocean Sciences*, edited by J. H. Steele et al., 1689–1705 pp., Elsevier, New York.

Roether W. and Schlitzer R., 1991. Eastern Mediterranean deep water renewal on the basis of chlorofluoromethane and tritium data. *Dynamics of Atmospheres and Oceans*, **15**, 333–354.

Roether W., Manca B.B., Klein B., Bregant D., Georgopoulos D., Beitzel V., Kovacevic V., and Luchetta A., 1996. Recent changes in Eastern Mediterranean deep waters. *Science*, **271**, 333–335.

Roether W., Klein B., Beitzel V., and Manca B.B., 1998. Property distributions and transient-tracer ages in Levantine Intermediate Water in the Eastern Mediterranean. *Journal of Marine Systems*, **18** , 71–87.

Roether W. and Lupton J.E., 2011. Tracers confirm downward mixing of Tyrrhenian Sea upper waters associated with the Eastern Mediterranean Transient. *Ocean Science*, **7**, 91–99, doi:10.5194/os-7-91-2011.

Sabine C.L., Feely R.A., Gruber N., Key R.M., Lee K., Bullister J.L., Wanninkhof R., Wong C.S., Wallace D.W.R., Tilbrook B., Millero F.J., Peng T.-H., Kozyr A., Ono T., Ríos A.F. 2004. The oceanic sink for anthropogenic CO2. *Science*, **305**, 367–371.

Sabine C.L. and Tanhua T., 2010. Estimation of anthropogenic CO2 inventories in the ocean. *Annual Review of Marine Science*, **2**,175–198.

Sanford E., Gaylord B., Hettinger A., Lenz E.A., Meyer K. and Hill T.M., 2014. Ocean acidification increases the vulnerability of native oysters to predation by invasive snails. *Royal Society Publishing*, doi: 10.1098/rspb.2013.2681.

Santana-Casiano J.M., Gonzalez-Davila M., and Laglera L.M., 2002. The carbon dioxide system in the Strait of Gibraltar. *Deep Sea Research Part II: Topical Studies in Oceanography*, **49**, 4145–4161.

Schlitzer R., Roether W., Oster H., Junghans H., Hausmann M., Johannsen H., and Michelato A., 1991. Chlorofluoromethane and oxygen in the eastern Mediterranean. *Deep Sea Research Part I: Oceanographic Research Papers*, **38**, 1531–1551.

Schlitzer R., 2014. Ocean Data View, http://odv.awi.de.

Schröder K., Gasparini G.P., Tangherini M., and Astraldi M., 2006. Deep and intermediate water in the western Mediterranean under the influence of the Eastern Mediterranean Transient. *Geophysical Research Letters*, **33** (L21607), doi:10.1029/2006GL027121.

Schröder A., Ribotti A., Borghini M., Sorgente R., Perilli A., and Gasparini G.P., 2008. An extensive western Mediterranean deep water renewal between 2004 and 2006. *Geophysical Research Letters*, **35** (L18605), doi:10.1029/2008GL035146.

Schneider A., Wallace D.W.R., and Körtzinger A., 2007. Alkalinity of the Mediterranean Sea. *Geophysical Research Letters*, **34**, L15608, doi:10.1029/2006GL028842.

Schneider A., Tanhua T., Körtzinger A., and Wallace D.W.R., 2010. High anthropogenic carbon content in the eastern Mediterranean. *Journal of Geophysical Research*, **115**, C12050, doi: 10.1029/2010JC006171.

Schneider A., Tanhua T., Roether W., and Steinfeldt R., 2014. Changes in ventilation of the Mediterranean Sea during the past 25 year. *Ocean Science*, **10**, 1–16, doi:10.5194/os-10-1-2014, 2014.

Seibel B.A., and Walsh P.J., 2001. Potential impacts of CO2 injection on deep-sea biota. *Science*, **294**, 319–320.

Sparnocchia S., Gasparini G.P., Astraldi M., Borghini M., and Pistek P., 1999. Dynamics and mixing of the Eastern Mediterranean outflow in the Tyrrhenian Sea. *Journal of Marine Systems*, **20**, 301–317.

Stöven T. and Tanhua T., 2014. Ventilation of the Mediterranean Sea constrained by multiple transient tracer measurements. *Ocean Science*, **10**, 439-457, doi:10.5194/os-10-439-2014.

Stratford K. and Williams R., 1997. A tracer study of the formation, dispersal, and renewal of Levantine Intermediate Water. *Journal of Geophysical Research*, **102** (C6), 12539–12549.

Stratford K., Williams R.G., and Drakopoulos P.G., 1998. Estimating climatological age from a model-derived oxygen-age relationship in the Mediterranean. *Journal of Marine Systems*, **18**, 215–226.

Touratier F. and Goyet C., 2004. Applying the new TrOCA approach to assess the distribution of anthropogenic CO2 in the Atlantic Ocean. *Journal of Marine Systems*, **46**, 181–197.

Touratier F., Goyet C., and Azouzi L., 2007. CFC-11, 114C, and 3H tracers as a means to assess anthropogenic CO2 concentrations in the ocean. *Tellus*, **59B**, 318–325.

Touratier F and Goyet C., 2009. Decadal evolution of anthropogenic CO2 in the northwestern Mediterranean Sea from the mid-1990s to the mid-2000s. *Deep Sea Research Part I: Oceanographic Research Papers*, **156**, 1708-1716.

Touratier F. and Goyet C., 2011. Impact of the Eastern Mediterranean Transient on the distribution of anthropogenic CO2 and first estimate of acidification for the Mediterranean Sea. *Deep Sea Research Part I: Oceanographic Research Papers*, **58**,1–15.

Touratier F., Guglielmi V., Goyet C., Prieur L., Pujo-Pay M., Conan P., and Falco C., 2012. Distributions of the carbonate system properties, anthropogenic CO2, and acidification during the 2008 BOUM cruisem (Mediterranean Sea). *Biogeosciences Discussion*, **9**, 2709–2753, doi:10.5194/bgd-9-2709-2012.

UNEP/MAP—Plan Bleu, 2009. State of the environment and development in the Mediterranean. UNEP/MAP—Blue Plan, Athens, 200 pp.

Uppström L.R., 1974. The boron/chlorinity ratio of the deep-sea water from the Pacific Ocean. *Deep Sea Research and Oceanographic Abstracts*, **21** (2), 161–162.

Vázquez-Rodríguez M., Touratier F., Lo Monaco C., Waugh D.W., Padin X.A., Bellerby R.G.J., Goyet C., Metzl N., Ríos A.F., and Pérez F.F., 2009. Anthropogenic carbon

distributions in the Atlantic Ocean: data-based estimates from the Arctic to the Antarctic. *Biogeosciences*, **6**, 439–451. www.biogeosciences.net/6/439/2009/, doi:10.5194/bg-6-439-2009.

Waugh D.W., Hall T.M., McNeil B.I., Key R., and Matear R.J., 2006. Anthropogenic CO2 in the oceans estimated using transit time distributions. *Tellus B*, **58**, 376–389, doi:10.1111/j.1600-10 0889.2006.00222.x.

Wolf-Gladrow D.A. and Rost B., 2014. Ocean Acidification and Oceanic Carbon Cycling. Global Environmental Change. *Handbook of Global Environmental Pollution*, **1**, 103–110.

Wüst G., 1961. On the vertical circulation of the Mediterranean Sea. *Journal of Geophysical Research*, **66** (10), 3261–3271, doi:10.1029/JZ066i010p03261.

Ziveri P., and Grelaud M., 2013a. Continuous thermosalinograph oceanography along Ángeles Alvariño cruise track MedSeA2013. Universitat Autònoma de Barcelona, doi:10.1594/PANGAEA.822153.

Ziveri P., and Grelaud M., 2013b. Physical oceanography during Ángeles Alvariño cruise MedSeA2013. Universitat Autònoma de Barcelona, doi:10.1594/PANGAEA.822162.

Ziveri P., and Grelaud M., 2013c. Physical oceanography measured on water bottle samples during Ángeles Alvariño cruise MedSeA2013. Universitat Autònoma de Barcelona, doi:10.1594/PANGAEA.822163.

http://odv.awi.de/en/data/ocean/carina_bottle_data/, CARINA project data collection—version 1.2.

http://www.climate.gov/

http://co2now.org/

http://medsea-project.eu/

http://medseaoceancruise.wordpress.com/

Article VII: What are the tipping points for the Mediterranean Sea Acidification?

Goyet, C., Hassoun, A.E.R., **Gemayel, E.**, et al. (2015)

Submitted to Climate Dynamics

What are the tipping points for the Mediterranean Sea acidification?

Catherine GOYET[1], Abed El Rahman HASSOUN[2], Elissar GEMAYEL[1,2], Franck TOURATIER[1], Marie ABBOUD-ABI SAAB[2] and Véronique GUGLIELMI[1]

[1]Université de Perpignan Via Domitia, IMAGES_ESPACE-DEV, 52 avenue Paul Alduy, 66860 Perpignan Cedex, France, and ESPACE-DEV UMR UG UA UM IRD, Maison de la télédétection, 500 rue Jean-François Breton, 34093 Montpellier Cedex 5, France.
[2]National Council for Scientific Research, National Center for Marine Sciences, Box 534, Batroun, Lebanon.

Abstract

This study aims to forecast the acidification variation (ΔpH) of the Mediterranean waters over the next few decades and beyond this century. In order to do so, we calculated and fitted the theoretical values based upon initial conditions from data of the 2013 MedSeA cruise. These estimates have been performed both for the Western and for the Eastern basins based upon their respective physical (temperature and salinity) and chemical (total alkalinity and total inorganic carbon) properties. The results allow us to point out four tipping points, including one when the Mediterranean Sea would become acid (pH<7).

In order to provide an associated time scale to the theoretical results we used two of the IPCC (2007) atmospheric CO_2 scenarios. Under the most optimistic scenario of the "Special Report: Emissions Scenarios" (SRES) of the IPCC (2007), the results indicate that in 2100, pH may decrease by 0.245 in the Western basin and 0.242 in the Eastern basin (compared to the pre-industrial pH). Whereas for the most pessimistic SRES scenario of the IPCC (2007), the results for year 2100, forecast a pH decrease of 0.462 and 0.457, for the Western and for the Eastern basins, respectively. Acidification, which increased unprecedentedly in recent years, will rise almost similarly in both basins after the end of this century. These results further suggest that both basins may become undersaturated (< 1) with respect to calcite and aragonite in deep Mediterranean waters (at the base of the mixed layer depth) by the end of the next century.

Keywords: Anthropogenic CO_2; Seawater acidification; Modeling; Carbonate system; Mediterranean Sea.

Introduction

Oceanic uptake of anthropogenic carbon dioxide (C_{ANT}) is altering the seawater chemistry of the world's oceans with various consequences on marine ecosystems. Ocean acidification is one of the consequences of approximately 79 million tons of carbon dioxide (CO_2) released into the atmosphere every day from fossil fuel burning, deforestation and cement production (IPCC, 2007). As a result of human activities, today's atmospheric CO_2 concentration is rising at a rate of ~ 0.5% $year^{-1}$ (Forster *et al.*, 2007), which is ~100 times faster than any change during the past 650 000 years (Royal Society, 2005 ; Siegenthaler *et al.*, 2005). The atmospheric increase of CO_2 from 2012 to 2013 was 2.9 microatmosphere (µatm), which is the largest annual increase for the period 1984-2013 (WMO, 2014). Oceans play a key role in the mitigation of the increasing atmospheric pCO_2. Approximately 25% of the total human emissions of CO_2 to the atmosphere is accumulating into the ocean (Sabine *et al.*, 2004 ; Mikaloff-Fletcher *et al.*, 2006 ; Le Quéré *et al.*, 2010 ; Sabine *et al.*, 2011). Without this buffer capacity of the oceans, the CO_2 content in the atmosphere would have been much higher and global warming and its consequences more dramatic.

Today there is a rapid population growth on the Mediterranean coast, from 165 million inhabitants in 2000 to 187 million in 2007, an increase of 13% (Eurostat, 2009). Although the Mediterranean Sea represents less than 1% of the global world's ocean surface (UNEP/MAP-Plan Bleu, 2009), it is under important anthropogenic pressure. Thus, the Mediterranean Sea is acidifying quickly and its marine ecosystems are under stress. A surface pH decrease of 0.05 unit has been recorded since the pre-industrial era (Dore *et al.*, 2009; Bates *et al.*, 2012) and models predict an additional pH decline by 0.3-0.5 pH unit during the 21st century depending upon which Intergovernmental Panel on Climate Change (IPCC) CO_2 emission scenario (Caldeira and Wickett, 2005 ; Orr *et al.*, 2005 ; Feely *et al.*, 2009) is used for the forecast. In the Mediterranean Sea, Géri *et al.* (2014) forecasted an evolution ranging between 0.3 and 0.4 pH unit decrease in the surface water of the Northwestern Mediterranean Sea by the end of this century. Nevertheless, little is known about the present and future situation of the seawater acidification in the Mediterranean waters, particularly in the deep waters, and its influences on marine organisms, community structure and the entire ecosystems.

In this paper, using the chemical equilibrium equations, we first calculate the acidification variations (ΔpH) due to the C_{ANT} penetration both into the Western and into the Eastern Mediterranean basins. Then, in order to present not only discrete but also continuous estimates of acidification, we fitted these results with simple functions (one for each basin). Subsequently, we present and discuss the impacts of this acidification on the carbonate saturation states in the Mediterranean Sea. In addition, we define four major tipping points of the Mediterranean Sea acidification.

Methodology

1.1. Data set

In order to illustrate the largest difference that can occur in the Mediterranean Sea we choose as initial conditions, data from two stations located at the extreme Northwestern and Eastern sides of the Mediterranean Sea.

Hydrologic properties [salinity, S and temperature, T (ºC)] were measured *in situ* and described earlier (Hassoun et al., 2015a). The precisions of the measurements were ± 0.001 ºC for T, and ± 0.0003 for S. For total alkalinity (A_T) and total dissolved inorganic carbon (C_T), seawater samples were collected at all stations throughout the water column. The accuracy of A_T and C_T measurements was determined to be ± 2 µmol.kg^{-1} for A_T and ± 4 µmol.kg^{-1} for C_T (Hassoun *et al.,* 2015b,c; Gemayel *et al.*, 2015a).

Next, in section 2.2, we describe the calculation of the theoretical pH variations, at the base of the wintertime mixed layer depth, as a function of theoretical anthropogenic carbon concentrations ranging from 0 to 3000 µmol.kg^{-1}.

1.2. Forecast of pH variations as a function of anthropogenic carbon

In order to forecast the Mediterranean Sea acidification beyond the end of this century, we calculate pH from the measured A_T (A_T^m) at the base of the wintertime mixed layer depth (Table 1) and a theoretical C_T calculated as follows:

At a given year C_T was calculated by adding a theoretical C_{ANT} concentration to the preindustrial C_T concentration (C_T^{preind}) , as follows:

$$C_T = C_T^{preind} + C_{ANT} \quad \text{(I)}$$

In order to calculate C_T^{preind} we made the assumption that the temporal variation of CO_2 fugacity (fCO_2) in seawater follows that of the atmosphere. Thus, C_T^{preind} is calculated from A_T^m, S^m, T^m, (fCO_2^c – 116), where fCO_2^c is calculated from A_T^m, S^m, T^m, C_T^m. The number "116" is the difference between the atmospheric preindustrial fCO_2 = 280 µatm and the measured atmospheric 2013 fCO_2 = 396 µatm (NOAA; http://co2now.org/current-co2/co2-now), thus 396 – 280 =116 µatm.

In order to provide a forecast over a very long range, we choose the theoretical values of C_{ANT} to increase from 0 to 3000 µmol.kg^{-1} (corresponding to an unlikely huge penetration of anthropogenic carbon that would, more than double the actual amount of C_T in the Mediterranean Sea).

Table 1. The 2013 measured S, T, A_T, C_T at the base of the wintertime mixed layer depth and the calculated $C_{Tpreindustrial}$ and $pH_{preindustrial}$ in the Western and Eastern basins of the Mediterranean Sea.

Parameters	Latitude (°N)	Longitude (°E)	Mixed Layer Depth (m)	S^m	T^m (°C)	A_T^m (µmol.kg^{-1})	C_T^m (µmol.kg^{-1})	pH^c	pH^{preind}	C_T^{preind} (µmol.kg^{-1})
Western basin	40.0736	5.94744	150	37.9812	13.487	2537	2261	8.087	8.215	2181
Eastern basin	34.22416	33.22504	200	39.0775	15.845	2634	2311	8.099	8.225	2224

pH^c was then calculated from T^m, A_T^m (Table 1), and C_T^m (Table 1 and Eq.I). The calculation was made according to the output conditions of temperature and pressure, based on the A_T-C_T combination and choosing the set of apparent constants (K_1 and K_2) of Goyet and Poisson (1989), the sulfate constants of Dickson (1990), the seawater scale and the borate constants of Uppström (1974). Note that the choice of constants here is not very important since we are looking at variations. The pre-industrial pH (pH^{preind}; Table 1) was calculated from the measured A_T^m (since A_T is not affected by the accumulation of C_{ANT} in seawater) and C_T^{preind} (from {A_T^m, S^m, T^m, [fCO_2^c – 116]} as mentioned above).

Thereafter, the pH variation (ΔpH) is calculated from the computed pH and the pre-industrial pH as follows:

$$\Delta pH = pH - pH_{preind} \quad \text{(II)}$$

For each basin, we then fitted the discrete values of ΔpH as a function of C_{ANT}.

2. Results and discussion

2.1. Acidification estimates of the Mediterranean Sea

The results are shown in Figure 1. It illustrates that the largest difference in ΔpH between the Western and the Eastern basins of the Mediterranean Sea will occur when C_{ANT} will range from 100 µmol.kg^{-1} to 900 µmol.kg^{-1}. This is due to the different oceanographic characteristics (T, S, A_T, and C_T) in each main basin. However, beyond this C_{ANT} range (corresponding to a decrease in pH larger than 1.3 pH unit), the chemical equilibrium of the CO_2/carbonate system in seawater will induce very similar variations of pH (ΔpH). For the sake of clarity, since the largest pH variations occur for C_{ANT} < 1500 µmol.kg^{-1}, in Figure 1, we have limited the x axis (C_{ANT}) to 2000 µmol.kg^{-1}.

This figure (Fig.1) clearly illustrates the seawater buffer effect, and thus the non-linear variation of pH as a function of C_{ANT} penetration. From C_{ANT} = 0 to C_{ANT} = 800 µmol.kg^{-1}, ΔpH will vary by -1.5 pH unit, while beyond this range, from C_{ANT} = 800 µmol.kg^{-1} to C_{ANT} = 1800 µmol.kg^{-1} the variation of pH will only be of -0.5 pH unit. Consequently, Fig.1 shows that the largest Mediterranean Sea pH decrease due to massive input of anthropogenic carbon (C_{ANT} > 1800 µmol.kg^{-1}) would remain close to -2 pH unit. Thus, the results of this model provide a reasonable limit of pH variations for future laboratory and mesocosms studies.

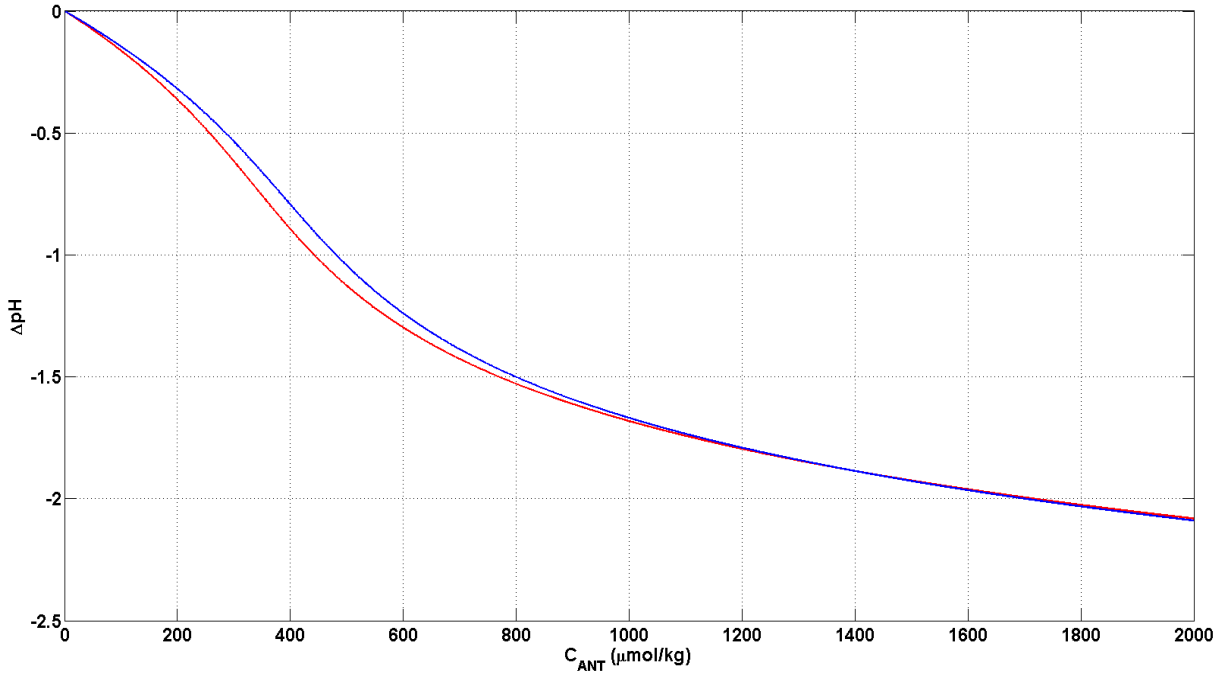

Fig.1. Theoretical estimates of pH variations as a function of C_{ANT} ($0 < C_{ANT} < 2000$ µmol.kg^{-1}) in the Western (red curve) and Eastern basins (blue curve) of the Mediterranean Sea.

In addition, since pH^c (Table 1) is > 7, this figure (Fig.1) illustrates that at ΔpH = -1.215 for the Western Mediterranean Sea (or at ΔpH = -1.225 for the Eastern Mediterranean Sea), the seawater pH will be neutral (pH = 7.00). Thus, the corresponding addition of C_{ANT} (548 µmol.kg^{-1} and 591 µmol.kg^{-1}, for the Western and Eastern basins the Mediterranean Sea, respectively), indicates a tipping point (TP_{pH7}), beyond which, the Mediterranean Sea waters will become acid (pH < 7.00).

In the Western basin, ΔpH follows a simple polynomial function of degree 7 (Eq.III; red line Fig.1) of C_{ANT} :

$$\Delta pH = 0.03895\ X^7 - 0.03946\ X^6 - 0.1747\ X^5 + 0.2054\ X^4 + 0.07289\ X^3 + 0.0001649\ X^2 - 0.3497\ X - 1.915 \quad \text{(III)}$$

with $X = (C_{ANT} - 1500)/866.5$ where the number "1500" represents the mean of C_{ANT} since we choose $0 < C_{ANT} < 3000$ µmol.kg^{-1}, and the number "866.5" represents the C_{ANT} standard deviation. The $r^2 = 0.9996$ of equation III indicates the goodness of this fit.

In the Eastern basin, ΔpH also follows a simple polynomial function of degree 7 (Eq.IV; green line Fig.1) of C_{ANT}:

$$\Delta pH = 0.0363\ X^7 - 0.0476\ X^6 - 0.1453\ X^5 + 0.2213\ X^4 + 0.009255\ X^3 + 0.01867\ X^2 - 0.3486\ X - 1.918 \quad \text{(IV)}$$

with X still equals to $(C_{ANT} - 1500)/866.5$. The $r^2 = 0.9997$ of equation IV indicates the goodness of this fit.

These fits (Eq.III and Eq.IV) are provided to forecast the pH variations in each basin of the Mediterranean Sea, based only upon C_{ANT} concentrations with $0 < C_{ANT} < 3000$ µmol.kg^{-1}. Inversely, it could be possible to estimate C_{ANT} from accurate measurements of ΔpH over several years (decades).

In figure 2, we have made a zoom of figure 1 for $0 < C_{ANT} < 700$ µmol.kg^{-1}, and we have added two strait lines which are the linear fits of each curve in the range $0 < C_{ANT} < 70$ µmol.kg^{-1} (corresponding to the present C_{ANT} penetration). Figure 2 illustrates that from now on, a linear interpolation will provide an unrealistic, very optimist (small) pH decrease. The chemical properties of seawater have now reached a tipping point where a small addition of anthropogenic carbon will induce a non-linear, relatively large pH drop (Fig. 2). This is happening now. As anthropogenic carbon continually penetrates into the Mediterranean Sea, the pH decreases more sharply from one day to the next.

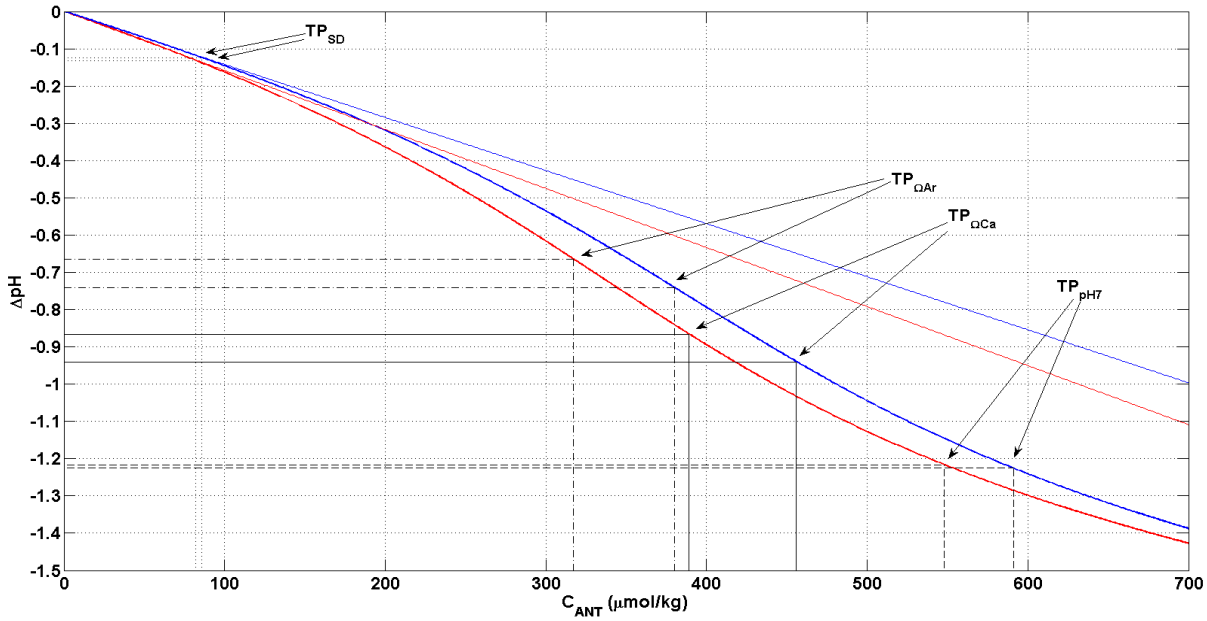

Fig.2. Zoom of the theoretical estimates of pH variations as a function of C_{ANT} in the Western and Eastern basins of the Mediterranean Sea. The red and green strait lines are the linear fits of the red and blue curves in the range $0 < C_{ANT} < 70$ µmol.kg^{-1}, respectively (Equations : ΔpH = - 0.00158439 C_{ANT} [red] and ΔpH = - 0.00142387 C_{ANT} [blue]).

The differences between ΔpH of the linear fits and the theoretical ΔpH (curves) as a function of C_{ANT} (< 1200 µmol.kg^{-1}, where the largest differences are observed), are shown in figure 3. This figure illustrates clearly a tipping point of "Sharp Decrease" in pH (TP_{SD}), at C_{ANT} = 82 µmol.kg^{-1} for the Western Mediterranean Sea (and at C_{ANT} = 86 µmol.kg^{-1} for the Eastern Mediterranean Sea), where the variation of pH deviates from a linear relationship with C_{ANT} penetration, and where a small addition of C_{ANT} provokes a sharp decrease in pH. Thus, today, a small additional input of anthropogenic carbon into the Mediterranean Sea would have a more significant impact than in the past, on its acidification and therefore on its ecosystems.

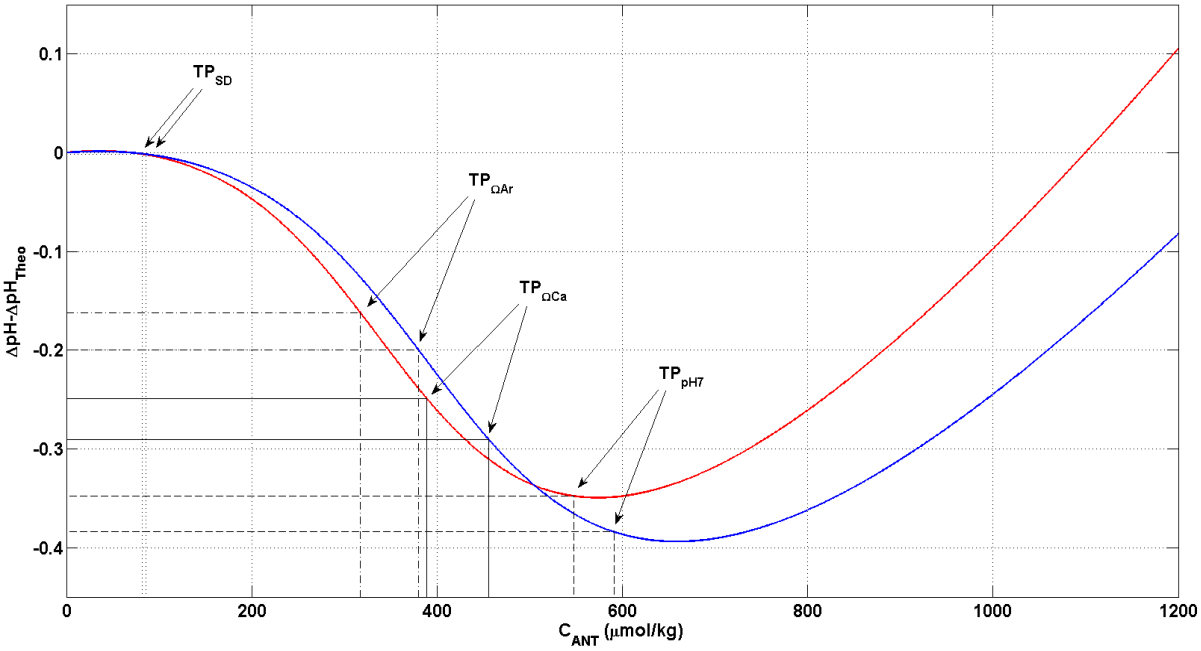

Fig.3. The distribution of differences between the experimental and theoretical ΔpH as a function of anthropogenic CO_2.

2.2. What are the consequences of the increasing anthropogenic CO_2 concentrations on the calcium carbonate (calcite and aragonite) saturation states in the Mediterranean Sea waters?

In order to assess the influence of the increasing C_{ANT} concentrations, we also computed (via the program "CO2Sys"), the calcium carbonate saturation via the two forms calcite and aragonite (Ω_{Ca} and Ω_{Ar}). As a reminder, Ω_{Ca} and Ω_{Ar} are proportional to the product of concentrations of calcium ions and carbonate ions dissolved in seawater (Ω_i = Cste x [Ca^{++}] x [CO_3^{--}]).

When $\Omega_i > 1$, there is oversaturation of the dissolved calcium carbonate. Thus, it will tend to precipitate. Corals and coralline sand are mainly made of calcite. Aragonite, which is mainly the result of the slow transformation of calcite, is mainly found in fossils.

When Ω_{Ar} (or Ω_{Ca}) is < 1, there is under-saturation of the dissolved calcium carbonate. Thus, it will tend to dissolve (shell and skeleton formation cannot occur). In seawater Ω_{Ar} is always inferior to Ω_{Ca}; aragonite is more soluble than calcite.

Therefore, the determination of when Ω_{Ar} = 1 and Ω_{Ca} = 1 will provide tipping points ($TP_{\Omega Ar}$ and $TP_{\Omega Ca}$), for the ecosystem equilibrium. The results indicate that these tipping points Ω_{Ar} = 1 and Ω_{Ca} = 1 will occur when C_{ANT} = 317 µmol.kg^{-1} and C_{ANT} = 389 µmol.kg^{-1}, respectively for the Western Mediterranean Sea, and when C_{ANT} = 380 µmol.kg^{-1} and C_{ANT} = 456 µmol.kg^{-1}, respectively for the Eastern Mediterranean Sea (Fig.3).

2.3. When would these tipping points (TP_{SD}, $TP_{\Omega Ar}$, $TP_{\Omega Ca}$, and TP_{pH7}), occur in the Mediterranean Sea waters?

Taking into account that fCO_2 in seawater (fCO_2^{sw}), follows that (fCO_2^{air}) of the atmosphere (Royal Society, 2005; Bates *et al.*, 2012 ; Zeebe, 2012), we can calculate the estimated anthropogenic carbon concentrations over the years. For instance, we can use results from both the most optimist/ecological (B1; fCO_2^{air} = 485 µatm and 540 µatm for year 2050 and 2100, respectively) and the most pessimistic (A1F1; fCO_2^{air} = 570 µatm and 940 µatm for year 2050 and 2100, respectively) of the SRES scenarios (IPCC 2007) to make such estimates at least to year 2100.

Then, assuming that ΔfCO_2 (fCO_2^{sw} - fCO_2^{air}) remains constant over time, we can compute the concentrations of anthropogenic carbon that penetrates into the seawater. Thus, for the Western basin, based upon the first scenario (B1), the C_{ANT} concentrations would be in the order of 122 and of 144 µmol kg^{-1} for the years 2050 and 2100, respectively, and based upon the second scenario (A1F1), C_{ANT} concentrations would be close to 154 and 241 µmol.kg^{-1} for the years 2050 to 2100, respectively (Fig.4). For the Eastern basin, based upon scenario B1, the C_{ANT} concentrations would be in the order of 134 and of 158 µmol kg^{-1} for the years 2050 and 2100, respectively, and based upon scenario A1F1, C_{ANT} concentrations would be close to 169 and 266 µmol.kg^{-1} for the years 2050 to 2100, respectively (Fig.4).

The results indicate that when C_{ANT} is equal to 240 µmol.kg^{-1} in seawater (about year 2100 according to scenario A1F1), the acidification variation will reach a value of 0.459 and 0,401pH unit in the Western and Eastern basins, respectively.

The variations of pH and anthropogenic CO_2 concentrations until the end of the 21st century are displayed in Fig.4. Estimated acidification variations from the present until the end of this century are presented in Table 2 for the two extreme SRES scenarios of the IPCC (2007). The results confirm that up to the end of this century, the Western basin (Fig.4a) is always more acidified than the Eastern one (Fig.4b). Figure 4a, b further illustrates the differences of acidification according to the two scenarios. Thus, by the end of this century, the expected decrease in pH in the Western basin will range from 0.245 to 0.462 (from 0.242 to 0.457 in the Eastern basin).

Note that for these calculations we assumed that the seawater temperature did not change. Now, if we take into account the probable increase in seawater temperature, the penetration of atmospheric CO_2 into the seawater will decrease, and thus slow down the penetration of anthropogenic carbon in seawater. For instance, a temperature increase of 2°C by 2050 (IPCC SRES scenarios; 2007) will reduce C_{ANT} by approximately 15 µmol.kg^{-1} and an increase of 4.5°C by 2100 (IPCC SRES scenarios; 2007), will reduce C_{ANT} by approximately 30 µmol.kg^{-1}. Thus, such temperature increase would induce in 2100 a pH variation ranging only from -0.19 to -0.37 pH unit. The amplitude of such pH decrease would, consequently, remain within the observed amplitude of the seasonal variations (Middelboe and Hansen, 2007; Abdelmongy and El-Moselhy, 2015).

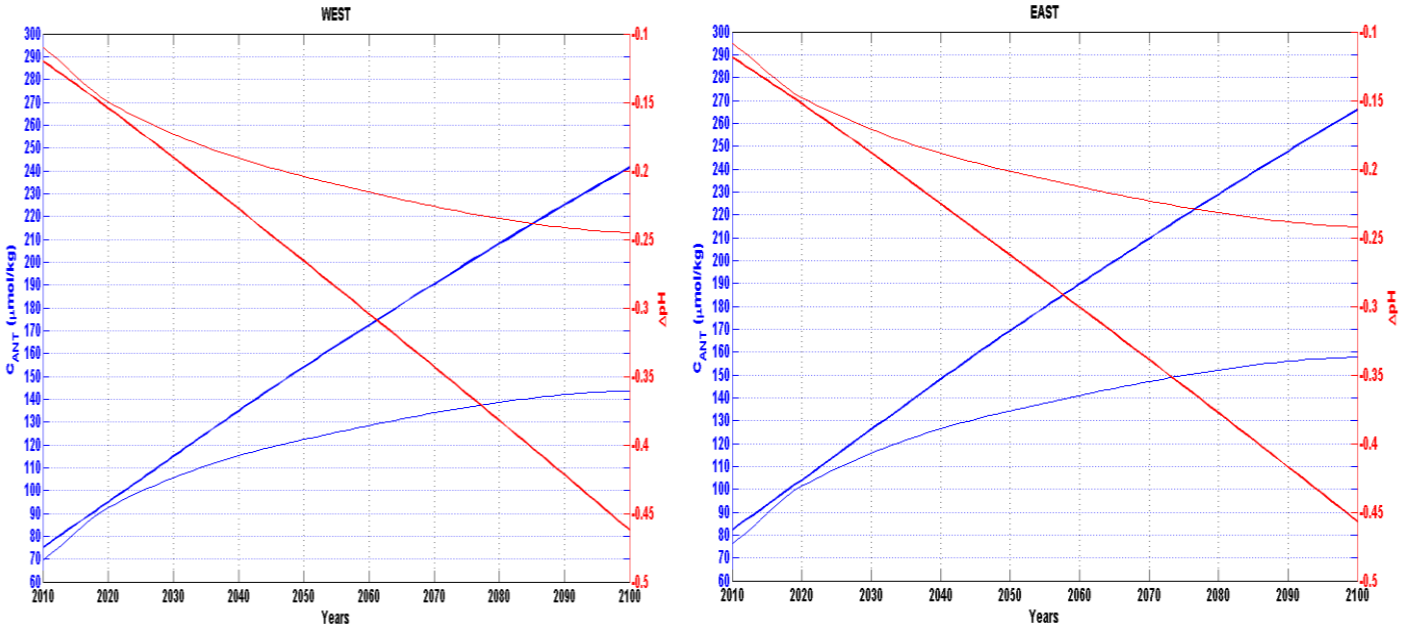

Fig.4.Variations of the anthropogenic CO_2 (left y axis in blue) and acidification (ΔpH; right y axis in red) in the a) Western Mediterranean basin and b) Eastern Mediterranean basin, from 2013 to the end of the 21st century (2100) according to the B1 (thin lines) and A1F1 (thick lines) SRES scenarios of the IPCC (2007).

At the global ocean scale, modelers have noted a decrease of 0.1 pH unit, between 1750 and 1994, in the ocean surface layers (equivalent to a 30% increase of $[H^+]$ ions ; Sabine *et al.*, 2004 ; Raven *et al.*, 2005 ; Orr *et al.*, 2005). However, time-series studies conducted in the North Pacific Ocean between 1988 and 2007 (Dore *et al.*, 2009) and in the North Atlantic Subtropical gyre between 1983 and 2011 (Bates *et al.*, 2012) have documented a significant long-term decreasing trend of 0.05 pH unit (0.0019 and 0.0017 unit yr^{-1} in the North Pacific and the North Atlantic respectively). At the end of the century, the model from Caldeira and Wickett (2003) predicted an increased acidification with a pH decrease between 0.3 and 0.4 pH unit. Similarly, Géri *et al.* (2014) and Yao et al. (2015) predicted the same range of pH decrease (0.3-0.4 pH unit) in the northwestern part of the Mediterranean Sea. Table 3 shows the results of calcium carbonate ions (calcite and aragonite) saturations at the base of the mixed layer depth, for both the Western and Eastern basins.

Table 2. The present and future Mediterranean Sea pH according to the anthropogenic CO_2 based on two extreme SRES scenarios of the IPCC (2007). B1 is the most optimistic scenario while A1F1 is the most pessimistic one.

Year	ΔfCO_2^{air} (µatm)		C_{ANT} (µmol.kg^{-1}) West/East		pH (pH unit)			
					Western basin		Eastern basin	
	B1	*A1F1*	*B1*	*A1F1*	*B1*	*A1F1*	*B1*	*A1F1*
2020	140	145	92/101	95/104	8.065	8.061	8.077	8.073
2050	205	290	122/134	154/169	8.011	7.949	8.024	7.962
2100	260	660	144/158	241/266	7.970	7.753	7.983	7.768

Table 3. The present and future Mediterranean calcium carbonate saturations (calcite, Ω_{Ca} and aragonite, Ω_{Ar}) at the base of the mixed layer depth, according to the anthropogenic CO_2 based on two extreme SRES scenarios of the IPCC (2007). B1 is the most optimistic scenario while A1F1 is the most pessimistic one.

Year	C_{ANT} (µmol.kg^{-1}) West/East		Western basin				Eastern basin			
			B1		*A1F1*		*B1*		*A1F1*	
	B1	*A1F1*	**ΩCa**	**ΩAr**	**ΩCa**	**ΩAr**	**ΩCa**	**ΩAr**	**ΩCa**	**ΩAr**
2020	92/101	95/104	4.37	2.81	4.33	2.79	5.04	3.26	5.00	3.23
2050	122/134	154/169	3.94	2.54	3.50	2.25	4.56	2.95	4.06	2.63
2100	144/158	241/266	3.64	2.34	2.35	1.51	4.23	2.74	2.77	1.79

While the main changes are largest at the ocean surface, the penetration of anthropogenic CO_2 into the ocean interior will alter the chemical composition over the 21st century down to several thousand meters (IPCC, 2014). Thus, as expected Ω_{Ca} and Ω_{Ar} decrease with the increasing C_{ANT} and acidification level (Table 3). According to the most pessimistic (A1F1) scenario of the IPCC (2007), the results show that the Mediterranean Sea waters will remain oversaturated with respect to calcite and aragonite until the end of this century (Table 3). Consequently, the impacts of the Mediterranean Sea acidification on calcareous shells would probably be very light until the end of this century. Yet, afterwards both basins will become undersaturated with respect to aragonite as soon as C_{ANT} = 380 µmol.kg^{-1} would have penetrated into the Mediterranean Sea. Both basins will then become undersaturated with respect to calcite as soon as C_{ANT} = 456 µmol.kg^{-1} would have penetrated in the Mediterranean Sea. Therefore, long before the Mediterranean Sea will become acid (pH < 7; C_{ANT} > 591 µmol.kg^{-1}), marine organisms depending upon formation of calcareous shells and skeletons will be vulnerable.

When water is undersaturated with respect to calcium carbonate ions, marine organisms can no longer form calcium carbonate shells (Raven *et al.*, 2005). Increasing atmospheric CO_2 concentrations lower oceanic pH and carbonate ion concentrations, thereby decreasing the saturation state with respect to calcium carbonate minerals (Feely *et al.*, 2004). The main driver of these changes is the direct geochemical effect due to the addition of anthropogenic CO_2 to the surface ocean (IPCC, 2007). After investigating the effects of CO_2-induced ocean acidification on calcification in 18 benthic marine organisms, Ries *et al.* (2009) suggested that the response of calcifying marine organisms to elevated atmospheric fCO_2 will be variable and complex. They found that oysters, scallops, and temperate corals grew thinner, weaker shells as acidity levels were increased. However, they indicated that some species, including blue crabs, lobsters, and shrimp, grew thicker shells that could make them more resistant to predators. Nevertheless, Mediterranean surface waters would remain oversaturated with respect to calcite and aragonite in surface layers (CIESM, 2008). However, the increasing acidification level could considerably decrease this saturated state by the end of this century. Although it may be assumed that the dissolution of calcium carbonate ions is not thermodynamically favorable and therefore not an anticipated problem in the Mediterranean Sea (CIESM, 2008), results from Table 3 suggest that over the very long term (beyond the century), this may become an issue.

High acidification levels can also influence the speciation of nutrients [the degree of limitation of phosphate ions, already a limiting factor for primary production (Berland *et al.*, 1980), will increase] and their trophic situations (worsening oligotrophy). This potentially affects the productivity, the entire structure of food webs as well as the carbon export.

3. Summary

In this paper, based upon the equations of the chemical equilibrium of the CO_2/carbonate system in seawater we first calculated the variation of pH (ΔpH) as a function of theoretical C_{ANT} concentrations ranging from 0 µmol.kg^{-1} to 3000 µmol.kg^{-1}, at the base of the mixed layer depth in waters of the Western and Eastern basins of the Mediterranean Sea. We then fitted these results with simple polynomial functions (one for each basin; Eq.III and IV for the Western and Eastern basin, respectively). The results show that the Western basin is acidifying faster than the Eastern basin. The difference in acidification between these two basins will reach its maximum (ΔpH = 0.101) when C_{ANT} will reach 395 µmol.kg^{-1}.

The results show that a linear interpolation cannot be used for C_{ANT} larger than 86 µmol.kg^{-1} since it will largely underestimates the pH variations. Thus, these results indicate the first tipping point (TP_{SD}) when the Mediterranean Sea acidification will sharply increase compared to the regular increase of C_{ANT}. This is happening now!

In order to provide an estimate of the dates corresponding to these variations, we made the reasonable assumption that surface seawater fCO_2 follows that of the atmosphere. Thus, based upon the SRES scenario B1 (optimist) and A1F1 (pessimistic) of the IPCC (2007), we could estimate the pH variations as a function of time. Therefore, by the end of this century, when C_{ANT} could reach 144 µmol.kg^{-1} (B1), or 241 µmol.kg^{-1} (A1F1), the pH variation would reach -0.245 and -0.462 pH unit, respectively, for the Western basin. For the Eastern basin, when C_{ANT} could reach 158 µmol.kg^{-1} (B1), or 266 µmol.kg^{-1} (A1F1), the pH variation would reach -0.242 and -0.457 pH unit, respectively. These variations would remain close to present amplitude of the observed seasonal variations of pH in the upper layer of the ocean.

One should keep in mind that in this study, the effect of the global warming was not taken into account and consequently, the estimated range of pH variations provides an upper limit. Global warming will mitigate the exchanges across the ocean-atmosphere interface, thus reducing the penetration of anthropogenic carbon and consequently the Mediterranean Sea acidification.

Although both basins are supersaturated with calcite and aragonite, the calcium carbonate saturation states are lower in the Western basin than those in the Eastern basin. The projected estimates of the calcite and aragonite tipping points ($TP_{\Omega Ar}$, $TP_{\Omega Ca}$) indicate that both basins may become undersaturated with respect to aragonite (and later to calcite), in Mediterranean waters only after the end of this century.

The next tipping point (TP_{pH7}), would occur when the Mediterranean Sea would become acid (pH<7) due to a large penetration of C_{ANT}.

In summary, this study highlights four tipping points. In each of the Western and Eastern basins of the Mediterranean Sea, these tipping points, calculated at the base of the mixed layer depth, are specific to the location. Nevertheless, they are reached for only slightly different concentrations of C_{ANT}. The tipping points with their limits of C_{ANT} and their significance are as follow:

1) TP_{SD}: when C_{ANT} would reach 86 µmol.kg^{-1} (or as soon as 82 µmol.kg^{-1} for the Western waters), the Mediterranean Sea acidification will intensify sharply,
2) $TP_{\Omega Ar}$: when C_{ANT} would reach 380 µmol.kg^{-1} (or as soon as 317 µmol.kg^{-1} for the Western waters), the Mediterranean Sea will become undersaturated with respect to aragonite,
3) $TP_{\Omega Ar}$: when C_{ANT} would reach 456 µmol.kg^{-1} (or as soon as 389 µmol.kg^{-1} for the Western waters), the Mediterranean Sea will become undersaturated with respect to calcite,
4) TP_{pH7}: when C_{ANT} would reach 591 µmol.kg^{-1} (or as soon as 548 µmol.kg^{-1} for the Western waters), the Mediterranean Sea will become acid (pH < 7).

When these tipping points will be reached? The first one TP_{SD} has already been reached. The three others $TP_{\Omega Ar}$, $TP_{\Omega Ca}$, and TP_{pH7} will probably be reached within the next century. The exact timing will strongly depend upon the politics of human activities, which will impact both global warming and the anthropogenic CO_2 raise both in the atmosphere and into the ocean.

Acknowledgment

This work was funded by the EC FP7 “Mediterranean Sea Acidification in a changing climate – MEDSEA” project (MedSeA; grant agreement 265103; medsea-project.eu). Authors are grateful to the National Council for Scientific Research (CNRS) in Lebanon for the PhD thesis scholarship granted to Miss Elissar GEMAYEL.

References

Abdelmongy A.S., K.M. El-Moselhy, 2015. Seasonal variations of the physical and chemical properties of seawater at the Northern Red Sea, Egypt. Open Journal of ocean and coastal sciences.ISSN(print): 2377-0007; ISSN(online): 2377-0015; DOI:10.15764/OCS.2015.01001. Vol.2, Num.1, January 2015.

Bates N.R., Best M.H.P., Neely K., Garley R., Dickson A.G. and Johnson R.J., 2012. Detecting anthropogenic carbon dioxide uptake and ocean acidification in the North Atlantic Ocean. *Biogeosciences*, **9**, 2509–2522. www.biogeosciences.net/9/2509/2012/, doi:10.5194/bg-9-2509-2012.

Berland B.R., Bonin D.J. and Maestrini S.Y., 1980. Azote ou phosphore ? Considérations sur le "paradoxe nutritionnel" de la mer méditerranée. *Oceanologica Acta*, **3** (1), 135-141.

Caldeira K. and Wickett M.E., 2003. Oceanography: Anthropogenic carbon and ocean pH. *Nature*, **425**, 365, doi:10.1038/425365a.

Caldeira K. and Wickett M.E., 2005. Ocean model predictions of chemistry changes from carbon dioxide emissions to the atmosphere and ocean. *Journal of Geophysical Research*, **110**, C09S04, doi:10.1029JC002671.

CIESM, 2008. Impacts of acidification on biological, chemical and physical systems in the Mediterranean and Black Seas. In: F. Briand (Ed.), No.36 in *CIESM Workshop Monographs*, Monaco, 124.

Dickson A.G., 1990. Standard potential of the reaction: AgCl(s) + 1/2H2 = Ag(s) + HCl(aq), and the standard acidity constant of the ion HSO4 in synthetic sea water from 273.15 to 318.15 K. *Journal of Chemical Thermodynamics*, **22**, 113-127.

Dore J.E., Lukas R., Sadler D.W., Church M.J., and Karl D.M., 2009. Physical and biogeochemical modulation of ocean acidification in the central North Pacific. *Proceedings of the National Academy of Sciences of the United States of America*, **106** (30), 12235–12240, doi: 10.1073/pnas.0906044106

DOE, 1994. Handbook of methods for the analysis of the various parameters of the carbon dioxide system in sea water. Version 2, A. G. Dickson & C. Goyet, eds., *ORNL/CDIAC-74*.

Eurostat, 2009. Population growth slowing and life expectancy increasing in the Euro-Mediterranean region, 2000-2007. *Statistics in focus* 66/2009.

Fabry V.J., Seibel B.A., Feely R.A., and Orr J.C., 2008. Impacts of ocean acidification on marine fauna and ecosystem processes. *ICES Journal of Marine Science*, **65** (3), 414–432.

Feely R.A., Sabine C.L., Lee K., Berelson W., Kleypas J., Fabry V.J. and Millero F.J., 2004. Impact of anthropogenic CO_2 on the CaCO3 system in the oceans. *Science*, **305** (5682), 362-366, doi: 10.1126/science.1097329.

Feely R.A., Doney S.C., and Cooley S.R., 2009. Ocean acidification: Present conditions and future changes in a high-CO_2 world. *Oceanography*, **22** (4), 36–47, doi:10.5670/oceanog.2009.95.

Gemayel Elissar, Hassoun Abed El Rahman, Abboud-Abi Saab Marie, Goyet Catherine, Krasakopoulo Evangelina, Touratier Franck and Ziveri Patrizia (2015a). Modelization of total inorganic carbon in surface waters of the Mediterranean Sea. Deep sea Research, part 1. (in revision)

Gemayel E., A.E.R. Hassoun, A. Benallal, C. Goyet, E. Krasakopoulou, M. Abboud-Abi Saab, Franck Touratier (2015b) Distribution of surface water pCO_2 and air-sea fluxes in the Mediterranean Sea during May 2013. *Journal of marine Systems (in revision)*

Géri P., El Yacoubi S. and Goyet C., 2014. Forecast of Sea Surface Acidification in the Northwestern Mediterranean Sea. *Journal of Computational Environmental Sciences*, Article ID 201819, 7 pp., doi:10.1155/2014/201819.

Goyet C. and Poisson A., 1989. New determination of carbonic-acid dissociation-constants in seawater as a function of temperature and salinity. *Deep Sea Research Part A: Oceanographic Research Papers*, **36** (11), 1635-1654.

Gypens N., Lancelot C. and Borges A.V., 2004. Carbon dynamics and CO2 air-sea exchanges in the eutrophied coastal waters of the Southern Bight of the North Sea: a modelling study. *Biogeosciences*, **1**, 147–157, doi: 10.5194/bg-1-147-2004

Gypens N., Borges A. V. and Lancelot C., 2009. Effect of eutrophication on air-sea CO2 fluxes in the coastal Southern North Sea: a model study of the past 50 years. *Global Change Biology*, **15**, 1040–1056, doi: 10.1111/j.1365-2486.2008.01773.x

Gypens N., Lacroix G., Lancelot C. and Borges A.V., 2011. Seasonal and inter-annual variability of air-sea CO_2 fluxes and seawater carbonate chemistry in the Southern North Sea. *Progress in Oceanography*, **88**, 59–77, doi: 10.1016/j.pocean.2010.11.004.

Hassoun A.E.R., Guglielmi V., Gemayel E., Goyet C., Abboud-Abi Saab M., Giani M., Ziveri P., Ingrosso G., Touratier F. (2015a) *Is the Mediterranean Sea circulation in a steady state?* Journal of Water Resources and Ocean Science, 4(1): 6-17, doi: 10.11648/j.wros.20150401.12

Hassoun A.E.R., E. Gemayel, E. Krasakopoulou, C. Goyet, M. Abboud-Abi Saab, Ziveri P., F. Touratier, V. Guglielmi, C. Falco (2015b). *Modeling of the total alkalinity and the total inorganic carbon in the Mediterranean.* Journal of Water Resources and Ocean Science, 4(1):24-32, doi:10.11648/j.wros.20150401.14

Hassoun A.E.R., E. Gemayel, C. Goyet, E. Krasakopoulou, M. Abboud-Abi Saab, V. Guglielmi, F. Touratier, C. Falco (2015c). Acidification of the Mediterranean Sea from anthropogenic carbon penetration. *Deep-Sea Research, Part I: Oceanographic Research Papers, (102) 1-15*, doi:10.1016/j.dsr.2015.04.005

IPCC, 2001. Climate Change 2001: Impacts, Adaptation and Vulnerability.

IPCC, 2007. Climate Change 2007: The Physical Science Basis. Contribution of Working Group I to the Fourth Assessment Report of the Intergovernmental Panel on Climate Change, ed. S Soloman, D Qin, D Manning, Z Chen, M Marquis, KB Averyt, et al. Cambridge, UK: Cambridge Univ. Press. 996 pp.

IPCC, 2014. Climate Change 2014: Impacts, Adaptation, and Vulnerability. The Fifth Assessment Report of the Intergovernmental Panel on Climate Change.

Le Quéré C., Takahashi T., Buitenhuis E.T., Rodenbeck C. and Sutherland S. C., 2010. Impact of climate change and variability on the global oceanic sink of CO_2. *Global Biogeochemical Cycles*, **24** (4), GB4007, doi:10.1029/2009GB003599.

Middelboe A.L., P.J. Hansen, 2007. High pH in shallow-water macroalgal habitats. Marine ecology progress series. Vol. 338:107-117.

Mikaloff-Fletcher S.E., Gruber N., Jacobson A.R., Doney S.C., Dutkiewicz S., Gerber M., Follows M., Cocco V.F., Lindsay K., Menemenlis D., Mouchet A., Moller S.A. and Sarmiento J., 2006. Inverse estimates of anthropogenic CO2 uptake, transport, and storage by the ocean. *Global Biogeochemical Cycles*, **20** (2), GB2002, doi:10.1029/2005GB002530.

Orr J.C., Fabry V.J., Aumont O., Bopp L., Doney S.C., Feely R.A., Gnanadesikan A., Gruber N., Ishida A., Joos F., Key R.M., Lindsay K., Maier-Reimer E., Matear R., Monfray P., Mouchet A., Najjar R.G., Plattner G.-K., Rodgers K.B., Sabine C.L., Sarmiento J.L., Schlitzer R., Slater R.D., Totterdell L.J., Weirig M.-F., Yamanaka Y. and Yool A., 2005. Anthropogenic ocean acidification over the twenty-first century and its impact on calcifying organisms. *Nature*, **437**, 681-686.

Pierrot D., Lewis E. and Wallace D.W.R., 2006. MS Excel Program Developed for CO2 System Calculations., *ORNL/CDIAC-105*. Carbon Dioxide Information Analysis Center, Oak Ridge National Laboratory, U.S. Department of Energy, Oak Ridge, Tennessee.

Raven J., Caldeira K., Elderfield H., Hoegh-Guldberg O., Liss P., Riebesell U., Shepherd J., Turley C. and Watson A., 2005. Ocean acidification due to increasing atmospheric carbon dioxide. *The Royal Society Policy Document*, 12/05, London.

Ries J.B., Cohen A.L., and McCorkle D.C., 2009. Marine calcifiers exhibit mixed responses to CO2-induced ocean acidification. *Geology*, **37** (12), 1131–1134, doi: 10.1130/G30210A.1.

Royal Society, 2005. Ocean acidification due to increasing atmospheric carbon dioxide. The Royal Society, London. Policy Document 12/05 ; p. 60.

Sabine C.L., Feely R.A., Gruber N., Key R.M., Lee K., Bullister J.L., Wanninkhof R., Wong C.S., Wallace D.W.R., Tilbrook B., Millero F.J., Peng T.-H., Kozyr A., Ono T. and Rios A.F., 2004. The Oceanic Sink for Anthropogenic CO2. *Science*, **305** (5682), 367-371, doi:10.1126/science.1097403.

Sabine C.L., Feely R.A., Wanninkhof R., Takahashi T., Khatiwala S., and Park G.-H., 2011. The global ocean carbon cycle. *Bulletin of the American Meteorological Society*, **92** (6), S100–S108, doi:10.1175/1520-0477-92.6.S1.

Siegenthaler U., Stocker T.F., Monnin E., Luethi D., Schwander J., Stauffer B., Raynaud D., Barnola J.-M., Fischer H., Masson-Delmotte V. and Jouzel J., 2005. Stable carbon cycle-climate relationship during the late Pleistocene. *Science*, **310** (5752), 1313-1317, doi: 10.1126/science.1120130.

Thomas H., England M.H. and Ittekkot V., 2001. An off-line 3D model of anthropogenic CO2 uptake by the oceans. *Geophysical Research Letters*, **28**, 547–550.

Touratier, F., V. Guglielmi, C. Goyet, L. Prieur, M. Pujo-Pay , P. Conan, and C. Falco (2012). Distribution of the carbonate system properties, anthropogenic CO_2, and acidification during the 2008 BOUM cruise (Mediterranean Sea). Biogeosciences Discussion, 9, 2709-2753. doi:10.5194/bgd-9-2709-2012

Touratier F. and C. Goyet (2004a). Definition, properties, and Atlantic Ocean distribution of the new tracer TrOCA. Journal of Marine Systems, 46, 169-179

Touratier F. and C. Goyet (2004b). Applying the new TrOCA approach to estimate the distribution of anthropogenic CO_2 in the Atlantic Ocean. Journal of Marine Systems, 46, 181-197

Touratier F., Azouzi L., and C. Goyet (2007). CFC-11, $\Delta^{14}C$, and ^{3}H tracers as a means to assess anthropogenic CO_2 concentrations in the ocean. Tellus, 59B, 318-325.

UNEP/MAP-Plan Bleu, 2009. State of the Environment and Development in the Mediterranean, UNEP/MAP-Plan Bleu, Athens.

Uppström L.R., 1974. The boron/chlorinity ratio of the deep-sea water from the Pacific Ocean. *Deep Sea Research and Oceanographic Abstracts*, **21** (2), 161-162.

Waugh D.W., Haine T.W.N. and Hall T.M., 2004. Transport times and anthropogenic carbon in the subpolar North Atlantic Ocean. *Deep-Sea Research Part I*, **51** (11), 1475–1491.

WMO, 2014. Record Greenhouse Gas Levels Impact Atmosphere and Oceans. Press Release No. 1002 by the World Meteorological Organization. http://www.wmo.int/pages/mediacentre/press_releases/pr_1002_en.html

Yao, K. M., Marcou, O., Goyet, C., Guglielmi, V., Touratier, F., Savy, J.-P. (2015). Understanding the dynamics patterns of the Mediterranean Sea pH over the last 17 years (1995-2011). *Journal of Marine Systems (soumis 2015)*

Yool A., Popova E.E. and Anderson T.R., 2011. Medusa-1.0: a new intermediate complexity plankton ecosystem model for the global domain. *Geoscientific Model Development*, **4** (2), 381-417, doi:10.5194/gmd-4-381.

Yool A., Popova E.E. and Anderson T.R., 2013. MEDUSA-2.0: an intermediate complexity biogeochemical model of the marine carbon cycle for climate change and ocean acidification studies. *Geoscientific Model Development*, **6** (5), 1767-1811, doi:10.5194/gmd-6-1767.

Zeebe R.E., 2012. History of Seawater Carbonate Chemistry, Atmospheric CO2, and Ocean Acidification. *The Annual Review of Earth and Planetary Sciences*, **40**, 141–165, doi: 10.1146/annurev-earth-042711-105521.

Chapitre IV : Conclusions Générales et Perspectives

'On sait toujours où commencer, mais très rarement où on termine'

Réflexion Personnelle

Conclusions Générales

Dans ce manuscrit de thèse sont abordées quatre thématiques principales qui incluent sept articles scientifiques au cours desquels on a appliqué différentes méthodes et approches qui nous ont permis : 1) d'analyser l'état de la circulation en Mer Méditerranée ; 2) d'estimer les flux air-mer de CO_2 à partir des données in situ de pCO_2^{sw} et/ou des données satellites ; 3) d'estimer l'alcalinité totale et le carbone inorganique total dans la colonne d'eau et dans les eaux de surface ; et 4) d'évaluer et prédire l'évolution de l'acidification dans la Mer Méditerranée.

On peut ainsi à partir du travail présenté tirer les conclusions principales suivantes :

On a tout d'abord abordé l'analyse de l'état de la circulation en Mer Méditerranée à travers le calcul et la comparaison des coefficients de mélange des masses d'eau pour les campagnes de Boum en 2008 et MedSeA en 2013. Les résultats montrent que les proportions des masses d'eau n'ont pas significativement changé pour les eaux de surface. Or cela n'est pas le cas pour les eaux intermédiaires et profondes où les coefficients de mélange ont été largement modifiés. Par exemple, le coefficient de mélange de l'eau d'origine Adriatique est toujours élevé dans le sous-bassin Ionien, mais il est plus faible que celui de l'eau d'origine Egéenne dans le sous-bassin Levantin. Une grande partie de ces modifications peut être attribuée au phénomène de l'EMT (Eastern Mediterranean Transient) qui affecte particulièrement le bassin Oriental. La Mer Méditerranée est alors sujette à des changements continus des masses d'eau qui sont en évolution permanente, ce qui remet en question l'hypothèse du 'régime permanent' ou 'quasi stationnaire'.

On s'est dirigé par la suite aux estimations ponctuelles et spatiales des flux de CO_2 à travers l'interface air-mer. Pour cela, on s'est référé aux données récentes de pCO_2 dans les eaux de surface (pCO_2^{sw}) mesurées durant la campagne MedSeA en mai 2013. L'analyse de ces données montre un gradient positif de l'Ouest vers l'Est d'environ 100 µatm observé durant une période de 20 jours. De ce fait, deux régimes différents de pCO_2^{sw} sont identifiés dans les bassins Ouest et Est dont les propriétés physico-bio-chimiques influencent différemment la variabilité de la pCO_2^{sw}. Dans le bassin Ouest, les variations de la pCO_2^{sw} ont été affectées par le mélange avec l'eau Atlantique ainsi que la forte variation de salinité, par contre dans le bassin Est ces variations ont été fortement dominées par les hautes températures de l'eau de surface. En considérant la variation Ouest-Est de la pCO_2^{sw} et la pCO_2 atmosphérique de 399 ppm, le déséquilibre air-mer (ΔpCO_2) a varié de - 31 µatm au niveau du détroit de Gibraltar pour atteindre + 57 µatm dans le sous-bassin Levantin. Ainsi, en moyenne en mai 2013, le calcul des flux journaliers de CO_2 indique que la Mer Méditerranée a été une source de CO_2 pour l'atmosphère avec un taux d'environ 1 $mmol.m^{-2}.jour^{-1}$.

A partir des données de la mission MedSeA on a pu présenter une estimation ponctuelle des flux journaliers de CO_2 couvrant un trajet Ouest-Est bien déterminé. Pour pouvoir estimer la

pCO_2^{sw} et en conséquent les flux de CO_2 sur une échelle spatiale qui couvre toute la Mer Méditerranée, on a pris dans une étude ultérieure l'exemple de deux campagnes océanographiques, qui sont respectivement la MedSeA et la Thresholds en mai 2007 et mai 2013. On a développé ainsi à partir de ces données, plusieurs équations pour estimer la pCO_2^{sw} à partir des données satellites de SST, Chla et CDOMi acquis du MODIS-A. La comparaison des différentes équations pour les mois de mai 2007 et 2013, a montré que la SST et la Chla sont plus convenables pour estimer la pCO_2^{sw} que la SST et le CDOMi. En outre l'équation développée pour le mois de mai 2013 a pu saisir 94 % de la gamme de pCO_2^{sw} initiale et a été donc utilisée pour cartographier les flux de CO_2 à l'interface air-mer sur l'ensemble de la Mer Méditerranée. En mai 2013, les flux de CO_2 ont varié de - 7 jusqu'à 2 $mmol.m^{-2}.jour^{-1}$, suivant un gradient Ouest-Est assez marqué. Les puits les plus importants pour le CO_2 atmosphérique ont été situés dans les sous-bassins Alboran, Ligurien et le Sud de la mer Tyrrhénienne ; tandis que les sources les plus importantes ont couvert le sous-bassin Levantin. En moyenne et sur une échelle couvrant presque la totalité de la Mer Méditerranée, les flux de CO_2 ont été de - 0.09 $mmol.m^{-2}.jour^{-1}$. Ces flux de CO_2 et contrairement à ceux calculés uniquement sur le trajet de la mission MedSeA, indiquent qu'en mai 2013, la Mer Méditerranée a été proche de l'équilibre avec l'atmosphère, avec un léger puits pour le CO_2 atmosphérique. Cette étude met en valeur les potentiels pour estimer les flux de CO_2 en Mer Méditerranée à partir de mesures directes de pCO_2^{sw} et des données satellites à haute résolution spatiale.

En ce qui concerne l'alcalinité totale (A_T) et le carbone inorganique total (C_T), leurs déterminations a lieu à travers des mesures discrètes et cela pour des échantillons collectés à des profondeurs prédéterminées. Dans le cas de manque de données, il est courant d'estimer les concentrations d'A_T et de C_T à travers d'autres paramètres mesurés en continu tel que la salinité et/ou la température. Dans un premier temps, les données physico-chimiques mesurées durant la mission MedSeA en mai 2013 ont présenté un très bon exemple pour ce genre d'application. Ainsi on a élaboré des relations linéaires pour estimer l'A_T et le C_T à partir de la salinité et cela au niveau de chaque bassin et sous-bassin de la Mer Méditerranée et pour plusieurs intervalles de profondeurs. Les relations établies dans cette étude sont caractérisées par leur aspect local et par leurs incertitudes proches de celles des mesures. Par exemple ces relations peuvent être utilisées pour estimer l'A_T et le C_T, respectivement dans les couches intermédiaires et profondes des sous-bassins Tyrrhénien et Alboran. Ainsi ces relations peuvent être facilement appliquées pour estimer d'une façon continue les concentrations d'A_T et de C_T, comme elles peuvent être introduites dans des modèles océaniques en 3D.

Dans un deuxième temps on s'est concentré sur l'estimation de l'A_T et du C_T uniquement dans les eaux de surface (< 10 m). En fait, en Mer Méditerranée, ces estimations sont limitées à des simulations numériques ou à des modèles empiriques développés pour des campagnes spécifiques. En outre, bien que l'estimation de l'A_T dans les eaux de surface fût largement abordée, celle du C_T reste encore très mal connue. On a présenté alors des régressions polynomiales pour estimer l'A_T et le C_T dans les eaux de surface à partir de la température et de la salinité; et cela par la compilation des données physico-chimiques de plusieurs

campagnes océanographiques qui ont eu lieu entre 1998 et 2013. Les résultats montrent que le RMSE de ± 10 µmol kg^{-1} d'un polynôme de second degré qui relie l'A_T à la température et la salinité, est plus petit que celui d'une relation linéaire (± 14 µmol.kg^{-1}) qui inclue uniquement la salinité. Ceci indique qu'il faudra tenir en compte de la contribution de la température afin de mieux déterminer les variations de l'A_T dans les eaux de surface. En outre ce modèle présente une équation plus globale et améliorée que celles déjà publiées pour la Mer Méditerranée. On a aussi présenté une première estimation du C_T moyen annuel dans les eaux de surface. Ainsi on a développé un modèle pour estimer le C_T à partir de la température et de la salinité par un polynôme du troisième degré et avec un RMSE de ± 14 µmol.kg^{-1}. On a pu montrer que pour les eaux de surface, l'effet de l'augmentation du CO_2 atmosphérique sur le C_T est négligeable par rapport aux variations saisonnières. Ceci est principalement dû à la ventilation relativement rapide des eaux qui transporte le CO_2 anthropique vers les couches les plus profondes. Ainsi, les deux équations proposées présentent des relations globales qui peuvent être appliquées pour estimer l'A_T et le C_T sur l'échelle de toute la Mer Méditerranée, puisqu'elles se basent sur des données physico-chimiques compilées à partir de plusieurs campagnes océanographiques, et sur un grand laps de temps. Comme exemple pratique, ces équations ont été appliquées sur les cartes climatologiques de température et de salinité du World Ocean Atlas pour cartographier les variabilités spatiales et saisonnières de l'A_T et du C_T dans les eaux de surface pour une moyenne de 7 ans (2005-2012).

Pour évaluer l'état de l'acidification en Mer Méditerranée, on a calculé à partir des données de la mission MedSeA en 2013 les distributions du CO_2 anthropique (C_{ANT}) ainsi que les variations de l'acidification et des taux de calcite et d'aragonite entre la période préindustrielle et l'année 2013. Les résultats montrent que toute la Mer Méditerranée est contaminée par le C_{ANT} avec des concentrations bien plus élevées que celles rapportées pour l'océan global. Dans le bassin Occidental, les eaux les plus contaminées par le C_{ANT} (> 60 µmol.kg^{-1}) ont été détectées dans les couches intermédiaires et profondes des sous-bassins Alboran, Liguro et Algéro-Provençal. Par contre dans le bassin Oriental, les plus faibles concentrations de C_{ANT} (~ 35 µmol.kg^{-1}) ont été détectées dans le sous-bassin Ionien et au Nord du sous-bassin Tyrrhénien. La variation de l'acidification de 0,055 à 0,156 unités de pH à confirmer que toutes les eaux méditerranéennes sont déjà acidifiées surtout dans le bassin Occidental. Malgré l'acidification élevée, la Mer Méditerranée reste sursaturée via à vis des minéraux du carbonate de calcium. Mais dans le bassin Occidental qui est le plus acidifié, le degré de saturation du calcite de l'aragonite est moins élevé par rapport au bassin Oriental, ce qui montre l'effet que pourra avoir l'augmentation du pH sur les organismes calcifiants.

Pour prédire la variation de l'acidification en Mer Méditerranée, on a calculé à partir des équations d'équilibre chimique du système des carbonates dans l'eau de mer, les variations du pH (ΔpH) en fonction de concentrations théoriques de C_{ANT} de 0 µmol.kg^{-1} à 3000 µmol.kg^{-1}, et cela en dessous de la couche de mélange dans les eaux du bassin Occidental et Oriental de la Mer Méditerranée. Les résultats montrent que le bassin Occidental s'acidifie plus rapidement que le bassin Oriental et que la différence de l'acidification entre ces deux bassins atteindra son maximum (= 0,101 ΔpH) lorsque le C_{ANT} sera de 395 µmol.kg^{-1}. En outre sur la

base de deux scénarios SRES de l'IPCC (2007): B1 (optimiste) et A1F1 (pessimiste), nous avons pu estimer les variations de pH en fonction du temps. A la fin de ce siècle et dans le bassin Occidental, quand le CANT pourrait atteindre 144 μmol.kg^{-1} (B1), ou 241 μmol.kg^{-1} (A1F1), la variation du pH correspondante sera, respectivement de - 0,245 ou - 0,462 unité. Dans le bassin Oriental, quand le CANT pourrait atteindre 158 μmol.kg^{-1} (B1), ou 266 μmol.kg^{-1} (A1F1), la variation du pH correspondante sera, respectivement de - 0,242 ou - 0,547 unité. On a aussi montré que le seuil en CANT de 86 μmol.kg^{-1} pour lequel l'acidification va fortement s'intensifier en Mer Méditerranée est déjà atteint. En outre les eaux profondes des bassins Occidental et Oriental deviendront sous saturés par rapport à la calcite et à l'aragonite d'ici la fin du siècle prochain.

Bien que les différents articles présentés dans cette thèse traitent différents aspects du système des carbonates, ces derniers restent fortement reliés entre eux. Ainsi on a abordé tout d'abord l'état la circulation générale en Mer Méditerranée qui régit largement la distribution des différents paramètres du système des carbonates. Ensuite on a mené une analyse des différentes propriétés physico-chimiques qui régulent la distribution de la pCO_2^{sw} dans les eaux de surface, et présenté à partir de ces données un calcul ponctuel des flux de CO_2 journaliers. En outre, on a présenté une première estimation de la pCO_2^{sw} à partir de différentes paramètres acquis par les images satellites. Ces dernières offrant l'avantage de couvrir une échelle spatiale très étendue et à haute résolution, ont permis de cartographier les flux de CO_2 sur une échelle qui couvre une grande partie de la Mer Méditerranée.

En outre, on a présenté des équations pour estimer la distribution de l'A_T et du C_T dans la colonne d'eau et dans les eaux de surface. On a ainsi montré qu'il est possible d'estimer ces deux paramètres par des relations simples qui nécessitent des mesures de la salinité et/ou de la température très largement disponibles. A partir des données d'A_T et de C_T, on termine par l'évaluation de l'état présent et la prédiction de l'acidification en Mer Méditerranée. On met ainsi en évidence un état alarmant vis-à-vis de l'acidification qui demande une prise de décision assez urgente pour pouvoir préserver 'notre' Mer Méditerranée, la '*Mare Nostrum*'.

Perspectives

Les articles présentés dans ce manuscrit répondent en plusieurs aspects à l'objectif principal de la thèse qui est de contribuer à l'estimation des paramètres du système des carbonates en Mer Méditerranée. Mais dans la vue de la continuité des travaux entamés durant cette thèse, de nombreuses perspectives pourront encore être abordées.

En Mer Méditerranée, les données d'A_T et de C_T sont beaucoup plus disponibles que celles de la pCO_2^{sw}. En fait la compilation des données d'environ vingt campagnes océanographiques nous a permis d'établir des relations pour estimer l'A_T et le C_T dans les eaux de surface. Suite à ces équations on a pu cartographier les variations spatiales et saisonnières de ces deux paramètres pour une moyenne de 7 ans (2005-2012) et sur une échelle spatiale qui couvre toute la Mer Méditerranée.

Dans un premier temps et à partir des champs d'A_T et de C_T, il sera donc possible de calculer et cartographier sur une moyenne de 7 ans (2005-2012), la pCO_2^{sw} et le flux de CO_2 à l'interface air-mer et cela au niveau de toute la Mer Méditerranée. En outre une comparaison avec les simulations de D'Ortenzio et al. (2008) pour les années 1998-2004, nous permettra d'évaluer l'évolution temporelle des flux de CO_2 suite à l'augmentation continue du CO_2 atmosphérique.

Dans un deuxième temps on pourra établir à partir de la même base de données des modèles qui estiment l'A_T et le C_T de la base de la couche de mélange jusqu'aux couches les plus profondes. Ces modèles nous permettront d'établir des relations théoriques pour prédire les variations du ΔpH ($pH - pH_{preind}$) en fonction du C_{ANT} et comparer avec les résultats théoriques: 'What are the tipping points for the Mediterranean Sea Acidification?'

En ce qui concerne l'estimation des paramètres du système des carbonates à partir des données d'images satellites, on s'est limité dans cette thèse à deux campagnes océanographiques en mai 2007 et 2013 et pour uniquement un seul paramètre qui est la pCO_2^{sw}. Les résultats de ce travail sont très prometteurs et ouvrent plusieurs perspectives pour l'application des images satellites en Mer Méditerranée, surtout que ce type de données a jusqu'à présent été très rarement utilisé.

On pourra tout d'abord se référer à d'autres campagnes que la Thresholds et la MedSeA pour estimer la pCO_2^{sw} à partir des images satellites de SST, Chla et CDOMi. On pourra prendre l'exemple des données de pCO_2^{sw} acquises à partir des bouées Carioca aux sites DYFAMED et BOUSSOLE dans la mer ligure, de la bouée Vida au golf de Trieste et des campagnes effectuées en mer Egée et au niveau du détroit de Gibraltar.

Ensuite, on pourra établir des équations qui permettent d'estimer l'A_T et le C_T à partir des données satellites de SST et SSS et comparer les résultats avec ceux dérivés à partir des données in situ. Bien qu'auparavant la SSS ne fût pas mesurée par les satellites, il est possible d'acquérir ce type de données par les satellites Aquarius du NASA (National Aeronautics and Space Administration) et SMOS (Soil Moisture and Ocean Salinity) de l'ESA (European Space Agency), respectivement à partir des années 2008 et 2010. Or il est important de noter que les images satellites actuelles de SSS sont d'une très faible résolution spatiale (de 0,25 à 1) et d'une faible précision de mesure (0,2 unité). Cela impose des limitations pour leurs applications directes en Mer Méditerranée, vu que cette dernière se caractérise par des variations très locales et spécifiques de SSS.

En outre, il sera possible d'établir des modèles pour estimer les variations décennales de la pCO_2^{sw}, l'A_T et/ou le C_T. Puisque les images satellites mensuelles pour la SST et la Chla et bientôt pour la SSS, sont disponibles pour une période de 10 ans; on pourra pour un paramètre donné calculer la moyenne annuelle pour chaque pixel de l'image (moyenne de 12 images mensuelles pour une année donnée), et puis calculer la moyenne décennale (moyenne des 10 images annuelles) pour toute la Mer Méditerranée.

En vue du manque de données vis-à-vis des mesures directes de pCO_2^{sw}, certaines perspectives restent pour le moment difficiles à entreprendre. Ainsi, une meilleure couverture spatiale et un échantillonnage plus dense pour la région permettrait de :

- Mieux caractériser et quantifier le cycle saisonnier et interannuel de la pCO_2^{sw}.
- Mieux expliquer les effets des propriétés physico-bio-chimiques dans les bassins Ouest et Est sur les distributions de la pCO_2^{sw}.
- Réduire l'incertitude sur les calculs des flux de CO_2 à l'interface air-mer et cela en se basant sur des mesures directes de pCO_2^{sw}.

A long terme, il serait donc important de s'orienter vers des études holistiques qui intégreraient l'analyse et l'évaluation des mesures répétitives sur l'échelle spatiale de toute la Mer Méditerranée ; et pour plusieurs paramètres du système des carbonates en particulier la pCO_2^{sw}, l'A_T, le C_T et le pH. Ceci permettrait de mieux apprécier le rôle de la Mer Méditerranée dans la séquestration du CO_2 atmosphérique et par la suite son rôle dans le ralentissement du changement climatique.

ANNEXES

Droits d'auteurs, Figure 2, Page 23

ELSEVIER LICENSE
TERMS AND CONDITIONS

Jun 24, 2015

This is a License Agreement between Elissar Gemayel ("You") and Elsevier ("Elsevier") provided by Copyright Clearance Center ("CCC"). The license consists of your order details, the terms and conditions provided by Elsevier, and the payment terms and conditions.

All payments must be made in full to CCC. For payment instructions, please see information listed at the bottom of this form.

Supplier	Elsevier Limited The Boulevard, Langford Lane Kidlington, Oxford,OX5 1GB,UK
Registered Company Number	1982084
Customer name	Elissar Gemayel
Customer address	IMAGES_ESPACE-DEV Perpignan, 66860
License number	3640250753139
License date	Jun 01, 2015
Licensed content publisher	Elsevier
Licensed content publication	Marine Chemistry
Licensed content title	Climatological distributions of pH, pCO2, total CO2, alkalinity, and CaCO3 saturation in the global surface ocean, and temporal changes at selected locations
Licensed content author	Taro Takahashi,S.C. Sutherland,D.W. Chipman,J.G. Goddard,Cheng Ho,Timothy Newberger,Colm Sweeney,D.R. Munro
Licensed content date	20 August 2014
Licensed content volume number	164
Licensed content issue number	n/a
Number of pages	31
Start Page	95
End Page	125
Type of Use	reuse in a thesis/dissertation
Portion	figures/tables/illustrations
Number of figures/tables/illustrations	1
Format	electronic
Are you the author of this Elsevier article?	No
Will you be translating?	No
Original figure numbers	Figure 12

Title of your thesis/dissertation	Contribution à l'estimation des paramètres du système des carbonates en Mer Méditerranée
Expected completion date	Sep 2015
Estimated size (number of pages)	200
Elsevier VAT number	GB 494 6272 12
Permissions price	0.00 USD
VAT/Local Sales Tax	0.00 USD / 0.00 GBP
Total	0.00 USD
Terms and Conditions	

INTRODUCTION

1. The publisher for this copyrighted material is Elsevier. By clicking "accept" in connection with completing this licensing transaction, you agree that the following terms and conditions apply to this transaction (along with the Billing and Payment terms and conditions established by Copyright Clearance Center, Inc. ("CCC"), at the time that you opened your Rightslink account and that are available at any time at http://myaccount.copyright.com).

GENERAL TERMS

2. Elsevier hereby grants you permission to reproduce the aforementioned material subject to the terms and conditions indicated.

3. Acknowledgement: If any part of the material to be used (for example, figures) has appeared in our publication with credit or acknowledgement to another source, permission must also be sought from that source. If such permission is not obtained then that material may not be included in your publication/copies. Suitable acknowledgement to the source must be made, either as a footnote or in a reference list at the end of your publication, as follows:

"Reprinted from Publication title, Vol /edition number, Author(s), Title of article / title of chapter, Pages No., Copyright (Year), with permission from Elsevier [OR APPLICABLE SOCIETY COPYRIGHT OWNER]." Also Lancet special credit - "Reprinted from The Lancet, Vol. number, Author(s), Title of article, Pages No., Copyright (Year), with permission from Elsevier."

4. Reproduction of this material is confined to the purpose and/or media for which permission is hereby given.

5. Altering/Modifying Material: Not Permitted. However figures and illustrations may be altered/adapted minimally to serve your work. Any other abbreviations, additions, deletions and/or any other alterations shall be made only with prior written authorization of Elsevier Ltd. (Please contact Elsevier at permissions@elsevier.com)

6. If the permission fee for the requested use of our material is waived in this instance, please be advised that your future requests for Elsevier materials may attract a fee.

7. Reservation of Rights: Publisher reserves all rights not specifically granted in the combination of (i) the license details provided by you and accepted in the course of this

licensing transaction, (ii) these terms and conditions and (iii) CCC's Billing and Payment terms and conditions.

8. License Contingent Upon Payment: While you may exercise the rights licensed immediately upon issuance of the license at the end of the licensing process for the transaction, provided that you have disclosed complete and accurate details of your proposed use, no license is finally effective unless and until full payment is received from you (either by publisher or by CCC) as provided in CCC's Billing and Payment terms and conditions. If full payment is not received on a timely basis, then any license preliminarily granted shall be deemed automatically revoked and shall be void as if never granted. Further, in the event that you breach any of these terms and conditions or any of CCC's Billing and Payment terms and conditions, the license is automatically revoked and shall be void as if never granted. Use of materials as described in a revoked license, as well as any use of the materials beyond the scope of an unrevoked license, may constitute copyright infringement and publisher reserves the right to take any and all action to protect its copyright in the materials.

9. Warranties: Publisher makes no representations or warranties with respect to the licensed material.

10. Indemnity: You hereby indemnify and agree to hold harmless publisher and CCC, and their respective officers, directors, employees and agents, from and against any and all claims arising out of your use of the licensed material other than as specifically authorized pursuant to this license.

11. No Transfer of License: This license is personal to you and may not be sublicensed, assigned, or transferred by you to any other person without publisher's written permission.

12. No Amendment Except in Writing: This license may not be amended except in a writing signed by both parties (or, in the case of publisher, by CCC on publisher's behalf).

13. Objection to Contrary Terms: Publisher hereby objects to any terms contained in any purchase order, acknowledgment, check endorsement or other writing prepared by you, which terms are inconsistent with these terms and conditions or CCC's Billing and Payment terms and conditions. These terms and conditions, together with CCC's Billing and Payment terms and conditions (which are incorporated herein), comprise the entire agreement between you and publisher (and CCC) concerning this licensing transaction. In the event of any conflict between your obligations established by these terms and conditions and those established by CCC's Billing and Payment terms and conditions, these terms and conditions shall control.

14. Revocation: Elsevier or Copyright Clearance Center may deny the permissions described in this License at their sole discretion, for any reason or no reason, with a full refund payable to you. Notice of such denial will be made using the contact information provided by you. Failure to receive such notice will not alter or invalidate the denial. In no event will Elsevier or Copyright Clearance Center be responsible or liable for any costs, expenses or damage incurred by you as a result of a denial of your permission request, other than a refund of the amount(s) paid by you to Elsevier and/or Copyright Clearance Center for denied permissions.

LIMITED LICENSE

The following terms and conditions apply only to specific license types:

15. Translation: This permission is granted for non-exclusive world English rights only unless your license was granted for translation rights. If you licensed translation rights you may only translate this content into the languages you requested. A professional translator must perform all translations and reproduce the content word for word preserving the integrity of the article. If this license is to re-use 1 or 2 figures then permission is granted for non-exclusive world rights in all languages.

16. Posting licensed content on any Website: The following terms and conditions apply as follows: Licensing material from an Elsevier journal: All content posted to the web site must maintain the copyright information line on the bottom of each image; A hyper-text must be included to the Homepage of the journal from which you are licensing athttp://www.sciencedirect.com/science/journal/xxxxx or the Elsevier homepage for books athttp://www.elsevier.com; Central Storage: This license does not include permission for a scanned version of the material to be stored in a central repository such as that provided by Heron/XanEdu. Licensing material from an Elsevier book: A hyper-text link must be included to the Elsevier homepage at http://www.elsevier.com . All content posted to the web site must maintain the copyright information line on the bottom of each image.

Posting licensed content on Electronic reserve: In addition to the above the following clauses are applicable: The web site must be password-protected and made available only to bona fide students registered on a relevant course. This permission is granted for 1 year only. You may obtain a new license for future website posting.

17. For journal authors: the following clauses are applicable in addition to the above:

Preprints:

A preprint is an author's own write-up of research results and analysis, it has not been peer-reviewed, nor has it had any other value added to it by a publisher (such as formatting, copyright, technical enhancement etc.).

Authors can share their preprints anywhere at any time. Preprints should not be added to or enhanced in any way in order to appear more like, or to substitute for, the final versions of articles however authors can update their preprints on arXiv or RePEc with their Accepted Author Manuscript (see below).

If accepted for publication, we encourage authors to link from the preprint to their formal publication via its DOI. Millions of researchers have access to the formal publications on ScienceDirect, and so links will help users to find, access, cite and use the best available version. Please note that Cell Press, The Lancet and some society-owned have different preprint policies. Information on these policies is available on the journal homepage.

Accepted Author Manuscripts: An accepted author manuscript is the manuscript of an article that has been accepted for publication and which typically includes author-incorporated changes suggested during submission, peer review and editor-author communications.

Authors can share their accepted author manuscript:

- - immediately
    - via their non-commercial person homepage or blog
    - by updating a preprint in arXiv or RePEc with the accepted manuscript
    - via their research institute or institutional repository for internal institutional uses or as part of an invitation-only research collaboration work-group
    - directly by providing copies to their students or to research collaborators for their personal use
    - for private scholarly sharing as part of an invitation-only work group on commercial sites with which Elsevier has an agreement
- - after the embargo period
    - via non-commercial hosting platforms such as their institutional repository
    - via commercial sites with which Elsevier has an agreement

In all cases accepted manuscripts should:

- - link to the formal publication via its DOI
- - bear a CC-BY-NC-ND license - this is easy to do
- - if aggregated with other manuscripts, for example in a repository or other site, be shared in alignment with our hosting policy not be added to or enhanced in any way to appear more like, or to substitute for, the published journal article.

Published journal article (JPA): A published journal article (PJA) is the definitive final record of published research that appears or will appear in the journal and embodies all value-adding publishing activities including peer review co-ordination, copy-editing, formatting, (if relevant) pagination and online enrichment.

Policies for sharing publishing journal articles differ for subscription and gold open access articles:

Subscription Articles: If you are an author, please share a link to your article rather than the full-text. Millions of researchers have access to the formal publications on ScienceDirect, and so links will help your users to find, access, cite, and use the best available version.

Theses and dissertations which contain embedded PJAs as part of the formal submission can be posted publicly by the awarding institution with DOI links back to the formal publications on ScienceDirect.

If you are affiliated with a library that subscribes to ScienceDirect you have additional private sharing rights for others' research accessed under that agreement. This includes use for classroom teaching and internal training at the institution (including use in course packs and courseware programs), and inclusion of the article for grant funding purposes.

Gold Open Access Articles: May be shared according to the author-selected end-user license and should contain a CrossMark logo, the end user license, and a DOI link to the formal publication on ScienceDirect.

Please refer to Elsevier's posting policy for further information.

18. For book authors the following clauses are applicable in addition to the above: Authors are permitted to place a brief summary of their work online only. You are not allowed to download and post the published electronic version of your chapter, nor may you scan the printed edition to create an electronic version. Posting to a repository: Authors are permitted to post a summary of their chapter only in their institution's repository.

19. Thesis/Dissertation: If your license is for use in a thesis/dissertation your thesis may be submitted to your institution in either print or electronic form. Should your thesis be published commercially, please reapply for permission. These requirements include permission for the Library and Archives of Canada to supply single copies, on demand, of the complete thesis and include permission for Proquest/UMI to supply single copies, on demand, of the complete thesis. Should your thesis be published commercially, please reapply for permission. Theses and dissertations which contain embedded PJAs as part of the formal submission can be posted publicly by the awarding institution with DOI links back to the formal publications on ScienceDirect.

Elsevier Open Access Terms and Conditions

You can publish open access with Elsevier in hundreds of open access journals or in nearly 2000 established subscription journals that support open access publishing. Permitted third party re-use of these open access articles is defined by the author's choice of Creative Commons user license. See our open access license policy for more information.

Terms & Conditions applicable to all Open Access articles published with Elsevier:

Any reuse of the article must not represent the author as endorsing the adaptation of the article nor should the article be modified in such a way as to damage the author's honour or reputation. If any changes have been made, such changes must be clearly indicated.

The author(s) must be appropriately credited and we ask that you include the end user license and a DOI link to the formal publication on ScienceDirect.

If any part of the material to be used (for example, figures) has appeared in our publication with credit or acknowledgement to another source it is the responsibility of the user to ensure their reuse complies with the terms and conditions determined by the rights holder.

Additional Terms & Conditions applicable to each Creative Commons user license:

CC BY: The CC-BY license allows users to copy, to create extracts, abstracts and new works from the Article, to alter and revise the Article and to make commercial use of the Article (including reuse and/or resale of the Article by commercial entities), provided the user gives appropriate credit (with a link to the formal publication through the relevant DOI), provides a link to the license, indicates if changes were made and the licensor is not represented as endorsing the use made of the work. The full details of the license are available at http://creativecommons.org/licenses/by/4.0.

CC BY NC SA: The CC BY-NC-SA license allows users to copy, to create extracts, abstracts and new works from the Article, to alter and revise the Article, provided this is not done for commercial purposes, and that the user gives appropriate credit (with a link to

the formal publication through the relevant DOI), provides a link to the license, indicates if changes were made and the licensor is not represented as endorsing the use made of the work. Further, any new works must be made available on the same conditions. The full details of the license are available at http://creativecommons.org/licenses/by-nc-sa/4.0.

CC BY NC ND: The CC BY-NC-ND license allows users to copy and distribute the Article, provided this is not done for commercial purposes and further does not permit distribution of the Article if it is changed or edited in any way, and provided the user gives appropriate credit (with a link to the formal publication through the relevant DOI), provides a link to the license, and that the licensor is not represented as endorsing the use made of the work. The full details of the license are available at http://creativecommons.org/licenses/by-nc-nd/4.0. Any commercial reuse of Open Access articles published with a CC BY NC SA or CC BY NC ND license requires permission from Elsevier and will be subject to a fee.

Commercial reuse includes:

- - Associating advertising with the full text of the Article
- - Charging fees for document delivery or access
- - Article aggregation
- - Systematic distribution via e-mail lists or share buttons

Posting or linking by commercial companies for use by customers of those companies.

20. Other Conditions:

v1.7

Questions? customercare@copyright.com or +1-855-239-3415 (toll free in the US) or +1-978-646-2777.

Droits d'auteurs, Figure 3, Page 30

Dear Dr. Gemayel—

My name is Jinny Nathans and I'm the Permissions Officer at AMS. Your question was referred to me. This signed message constitutes permission to use the material requested in your email below.

You may use the figure in your thesis with the following conditions:

+ please include the complete bibliographic citation of the original source, and
+ please include the following statement with that citation: ©American Meteorological Society. Used with permission.

Thanks very much for your request and if you need any further information, please get in touch with me. My contact information is below.

Regards,

Jinny Nathans
Permissions Officer
American Meteorological Society

jnathans@ametsoc.org
617 226-3905

Dear Sir/Madam,

I am third year PhD student in the process of writing my thesis which I intend to submit by the end of June 2015. In this manner I would appreciate your approval to reproduce in my thesis the Figure 1 of the article: Accadia, C., Zecchetto, S., Lavagnini, A., Speranza, A., 2007. Comparison of 10-m Wind Forecasts from a Regional Area Model and QuikSCAT Scatterometer Wind Observations over the Mediterranean Sea. Mon. Weather Rev. 135 (5), 1945-1960. 10.1175/mwr3370.1

The figure will be included with no modifications and collated to a paragraph where I introduce the general wind regime in the Mediterranean Sea. The thesis will be submitted electronically to the administration with no hard copy distributions.
Also note that I do not intend to distribute this figure or my thesis for commercial purposes

Please inform me how to proceed on this manner
Best regards,
Elissar

Droits d'auteurs, Figure 4, Page 32

SPRINGER LICENSE
TERMS AND CONDITIONS

Jun 24, 2015

This is a License Agreement between Elissar Gemayel ("You") and Springer ("Springer") provided by Copyright Clearance Center ("CCC"). The license consists of your order details, the terms and conditions provided by Springer, and the payment terms and conditions.

All payments must be made in full to CCC. For payment instructions, please see information listed at the bottom of this form.

License Number	3640260257391
License date	Jun 01, 2015
Licensed content publisher	Springer
Licensed content publication	Springer eBook
Licensed content title	Circulation in the Mediterranean Sea
Licensed content author	Claude Millot
Licensed content date	Jan 1, 2005
Type of Use	Thesis/Dissertation
Portion	Figures
Author of this Springer article	No
Order reference number	None
Original figure numbers	Figure 2
Title of your thesis / dissertation	Contribution à l'estimation des paramètres du système des carbonates en Mer Méditerranée
Expected completion date	Sep 2015
Estimated size(pages)	200
Total	0.00 USD
Terms and Conditions	

Introduction
The publisher for this copyrighted material is Springer Science + Business Media. By clicking "accept" in connection with completing this licensing transaction, you agree that the following terms and conditions apply to this transaction (along with the Billing and Payment terms and conditions established by Copyright Clearance Center, Inc. ("CCC"), at the time that you opened your Rightslink account and that are available at any time at

http://myaccount.copyright.com).

Limited License
With reference to your request to reprint in your thesis material on which Springer Science and Business Media control the copyright, permission is granted, free of charge, for the use indicated in your enquiry.

Licenses are for one-time use only with a maximum distribution equal to the number that you identified in the licensing process.

This License includes use in an electronic form, provided its password protected or on the university's intranet or repository, including UMI (according to the definition at the Sherpa website: http://www.sherpa.ac.uk/romeo/). For any other electronic use, please contact Springer at (permissions.dordrecht@springer.com or permissions.heidelberg@springer.com).

The material can only be used for the purpose of defending your thesis limited to university-use only. If the thesis is going to be published, permission needs to be re-obtained (selecting "book/textbook" as the type of use).

Although Springer holds copyright to the material and is entitled to negotiate on rights, this license is only valid, subject to a courtesy information to the author (address is given with the article/chapter) and provided it concerns original material which does not carry references to other sources (if material in question appears with credit to another source, authorization from that source is required as well).

Permission free of charge on this occasion does not prejudice any rights we might have to charge for reproduction of our copyrighted material in the future.

Altering/Modifying Material: Not Permitted
You may not alter or modify the material in any manner. Abbreviations, additions, deletions and/or any other alterations shall be made only with prior written authorization of the author(s) and/or Springer Science + Business Media. (Please contact Springer at (permissions.dordrecht@springer.com or permissions.heidelberg@springer.com)

Reservation of Rights
Springer Science + Business Media reserves all rights not specifically granted in the combination of (i) the license details provided by you and accepted in the course of this licensing transaction, (ii) these terms and conditions and (iii) CCC's Billing and Payment terms and conditions.

Copyright Notice:Disclaimer
You must include the following copyright and permission notice in connection with any reproduction of the licensed material: "Springer and the original publisher /journal title, volume, year of publication, page, chapter/article title, name(s) of author(s), figure number(s), original copyright notice) is given to the publication in which the material was originally published, by adding; with kind permission from Springer Science and Business Media"

Warranties: None
Example 1: Springer Science + Business Media makes no representations or warranties with

respect to the licensed material.

Example 2: Springer Science + Business Media makes no representations or warranties with respect to the licensed material and adopts on its own behalf the limitations and disclaimers established by CCC on its behalf in its Billing and Payment terms and conditions for this licensing transaction.

Indemnity
You hereby indemnify and agree to hold harmless Springer Science + Business Media and CCC, and their respective officers, directors, employees and agents, from and against any and all claims arising out of your use of the licensed material other than as specifically authorized pursuant to this license.

No Transfer of License
This license is personal to you and may not be sublicensed, assigned, or transferred by you to any other person without Springer Science + Business Media's written permission.

No Amendment Except in Writing
This license may not be amended except in a writing signed by both parties (or, in the case of Springer Science + Business Media, by CCC on Springer Science + Business Media's behalf).

Objection to Contrary Terms
Springer Science + Business Media hereby objects to any terms contained in any purchase order, acknowledgment, check endorsement or other writing prepared by you, which terms are inconsistent with these terms and conditions or CCC's Billing and Payment terms and conditions. These terms and conditions, together with CCC's Billing and Payment terms and conditions (which are incorporated herein), comprise the entire agreement between you and Springer Science + Business Media (and CCC) concerning this licensing transaction. In the event of any conflict between your obligations established by these terms and conditions and those established by CCC's Billing and Payment terms and conditions, these terms and conditions shall control.

Jurisdiction
All disputes that may arise in connection with this present License, or the breach thereof, shall be settled exclusively by arbitration, to be held in The Netherlands, in accordance with Dutch law, and to be conducted under the Rules of the 'Netherlands Arbitrage Instituut' (Netherlands Institute of Arbitration).***OR:***

All disputes that may arise in connection with this present License, or the breach thereof, shall be settled exclusively by arbitration, to be held in the Federal Republic of Germany, in accordance with German law.

Other terms and conditions:

v1.3

Questions? customercare@copyright.com or +1-855-239-3415 (toll free in the US) or +1-978-646-2777.

Droits d'auteurs, Figure 8, Page 38

ELSEVIER LICENSE
TERMS AND CONDITIONS

Jun 24, 2015

This is a License Agreement between Elissar Gemayel ("You") and Elsevier ("Elsevier") provided by Copyright Clearance Center ("CCC"). The license consists of your order details, the terms and conditions provided by Elsevier, and the payment terms and conditions.

All payments must be made in full to CCC. For payment instructions, please see information listed at the bottom of this form.

Supplier	Elsevier Limited The Boulevard,Langford Lane Kidlington,Oxford,OX5 1GB,UK
Registered Company Number	1982084
Customer name	Elissar Gemayel
Customer address	IMAGES_ESPACE-DEV Perpignan, 66860
License number	3640260502630
License date	Jun 01, 2015
Licensed content publisher	Elsevier
Licensed content publication	Deep Sea Research Part I: Oceanographic Research Papers
Licensed content title	Satellite-driven modeling of the upper ocean mixed layer and air–sea CO2 flux in the Mediterranean Sea
Licensed content author	Fabrizio D'Ortenzio,David Antoine,Salvatore Marullo
Licensed content date	April 2008
Licensed content volume number	55
Licensed content issue number	4
Number of pages	30
Start Page	405
End Page	434
Type of Use	reuse in a thesis/dissertation
Intended publisher of new work	other
Portion	figures/tables/illustrations
Number of figures/tables/illustrations	1
Format	both print and electronic
Are you the author of this Elsevier article?	No
Will you be translating?	No
Original figure numbers	Figure 10

Title of your thesis/dissertation	Contribution à l'estimation des paramètres du système des carbonates en Mer Méditerranée
Expected completion date	Sep 2015
Estimated size (number of pages)	200
Elsevier VAT number	GB 494 6272 12
Permissions price	0.00 USD
VAT/Local Sales Tax	0.00 USD / 0.00 GBP
Total	0.00 USD
Terms and Conditions	

INTRODUCTION

1. The publisher for this copyrighted material is Elsevier. By clicking "accept" in connection with completing this licensing transaction, you agree that the following terms and conditions apply to this transaction (along with the Billing and Payment terms and conditions established by Copyright Clearance Center, Inc. ("CCC"), at the time that you opened your Rightslink account and that are available at any time athttp://myaccount.copyright.com).

GENERAL TERMS

2. Elsevier hereby grants you permission to reproduce the aforementioned material subject to the terms and conditions indicated.

3. Acknowledgement: If any part of the material to be used (for example, figures) has appeared in our publication with credit or acknowledgement to another source, permission must also be sought from that source. If such permission is not obtained then that material may not be included in your publication/copies. Suitable acknowledgement to the source must be made, either as a footnote or in a reference list at the end of your publication, as follows:

"Reprinted from Publication title, Vol /edition number, Author(s), Title of article / title of chapter, Pages No., Copyright (Year), with permission from Elsevier [OR APPLICABLE SOCIETY COPYRIGHT OWNER]." Also Lancet special credit - "Reprinted from The Lancet, Vol. number, Author(s), Title of article, Pages No., Copyright (Year), with permission from Elsevier."

4. Reproduction of this material is confined to the purpose and/or media for which permission is hereby given.

5. Altering/Modifying Material: Not Permitted. However figures and illustrations may be altered/adapted minimally to serve your work. Any other abbreviations, additions, deletions and/or any other alterations shall be made only with prior written authorization of Elsevier Ltd. (Please contact Elsevier at permissions@elsevier.com)

6. If the permission fee for the requested use of our material is waived in this instance, please be advised that your future requests for Elsevier materials may attract a fee.

7. Reservation of Rights: Publisher reserves all rights not specifically granted in the combination of (i) the license details provided by you and accepted in the course of this

licensing transaction, (ii) these terms and conditions and (iii) CCC's Billing and Payment terms and conditions.

8. License Contingent Upon Payment: While you may exercise the rights licensed immediately upon issuance of the license at the end of the licensing process for the transaction, provided that you have disclosed complete and accurate details of your proposed use, no license is finally effective unless and until full payment is received from you (either by publisher or by CCC) as provided in CCC's Billing and Payment terms and conditions. If full payment is not received on a timely basis, then any license preliminarily granted shall be deemed automatically revoked and shall be void as if never granted. Further, in the event that you breach any of these terms and conditions or any of CCC's Billing and Payment terms and conditions, the license is automatically revoked and shall be void as if never granted. Use of materials as described in a revoked license, as well as any use of the materials beyond the scope of an unrevoked license, may constitute copyright infringement and publisher reserves the right to take any and all action to protect its copyright in the materials.

9. Warranties: Publisher makes no representations or warranties with respect to the licensed material.

10. Indemnity: You hereby indemnify and agree to hold harmless publisher and CCC, and their respective officers, directors, employees and agents, from and against any and all claims arising out of your use of the licensed material other than as specifically authorized pursuant to this license.

11. No Transfer of License: This license is personal to you and may not be sublicensed, assigned, or transferred by you to any other person without publisher's written permission.

12. No Amendment Except in Writing: This license may not be amended except in a writing signed by both parties (or, in the case of publisher, by CCC on publisher's behalf).

13. Objection to Contrary Terms: Publisher hereby objects to any terms contained in any purchase order, acknowledgment, check endorsement or other writing prepared by you, which terms are inconsistent with these terms and conditions or CCC's Billing and Payment terms and conditions. These terms and conditions, together with CCC's Billing and Payment terms and conditions (which are incorporated herein), comprise the entire agreement between you and publisher (and CCC) concerning this licensing transaction. In the event of any conflict between your obligations established by these terms and conditions and those established by CCC's Billing and Payment terms and conditions, these terms and conditions shall control.

14. Revocation: Elsevier or Copyright Clearance Center may deny the permissions described in this License at their sole discretion, for any reason or no reason, with a full refund payable to you. Notice of such denial will be made using the contact information provided by you. Failure to receive such notice will not alter or invalidate the denial. In no event will Elsevier or Copyright Clearance Center be responsible or liable for any costs, expenses or damage incurred by you as a result of a denial of your permission request, other than a refund of the amount(s) paid by you to Elsevier and/or Copyright Clearance Center for denied permissions.

LIMITED LICENSE

The following terms and conditions apply only to specific license types:

15. **Translation**: This permission is granted for non-exclusive world **English** rights only unless your license was granted for translation rights. If you licensed translation rights you may only translate this content into the languages you requested. A professional translator must perform all translations and reproduce the content word for word preserving the integrity of the article. If this license is to re-use 1 or 2 figures then permission is granted for non-exclusive world rights in all languages.

16. **Posting licensed content on any Website**: The following terms and conditions apply as follows: Licensing material from an Elsevier journal: All content posted to the web site must maintain the copyright information line on the bottom of each image; A hyper-text must be included to the Homepage of the journal from which you are licensing athttp://www.sciencedirect.com/science/journal/xxxxx or the Elsevier homepage for books athttp://www.elsevier.com; Central Storage: This license does not include permission for a scanned version of the material to be stored in a central repository such as that provided by Heron/XanEdu.

Licensing material from an Elsevier book: A hyper-text link must be included to the Elsevier homepage at http://www.elsevier.com . All content posted to the web site must maintain the copyright information line on the bottom of each image.

Posting licensed content on Electronic reserve: In addition to the above the following clauses are applicable: The web site must be password-protected and made available only to bona fide students registered on a relevant course. This permission is granted for 1 year only. You may obtain a new license for future website posting.

17. **For journal authors:** the following clauses are applicable in addition to the above:

Preprints:

A preprint is an author's own write-up of research results and analysis, it has not been peer-reviewed, nor has it had any other value added to it by a publisher (such as formatting, copyright, technical enhancement etc.).

Authors can share their preprints anywhere at any time. Preprints should not be added to or enhanced in any way in order to appear more like, or to substitute for, the final versions of articles however authors can update their preprints on arXiv or RePEc with their Accepted Author Manuscript (see below).

If accepted for publication, we encourage authors to link from the preprint to their formal publication via its DOI. Millions of researchers have access to the formal publications on ScienceDirect, and so links will help users to find, access, cite and use the best available version. Please note that Cell Press, The Lancet and some society-owned have different preprint policies. Information on these policies is available on the journal homepage.

Accepted Author Manuscripts: An accepted author manuscript is the manuscript of an article that has been accepted for publication and which typically includes author-incorporated changes suggested during submission, peer review and editor-author

communications.

Authors can share their accepted author manuscript:

- - immediately
    - via their non-commercial person homepage or blog
    - by updating a preprint in arXiv or RePEc with the accepted manuscript
    - via their research institute or institutional repository for internal institutional uses or as part of an invitation-only research collaboration work-group
    - directly by providing copies to their students or to research collaborators for their personal use
    - for private scholarly sharing as part of an invitation-only work group on commercial sites with which Elsevier has an agreement
- - after the embargo period
    - via non-commercial hosting platforms such as their institutional repository
    - via commercial sites with which Elsevier has an agreement

In all cases accepted manuscripts should:

- - link to the formal publication via its DOI
- - bear a CC-BY-NC-ND license - this is easy to do
- - if aggregated with other manuscripts, for example in a repository or other site, be shared in alignment with our hosting policy not be added to or enhanced in any way to appear more like, or to substitute for, the published journal article.

Published journal article (JPA): A published journal article (PJA) is the definitive final record of published research that appears or will appear in the journal and embodies all value-adding publishing activities including peer review co-ordination, copy-editing, formatting, (if relevant) pagination and online enrichment.

Policies for sharing publishing journal articles differ for subscription and gold open access articles:

Subscription Articles: If you are an author, please share a link to your article rather than the full-text. Millions of researchers have access to the formal publications on ScienceDirect, and so links will help your users to find, access, cite, and use the best available version.

Theses and dissertations which contain embedded PJAs as part of the formal submission can be posted publicly by the awarding institution with DOI links back to the formal publications on ScienceDirect.

If you are affiliated with a library that subscribes to ScienceDirect you have additional private sharing rights for others' research accessed under that agreement. This includes use for classroom teaching and internal training at the institution (including use in course packs and courseware programs), and inclusion of the article for grant funding purposes.

Gold Open Access Articles: May be shared according to the author-selected end-user

license and should contain a CrossMark logo, the end user license, and a DOI link to the formal publication on ScienceDirect.

Please refer to Elsevier's posting policy for further information.

18. **For book authors** the following clauses are applicable in addition to the above: Authors are permitted to place a brief summary of their work online only. You are not allowed to download and post the published electronic version of your chapter, nor may you scan the printed edition to create an electronic version. **Posting to a repository:** Authors are permitted to post a summary of their chapter only in their institution's repository.

19. **Thesis/Dissertation**: If your license is for use in a thesis/dissertation your thesis may be submitted to your institution in either print or electronic form. Should your thesis be published commercially, please reapply for permission. These requirements include permission for the Library and Archives of Canada to supply single copies, on demand, of the complete thesis and include permission for Proquest/UMI to supply single copies, on demand, of the complete thesis. Should your thesis be published commercially, please reapply for permission. Theses and dissertations which contain embedded PJAs as part of the formal submission can be posted publicly by the awarding institution with DOI links back to the formal publications on ScienceDirect.

Elsevier Open Access Terms and Conditions

You can publish open access with Elsevier in hundreds of open access journals or in nearly 2000 established subscription journals that support open access publishing. Permitted third party re-use of these open access articles is defined by the author's choice of Creative Commons user license. See our open access license policy for more information.

Terms & Conditions applicable to all Open Access articles published with Elsevier:

Any reuse of the article must not represent the author as endorsing the adaptation of the article nor should the article be modified in such a way as to damage the author's honour or reputation. If any changes have been made, such changes must be clearly indicated.

The author(s) must be appropriately credited and we ask that you include the end user license and a DOI link to the formal publication on ScienceDirect.

If any part of the material to be used (for example, figures) has appeared in our publication with credit or acknowledgement to another source it is the responsibility of the user to ensure their reuse complies with the terms and conditions determined by the rights holder.

Additional Terms & Conditions applicable to each Creative Commons user license:

CC BY: The CC-BY license allows users to copy, to create extracts, abstracts and new works from the Article, to alter and revise the Article and to make commercial use of the Article (including reuse and/or resale of the Article by commercial entities), provided the user gives appropriate credit (with a link to the formal publication through the relevant DOI), provides a link to the license, indicates if changes were made and the licensor is not represented as endorsing the use made of the work. The full details of the license are available at http://creativecommons.org/licenses/by/4.0.

CC BY NC SA: The CC BY-NC-SA license allows users to copy, to create extracts, abstracts and new works from the Article, to alter and revise the Article, provided this is not done for commercial purposes, and that the user gives appropriate credit (with a link to the formal publication through the relevant DOI), provides a link to the license, indicates if changes were made and the licensor is not represented as endorsing the use made of the work. Further, any new works must be made available on the same conditions. The full details of the license are available at http://creativecommons.org/licenses/by-nc-sa/4.0.

CC BY NC ND: The CC BY-NC-ND license allows users to copy and distribute the Article, provided this is not done for commercial purposes and further does not permit distribution of the Article if it is changed or edited in any way, and provided the user gives appropriate credit (with a link to the formal publication through the relevant DOI), provides a link to the license, and that the licensor is not represented as endorsing the use made of the work. The full details of the license are available at http://creativecommons.org/licenses/by-nc-nd/4.0. Any commercial reuse of Open Access articles published with a CC BY NC SA or CC BY NC ND license requires permission from Elsevier and will be subject to a fee.

Commercial reuse includes:

- - Associating advertising with the full text of the Article
- - Charging fees for document delivery or access
- - Article aggregation
- - Systematic distribution via e-mail lists or share buttons

Posting or linking by commercial companies for use by customers of those companies.

20. **Other Conditions**:

v1.7

Questions? customercare@copyright.com or +1-855-239-3415 (toll free in the US) or +1-978-646-2777.

Droits d'auteurs, Figure 9, Page 39

ELSEVIER LICENSE
TERMS AND CONDITIONS

Jun 24, 2015

This is a License Agreement between Elissar Gemayel ("You") and Elsevier ("Elsevier") provided by Copyright Clearance Center ("CCC"). The license consists of your order details, the terms and conditions provided by Elsevier, and the payment terms and conditions.

All payments must be made in full to CCC. For payment instructions, please see information listed at the bottom of this form.

Supplier	Elsevier Limited The Boulevard,Langford Lane Kidlington,Oxford,OX5 1GB,UK
Registered Company Number	1982084
Customer name	Elissar Gemayel
Customer address	IMAGES_ESPACE-DEV Perpignan, 66860
License number	3640260761132
License date	Jun 01, 2015
Licensed content publisher	Elsevier
Licensed content publication	Deep Sea Research Part I: Oceanographic Research Papers
Licensed content title	Carbon fluxes in the mixed layer of the Mediterranean Sea in the 1980s and the 2000s
Licensed content author	Vincent Taillandier,Fabrizio D'Ortenzio,David Antoine
Licensed content date	July 2012
Licensed content volume number	65
Licensed content issue number	n/a
Number of pages	12
Start Page	73
End Page	84
Type of Use	reuse in a thesis/dissertation
Intended publisher of new work	other
Portion	figures/tables/illustrations
Number of figures/tables/illustrations	1
Format	both print and electronic
Are you the author of this Elsevier article?	No
Will you be translating?	No
Original figure numbers	Figure 4

Title of your thesis/dissertation	Contribution à l'estimation des paramètres du système des carbonates en Mer Méditerranée
Expected completion date	Sep 2015
Estimated size (number of pages)	200
Elsevier VAT number	GB 494 6272 12
Permissions price	0.00 USD
VAT/Local Sales Tax	0.00 USD / 0.00 GBP
Total	0.00 USD
Terms and Conditions	

INTRODUCTION

1. The publisher for this copyrighted material is Elsevier. By clicking "accept" in connection with completing this licensing transaction, you agree that the following terms and conditions apply to this transaction (along with the Billing and Payment terms and conditions established by Copyright Clearance Center, Inc. ("CCC"), at the time that you opened your Rightslink account and that are available at any time athttp://myaccount.copyright.com).

GENERAL TERMS

2. Elsevier hereby grants you permission to reproduce the aforementioned material subject to the terms and conditions indicated.

3. Acknowledgement: If any part of the material to be used (for example, figures) has appeared in our publication with credit or acknowledgement to another source, permission must also be sought from that source. If such permission is not obtained then that material may not be included in your publication/copies. Suitable acknowledgement to the source must be made, either as a footnote or in a reference list at the end of your publication, as follows:

"Reprinted from Publication title, Vol /edition number, Author(s), Title of article / title of chapter, Pages No., Copyright (Year), with permission from Elsevier [OR APPLICABLE SOCIETY COPYRIGHT OWNER]." Also Lancet special credit - "Reprinted from The Lancet, Vol. number, Author(s), Title of article, Pages No., Copyright (Year), with permission from Elsevier."

4. Reproduction of this material is confined to the purpose and/or media for which permission is hereby given.

5. Altering/Modifying Material: Not Permitted. However figures and illustrations may be altered/adapted minimally to serve your work. Any other abbreviations, additions, deletions and/or any other alterations shall be made only with prior written authorization of Elsevier Ltd. (Please contact Elsevier at permissions@elsevier.com)

6. If the permission fee for the requested use of our material is waived in this instance, please be advised that your future requests for Elsevier materials may attract a fee.

7. Reservation of Rights: Publisher reserves all rights not specifically granted in the combination of (i) the license details provided by you and accepted in the course of this

licensing transaction, (ii) these terms and conditions and (iii) CCC's Billing and Payment terms and conditions.

8. License Contingent Upon Payment: While you may exercise the rights licensed immediately upon issuance of the license at the end of the licensing process for the transaction, provided that you have disclosed complete and accurate details of your proposed use, no license is finally effective unless and until full payment is received from you (either by publisher or by CCC) as provided in CCC's Billing and Payment terms and conditions. If full payment is not received on a timely basis, then any license preliminarily granted shall be deemed automatically revoked and shall be void as if never granted. Further, in the event that you breach any of these terms and conditions or any of CCC's Billing and Payment terms and conditions, the license is automatically revoked and shall be void as if never granted. Use of materials as described in a revoked license, as well as any use of the materials beyond the scope of an unrevoked license, may constitute copyright infringement and publisher reserves the right to take any and all action to protect its copyright in the materials.

9. Warranties: Publisher makes no representations or warranties with respect to the licensed material.

10. Indemnity: You hereby indemnify and agree to hold harmless publisher and CCC, and their respective officers, directors, employees and agents, from and against any and all claims arising out of your use of the licensed material other than as specifically authorized pursuant to this license.

11. No Transfer of License: This license is personal to you and may not be sublicensed, assigned, or transferred by you to any other person without publisher's written permission.

12. No Amendment Except in Writing: This license may not be amended except in a writing signed by both parties (or, in the case of publisher, by CCC on publisher's behalf).

13. Objection to Contrary Terms: Publisher hereby objects to any terms contained in any purchase order, acknowledgment, check endorsement or other writing prepared by you, which terms are inconsistent with these terms and conditions or CCC's Billing and Payment terms and conditions. These terms and conditions, together with CCC's Billing and Payment terms and conditions (which are incorporated herein), comprise the entire agreement between you and publisher (and CCC) concerning this licensing transaction. In the event of any conflict between your obligations established by these terms and conditions and those established by CCC's Billing and Payment terms and conditions, these terms and conditions shall control.

14. Revocation: Elsevier or Copyright Clearance Center may deny the permissions described in this License at their sole discretion, for any reason or no reason, with a full refund payable to you. Notice of such denial will be made using the contact information provided by you. Failure to receive such notice will not alter or invalidate the denial. In no event will Elsevier or Copyright Clearance Center be responsible or liable for any costs, expenses or damage incurred by you as a result of a denial of your permission request, other than a refund of the amount(s) paid by you to Elsevier and/or Copyright Clearance Center for denied permissions.

LIMITED LICENSE

The following terms and conditions apply only to specific license types:

15. **Translation**: This permission is granted for non-exclusive world **English** rights only unless your license was granted for translation rights. If you licensed translation rights you may only translate this content into the languages you requested. A professional translator must perform all translations and reproduce the content word for word preserving the integrity of the article. If this license is to re-use 1 or 2 figures then permission is granted for non-exclusive world rights in all languages.

16. **Posting licensed content on any Website**: The following terms and conditions apply as follows: Licensing material from an Elsevier journal: All content posted to the web site must maintain the copyright information line on the bottom of each image; A hyper-text must be included to the Homepage of the journal from which you are licensing athttp://www.sciencedirect.com/science/journal/xxxxx or the Elsevier homepage for books athttp://www.elsevier.com; Central Storage: This license does not include permission for a scanned version of the material to be stored in a central repository such as that provided by Heron/XanEdu.

Licensing material from an Elsevier book: A hyper-text link must be included to the Elsevier homepage at http://www.elsevier.com . All content posted to the web site must maintain the copyright information line on the bottom of each image.

Posting licensed content on Electronic reserve: In addition to the above the following clauses are applicable: The web site must be password-protected and made available only to bona fide students registered on a relevant course. This permission is granted for 1 year only. You may obtain a new license for future website posting.

17. **For journal authors:** the following clauses are applicable in addition to the above:

Preprints:

A preprint is an author's own write-up of research results and analysis, it has not been peer-reviewed, nor has it had any other value added to it by a publisher (such as formatting, copyright, technical enhancement etc.).

Authors can share their preprints anywhere at any time. Preprints should not be added to or enhanced in any way in order to appear more like, or to substitute for, the final versions of articles however authors can update their preprints on arXiv or RePEc with their Accepted Author Manuscript (see below).

If accepted for publication, we encourage authors to link from the preprint to their formal publication via its DOI. Millions of researchers have access to the formal publications on ScienceDirect, and so links will help users to find, access, cite and use the best available version. Please note that Cell Press, The Lancet and some society-owned have different preprint policies. Information on these policies is available on the journal homepage.

Accepted Author Manuscripts: An accepted author manuscript is the manuscript of an article that has been accepted for publication and which typically includes author-incorporated changes suggested during submission, peer review and editor-author

communications.

Authors can share their accepted author manuscript:

- - immediately
    - via their non-commercial person homepage or blog
    - by updating a preprint in arXiv or RePEc with the accepted manuscript
    - via their research institute or institutional repository for internal institutional uses or as part of an invitation-only research collaboration work-group
    - directly by providing copies to their students or to research collaborators for their personal use
    - for private scholarly sharing as part of an invitation-only work group on commercial sites with which Elsevier has an agreement
- - after the embargo period
    - via non-commercial hosting platforms such as their institutional repository
    - via commercial sites with which Elsevier has an agreement

In all cases accepted manuscripts should:

- - link to the formal publication via its DOI
- - bear a CC-BY-NC-ND license - this is easy to do
- - if aggregated with other manuscripts, for example in a repository or other site, be shared in alignment with our hosting policy not be added to or enhanced in any way to appear more like, or to substitute for, the published journal article.

Published journal article (JPA): A published journal article (PJA) is the definitive final record of published research that appears or will appear in the journal and embodies all value-adding publishing activities including peer review co-ordination, copy-editing, formatting, (if relevant) pagination and online enrichment.

Policies for sharing publishing journal articles differ for subscription and gold open access articles:

Subscription Articles: If you are an author, please share a link to your article rather than the full-text. Millions of researchers have access to the formal publications on ScienceDirect, and so links will help your users to find, access, cite, and use the best available version.

Theses and dissertations which contain embedded PJAs as part of the formal submission can be posted publicly by the awarding institution with DOI links back to the formal publications on ScienceDirect.

If you are affiliated with a library that subscribes to ScienceDirect you have additional private sharing rights for others' research accessed under that agreement. This includes use for classroom teaching and internal training at the institution (including use in course packs and courseware programs), and inclusion of the article for grant funding purposes.

Gold Open Access Articles: May be shared according to the author-selected end-user

license and should contain a CrossMark logo, the end user license, and a DOI link to the formal publication on ScienceDirect.

Please refer to Elsevier's posting policy for further information.

18. **For book authors** the following clauses are applicable in addition to the above: Authors are permitted to place a brief summary of their work online only. You are not allowed to download and post the published electronic version of your chapter, nor may you scan the printed edition to create an electronic version. **Posting to a repository:** Authors are permitted to post a summary of their chapter only in their institution's repository.

19. **Thesis/Dissertation**: If your license is for use in a thesis/dissertation your thesis may be submitted to your institution in either print or electronic form. Should your thesis be published commercially, please reapply for permission. These requirements include permission for the Library and Archives of Canada to supply single copies, on demand, of the complete thesis and include permission for Proquest/UMI to supply single copies, on demand, of the complete thesis. Should your thesis be published commercially, please reapply for permission. Theses and dissertations which contain embedded PJAs as part of the formal submission can be posted publicly by the awarding institution with DOI links back to the formal publications on ScienceDirect.

Elsevier Open Access Terms and Conditions

You can publish open access with Elsevier in hundreds of open access journals or in nearly 2000 established subscription journals that support open access publishing. Permitted third party re-use of these open access articles is defined by the author's choice of Creative Commons user license. See our open access license policy for more information.

Terms & Conditions applicable to all Open Access articles published with Elsevier:

Any reuse of the article must not represent the author as endorsing the adaptation of the article nor should the article be modified in such a way as to damage the author's honour or reputation. If any changes have been made, such changes must be clearly indicated.

The author(s) must be appropriately credited and we ask that you include the end user license and a DOI link to the formal publication on ScienceDirect.

If any part of the material to be used (for example, figures) has appeared in our publication with credit or acknowledgement to another source it is the responsibility of the user to ensure their reuse complies with the terms and conditions determined by the rights holder.

Additional Terms & Conditions applicable to each Creative Commons user license:

CC BY: The CC-BY license allows users to copy, to create extracts, abstracts and new works from the Article, to alter and revise the Article and to make commercial use of the Article (including reuse and/or resale of the Article by commercial entities), provided the user gives appropriate credit (with a link to the formal publication through the relevant DOI), provides a link to the license, indicates if changes were made and the licensor is not represented as endorsing the use made of the work. The full details of the license are

available at http://creativecommons.org/licenses/by/4.0.

CC BY NC SA: The CC BY-NC-SA license allows users to copy, to create extracts, abstracts and new works from the Article, to alter and revise the Article, provided this is not done for commercial purposes, and that the user gives appropriate credit (with a link to the formal publication through the relevant DOI), provides a link to the license, indicates if changes were made and the licensor is not represented as endorsing the use made of the work. Further, any new works must be made available on the same conditions. The full details of the license are available at http://creativecommons.org/licenses/by-nc-sa/4.0.

CC BY NC ND: The CC BY-NC-ND license allows users to copy and distribute the Article, provided this is not done for commercial purposes and further does not permit distribution of the Article if it is changed or edited in any way, and provided the user gives appropriate credit (with a link to the formal publication through the relevant DOI), provides a link to the license, and that the licensor is not represented as endorsing the use made of the work. The full details of the license are available at http://creativecommons.org/licenses/by-nc-nd/4.0. Any commercial reuse of Open Access articles published with a CC BY NC SA or CC BY NC ND license requires permission from Elsevier and will be subject to a fee.

Commercial reuse includes:

- - Associating advertising with the full text of the Article
- - Charging fees for document delivery or access
- - Article aggregation
- - Systematic distribution via e-mail lists or share buttons

Posting or linking by commercial companies for use by customers of those companies.

20. **Other Conditions**:

v1.7

Questions? customercare@copyright.com or +1-855-239-3415 (toll free in the US) or +1-978-646-2777.

Droits d'auteurs, Article VI, Pages 153-181

ELSEVIER LICENSE
TERMS AND CONDITIONS

Jun 24, 2015

This is a License Agreement between Elissar Gemayel ("You") and Elsevier ("Elsevier") provided by Copyright Clearance Center ("CCC"). The license consists of your order details, the terms and conditions provided by Elsevier, and the payment terms and conditions.

All payments must be made in full to CCC. For payment instructions, please see information listed at the bottom of this form.

Supplier	Elsevier Limited The Boulevard,Langford Lane Kidlington,Oxford,OX5 1GB,UK
Registered Company Number	1982084
Customer name	Elissar Gemayel
Customer address	IMAGES_ESPACE-DEV Perpignan, 66860
License number	3640261058167
License date	Jun 01, 2015
Licensed content publisher	Elsevier
Licensed content publication	Deep Sea Research Part I: Oceanographic Research Papers
Licensed content title	Acidification of the Mediterranean Sea from anthropogenic carbon penetration
Licensed content author	None
Licensed content date	August 2015
Licensed content volume number	102
Licensed content issue number	n/a
Number of pages	15
Start Page	1
End Page	15
Type of Use	reuse in a thesis/dissertation
Portion	full article
Format	both print and electronic
Are you the author of this Elsevier article?	Yes
Will you be translating?	No
Title of your thesis/dissertation	Contribution à l'estimation des paramètres du système des carbonates en Mer Méditerranée
Expected completion date	Sep 2015
Estimated size (number of pages)	200

Elsevier VAT number	GB 494 6272 12
Permissions price	0.00 USD
VAT/Local Sales Tax	0.00 USD / 0.00 GBP
Total	0.00 USD
Terms and Conditions	

INTRODUCTION

1. The publisher for this copyrighted material is Elsevier. By clicking "accept" in connection with completing this licensing transaction, you agree that the following terms and conditions apply to this transaction (along with the Billing and Payment terms and conditions established by Copyright Clearance Center, Inc. ("CCC"), at the time that you opened your Rightslink account and that are available at any time athttp://myaccount.copyright.com).

GENERAL TERMS

2. Elsevier hereby grants you permission to reproduce the aforementioned material subject to the terms and conditions indicated.

3. Acknowledgement: If any part of the material to be used (for example, figures) has appeared in our publication with credit or acknowledgement to another source, permission must also be sought from that source. If such permission is not obtained then that material may not be included in your publication/copies. Suitable acknowledgement to the source must be made, either as a footnote or in a reference list at the end of your publication, as follows:

"Reprinted from Publication title, Vol /edition number, Author(s), Title of article / title of chapter, Pages No., Copyright (Year), with permission from Elsevier [OR APPLICABLE SOCIETY COPYRIGHT OWNER]." Also Lancet special credit - "Reprinted from The Lancet, Vol. number, Author(s), Title of article, Pages No., Copyright (Year), with permission from Elsevier."

4. Reproduction of this material is confined to the purpose and/or media for which permission is hereby given.

5. Altering/Modifying Material: Not Permitted. However figures and illustrations may be altered/adapted minimally to serve your work. Any other abbreviations, additions, deletions and/or any other alterations shall be made only with prior written authorization of Elsevier Ltd. (Please contact Elsevier at permissions@elsevier.com)

6. If the permission fee for the requested use of our material is waived in this instance, please be advised that your future requests for Elsevier materials may attract a fee.

7. Reservation of Rights: Publisher reserves all rights not specifically granted in the combination of (i) the license details provided by you and accepted in the course of this licensing transaction, (ii) these terms and conditions and (iii) CCC's Billing and Payment terms and conditions.

8. License Contingent Upon Payment: While you may exercise the rights licensed immediately upon issuance of the license at the end of the licensing process for the

transaction, provided that you have disclosed complete and accurate details of your proposed use, no license is finally effective unless and until full payment is received from you (either by publisher or by CCC) as provided in CCC's Billing and Payment terms and conditions. If full payment is not received on a timely basis, then any license preliminarily granted shall be deemed automatically revoked and shall be void as if never granted. Further, in the event that you breach any of these terms and conditions or any of CCC's Billing and Payment terms and conditions, the license is automatically revoked and shall be void as if never granted. Use of materials as described in a revoked license, as well as any use of the materials beyond the scope of an unrevoked license, may constitute copyright infringement and publisher reserves the right to take any and all action to protect its copyright in the materials.

9. Warranties: Publisher makes no representations or warranties with respect to the licensed material.

10. Indemnity: You hereby indemnify and agree to hold harmless publisher and CCC, and their respective officers, directors, employees and agents, from and against any and all claims arising out of your use of the licensed material other than as specifically authorized pursuant to this license.

11. No Transfer of License: This license is personal to you and may not be sublicensed, assigned, or transferred by you to any other person without publisher's written permission.

12. No Amendment Except in Writing: This license may not be amended except in a writing signed by both parties (or, in the case of publisher, by CCC on publisher's behalf).

13. Objection to Contrary Terms: Publisher hereby objects to any terms contained in any purchase order, acknowledgment, check endorsement or other writing prepared by you, which terms are inconsistent with these terms and conditions or CCC's Billing and Payment terms and conditions. These terms and conditions, together with CCC's Billing and Payment terms and conditions (which are incorporated herein), comprise the entire agreement between you and publisher (and CCC) concerning this licensing transaction. In the event of any conflict between your obligations established by these terms and conditions and those established by CCC's Billing and Payment terms and conditions, these terms and conditions shall control.

14. Revocation: Elsevier or Copyright Clearance Center may deny the permissions described in this License at their sole discretion, for any reason or no reason, with a full refund payable to you. Notice of such denial will be made using the contact information provided by you. Failure to receive such notice will not alter or invalidate the denial. In no event will Elsevier or Copyright Clearance Center be responsible or liable for any costs, expenses or damage incurred by you as a result of a denial of your permission request, other than a refund of the amount(s) paid by you to Elsevier and/or Copyright Clearance Center for denied permissions.

LIMITED LICENSE

The following terms and conditions apply only to specific license types:

15. **Translation**: This permission is granted for non-exclusive world **English** rights only unless your license was granted for translation rights. If you licensed translation rights you may only translate this content into the languages you requested. A professional

translator must perform all translations and reproduce the content word for word preserving the integrity of the article. If this license is to re-use 1 or 2 figures then permission is granted for non-exclusive world rights in all languages.

16. **Posting licensed content on any Website**: The following terms and conditions apply as follows: Licensing material from an Elsevier journal: All content posted to the web site must maintain the copyright information line on the bottom of each image; A hyper-text must be included to the Homepage of the journal from which you are licensing athttp://www.sciencedirect.com/science/journal/xxxxx or the Elsevier homepage for books athttp://www.elsevier.com; Central Storage: This license does not include permission for a scanned version of the material to be stored in a central repository such as that provided by Heron/XanEdu.

Licensing material from an Elsevier book: A hyper-text link must be included to the Elsevier homepage at http://www.elsevier.com . All content posted to the web site must maintain the copyright information line on the bottom of each image.

Posting licensed content on Electronic reserve: In addition to the above the following clauses are applicable: The web site must be password-protected and made available only to bona fide students registered on a relevant course. This permission is granted for 1 year only. You may obtain a new license for future website posting.

17. **For journal authors:** the following clauses are applicable in addition to the above:

Preprints:

A preprint is an author's own write-up of research results and analysis, it has not been peer-reviewed, nor has it had any other value added to it by a publisher (such as formatting, copyright, technical enhancement etc.).

Authors can share their preprints anywhere at any time. Preprints should not be added to or enhanced in any way in order to appear more like, or to substitute for, the final versions of articles however authors can update their preprints on arXiv or RePEc with their Accepted Author Manuscript (see below).

If accepted for publication, we encourage authors to link from the preprint to their formal publication via its DOI. Millions of researchers have access to the formal publications on ScienceDirect, and so links will help users to find, access, cite and use the best available version. Please note that Cell Press, The Lancet and some society-owned have different preprint policies. Information on these policies is available on the journal homepage.

Accepted Author Manuscripts: An accepted author manuscript is the manuscript of an article that has been accepted for publication and which typically includes author-incorporated changes suggested during submission, peer review and editor-author communications.

Authors can share their accepted author manuscript:

- - immediately
    - via their non-commercial person homepage or blog
    - by updating a preprint in arXiv or RePEc with the accepted

manuscript
    - via their research institute or institutional repository for internal institutional uses or as part of an invitation-only research collaboration work-group
    - directly by providing copies to their students or to research collaborators for their personal use
    - for private scholarly sharing as part of an invitation-only work group on commercial sites with which Elsevier has an agreement
- - after the embargo period
    - via non-commercial hosting platforms such as their institutional repository
    - via commercial sites with which Elsevier has an agreement

In all cases accepted manuscripts should:

- - link to the formal publication via its DOI
- - bear a CC-BY-NC-ND license - this is easy to do
- - if aggregated with other manuscripts, for example in a repository or other site, be shared in alignment with our hosting policy not be added to or enhanced in any way to appear more like, or to substitute for, the published journal article.

Published journal article (JPA): A published journal article (PJA) is the definitive final record of published research that appears or will appear in the journal and embodies all value-adding publishing activities including peer review co-ordination, copy-editing, formatting, (if relevant) pagination and online enrichment.

Policies for sharing publishing journal articles differ for subscription and gold open access articles:

Subscription Articles: If you are an author, please share a link to your article rather than the full-text. Millions of researchers have access to the formal publications on ScienceDirect, and so links will help your users to find, access, cite, and use the best available version.

Theses and dissertations which contain embedded PJAs as part of the formal submission can be posted publicly by the awarding institution with DOI links back to the formal publications on ScienceDirect.

If you are affiliated with a library that subscribes to ScienceDirect you have additional private sharing rights for others' research accessed under that agreement. This includes use for classroom teaching and internal training at the institution (including use in course packs and courseware programs), and inclusion of the article for grant funding purposes.

Gold Open Access Articles: May be shared according to the author-selected end-user license and should contain a CrossMark logo, the end user license, and a DOI link to the formal publication on ScienceDirect.

Please refer to Elsevier's posting policy for further information.

18. **For book authors** the following clauses are applicable in addition to the above: Authors are permitted to place a brief summary of their work online only. You

are not allowed to download and post the published electronic version of your chapter, nor may you scan the printed edition to create an electronic version. **Posting to a repository:** Authors are permitted to post a summary of their chapter only in their institution's repository.

19. **Thesis/Dissertation**: If your license is for use in a thesis/dissertation your thesis may be submitted to your institution in either print or electronic form. Should your thesis be published commercially, please reapply for permission. These requirements include permission for the Library and Archives of Canada to supply single copies, on demand, of the complete thesis and include permission for Proquest/UMI to supply single copies, on demand, of the complete thesis. Should your thesis be published commercially, please reapply for permission. Theses and dissertations which contain embedded PJAs as part of the formal submission can be posted publicly by the awarding institution with DOI links back to the formal publications on ScienceDirect.

Elsevier Open Access Terms and Conditions

You can publish open access with Elsevier in hundreds of open access journals or in nearly 2000 established subscription journals that support open access publishing. Permitted third party re-use of these open access articles is defined by the author's choice of Creative Commons user license. See our open access license policy for more information.

Terms & Conditions applicable to all Open Access articles published with Elsevier:

Any reuse of the article must not represent the author as endorsing the adaptation of the article nor should the article be modified in such a way as to damage the author's honour or reputation. If any changes have been made, such changes must be clearly indicated.

The author(s) must be appropriately credited and we ask that you include the end user license and a DOI link to the formal publication on ScienceDirect.

If any part of the material to be used (for example, figures) has appeared in our publication with credit or acknowledgement to another source it is the responsibility of the user to ensure their reuse complies with the terms and conditions determined by the rights holder.

Additional Terms & Conditions applicable to each Creative Commons user license:

CC BY: The CC-BY license allows users to copy, to create extracts, abstracts and new works from the Article, to alter and revise the Article and to make commercial use of the Article (including reuse and/or resale of the Article by commercial entities), provided the user gives appropriate credit (with a link to the formal publication through the relevant DOI), provides a link to the license, indicates if changes were made and the licensor is not represented as endorsing the use made of the work. The full details of the license are available at http://creativecommons.org/licenses/by/4.0.

CC BY NC SA: The CC BY-NC-SA license allows users to copy, to create extracts, abstracts and new works from the Article, to alter and revise the Article, provided this is not done for commercial purposes, and that the user gives appropriate credit (with a link

to the formal publication through the relevant DOI), provides a link to the license, indicates if changes were made and the licensor is not represented as endorsing the use made of the work. Further, any new works must be made available on the same conditions. The full details of the license are available at http://creativecommons.org/licenses/by-nc-sa/4.0.

CC BY NC ND: The CC BY-NC-ND license allows users to copy and distribute the Article, provided this is not done for commercial purposes and further does not permit distribution of the Article if it is changed or edited in any way, and provided the user gives appropriate credit (with a link to the formal publication through the relevant DOI), provides a link to the license, and that the licensor is not represented as endorsing the use made of the work. The full details of the license are available at http://creativecommons.org/licenses/by-nc-nd/4.0. Any commercial reuse of Open Access articles published with a CC BY NC SA or CC BY NC ND license requires permission from Elsevier and will be subject to a fee.

Commercial reuse includes:

- - Associating advertising with the full text of the Article
- - Charging fees for document delivery or access
- - Article aggregation
- - Systematic distribution via e-mail lists or share buttons

Posting or linking by commercial companies for use by customers of those companies.

20. **Other Conditions**:

v1.7

Questions? customercare@copyright.com or +1-855-239-3415 (toll free in the US) or +1-978-646-2777.

Résumé

L'objectif de la thèse s'inscrit dans le contexte de l'acidification des océans. Après avoir analysé l'état la circulation générale en Mer Méditerranée, j'ai étudié les différentes propriétés physico-chimiques qui régulent la distribution de la pression partielle du CO_2 dans les eaux de surface (pCO_2^{sw}), et présenté un calcul ponctuel des flux de CO_2 journaliers. En outre, j'ai estimé la pCO_2^{sw} à partir de différents paramètres acquis par les images satellites, et cartographié les flux de CO_2 sur l'échelle de toute la Mer Méditerranée. Par la suite, j'ai établi des équations pour estimer les distributions de l'alcalinité totale (A_T) et du carbone inorganique total (C_T) dans la colonne d'eau et dans les eaux de surface. Il est donc possible d'estimer ces deux paramètres par des relations simples qui nécessitent des mesures de salinité et/ou de température. A partir des données d'A_T et de C_T, il est aussi possible de déterminer l'état présent et d'estimer l'acidification future de la Mer Méditerranée.

Mots clés : Mer Méditerranée ; système des carbonates ; images satellites ; flux de CO_2 ; acidification

Abstract

The objectif of the thesis is in the context of ocean acidification. After analyzing the general circulation in the Mediterranean Sea, I studied the different physico-chemical properties that regulate the distribution of the partial pressure of CO_2 in surface waters (pCO_2^{sw}), and presented a local calculation of the daily CO_2 fluxes. I also estimated the pCO_2^{sw} from different parameters acquired from the satellite images, and mapped the CO_2 fluxes on the scale of the entire Mediterranean Sea. Later on, I established equations to estimate the distributions of total alkalinity (A_T) and total inorganic carbon (C_T) in the water column and in surface waters. Therefore, it is possible to estimate these two parameters from simple relationships that require measurements of salinity and/or temperature. Based on the data of A_T and C_T, it is also possible to determine the present state and estimate acidification of the Mediterranean Sea in the future.

Keywords: Mediterranean Sea; carbonates system; satellite images; CO_2 fluxes; acidification